10. SITE 639[1]

Shipboard Scientific Party[2]

HOLE 639A

Date occupied: 23 May 1985

Date departed: 25 May 1985

Time on hole: 2 days, 14 hr

Position: 42°08.6′N, 12°14.9′W

Water depth (sea level, corrected m, echo-sounding): 4720

Water depth (rig floor, corrected m, echo-sounding): 4730

Bottom felt (m, drill pipe): 4735

Penetration (m): 89.8

Number of cores: 10

Total length of cored section (m): 89.8

Total core recovered (m): 35.43

Core recovery (%): 39

Deepest sedimentary unit cored:
Depth sub-bottom (m): 89.8
Nature: dolomite
Age: latest Jurassic/earliest Cretaceous
Measured vertical sound velocity (km/s): 5.9–6.8

HOLE 639B

Date occupied: 26 May 1985

Date departed: 27 May 1985

Time on hole: 1 day, 6 hr

Position: 42°08.6′N, 12°15.0′W (200 m west of Hole 639A)

Water depth (sea level, corrected m, echo-sounding): 4735

Water depth (rig floor, corrected m, echo-sounding): 4745

Bottom felt (m, drill pipe): 4758

Penetration (m): 80

Number of cores: 4

Total length of cored section (m): 23.7

Total core recovered (m): 12.3

Core recovery (%): 38

Deepest sedimentary unit cored:
Depth sub-bottom (m): 80
Nature: dolomite
Age: Late Jurassic/earliest Cretaceous
Measured vertical sound velocity (km/s): 6.5–6.7

HOLE 639C

Date occupied: 27 May 1985

Date departed: 27 May 1985

Time on hole: 14 hr

Position: 42°08.6′N, 12°15.1′W (300 m west of Hole 639A)

Water depth (sea level, corrected m, echo-sounding): 4756

Water depth (rig floor, corrected m, echo-sounding): 4766

Bottom felt (m, drill pipe): 4792

Penetration (m): 100.4

Number of cores: 2

Total length of cored section (m): 22.4

Total core recovered (m): 4.8

Core recovery (%): 22

Deepest sedimentary unit cored:
Depth sub-bottom (m): 100.4
Nature: dolomite
Age: Late Jurassic/earliest Cretaceous

HOLE 639D

Date occupied: 27 May 1985

Date departed: 1 June 1985

Time on hole: 6 days, 21 hr

Position: 42°08.6′N, 12°15.3′W (500 m west of Hole 639A)

---

[1] Boillot, G., Winterer, E. L., Meyer, A. W., et al., *Proc. Init. Repts. (Pt. A), ODP*, 103.

[2] Gilbert Boillot (Co-Chief Scientist), Laboratoire de Géodynamique Sous-Marine, Université Pierre et Marie Curie, B.P. 48, 06230, Villefranche-sur-Mer, France; Edward L. Winterer (Co-Chief Scientist), Graduate Research Division A-012-W, Scripps Institution of Oceanography, La Jolla, CA 92093; Audrey W. Meyer (ODP Staff Scientist), Ocean Drilling Program, Texas A&M University, College Station, TX 77843-3469; Joseph Applegate, Department of Geology, Florida State University, Tallahassee, FL 32306; Mariam Baltuck, Department of Geology, Tulane University, New Orleans, LA 70118 (current address: NASA Headquarters, Code EEL, Washington, D.C. 20546); James A. Bergen, Department of Geology, Florida State University, Tallahassee, FL 32306; M. C. Comas, Departamento Estratigrafia y Paleontologia, Facultad de Ciencias, Universidad de Granada, 18001 Granada, Spain; Thomas A. Davies, Institute for Geophysics, University of Texas at Austin, 4920 North IH 35, Austin, TX 78751; Keith Dunham, Department of Atmospheric and Oceanic Sciences, University of Michigan, 2455 Hayward Avenue, Ann Arbor, MI 48109 (current address: P.O. Box 13, Pequat Lakes, MN 56478); Cynthia A. Evans, Department of Geology, Colgate University, Hamilton, NY 13346 (current address: Lamont-Doherty Geological Observatory, Palisades, NY 10964); Jacques Girardeau, Laboratoire de Materiaux Terrestres, I.P.G., 4 Place Jussieu, 75252 Paris Cedex 05, France; David Goldberg, Lamont-Doherty Geological Observatory, Palisades, NY 10964; Janet Haggerty, Department of Geology, University of Tulsa, 600 S. College Avenue, Tulsa, OK 74104; Lubomir F. Jansa, Atlantic Geoscience Center, Bedford Institute of Oceanography, Dartmouth, Nova Scotia B2Y 4A2, Canada; Jeffrey A. Johnson, Department of Earth and Space Sciences, University of California, Los Angeles, CA 90024 (current address: 9449 Briar Forest Drive, No. 3544, Houston, TX 77063); Junzo Kasahara, Earthquake Research Institute, University of Tokyo, 1,1,1 Yayoi, Bunkyo, Tokyo 113, Japan (current address: Nippon Schlumberger K.K., 2-1 Fuchinobe, 2-Chome, Sagamihara-shi, Kanagawa-ken, 229, Japan); Jean-Paul Loreau, Laboratoire de Géologie, Museum National D'Histoire Naturelle, 43 Rue Buffon, 75005 Paris, France; Emilio Luna, Hispanoil, Pez Volador No. 2, 28007 Madrid, Spain; Michel Moullade, Laboratoire de Géologie et Micropaleontologie Marines, Université de Nice, Parc Valrose, 06034 Nice Cedex, France; James Ogg, Geological Research Division A-012, Scripps Institution of Oceanography, La Jolla, CA 92093 (current address: Dept. Earth and Atmospheric Sciences, Purdue University, W. Lafayette, IN 47907); Massimo Sarti, Istituto di Geologia, Universitá di Ferrara, Corso Ercole d'Este, 32, 4410 Ferrara, Italy; Jürgen Thurow, Institut und Museum für Geologie und Paleontologie, Universität Tübingen, Sigwartstr. 10, D-7400 Tübingen, Federal Republic of Germany; Mark A. Williamson, Atlantic Geoscience Centre, Geological Survey of Canada, Bedford Institute of Oceanography, Box 1006, Dartmouth, Nova Scotia B2Y 4A2, Canada (current address: Shell Canada Ltd., P.O. Box 100, Stn. M, Calgary, Alberta T2P 2H5, Canada).

Water depth (sea level, corrected m, echo-sounding): 4748

Water depth (rig floor, corrected m, echo-sounding): 4758

Bottom felt (m, drill pipe): 4753

Penetration (m): 293.1

Number of cores: 13

Total length of cored section (m): 115.5

Total core recovered (m): 24.15

Core recovery (%): 21

Deepest sedimentary unit cored:
Depth sub-bottom (m): 293.1
Nature: limestone
Age: Late Jurassic (Tithonian)
Measured vertical sound velocity (km/s): 3.0–5.1

HOLE 639E

Date occupied: 6 June 1985

Date departed: 7 June 1985

Time on hole: 1 day, 7 hr

Position: 42°08.6′N, 12°15.4′W (700 m west of Hole 639A)

Water depth (sea level, corrected m, echo-sounding): 4754

Water depth (rig floor, corrected m, echo-sounding): 4764

Bottom felt (m, drill pipe): 4770

Penetration (m): 237.9

Number of cores: 4

Total length of cored section (m): 38.5

Total core recovered (m): 1.2

Core recovery (%): 3

Deepest sedimentary unit cored:
Depth sub-bottom (m): 209.1
Nature: limestone
Age: Late Jurassic (Tithonian)
Measured vertical sound velocity (km/s): 3.8

HOLE 639F

Date occupied: 7 June 1985

Date departed: 8 June 1985

Time on hole: 19 hr

Position: 42°08.6′N, 12°15.5′W (800 m west of Hole 639A)

Water depth (sea level, corrected m, echo-sounding): 4754

Water depth (rig floor, corrected m, echo-sounding): 4764

Bottom felt (m, drill pipe): 4771

Penetration (m): 250.8

Number of cores: 2

Total length of cored section (m): 13.0

Total core recovered (m): 0.6

Core recovery (%): 5

Igneous or metamorphic basement:
Depth sub-bottom (m): 247.3 (top?); 250.8 (bottom of hole)
Nature: metadacite(?)
Velocity range (km/s): 6.2–6.6

Principal results: Six holes were drilled at Site 639 to sample the stratigraphic section from the top of the carbonate platform to the basement. As shown in Figure 1, the holes are arrayed along an east-west line measuring 800 m from Hole 639A at the east end of the line to Hole 639F at the west end. The six holes sample a section of Mesozoic strata estimated to be about 300–500 m thick, ranging from late Tithonian to early Valanginian age. The section dips east and subcrops on a westward-sloping submarine erosion surface, now buried beneath an onlapping wedge of nearly horizontal Neogene pelagic ooze. Impossible drilling conditions blocked our attempts to core through the entire section from the Lower Cretaceous to basement rock at Hole 639A; we, therefore, stepped progressively west down the subcrop to construct a composite section. At each of the holes except Hole 639D, the pipe, after penetrating only a few meters or tens of meters of dolomite, stuck in the hole, probably because of extensive brecciation and loose connections among breccia blocks. At Hole 639D, the dolomite breccia was only about 15 m thick, and we could, therefore, continue into the underlying upper Tithonian limestone for about 95 m until the bit failed.

The reconstructed section of rocks at Site 639 is depicted in Figure 1. Measurements on cores from Holes 639A and 639D show that the local dip ranges between about 15° and 45°, averaging about 25°–30°, and both seismic and shipboard magnetic data indicate that the beds dip east. Seismic profiles and the results of Site 638 studies (this volume), indicate that the regional dip east of Site 639 is only about 10°. Faulting near Site 639 may be responsible for the steep dips, and the section may be partly repeated by faulting, resulting in a falsely high estimate of the thickness of the carbonate-platform rocks.

The generalized section (Fig. 1), synthesized from the strata cored at each of the holes, is as follows:

Lithologic Unit I: Neogene ooze, marl, and clay, probably including turbidites. This unit is 21.6 m thick at Hole 639A and thickens to about 235 m (uncored) in Hole 639F. The oldest strata cored are late Miocene at Hole 639A, and mid-Pliocene fossils occur within 10 m of the base of the unit in Hole 639B.

Lithologic Unit II: Undated brown silty clay. This unit, only about 2 m thick and occurring only in Hole 639C, is similar to brown clay on the Mesozoic/Neogene unconformity at Sites 637 and 640. Unit II contains ichthyoliths, dated by P. Doyle (pers. comm., 1985) as being late or middle Eocene, but has no other fossils.

Talus and Slide Unit: Treated as part of lithologic Unit VI in the "Sediment Lithology" section (this chapter). Brecciated dolomite, limestone, and fragments of sandstone and metamorphosed sandstone in Holes 639D, 639E, and 639F are interpreted as being talus and rock slides from the slopes above, emplaced before the Neogene and probably before deposition of the brown clay of Unit II. The displaced material has its maximum thickness of about 20 m in Hole 639E.

Lithologic Unit III: Lower Valanginian calpionellid-bearing marlstone, passing upward into marl with thin sandstone interbeds. This unit occurs only in Hole 639A, where it has a stratigraphic thickness of about 49 m.

Lithologic Unit IV: Dolomite, commonly fractured and vuggy, with internal sediments in fractures and vugs; originally skeletal grainstone/packstone and framestone/wackestone. No age-diagnostic fossils occur. Stratigraphic thickness is estimated as being 215 m, but it could be as much as 365 m.

Lithologic Unit V: Limestone, clayey limestone, marlstone, and sandstone. This unit is Tithonian, according to the occurrence of *Anchispiracyclina lusitanica*. A stratigraphic thickness of about 95 m was cored in Hole 639D, but the unit may be as thick as 200 m.

A possible conglomerate unit (treated as part of lithologic Unit VI in the "Sediment Lithology" section, this chapter) occurs as a polymict assortment of quartzite, pisolitic claystone, and conglomerate fragments with the igneous rocks in Hole 639E and suggests that a basal conglomerate may lie between the Tithonian limestone of Unit V and basement rock. Clasts from this unit may be present in the toe of the proposed talus unit in Hole 639F.

Basement(?) rock (treated as part of lithologic Unit VI in "Sediment Lithology" section, this chapter) has large pieces of (hydrothermally?) altered silicic volcanic or hypabyssal rocks of rhyolitic or rhyodacitic composition at the bottom of Hole 639F and in the next-to-last core of Hole 639E. We interpret these rocks as belonging to the basement, but they could plausibly be clasts in a conglomerate.

Gamma-ray, induction, sonic, density, and multichannel-sonic logs were obtained for most of the Mesozoic section in Hole 639D.

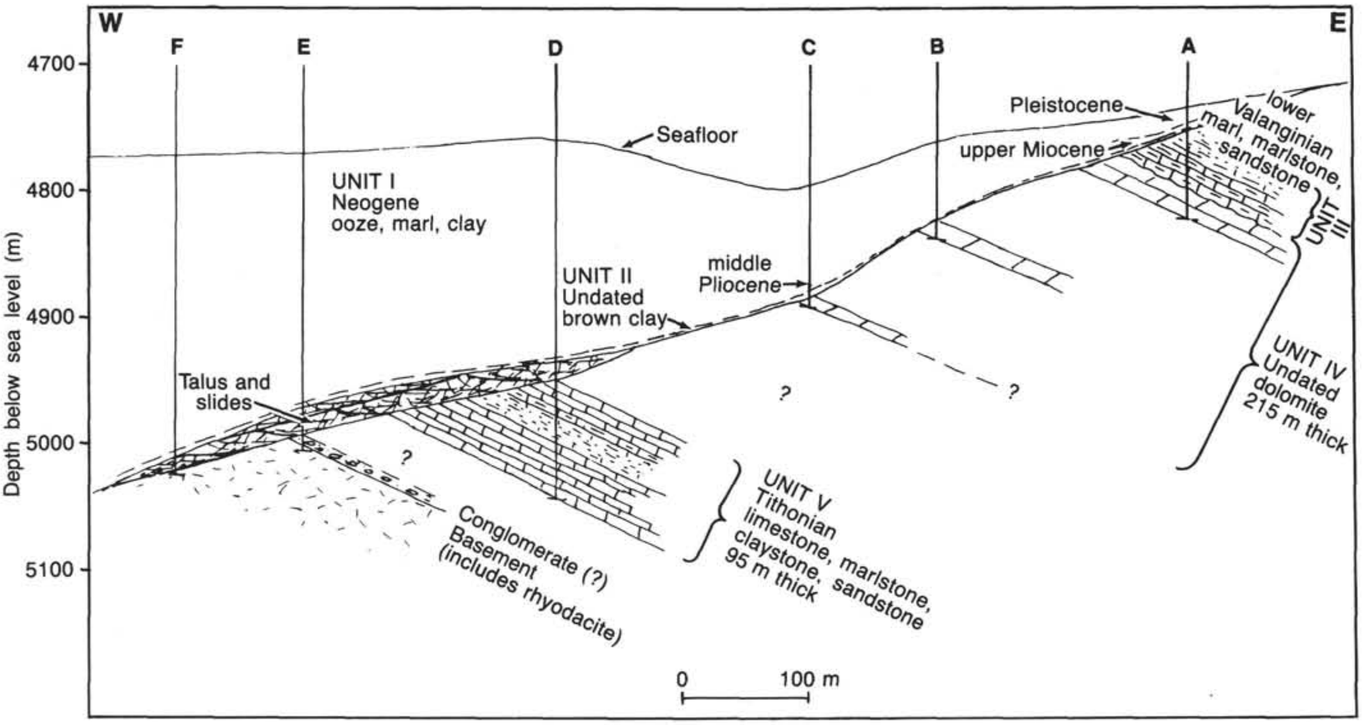

Figure 1. Geologic cross section through holes drilled at Site 639. A uniform local dip of 30° is assumed, indicated by the average of measurements on cores. Regional dip, as estimated from seismic data, is about 10°. No faults are shown although some could exist. Blank spaces in the cross section indicate parts of the section unsampled during coring for which stratigraphic assignment cannot be made confidently. The brown clay, Unit II, is shown extending across the whole of the erosion surface that truncates the Mesozoic. The inferred talus and rock-slide unit is drawn so that the displaced limestone at the top of the unit has a possible source farther up the slope, on limestone not covered by the dolomite talus. The rhyodacite drawn here as basement rock may be part of the conglomerate, and the basement may include many rocks besides rhyodacite.

BACKGROUND AND OBJECTIVES

As we left Site 638 and prepared to drill at Site 639, we realized that the results of drilling at Site 638 forced a reassessment of the regional seismic stratigraphy. At least 350 m of Barremian marlstone and Valanginian–Hauterivian turbidite sandstone beds certainly lie below the conspicuous seismic reflector thought from previous studies (Mougenot et al., 1985; G. Boillot, pers. comm., 1985) to mark the top of the Upper Jurassic–lowest Cretaceous shallow-water carbonate platform. These marlstone and sandstone beds constitute the relatively transparent seismic unit labeled "5" on Figure 2C. The top of the carbonate platform must, therefore, be lower, and as we approached Site 639, we presumed it to be delineated by the strong reflector at the base of seismic unit 5.

Because the pipe stuck in Hole 638C and unfortunately prevented our reaching this deep reflector, we planned to continue our effort to construct a stratigraphic column extending through the carbonate platform and into the crystalline basement by drilling Site 639 about 3 km west of Site 638, at a place where the deep reflector is near the seafloor (Fig. 2C), along a partly buried steep submarine escarpment.

The seismic record is unclear below seismic unit 5, probably because the sound velocity in carbonate-platform rocks and in crystalline basement rocks is roughly the same. It is therefore difficult to estimate accurately the thickness of the pre-rift sequence and hence the depth to the basement at the place chosen for Site 639. The results of dredging about 6 km north of Site 639, on the continuation of the west-facing slope where the escarpment rises about 800 m above the abyssal plain (Fig. 2B, locality DR03), furnish some clues to the depth to the basement. The rocks collected in the dredge include basement rocks, carbonate-platform rocks (Berriasian?), and unfossiliferous sandstone (Mougenot et al., 1985). The seismic line recorded near the dredge site (Fig. 3D, Site 638 chapter, this volume) clearly shows that the transparent layer identified at Site 638 as being Valanginian and Hauterivian sandstone and marl crops out on the upper slopes of the escarpment, where the layer is about 350 m thick. Therefore, the basement and carbonate rocks recovered by the dredge came from the lower 450 m of the escarpment, which, in turn, implies a maximum thickness of the platform carbonates of somewhat less than 450 m and, thus, possibly within the limits of a single-bit hole.

The main scientific objective at Site 639 was thus to collect data on the evolution of the Galicia margin from the time sedimentation began on the Hercynian basement through the time of disintegration of the carbonate platform at the onset of rifting.

OPERATIONS

Approach to Site 639

We had seen before leaving Site 638 that a favorable place to drill through the top of the carbonate platform was along seismic profile GP-101, at shotpoint 3025 (Fig. 2C), but we decided to make a short survey in the area just south of that place to attempt to find an even more attractive site. The ship followed approximately along the track shown in Figure 3, which is a chart constructed after we had already dropped the beacon at Site 639 (at 0946 hr on 23 May 1985), when adequate satellite positions became available. During the survey itself, we obtained not one usable satellite fix. The chart shows that Site 639 is about 1 km southwest of shotpoint 3025, but the seismic-reflection profile (Fig. 4) and the 3.5-kHz echo-sounding record (Fig. 5) taken from *JOIDES Resolution* during the final approach show con-

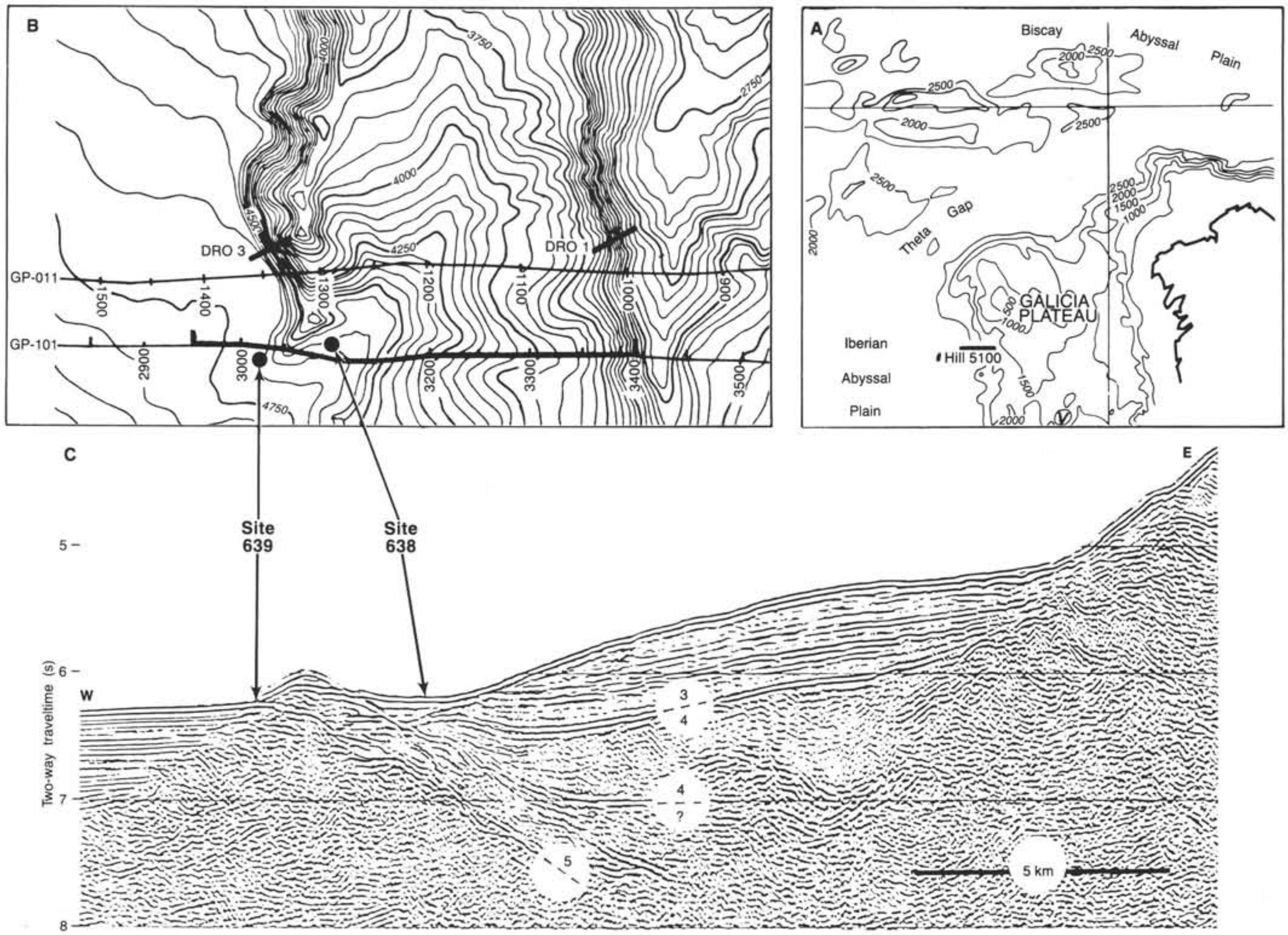

Figure 2. A. Galicia margin. Location of profile shown in Figure 2C is indicated by heavy solid line. B. Sea Beam map (Sibuet et al., this volume) of the area near Site 639, showing the location of dredge localities DR01 and DR03 (Mougenot et al., 1985), Sites 638 and 639, and multichannel seismic profiles shown in Figures 2C and 26. C. IFP multichannel seismic profile GP-101 from shotpoint 2950 to 3400, showing the location of Sites 638 and 639. Post-rift strata, 3; syn-rift strata, 4 and 5. Courtesy of L. Montadert.

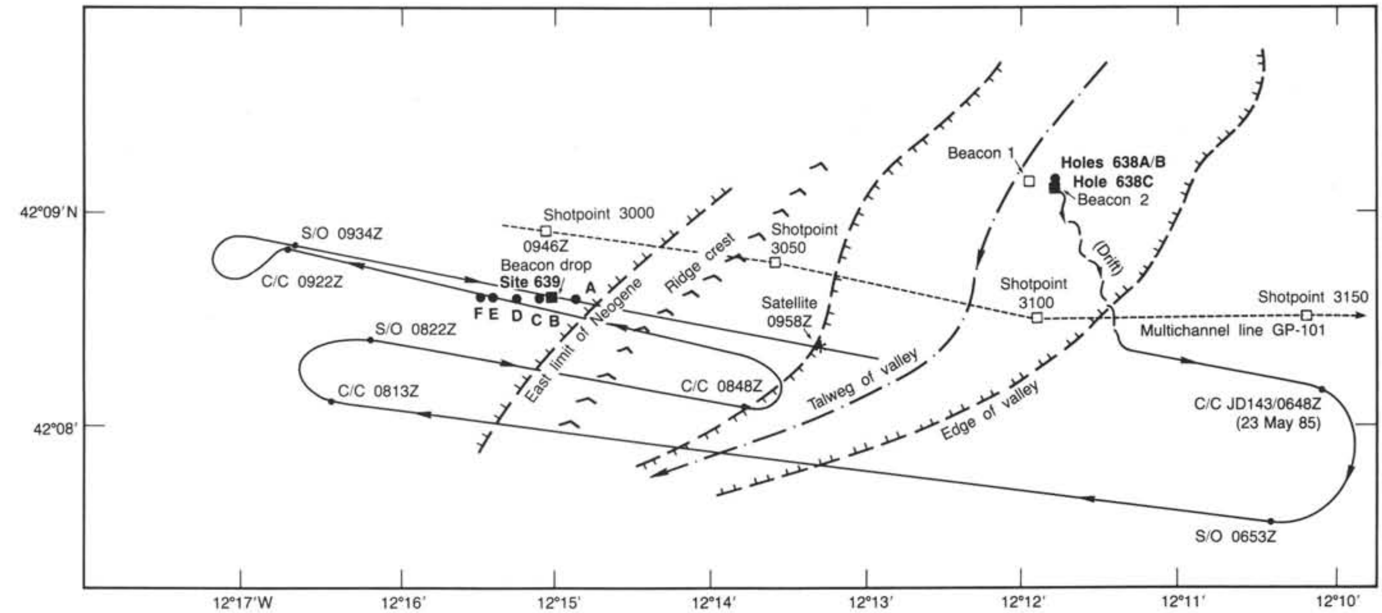

Figure 3. Approach to Site 639 from Site 638. The location of the six holes, 639A through 639F, is shown.

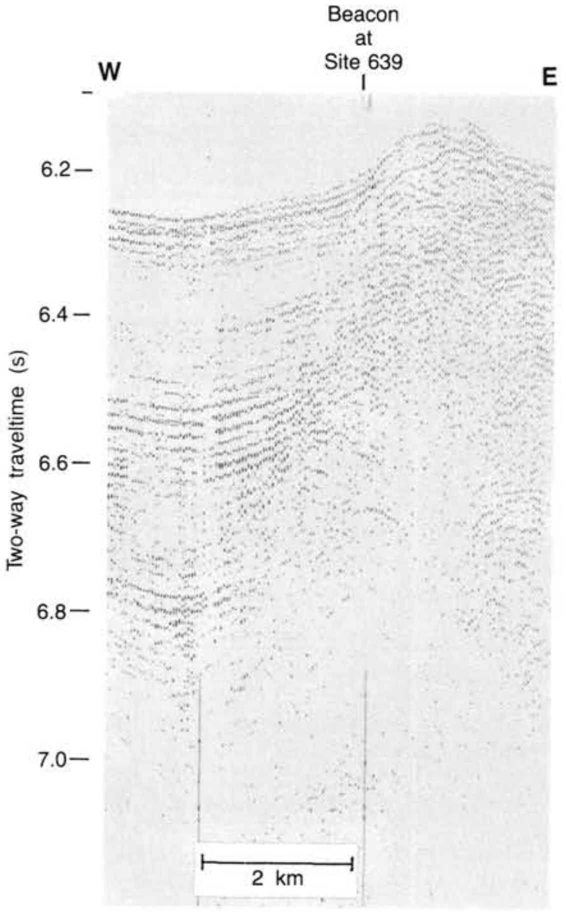

Figure 4. Seismic-reflection profile made from *JOIDES Resolution* during the approach to Site 639, showing position of the acoustic beacon at Hole 639B. Location of trackline shown in Figure 3.

ditions similar to those at shotpoint 3025. The site is close to where Neogene sediments lap out against the hill to the east, and the top of the strong reflector that we supposed to be the top of carbonate platform is near but not at the seafloor. We thus had located a thickness of Neogene sediments sufficient to bury the bottom-hole assembly (BHA) before starting to core hard rocks.

Coring Operations at Site 639

Technical drilling difficulties at this site forced us to drill six shallow holes rather than one deep hole. The six holes constitute a transect 800 m long from east to west, each hole drilling through a thicker sequence of Neogene sediments to reach a level deeper in the Mesozoic carbonate rocks, as shown in the cross section in Figure 1.

Hole 639A

Close study of the 3.5-kHz and seismic profiles persuaded us that we should spud Hole 639A about 100 m east of the beacon to increase our chances of coring the lower part of the sedimentary sequence overlying the strong reflector. Hole 639A spudded at 2000 hr on 23 May, when the driller noted a weight loss at a depth of 4735 m below the derrick floor (4725 mbsl), and a core obtained from 4735 to 4737 m returned Quaternary ooze that had been squeezed up into the core barrel for a distance of nearly 7 m (Table 1).

The next two cores to a depth of 21.5 mbsf returned Neogene ooze, but near the top of the interval spanned by Core 103-639A-4R, from 21.5 to 31.9 mbsf, the coring rate slowed markedly, indicating firmer sediments. The core returned about 10 cm of light-gray ooze, overlying about 50 cm of rusty yellow silt and clay containing weathered chunks of sandstone. Coring went faster again for Cores 103-639A-5R and 103-639A-6R, in yellowish and reddish marl, then slowed again in Cores 103-639A-7R and 103-639A-8R, in somewhat harder marlstone.

At the bottom of Core 103-639A-8R, at a depth of about 70 mbsf, the bit struck something even harder to drill, and a piece of pale-brown dolomite in the core catcher confirmed that we had struck the top of the carbonate platform for which we had been aiming since beginning to drill at Site 638, on 5 May. The following core cut in only about 1 hr, but the driller reported a tendency for the pipe to torque. When the drill string was pulled up off the bottom of the hole just before retrieving this core, the pipe became stuck, and only a strong set of pulls freed it. Core 103-639A-9R contained 16 pieces of dolomite, none longer than about 10 cm. The following core, Core 103-639A-10R, was the last from this hole, not only because the core was difficult to cut owing to the pipe torquing and because the pipe became stuck again but also because the core barrel itself was stuck and could not be retrieved with the overshot device. We, therefore, had to abandon the hole and trip all the drill string back onto the ship to free the core barrel, which contained about 2 m of dolomite broken into small pieces, as in the preceding core.

The drilling problems posed by the dolomite in this hole (torquing during coring, sticking of the pipe, plugging of the bit, and poor recovery rates of small pieces of rock) were to plague us at each of the other holes drilled at this site.

Hole 639B

Before beginning Hole 639B, we moved the ship 100 m west from Hole 639A, lowered the drill string to find the seafloor, and struck firm bottom at a depth of 4715 m below the derrick floor. Given the general westward slope of the bottom, which we knew from our echo-sounding profile, and taking into account the firm substrate, we surmised that a small deviation in the drill string from vertical (even only 2°) had planted the bit on the hillslope a short distance *east* of Hole 639A. We elected to treat this misadventure as an engineering soil test and moved the ship another 100 m to the west to a position directly over the acoustic beacon.

Hole 639B spudded at 1330 hr on 26 May, when the driller said the weight gauge showed a weight loss at a depth of 4758 m below the derrick floor, and the coring bit advanced to take a "mud-line" core from the seafloor to a depth of about 7 mbsf (Core 103-639B-1R). As usual in such soft sediments, the core barrel was full, owing to sediment being squeezed into the barrel from an area larger than the core liner.

The interval from 7.2 to 63.5 mbsf was drilled without taking any cores. At 63.5 m, the bit struck a firm level, and Core 103-639B-2R was taken in the interval 63.5–66.5 mbsf, recovering about 70 cm of brownish dolomite similar to that cored in Hole 639A. The next core, to a depth of 76 mbsf, cut with the familiar difficulties we had already experienced in the dolomite. In the middle of cutting the next core, Core 103-639B-4R, at a depth of 80 mbsf, the pipe began sticking dangerously and the ODP operations manager advised us to abandon the hole. Besides the surface ooze, we had penetrated 16.5 m into the dolomite and recovered slightly less than 3 m of core.

Hole 639C

For Hole 639C, we moved the ship 100 m farther to the west (Figs. 1 and 3), not having to do more than pull the pipe up to a

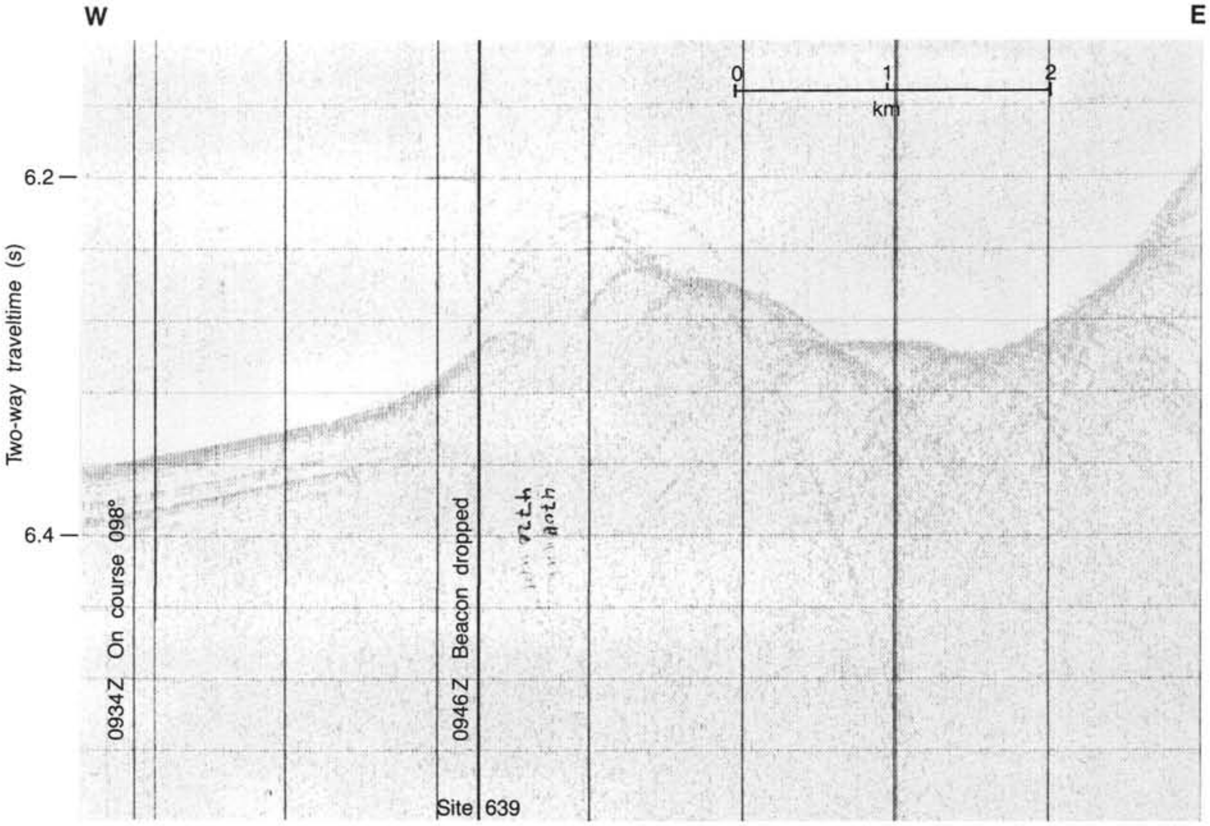

Figure 5. The 3.5-kHz echo-sounding record made from *JOIDES Resolution* during the approach to Site 639, showing the location of the acoustic beacon at Hole 639B. Location of trackline shown in Figure 3.

position safely above the seafloor during the move. At 1230 hr on 27 May, we spudded at a depth of 4792 m below the derrick floor, as estimated by the driller from the point at which his gauge showed a weight loss. Without taking any cores, we drilled ahead until meeting the first indication of firm material, which occurred at a depth of 78 mbsf. Core 103-639C-1R, taken from 78–90.8 mbsf, recovered only Pliocene ooze, so we decided to continue washing ahead, keeping the core barrel in place. At a depth of about 97 mbsf, the drilling became slower and the pipe began sticking again. We pushed ahead to a depth of 100.4 mbsf and recovered the core barrel, which contained about 1.7 m of brown silty clay at the top and about 60 cm of dolomite at the bottom. The sticking of the pipe led the ODP operations manager again to advise us to abandon the hole.

Hole 639D

This time we moved the ship 200 m west of Hole 639C, to a point 500 m west of Hole 639A, again with the pipe suspended slightly above the seafloor. The depth at Hole 639D, as measured by the drill according to weight loss, was 4753 m below the derrick floor; we had, however, expected the seafloor to deepen westward. We surmised that a small valley, too small to show on the echo-soundings (Fig. 5), cuts between Holes 639C and 639D, as shown in Figure 1.

Drilling at Hole 639D was much more successful than at the preceding three holes. Beneath a thickness of about 178 m of soft Neogene sediments, which were washed without coring, we cored about 2 m of brown clay and then about 113 m of dolomite and limestone. At a total depth of 293.1 mbsf, the bit refused to turn; thus, we surmised that it had lost a cone.

We then commenced preparations for logging by first conditioning the hole, next dropping the coring bit, filling the part of the hole we intended to log with mud, and then pulling the BHA up to about 186 mbsf to enable logging of the limestone and dolomite section below that depth. Three successful logging runs were made, but the tools could not descend lower than 264 mbsf because of fill in the hole. Logging was completed and the tools retrieved by 0600 hr on 1 June. Once the bit had cleared the seafloor, we pulled out of the hole under way, the ship steaming slowly on thruster power toward the next site.

Hole 639E

After logging at Hole 638C and then drilling at Site 640, we returned to Site 639 to continue to core a more-or-less complete section to the basement rock. We thus continued our strategy of stepping westward to reach deeper levels (Fig. 1). Hole 639E was located 200 m west of Hole 639D. No cores were taken between the seafloor (tagged at 4770 m below the derrick floor by a decrease on the weight indicator), and the bit was washed ahead to 199 mbsf, where firm rock was met. Intermittent difficulty with torquing and sticking of the pipe vexed us through Core 103-639E-4R, at a depth of 238 mbsf, where the pipe stuck firmly while the driller was running back to bottom to begin the next core. The ODP operations manager advised us that we must abandon the hole. The pipe was pulled back up above the seafloor, and at 1345 hr on 7 June, we were ready to move away from Hole 639E to drill the next hole in the series.

Hole 639F

Hole 639F is located 100 m west of Hole 639E, which is 800 m west of Hole 639A. The same tactics were used as at Hole 639E: we washed through the Neogene until striking a hard layer. The seafloor was felt, by weight loss, at 4771 m below the derrick floor, and the first hard rock was met at 238 mbsf. Core

Table 1. Coring summary, Site 639.

Core no.	Date (mo./day) 1985	Time (hr)	Sub-bottom top (m)	Sub-bottom bottom (m)	Length cored (m)	Length recovered[a] (m)	Percentage recovered
Hole 639A							
1R	05/23	2145	0.0	2.3	2.3	6.8	296.0
2R	05/23	2345	2.3	12.0	9.7	7.0	71.0
3R	05/24	0200	12.0	21.5	9.5	5.7	59.0
4R	05/24	0445	21.5	31.9	10.4	0.5	5.0
5R	05/24	0715	31.9	41.6	9.7	2.7	27.0
6R	05/24	0930	41.6	51.2	9.6	3.2	33.0
7R	05/24	1240	51.2	60.8	9.6	4.2	44.0
8R	05/24	1615	60.8	70.4	9.6	2.5	26.0
9R	05/24	2125	70.4	80.1	9.7	1.0	10.0
10R	05/24	2245	80.1	89.8	9.7	2.1	21.0
Hole 639B							
1R	05/26	1505	0.0	7.2	7.2	9.7	135.0
2R	05/26	2115	63.5	66.5	3.0	0.7	24.0
3R	05/27	0030	66.5	76.0	9.5	1.1	11.0
4R	05/27	0715	76.0	80.0	4.0	0.8	18.0
Hole 639C							
1R	05/27	1809	78.0	90.8	12.8	2.5	19.0
2R	05/27	2045	90.8	100.4	9.6	2.4	24.0
Hole 639D							
1W	05/28	0700	177.6	179.6	2.0	0.8	39.0
2R	05/28	0945	179.6	187.3	7.7	0.2	2.0
3R	05/28	1230	187.3	196.8	9.5	0.9	9.0
4R	05/28	1830	196.8	206.5	9.7	0.3	3.0
5R	05/28	2330	206.5	216.0	9.5	3.0	31.0
6R	05/29	0340	216.0	225.6	9.6	3.0	31.0
7R	05/29	0745	225.6	235.2	9.6	2.2	22.0
8R	05/29	1100	235.2	244.9	9.7	1.7	17.0
9R	05/29	1515	244.9	254.5	9.6	0.4	4.0
10R	05/29	2015	254.5	264.1	9.6	1.8	18.0
11R	05/30	0045	264.1	273.8	9.7	2.4	24.0
12R	05/30	0730	273.8	283.4	9.6	3.3	34.0
13R	05/30	1415	283.4	293.1	9.7	3.1	32.0
Hole 639E							
1R	06/06	2000	199.4	209.1	9.7	0.6	6.0
2R	06/07	0000	209.1	218.6	9.5	0.4	3.0
3R	06/07	0445	218.6	228.2	9.6	0.2	2.0
4R	06/07	1000	228.2	237.9	9.7	TR	<1.0
Hole 639F							
1R	06/07	2230	237.8	247.3	9.5	0.4	4.0
2R	06/08	1020	247.3	250.8	3.5	0.2	6.0

[a] TR = trace recovery.

103-639F-1R cut more-or-less normally, with the usual moderate torquing and sticking, but on Core 103-639F-2R, these problems became so severe that the ODP operations manager again had to order abandonment of the hole. Having recovered some igneous rocks in Core 103-639F-2R, we decided that the essential objectives of drilling at Site 639 had been accomplished, and we elected to abandon the site. To save time, the pipe with the core barrel still inside, was pulled out of the hole. At 0215 hr on 8 June, we began moving to the next site while steaming slowly with thruster power and pulling pipe.

SEDIMENT LITHOLOGY

The description of sediment lithology at Site 639 is a composite description of material recovered in Holes 639A through 639F (Fig. 6 and Table 2). Lithologic Unit I consists of Cenozoic clayey nannofossil ooze, nannofossil marl, and calcareous clay recovered from Holes 639A through 639D. The thickest recovered interval is 21.6 m in Hole 639A, but if the entire section above Core 103-639D-1W is part of lithologic Unit I, the maximum thickness is 185.0 m. Lithologic Unit I unconformably overlies 1.9 m of brown clay of lithologic Unit II, recovered only in Hole 639C. The age of lithologic Unit II can be bracketed only as older than early middle Pliocene and younger than Valanginian. Lithologic Units II and III were not recovered from the same holes, and lithologic Unit II is inferred to have an irregular and patchy distribution above an unconformable surface. Lithologic Unit III consists of 48.7 m of Lower Cretaceous pale-yellow marl/marlstone recovered only in Hole 639A. Dips of as much as 46° are measured in lithologic Unit III. Lithologic Unit IV, consisting of dolomite recovered from Holes 639A through 639D, has a maximum cored thickness of 19.6 m in Hole 639A; no age-diagnostic fossils were found within it. Dips of as much as 30° are commonly measured in lithologic Unit IV. Neither the upper nor lower contacts of lithologic Unit IV were recovered. Lithologic Unit V consists of 94.1 m of Upper Jurassic limestone, marlstone, and sandstone recovered from

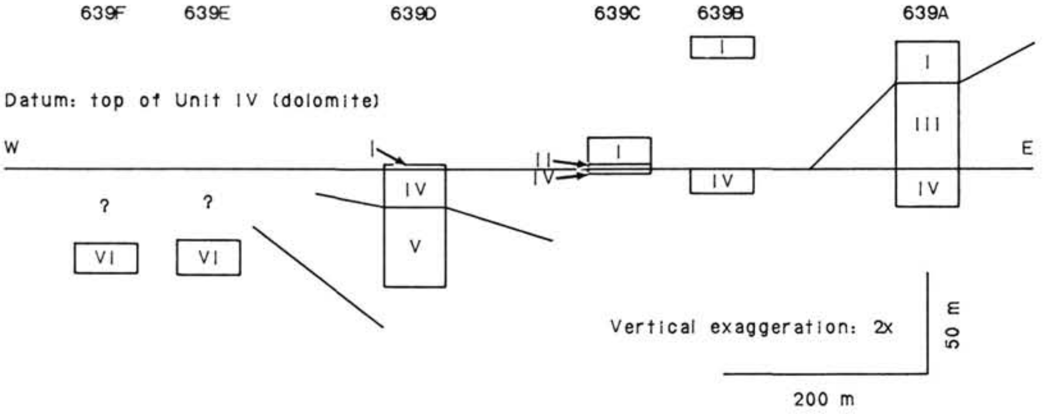

Figure 6. Correlation of Site 639 lithologic Units I through VI. See Table 2 for definition of these units; more detailed discussion of units is given in the text.

Table 2. Lithologic units recovered at Site 639.

Lithologic units	Lithology	Cores	Sub-bottom depth (m)
I	Clayey nannofossil ooze, nannofossil marl, and calcareous clay	103-639A-1R-1, 0 cm, to 103-639A-4R-1, 10 cm	0–21.6
		103-639B-1R-1, 0 cm, to 103-639B-1R, CC, 0 cm	0–63.5
		103-639C-1R-1, 0 cm, to 103-639C-1R-2, 59 cm	0–95.0
		103-639D-1R-1, 0 cm, to 103-639D-1R, CC, 10 cm	0–185.0
II	Brown clay	103-639C-2R-1, 0 cm, to 103-639C-2R-2, 41 cm	95.0–[a]96.8
III	Mottled pale-yellow marl/marlstone	103-639A-4R-1, 10 cm, to 103-639A-8R, CC, 7 cm	21.6–70.3
IV	Dolomite	103-639A-8R, CC, 7 cm, to 103-639A-10R-2, 125 cm	70.3–89.8
		103-639B-2R-1, 0 cm, to 103-639B-4R, CC, 20 cm	[b]63.5–80.0
		103-639C-2R, 41 cm, to 103-639C-2R-2, 102 cm	96.8–100.4
		103-639D-2R, CC, 0 cm, to 103-639D-4R-1, 9 cm	[c]185.0–199.0
V	Clayey limestone, limestone, marlstone, sandstone	103-639D-4R-1, 9 cm, to 103-639D-13R, CC, 36 cm	199.0–293.1
VI	Problematic interval	103-639E-1R-1, 0 cm, to 103-639E-4R, CC, 5 cm	199.4–237.9
		103-639F-1R-1, 0 cm, to 103-639F-2R, CC, 27 cm	237.8–250.8

∼∼∼∼ Unconformity.
– – – – Unit boundary (contact not recovered).
[a] First hard layer encountered.
[b] Last 3 m of core drilled with difficulty.
[c] Based on logging results.

Hole 639D. Pieces of widely differing sediment types, including igneous and metamorphic rocks that may be from the basement, were recovered in Holes 639E and 639F. In the two holes, a total of 51.5 m of these rocks were cored and 1.6 m were recovered. They are grouped into lithologic Unit VI, termed a "problematic interval," because of the uncertain stratigraphic significance of these pieces.

Lithologic Unit I: Clayey Nannofossil Ooze, Nannofossil Marl, and Calcareous Clay

Unit I is 185.0 m thick and consists of vaguely rhythmic gradational alternations (on the scale of from 10 cm to 2.5 m) of gray, light brownish gray, light-olive gray, and olive-gray nannofossil marl and white, light-gray, gray, and very pale-brown clayey nannofossil ooze. In addition, a light brownish gray calcareous clay occurs in the uppermost 65 cm of Section 103-639A-1R-1, and 30 cm of olive-gray clay occurs at the top of Section 103-639A-2R-1. The sediments are soft and generally highly disturbed by drilling, although firmness increases and drilling disturbance decreases in Core 103-639A-3R. Except for some faint parallel lamination in the interval from Samples 103-639A-1R-1, 125 cm, to 103-639A-1R-2, 35 cm, and rare trace fossils, primary sedimentary structures are not observed. However, the entire sequence may be thoroughly bioturbated. Bands, blebs, and specks of purplish stain, which occur throughout lithologic Unit I, are attributed to the presence of an iron-manganese oxide.

Compositionally, in addition to abundant nannofossils and clay, the marl and clayey ooze contain as much as 10% quartz silt, 2% mica, and trace amounts of zircon, glauconite, zeolite minerals, and various opaque minerals including pyrite. Foraminifers are ubiquitous in amounts of as great as 7% and an exceptional 35% in Sample 103-639A-3R-3, 86–97 cm.

The base of Unit I, recovered only in Hole 639A (Sample 103-639A-4R-1, 10 cm) is sharp, placing white nannofossil ooze depositionally above strongly limonite-stained Lower Cretaceous(?) sandy silt and silty clay. In every hole, the lower contact is undoubtedly unconformable.

The Cenozoic sediments at Hole 639A are typical of pelagic carbonates deposited above the carbonate compensation depth (CCD). The clay-rich intervals in Samples 103-639A-1R-1, 0–65 cm, and 103-639A-2R-1, 0–30 cm, and the faintly rhythmic variation in clay content may be related to the increased influx of clay during Pliocene–Pleistocene glacial episodes, perhaps in distal turbid flows or in nepheloid layers.

Lithologic Unit II: Brown Clay

Lithologic Unit II, recovered only in Hole 639C, is 1.91 m thick and consists of interlayered dark-brown to light reddish brown (5YR4/2, 5YR6/4) clay, commonly variegated in pink and yellow shades. Pale-olive (5Y6/4) clayey silt with limonite-stained sandy patches is also present. In Hole 639C, the clay, overlain by Pliocene clayey nannofossil ooze (lithologic Unit I), overlies dolomite (lithologic Unit IV). Neither contact was actually recovered. The clay is highly recrystallized and barren of fossils.

Because the clay was recovered from only one hole, it is inferred to have an irregular and patchy distribution above an unconformable surface. The clay is similar to the clay that overlies ultramafic basement rock at Hole 637A (lithologic Unit III, Samples 103-637A-20R-1, 0 cm, to 103-637A-23R-2, 135 cm; see Site 637 chapter, this volume), the slumped clay in Hole 638B (in lithologic Unit I, Sample 103-638B-18R-1, 15–70 cm; see Site 638 chapter, this volume), and the brown clay in Hole 640A (lithologic Unit I, Samples 103-640A-1R-1, 0 cm, to 640A-2R-2, 47 cm; see Site 640 chapter, this volume). This unit probably has regional extent.

Lithologic Unit III: Mottled Pale-Yellow Marl/Marlstone

Unit III is 48.7 m thick and consists of relatively structureless and homogeneous pale-yellow to light-gray nannofossil marl/marlstone; the marl is mottled light reddish brown, light brown, and pinkish gray in Cores 103-639A-6R and 103-639A-7R. The carbonate content, as determined by shipboard carbonate-bomb analysis (see "Inorganic Chemistry" section, this chapter), ranges from 42% to 68%. Silt-sized quartz and feldspar, mica, hematite, glauconite, foraminifers, and mollusks are present as trace to accessory constituents. Apparent dips of as much as 46° (Section 103-639A-7R-1) are measured.

The top of Unit III, in Core 103-639A-4R, is marked by limonite-stained sandstone occurring as pebble-sized clasts in a limonite-stained sandy silt and silty clay. This highly oxidized pebbly zone immediately beneath the unconformity separating Unit III from the overlying Cenozoic Unit I may be a residual weathering zone, which includes debris shed from upslope, a slope that may be fault controlled. Core 103-639A-4R is included in Unit III because of its oxidized character. A strong possibility exists, however, that the sediment of Core 103-639A-4R beneath the marl and ooze of Cenozoic Unit I is some sort of talus or residual weathering horizon significantly younger than the rest of Unit III. An alternative possibility is that this interval is somehow related to lithologic Unit II.

Limonite-stained fine-grained sandstone is present as clasts, stringers, and pieces in the interval from Samples 103-639A-4R-1, 10 cm, to 103-639A-6R-1, 36 cm (Fig. 7). The sandstone intervals in Cores 103-639A-5R and 103-639A-6R are from 5 mm to 10 cm thick and disturbed by drilling. Whether the sandstone occurs as displaced clasts or as true interbeds is unclear. Since the sandstone is commonly associated with light-olive gray, bioturbated, quartz-silt-bearing calcareous clay and since this same calcareous clay occurs in burrows in the marl, the sandstones are most likely true interbeds. Sedimentary structures are generally not observed in the sandstone, but the style of lamination and the water-escape structures in Sample 103-639A-6R-1, 10–15 cm, suggest that the sandstone is part of a turbidite. Sample 103-639A-6R-1, 36 cm, is the lowermost occurrence of sandstone at Hole 639A. The sandstone is subarkosic and carbonate cemented. Except for the high degree of oxidation, it has a composition similar to the Valanginian sandstone recovered at Site 638 (see Site 638 chapter, this volume). The oxidation is probably associated with the unconformity.

Recovery is poor in Core 103-639A-4R, and drilling disturbance is high. A peculiar feature, however, is the presence of gray clay in the interval from Samples 103-639A-4R-1, 24 cm, to 103-639A-4R, CC, 10 cm, and of a single, gray calcite-cemented pebble of sandstone that is indistinguishable from Valanginian sandstone recovered at Site 638. The gray, unoxidized clay is in stark contrast to the highly oxidized intervals above and below. The gray material may have been slumped, or possibly it is contamination from the previous site, perhaps stuck in the drill string and dislodged only at this stage of the drilling.

Changes in the degree of lithification are noticable downhole in Unit III. Cores 103-639A-5R and 103-639A-6R are stiff marls, easily indented by a fingernail. In Core 103-639A-8R, lithification has advanced to the extent that the marl may be termed "marlstone." The transition to marlstone occurs in Core 103-639A-7R, which contains dominantly marlstone in gradational contact with 10–20-cm-thick intervals of soft marl. The increase in degree of lithification correlates with a change in the percentage of micrite and disaggregated calcite and dolomite rhombs, from <10% in the marl to as much as 42% in the marlstone, as determined by smear slide observation (see core-description forms, this chapter).

Primary sedimentary structures are rare. The only intervals in which bedding is recognized are in Section 103-639A-8R-1 and Sample 103-639A-6R-2, 60–90 cm, with apparent dips of 30° and 45°, respectively. Features recognizable as trace fossils are rare. In Sample 103-639A-7R-2, 48–52 cm, a large (1 cm across) burrow is ringed with pyrite. Fractures exist, and where mottling of pale-yellow and light reddish brown is well developed, such as in Sample 103-639A-6R-2, 61–80 cm, the pale-yellow coloration occurs in a zone as much as 1-cm wide, bordering the fractures. Associated with the fractures are also (1) yellowish brown sparry calcite filling the fractures, (2) limonite staining, and (3) 1-mm spots of iron/manganese precipitate (Fig. 8). Away from the fractures, radial dendritic patterns as much as 6 mm across of iron/manganese precipitates and limonite micronodules (Sample 103-639A-7R-2, 11 cm) also occur. Unit III is clearly oxidized.

The abundant nannofossils indicate sedimentation above the CCD. The occurrence in Cores 103-639A-5R and 103-639A-6R of sandstone suggests that low-density turbid flows may have been introducing terrigenous clay throughout the predominately pelagic deposition of Unit III.

The contact between Units III and IV was not recovered but is placed at Sample 103-639A-8, CC, 7 cm, between marlstone above and dolomite below.

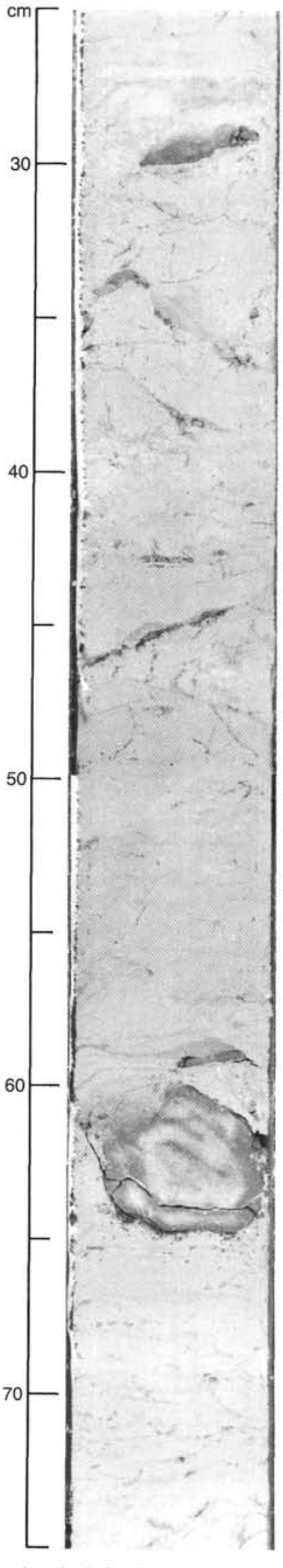

Figure 7. Sandstone interbeds in the marlstone of lithologic Unit III (Sample 103-639A-5R-2, 25–75 cm).

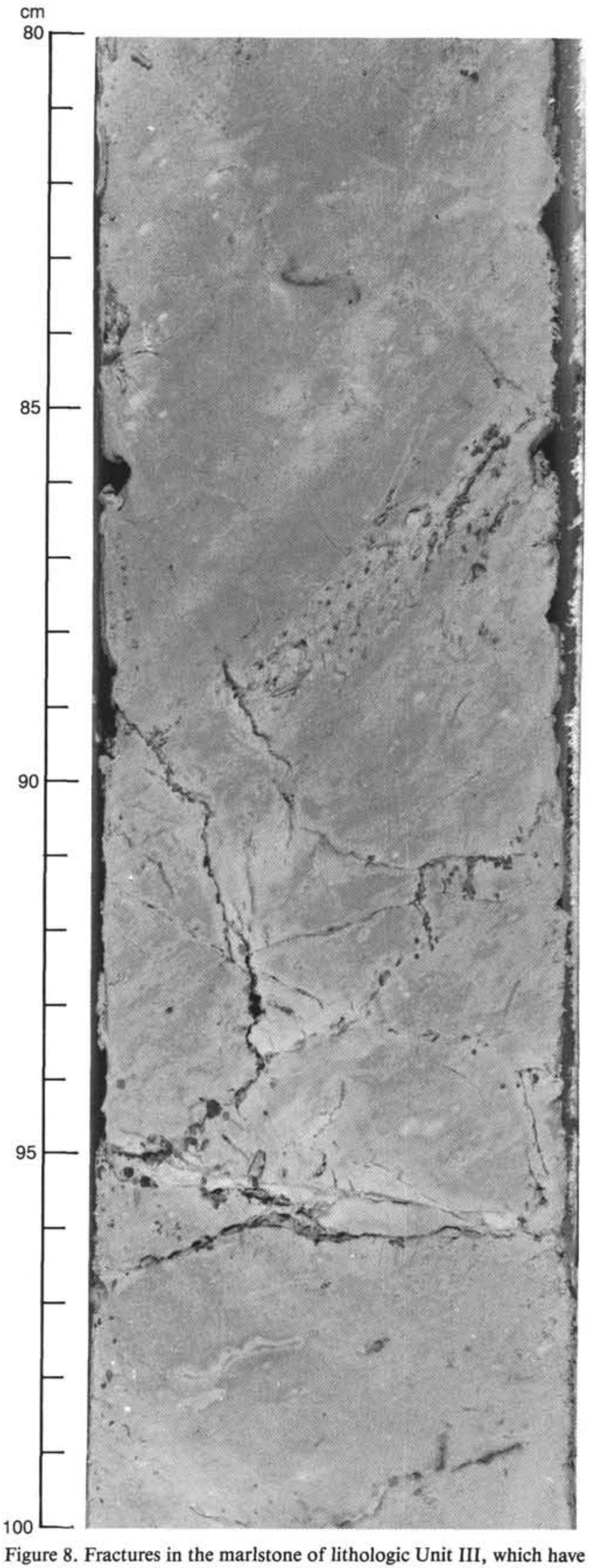

Figure 8. Fractures in the marlstone of lithologic Unit III, which have a border of bleached pale-yellow marlstone, calcite cementation, and spots of iron/manganese oxide precipitate (Sample 103-639A-6R-2, 80–100 cm).

Lithologic Unit IV: Dolomite

Dolomite attributed to lithologic Unit IV occurs in Holes 639A through 639D (Table 2); similar dolomite also occurs in Core 103-639E-2R, but is assigned to lithologic Unit VI (see following text). The minimum thickness of dolomite is 19.5 m, based on the longest coring interval in a single hole (Samples 103-639D-2R, CC, 0 cm, to 103-639D-4R-1, 9 cm). A maximum thickness of 275 m can be calculated by construction of a cross section from drilling results at Holes 639A and 639D, assuming an 8° dip to the east and no faults between the holes. The dolomite was difficult to drill, causing high torque; generally only irregular pieces less than 10 cm long were recovered. The longest continuous piece was 36 cm (Sample 103-639B-2R-1, 10-46 cm). The pieces commonly are shaped in a way that is difficult to attribute entirely to drilling artifacts. This and the presence of a yellowish dolomicrite coating on many of the pieces suggest that the rock is rubbly and fractured in place. No allochthonous material indicating sedimentary mass transport was recovered.

The contact of the dolomite with the overlying lithologic Unit III was not recovered. Although several percent of dolomite rhombs are reported from smear slides in lithologic Unit III, shipboard x-ray diffraction analysis found no dolomite in detectable amounts. This may suggest a sharp break between lithologic Unit IV dolomite and essentially undolomitized overlying beds. The contact between the dolomite and the underlying Unit V was not recovered. That the uppermost clayey limestone of Unit V appears to be slightly dolomitized suggests a downward gradational dolomitic front.

In all holes drilled at Site 639, the dolomite is similar and consists of a fine- to coarse-grained (15–800 microns; average 300 microns) mosaic of subhedral dolomite crystals. Vuggy and intercrystalline porosity is present (Fig. 9). The vugs are as much as 1 cm across and are lined with drusy dolomite. Porosity ranges from 2% to 9% (see "Physical Properties" section, this chapter). Thin-section observations show that, within irregularly shaped areas, dolomite-crystal size is generally uniform and different from that in adjacent areas. Likewise, within irregularly shaped areas, the clarity of the dolomite may be different from that in adjacent areas. Single crystals commonly have a zoned, rhombohedral-shaped core of impurities. In Sample 103-639D-3R-1, 88–91 cm, eight zonations were counted. Only locally can the original sedimentary structures and the nature of the allochems be recognized from the patterns of impurities.

The dolomite is divided into two broad types, according to texture and composition of the original rock: (1) light brownish gray grainstone to packstone, and (2) dark grayish brown skeletal wackestone. The grainstone-to-packstone type (Fig. 9) has round ghosts, about 0.5 mm in diameter, of echinoderm debris with syntaxial overgrowths, foraminifers, sponges, red algae, corals, bivalves, and gastropods. The dark grayish brown skeletal wackestone type is commonly marbled and shows a complex system of cavities, vugs, and fractures filled with various cements and internal sediments (Fig. 10). Allochems recognized in these wackestones include echinoderm debris, high-spired gastropods and other mollusks, oncoids, intraclasts, and unidentifiable plate-like structures, which on a slabbed surface are 1 mm by 2–30 mm and filled with clear sparry dolomite (Fig. 11). These structures bear some similarities to phylloid algae, but no internal structure remains that allows an identification. Large intraclasts as much as 6 cm in length are present in the wackestone lithology. In Sample 103-639B-2R-1, 65–67 cm, an intraclast has a spar-filled fracture that predates its transport as an intraclast (Fig. 11). Filled vugs and cavities are also common. Sample 103-639A-10R-2, 16–21 cm, illustrates the complexity of void filling (Fig. 12). In this example, baroque (curved-faced) dolomite represents a cavity filling and partly replaces internal sediment. Two types of laminated, geopetal internal sediments are present: (1) dark grayish brown (2.5Y 4/2), fine-grained, crystalline dolomite, which was originally micrite, and (2) pale-yellow (2.5Y 7.5/4) dolomicrite to dolomicrosparite, which contains laminations of silt- and sand-sized dolomite rhombs. Many of these voids and cavities may be related to the open framework of a bioherm. Some elongate structures, filled with dolomite, bear certain similarities to stromatactis (e.g., Samples 103-639A-10R-2, 117–129 cm, and 103-639B-2R-1, 52–56 cm).

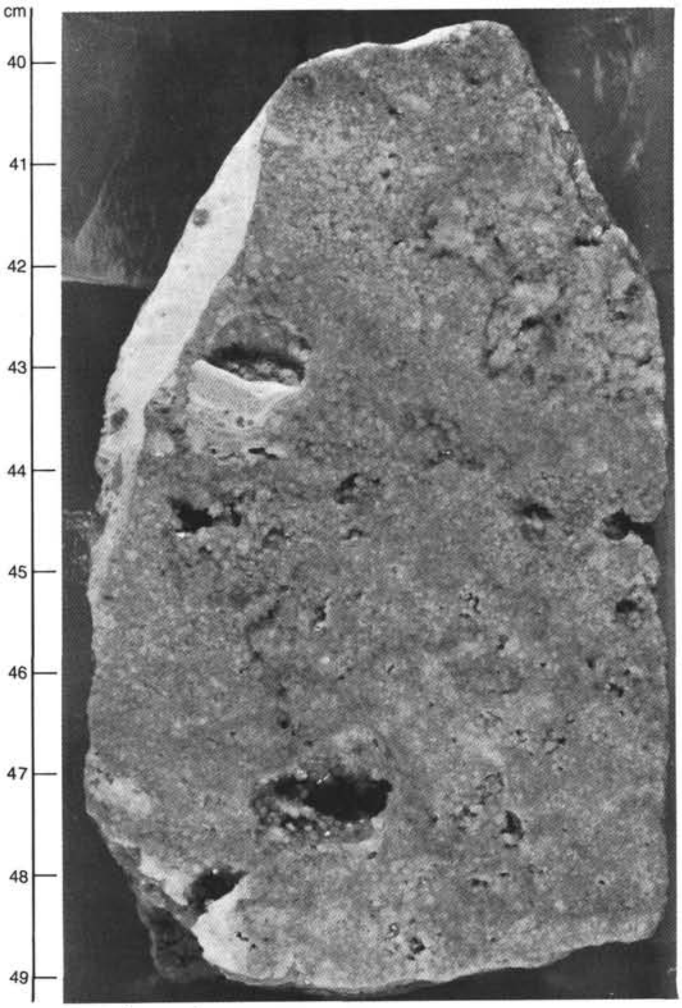

Figure 9. Vuggy and intercrystalline porosity in light brownish gray dolomitic grainstone to packstone (Sample 103-639A-10R-1, 40–49 cm).

Several sets of fractures were observed in the dolomite. Most obvious under the microscope are those filled by clear, white dolomite. The boundary between clear and impure dolomite commonly crosses a single crystal (Sample 103-639A-10R-1, 15–18 cm). These filled fractures range in width from 1 to 10 mm and in length from 1 to more than 4 cm. Development and cementation of fractures in these samples seem to predate one phase of dolomitization.

A second variety of fractures is filled with yellow (2.5Y 8/6) dolomicrite-to-dolomicrosparite internal sediment (Fig. 13). Locally the sediment is laminated with silt- and sand-sized dolomite crystals. In places, the internal sediment is recrystallized, and some dolomite rhombs have tiny overgrowths (Sample 103-639A-10R-1, 147–149 cm). Laminations are complex, varying from planar, either parallel or perpendicular to the fracture wall, to curved (Sample 103-639A-10R-1, 15–18 cm). In places, the

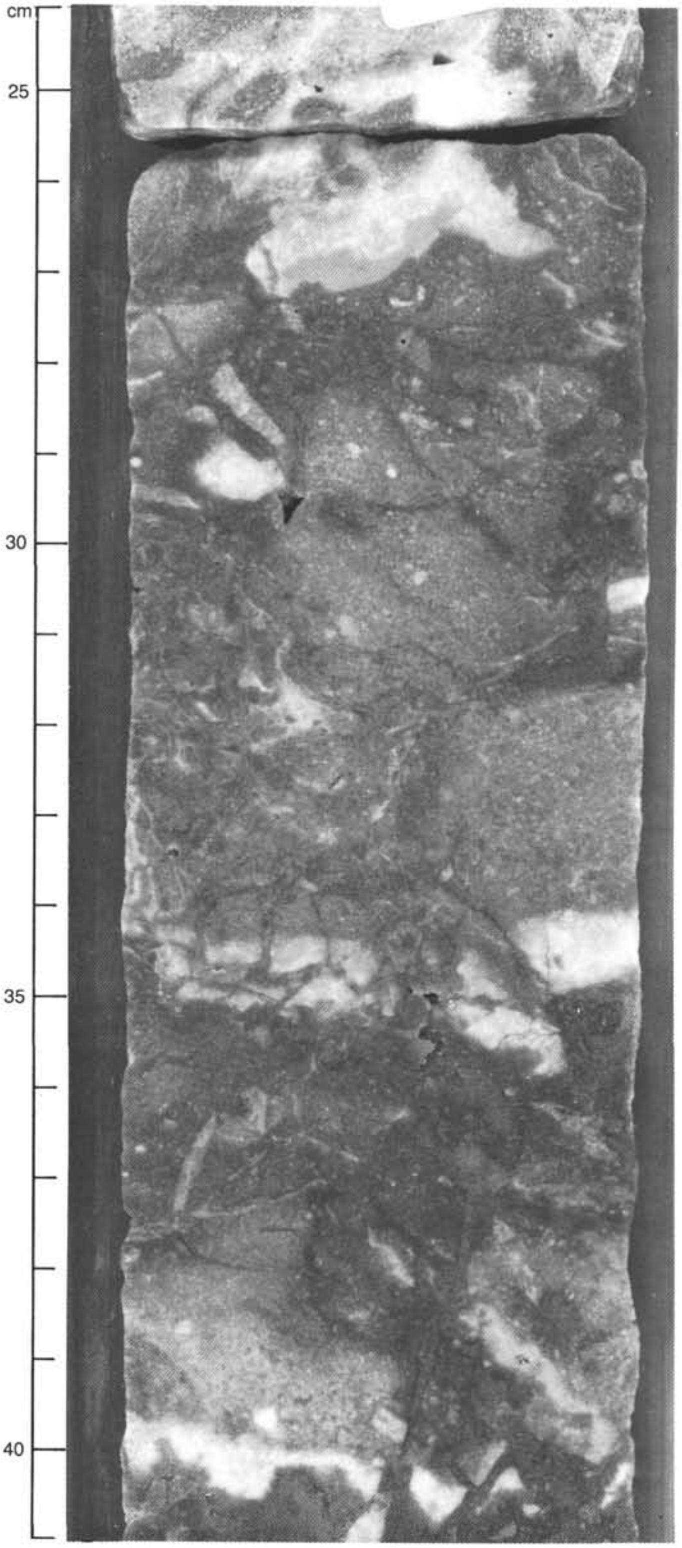

Figure 10. Marbled aspect of dark grayish brown dolomitic wackestone (Sample 103-639B-2R-1, 24–41 cm).

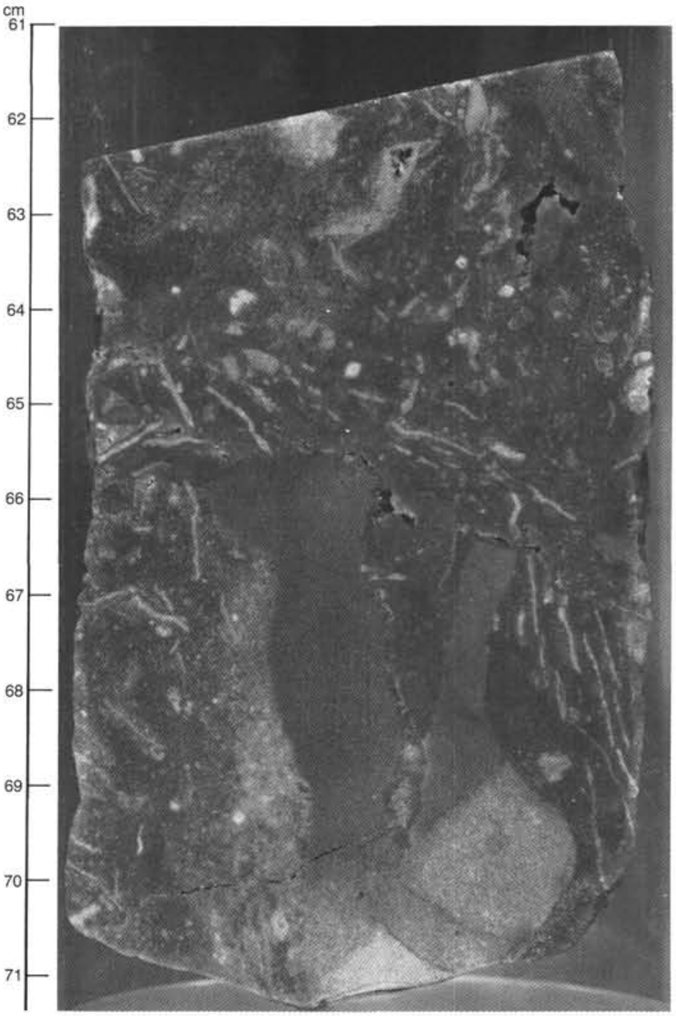

Figure 11. Dark grayish brown dolomitic wackestone showing unidentified plate- to tube-like spar-filled structures and large intraclasts (Sample 103-639B-2R-1, 61–71 cm).

fractures are filled with material clearly derived from the adjacent wall of the fracture. The fractures are as much as 1 cm wide, and some are at least 7 cm long. The fractures cut all structural elements of the dolomite and, thus, are one of the last events in the rock history. However, whether the brecciation and sediment infilling postdates the latest stage of dolomitization is unclear. This final stage of fracturing and fracture filling may mean that the rocks were exposed to weathering before being buried by the Valanginian marlstone.

The depositional environment of Unit IV was probably a shallow-marine, normal-salinity, carbonate platform, perhaps having local development of bioherms. This conclusion is highly tentative, however, and a deeper water, resedimented deposit, such as talus, cannot be entirely dismissed.

The diagenetic history of these rocks is extremely complex, and the sequence of events cannot yet be clearly discerned. Shipboard sedimentologists propose several possible scenarios, which are described as follows:

1. Deposition of limestone on a shallow-water platform, perhaps with local biohermal development. Primary voids and cavities are filled with penecontemporaneous calcite cement and internal sediment. Dissolution may have enhanced initial porosity.
2. Brittle fracturing. Fractures are cemented by sparry calcite and/or dolomite.
3. Pervasive dolomitization. Voids may have been formed during this process.

All shipboard sedimentologists accept these three stages, but further details of the dolomitization process are more controversial. This subject will be discussed in a separate chapter in the

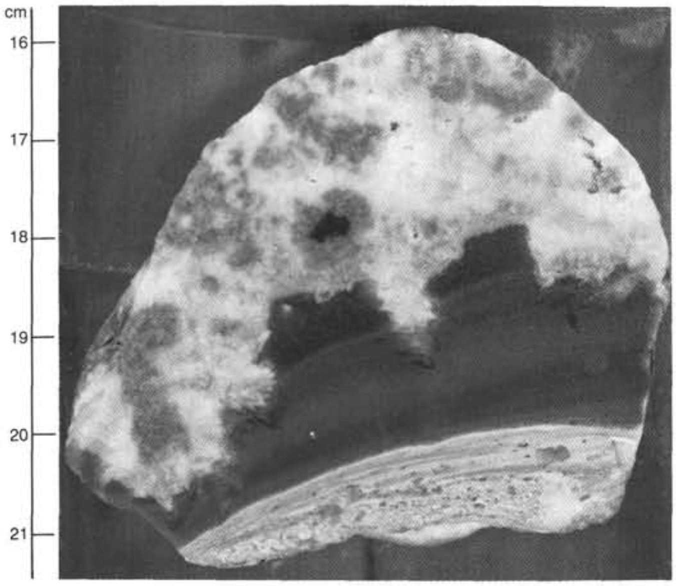

Figure 12. Complex fill of a large cavity in dolomite (Sample 103-639A-10R-2, 16–21 cm).

Leg 103 Part B volume. Clearly, the dolomite has a complicated history of brecciation and recrystallization.

Lithologic Unit V: Clayey Limestone, Limestone, Marlstone, and Sandstone

Lithologic Unit V consists of 94.1 m of light-gray to light brownish gray limestone. Limestone attributed to lithologic Unit V was recovered only in Hole 639D; similar limestone also occurs in Core 103-639E-1R but is assigned to lithologic Unit VI (see following text). The contact of lithologic Unit V with lithologic Unit IV was not recovered, and the boundary between the two units is placed beneath a piece of dolomite in Sample 103-639D-4R-1, 9 cm. The limestone and clayey limestone are dominantly skeletal-peloidal packstone to wackestone. Bedding is rare, but, where observed, dips range to as much as 30°. Bioturbation may have obscured the bedding. The contact between different textures is generally gradational over 1-3 cm. Carbonate-bomb analyses (see "Inorganic Geochemistry" section, this chapter) indicate a general decrease in clay content downhole so that the packstone and wackestone in Cores 103-639D-4R to 103-639D-10R have more than 10% clay and are termed "clayey limestone," whereas in Cores 103-639D-11R to 103-639D-13R they have less than 10% clay and are termed "limestone."

Lithologic Unit V may be loosely subdivided into three parts (upper clayey limestone, middle clayey limestone and sandstone, lower oncolitic limestone), which correspond well to subdivisions based on logging results (see "Logging Results" section, this chapter).

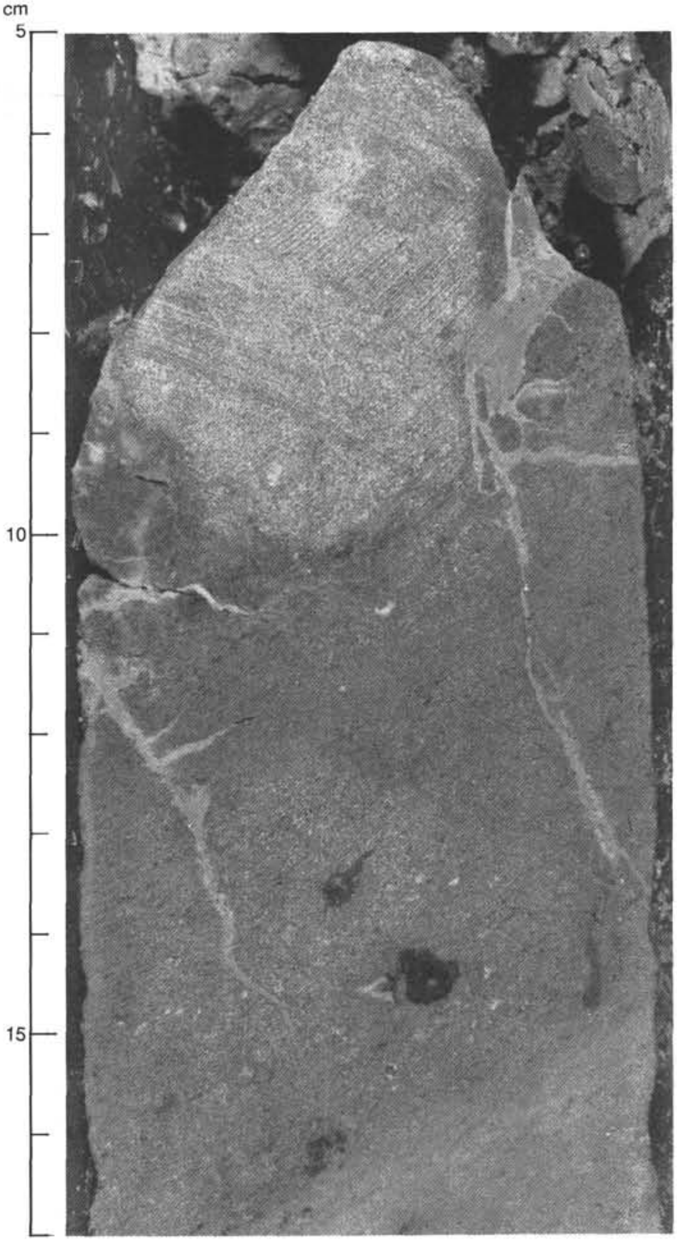

Figure 13. Late-stage fractures in dolomite, which are filled with yellowish dolomicrite to dolomicrosparite internal sediment (Sample 103-639A-8R, CC, 5–17 cm).

Upper Clayey Limestone (Cores 103-639D-4R and 103-639D-5R)

The upper part of lithologic Unit V is characterized by the abundance of a diverse, biohermal fauna. The clayey limestone is dominantly skeletal-peloidal packstone to wackestone with interbeds of marlstone, calcareous silt, and silty clay in Core 103-639D-5R. Locally, the skeletal debris is large enough to term the rock floatstone. Allochems identified include solitary corals, siliceous sponges, calcisponges, unidentified hydrozoans, mollusk fragments, serpulid worm tubes, echinoderm debris, pelecypods, ostracodes, algal debris, and large benthic foraminifers. Large skeletal debris is commonly bored, and a coral in growth position is preserved in Sample 103-639D-5R-2, 16–30 cm. Quartz silt and dolomite rhombs are present in trace amounts. Some of the bioclasts are partly silicified.

Middle Clayey Limestone and Sandstone (Cores 103-639D-6R through 103-639D-8R)

The middle part of lithologic Unit V is characterized by the influx of terrigenous clastic detritus and by the lack of corals. The interval consists of light-gray, light yellowish brown to light reddish brown clayey limestone with interbeds (about 15 cm thick) of light yellowish brown silty marlstone and silty calcareous clay. Coarse-grained sandstone, pale-olive siltstone, and olive clay are present in Core 103-639D-8R. The contacts between the various sediment and rock types were generally not recovered, but where observed, they are gradational over 1-5 cm.

Logging data (see "Logging Results" section, this chapter) indicate that many sandstone and siltstone beds are present in this interval that were not recovered in the cores.

The clayey limestone includes skeletal wackestone to fossiliferous mudstone containing large benthic foraminifers, mollusks, ostracodes, pelecypods, echinoderm debris, and rare oncoids. The marlstone and calcareous clay is characterized by 5-20-mm-thick laminations of large benthic foraminifers having normal grading of their abundance over a 5-15-cm interval. This is one of the few clear examples of current activity in lithologic Unit V. The sandstone beds are massive, poorly sorted, and as much as 15 cm thick. They are quartz-rich and contain a component of rounded carbonate bioclasts. Locally, quartz grains are coated by micrite.

Lower Oncolitic Limestone (Cores 103-639D-9R through 103-639D-13R)

The lower part of lithologic Unit V is dominantly light-gray skeletal-peloidal packstone to wackestone with abundant stylolites. Oncoids (as much as 10%) that average 2 mm in diameter (Fig. 14) and appear to float in a finer grained peloidal matrix are characteristic. Although not abundant, grainstone and fossiliferous mudstone are also present. The oncoids have nuclei of skeletal debris, micrite, or microsparite, and the coatings vary from thick to superficial. Fossils include mollusks, ostracodes, and large benthic foraminifers. In general, the fauna are less diverse and less abundant than in the overlying intervals.

Diagenesis

The limestone and clayey limestone of lithologic Unit V have undergone minor recrystallization, replacing micrite with microspar and high-magnesium calcite and aragonite with coarse sparry calcite. Low-magnesium calcite skeletal debris has not been replaced. Skeletal debris is commonly extensively micritized. Dolomite is present in the upper part. Silica replaces some shells and hydrozoans, and a silica nodule, greater than 4 cm across, is present in Sample 103-639D-5R-2, 136–145 cm. Limonite-stained, clayey(?) stylolitic bands as much as 2 cm thick are common. In them, benthic foraminifers as well as insoluble residues and dolomite rhombs are concentrated. Vertical, sparry-calcite-filled veins (1 × 50 mm) are also present. The overall degree of recrystallization and brecciation is strikingly less than in the overlying dolomite of lithologic Unit IV.

Sedimentary Environment

The abundance of skeletal debris and especially of a biohermal fauna suggests a normal-salinity, shallow-water carbonate platform for the depositional environment of the upper part of the limestone. The presence of quartz silt and clay testifies to a persistent terrigenous influence. The occurrence of calpionellids and nannofossils suggests to the shipboard paleontologists that these rocks may have been resedimented into slightly deeper water. Some sedimentological evidence for minor transport exists, but no direct evidence indicates that the sediment was transported into deeper water.

The influx of clastic detritus (some of which is very coarse) in the middle part of lithologic Unit V suggests river supply to a shallow inner shelf. Owing to poor preservation and incomplete recovery, sedimentological criteria for the actual mode of sand transport are lacking.

In the lower part of lithologic Unit V, the impoverished fauna, the abundance of oncoids and large benthic foraminifers, and the lack of clastic detritus suggest deposition in a low-energy environment such as a shelf lagoon, despite the rarity of algae.

The clastic sediments in the middle part of this unit may be an expression of a regional regression or of a tectonic event, both known to occur near the Jurassic/Cretaceous boundary. The regression is commonly associated with widespread distribution of Purbeckian and Wealden facies (Ziegler, 1975, 1982; Jansa and Wiedmann, 1982).

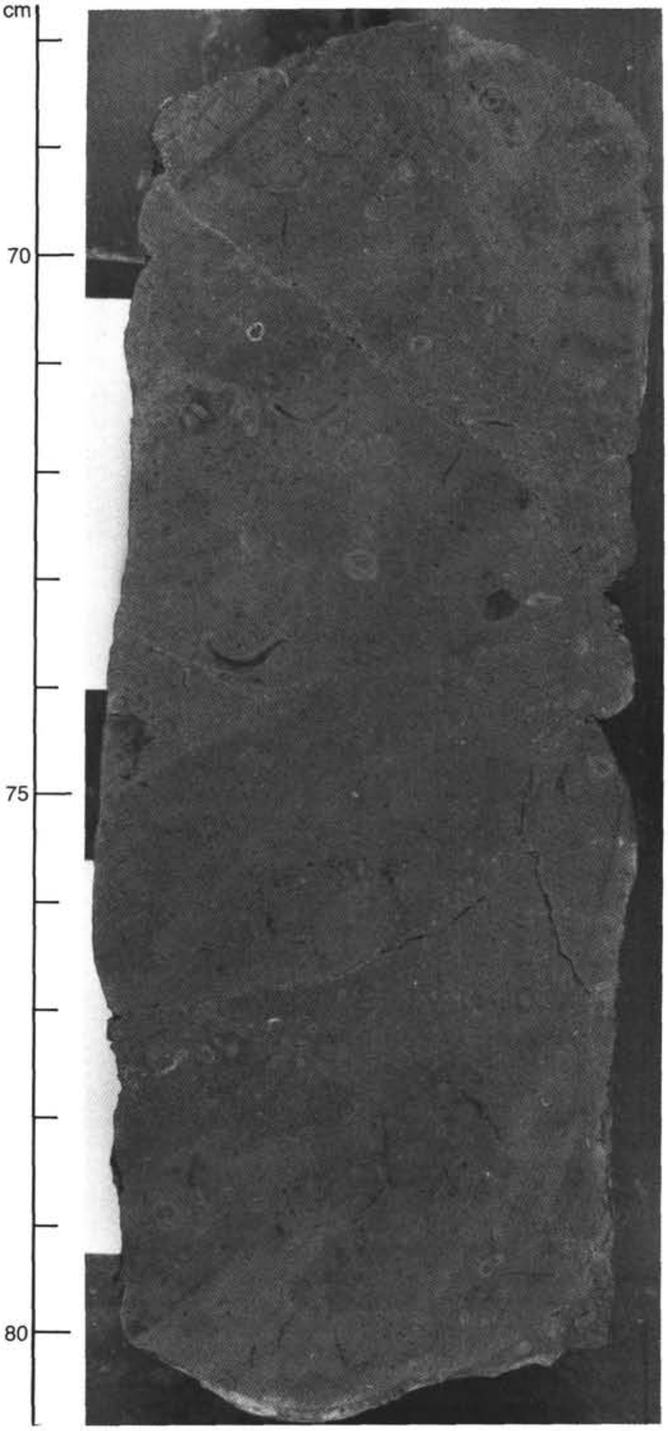

Figure 14. Skeletal-peloidal packstone to wackestone with oncoids, lithologic Unit V (Sample 103-639D-13R-1, 68–81 cm).

Lithologic Unit V bears certain similarities to other Late Jurassic carbonate-platform deposits such as in the Lusetanian Basin of Portugal (Cabo Espichel), southern Spain, and the eastern North American margin (Scotian Basin) (Eliuk, 1978; Jansa, 1981).

Lithologic Unit VI: Problematic Interval of Different Lithologies

The interval from Samples 103-639E-1R-1, 0 cm, to 103-639E-4R, CC, 5 cm, and from Samples 103-639F-1R-1, 0 cm, to 103-639F-2, CC, 27 cm, consists of pieces, many of which are unoriented and some of which are mixed by drilling, of different rock types. In Holes 639E and 639F, 51.5 m of this interval were cored, and 1.6 m of Unit VI were recovered. The recovered pieces range in size from 1–12 cm in length, though most are less than 5 cm. Most are angular, although several pieces are subrounded. We consider these pieces and this unit to be problematic because of the heterogeneous composition of the material, the small volume of recovery, and the uncertain stratigraphic relationship to Units I through V.

Lithologies arranged in the approximate order of recovery include the following:

Lithology 1. Brownish yellow limestone composing all Section 103-639E-1R-1. The limestone is dominantly fossiliferous mudstone and wackestone containing gastropods, pelecypod debris, large oyster fragments, and rare large benthic foraminifers. Other varieties include pink mudstone, skeletal-oncolitic packstone with large oyster fragments, and quartz-silt-bearing pelletal-oncolitic grainstone. The limestone is similar to the limestone in Unit V, although finer grained.

Lithology 2. Highly fractured, grayish brown, coarse-grained, crystalline dolomite and dolomite breccia composing all of Section 103-639E-2R-2 and Sample 103-639E-2R, CC. The fractures are filled with white sparry dolomite and locally constitute as much as 50% of the rock. Some fractures are filled with yellow clayey dolomicrite, dolomicrosparite, and dolomite (brecciated host rock). The dolomite is similar to dolomite in Unit IV.

Lithology 3. Dark yellowish brown silicic breccia. Clasts in the breccia are fine-grained quartzite, some of which are highly strained. The matrix is silicified.

Lithology 4. Dark reddish brown, pisolite-bearing claystone and siltstone. The presence of the authigenic minerals chlorite, sericite, and muscovite indicates either deep burial diagenesis or low-grade metamorphism. Metamorphic foliation is absent.

Lithology 5. Dark yellowish brown and reddish brown very fine-grained quartz sandstone and siltstone. The framework consists of monocrystalline quartz having less than 5% feldspar. The sandstone and siltstone have a well-compacted fabric, pressure-solution grain boundaries, and silica cement. Recrystallized matrix and/or authigenic interstitial material is rare and consists of sericite, chlorite, and ferruginous minerals. Metamorphic foliation is present in some pieces.

Lithology 6. Metamorphosed-granule conglomerate in which the clasts are rounded quartz and fine-grained siliciclastic sedimentary rocks. The clasts and the material between the clasts have a similar composition. Chlorite, sericite, and biotite both in the clasts and between the clasts indicate low-grade (low greenschist) metamorphism. Although the rock is weakly foliated, original sedimentary features remain.

Lithology 7. Pale-brown fossiliferous mudstone containing thin-walled bivalves, gastropods, serpulid worm tubes, and fine-grained molluscan debris.

Lithology 8. Altered silicic hypabyssal rock of rhyolitic to rhyodacitic composition (see "Basement Rocks" section, this chapter).

Locally a yellowish red clay coats and glues pieces of the hard rock.

A vague stratigraphic ordering appears in this unit. The limestone and highly fractured dolomite (lithologies 1 and 2) occur at the top of Unit VI. Both are mixed with lithologies 3 through 6, however. Lithologies 3 through 6 are described in their general order of occurrence but are mixed throughout this unit. The silicic hypabyssal rocks are at or near the bottom of both Holes 639E and 639F (Samples 103-639E-3R, CC, 6–27 cm, and 103-639F-2R, CC, 8–27 cm).

The stratigraphic significance of Unit VI remains ambiguous. Several explanations are possible:

1. The least complicated explanation for Unit VI is that it is a pre-Unit II submarine scree and slide deposit. The stratigraphy within Unit VI could be explained as follows. The limestone and dolomite at the top is Unit V and IV material transported as a rather coherent slide block. The mixed lithologies (lithologies 3 through 6) are derived from basement rock and/or a conglomerate cropping out farther up the paleoslope. The volcanic rocks at the bottom are either *in-situ* basement rock or large blocks of basement not far traveled.

2. The interval is a basal conglomerate resting on Hercynian basement. If this is true, the basement is here composed of lightly metamorphosed Paleozoic clastic sedimentary rocks and hypabyssal volcanic rocks, as indicated by the composition of the recovered clasts. The limestone in Section 103-639E-1R-1 could be *in-situ* lithologic Unit V in this explanation. A problem with this explanation is the occurrence of supposedly younger lithologies: (1) dolomite (lithology 1), which is similar to dolomite in Unit IV, and (2) fossiliferous mudstone, which is similar to limestone in Unit V, intermixed with the other lithologies. A highly speculative and whimsical explanation for these "younger" lithologies is to fault them into their present position.

3. The interval is a post-Hercynian (Permian to Triassic?) stratigraphic sequence highly disturbed by drilling, or it is a conglomerate lens within or underlying Unit V. This explanation shares the same problems evident in explanation 2.

BASEMENT ROCKS

Igneous rocks were recovered at the bottom of Holes 639E and 639F; the base of both holes revealed a pinkish gray silicic volcanic rock. About 20 cm (three pieces) of this rock were recovered in the core catcher of Core 103-639E-3R, and three cobble-sized pieces constituting about 25 cm were recovered in the core catcher of Core 103-639F-2R. The overlying rocks in both holes represent many sedimentary rock types, including clayey limestone, fossiliferous mudstone, crystalline dolomite, metaquartzite breccia, pisolite-bearing metaclaystone, metagraywacke, metagranule conglomerate, and metaquartz sandstone (see "Sediment Lithology" section, this chapter). Small pebbles of recrystallized cherty material and pisolite-bearing metaclaystone were recovered between the volcanic rock pieces in Sample 103-639E-3R, CC. Because their size is small, their stratigraphic position relative to the surrounding pieces of volcanic rock is unknown; they may have been situated above the volcanic rock and have slipped down between the other pieces during the drilling or recovery process.

Some of the sedimentary rocks recovered from Holes 639E and 639F show evidence of low-grade metamorphic transformation or contain clasts of strongly deformed quartzite.

In addition to the description of the subvolcanic rocks, a brief description of the metamorphic paragenesis is also included in this section.

Petrographic Description

Volcanic Rocks (Samples 103-639E-3R, CC, 20–23 cm; 103-639F-2R, CC, 9–11 cm; 103-639F-2R, CC, 18–20 cm)

Because the volcanic rocks recovered from both holes appear to have the same petrology, they are described together here. Descriptions of the rock in hand specimens are ambiguous. The rocks from Hole 639E have a pinkish cast and look so similar to some of the overlying pieces of sandstone that they were originally described as such. The pieces from Hole 639F are altered to a lesser extent and were first described as hypabyssal rocks of granitic composition. Small grains of quartz, altered feldspar, and mica were identified.

In thin section, the rocks display an altered volcanic, possibly hypabyssal, texture. They are relatively phenocryst-rich rocks having a silicic composition, probably rhyolite or rhyodacite. However, the pervasive alteration makes a more definite assessment of rock type difficult. Two thin sections from Hole 639F and one from Hole 639E samples were made and described on board.

The phenocryst assemblages constitute about 20% of the rock from Hole 639F and include alkali feldspars (about 15% of the rock), quartz (2%-3%), micas (10% to 15%, both muscovite and biotite), and 1%-2% altered mafic minerals (which were probably originally hornblende). Accessory minerals include zircon, rutile (associated with chloritized biotite), magnetite, and apatite. The groundmass contains a spherulitic material (Fig. 15), which is interpreted as being either a primary spherulitic quench texture (presumably composed of a mixture of alkali feldspar-quartz proto-crystals) or secondary rosettes of alteration phases, also typical of altered silicic volcanic rocks. Throughout all the thin sections, these rosettes/spherulites are uniform in size, shape, abundance, and relationship to the phenocrysts. They are rounded and are about 1 mm in diameter. Interstitial to both the rosettes/spherulites and phenocrysts are areas comprising fine quartz, feldspar, and chloritized mica, representing recrystallized and altered groundmass, possibly glass.

The feldspar phenocrysts (both albitic plagioclase, An 10-20, and K-feldspar, probably sanidine) are euhedral and 1-5 mm in size (Fig. 16). Few crystals are resorbed, and compositional zonation is not observed. The feldspars are highly sericitized and contain some zoisite, especially within the interior of the grains. Abundant muscovite and chlorite are present in both the altered groundmass and as coarser booklets of mica, which probably represent original phenocrysts of muscovite and biotite. The biotite has been chloritized and partly replaced by opaque minerals. Small hornblende crystals, which are recognized by grain outline, have been replaced by chlorite and chlorite + epidote assemblages.

In the thin section, the rock from Hole 639E (Sample 103-639E-3R, CC, 20-23 cm) is similar to rocks from Hole 639F but is finer grained. It also appears to have a composition slightly different from the rocks at Hole 639F, which have a plagioclase

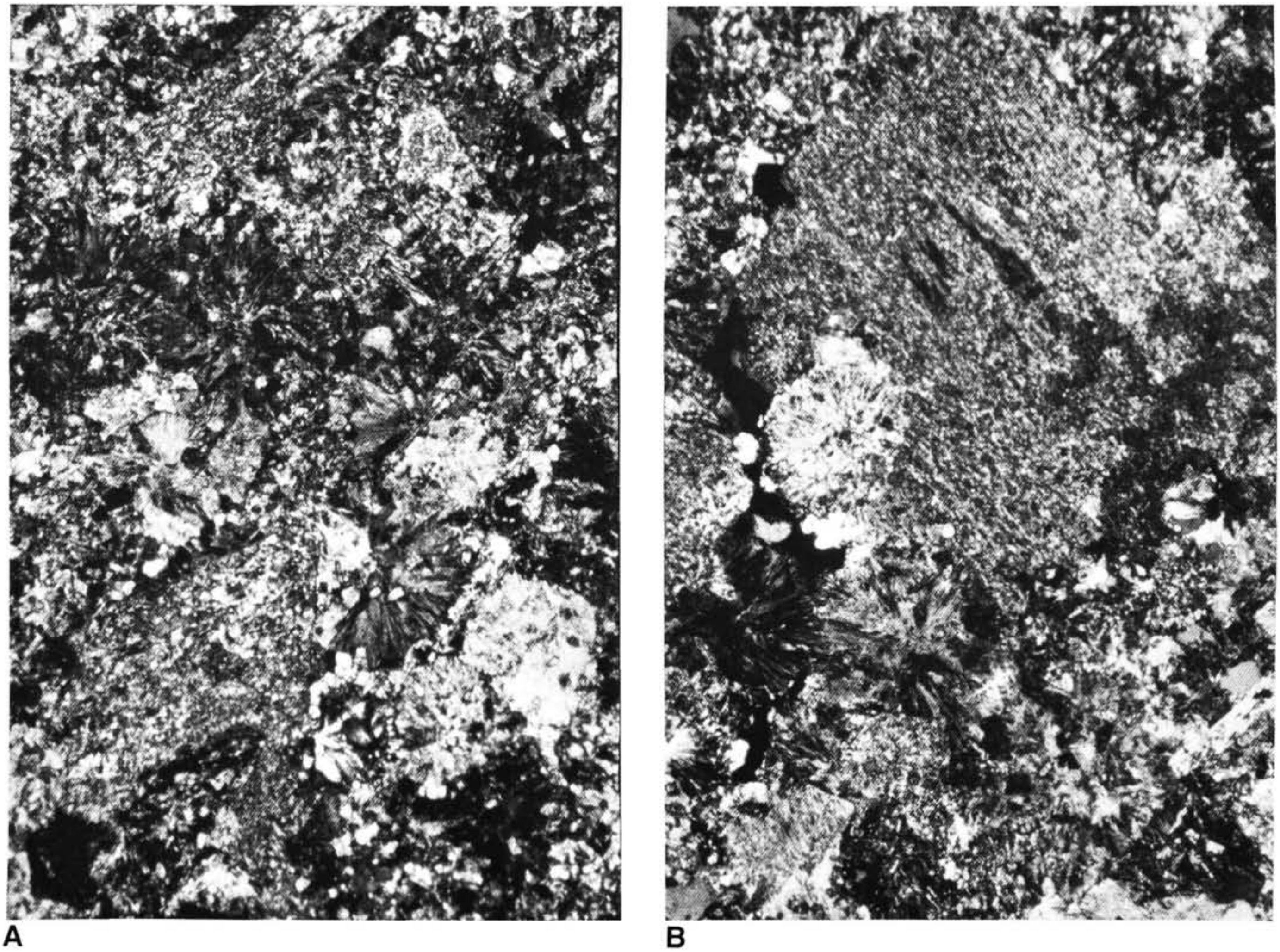

Figure 15. Photomicrographs of representative features in groundmass of rhyolitic rocks from Hole 639F. A. Sample 103-639F-2R, CC, 18-20 cm. Altered feldspar phenocryst (right center) surrounded by radiating groundmass material. Field of view is 3.6 × 2.4 mm. B. Sample 103-639F-2R, CC, 9-11 cm. Altered feldspar phenocryst surrounded by radiating structures in the groundmass. Field of view is 3.6 × 2.4 mm.

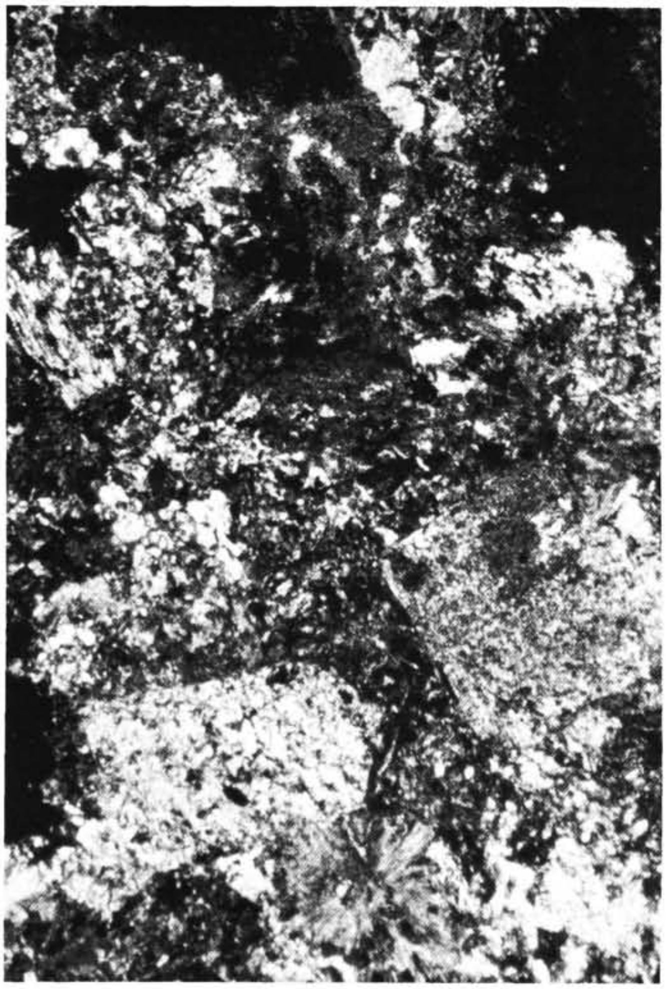

Figure 16. Sample 103-639F-2R, CC, 9-11 cm. Euhedral feldspar phenocrysts in rhyolite. Field of view is 3.6 × 2.4 mm.

phenocryst composition closer to An 20-30. Rock from Hole 639E is also altered to a greater extent, as evidenced by veinlets of recrystallized quartz and heavily altered opaque patches.

Metamorphic Sedimentary Rocks (Samples 103-639F-1R-1, 1-8 cm; 103-639F-2R, CC, 1-4 cm; 103-639E-3R-1, 18-21 cm)

Although most of the rocks discussed here still display their primary sedimentary textures, they differ from the overlying Mesozoic sedimentary rocks by the transformation of their clayey matrix or interstitial phases into a sericite-chlorite assemblage and by the partial recrystallization of their quartz clasts, owing to pressure solution. This is seen in the metagraywackes (Sample 103-639F-1R-1, 1-8 cm) and in the quartz sandstones (Sample 103-639F-2R, CC, 1-4 cm). Development of a slight schistosity is also seen in the metamorphic pisolite-bearing claystone (Sample 103-639E-3R-1, 18-21 cm) and in a metamorphic granule-conglomerate exhibiting a sericite-chlorite-biotite paragenesis in the matrix as well as in the clasts, indicating lower greenschist-facies conditions (<300°C) for their crystallization.

Metamorphic Quartzite Breccia (Sample 103-639E-3R-1, 21-24 cm)

Fragments of strongly deformed and recrystallized quartzite occur in Sample 103-639E-3R-1, 21-24 cm, which is a recrystallized quartzite sedimentary breccia. Grain size of the quartzite fragments is variable (1-10 mm). The interlocking quartz grains (0.1 mm) are strained and show a strong preferred crystallographic orientation defining a good foliation. The clasts, probably from Hercynian mylonites, are partly recrystallized, show resorbed contours, and are commonly rimmed by quartz grains with a comb structure (Fig. 17). The matrix consists of finely recrystallized quartz (<0.1 mm), which is unstrained and lacks a preferred orientation. It contains strained, large (0.5-1 mm), rounded individual quartz clasts and isolated rhombs of late-formed dolomite (euhedral-subhedral).

Discussion

The volcanic rocks recovered in Holes 639E and 639F may represent extrusive flows or dikes intrusive into shallow crustal levels, as evidenced by their small grain size (<0.1 mm) and porphyritic texture. Although heavily altered and leached, possibly by hydrothermal processes, the volcanic rocks have not been dynamically metamorphosed; the preserved textures are undeformed and igneous.

The metasedimentary rocks and metaquartzite breccia are possibly Paleozoic rocks. None of the overlying Mesozoic sandstones are pure quartzite; rather, they contain abundant feldspar and mica and are cemented by carbonate material. This is not a conclusive argument against a Mesozoic age for the metasandstones. If the sandstones were Mesozoic, it would be difficult to explain their metamorphic transformation and the appearance of a weak schistosity either by burial diagenesis (the overlying sedimentary cover is relatively thin) or by contact metamorphism owing to the intrusion of the volcanic rocks. On the other hand, they are similar to some Carboniferous and Permian rocks from Spain and Portugal. The age of neither the metasedimentary rocks nor the silicic volcanic rocks can be determined aboard the drilling vessel.

The stratigraphic position of all these rocks is uncertain. Because a small amount of volcanic rock was recovered from both Holes 639E and 639F (total of about 40 cm) and a variety of rock types was recovered together with the volcanic rocks in both holes, these rocks probably all represent fragments of a breccia or talus pile. Their presence, however, indicates the existence of basement outcrops in the area, beneath the Mesozoic cover.

BIOSTRATIGRAPHY

Six holes were drilled at Site 639 on the Iberian margin to penetrate and recover a composite section through hard dolomite (lithologic Unit IV; see "Sediment Lithology" section, this chapter), limestone (lithologic Unit V), and into basement rock. Foraminifers, nannofossils, radiolarians, and calpionellids, examined in core catchers, specific intervals, and thin sections, allow the recognition of sediments as old as Tithonian. The youngest sediments recovered at Site 639 are Pleistocene.

In Hole 639A, an abundant and well-preserved planktonic foraminiferal fauna and nannofossil flora indicates the presence of an unconformity within lithologic Unit I separating the lower Pleistocene (Sample 103-639A-3R-3, 102 cm) from upper Miocene sediments (Sample 103-639A-3R-4, 19 cm). Similarly, an unconformity is present somewhere between Samples 103-639A-4R-1, 1 cm, and 103-639A-4R, CC, i.e., between the Miocene nannofossil ooze of lithologic Unit I and the pale-yellow reddish brown marlstone of underlying lithologic Unit III. A poorly preserved, sporadic benthic foraminiferal fauna and a poorly preserved nannofossil flora indicate that the marlstone is of early-late Valanginian age. Poorly preserved, recrystallized radiolarians are also present and are typical of the Upper Jurassic and Lower Cretaceous. Calpionellid specimens observed in thin section are relatively rare but seem to confirm an early Valan-

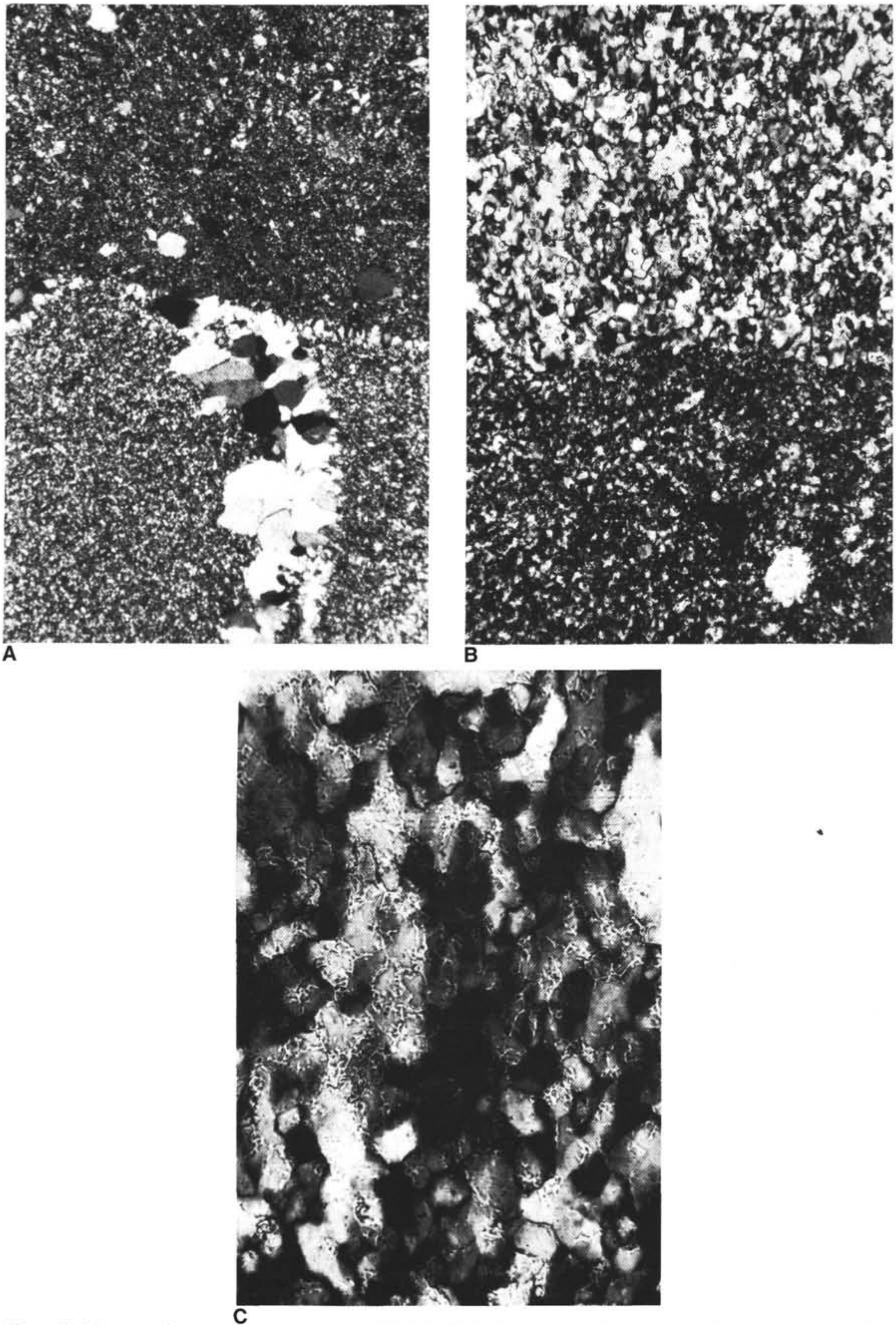

Figure 17. Metamorphic quartzite breccia, Sample 103-639E-3R-1, 21–24 cm. A. Quartzite clast rimmed with recrystallized quartz in quartz matrix. Field of view is 3.6 × 2.4 mm. B. Foliated quartzite clast in fine-grained, unfoliated, recrystallized quartz matrix. Field of view is 0.6 × 0.4 mm. C. Close up of foliated clast in B. Field of view is 0.36 × 0.24 mm.

ginian age for these sediments. No identifiable fossils were recovered from the dolomite sediments (lithologic Unit IV) below Sample 103-639A-8R, CC.

Holes 639B and 639C produced only one and two cores, respectively, before encountering the hard dolomite of Unit IV (characterized by nonidentifiable fossils). Planktonic foraminifers and nannofossils indicate a Pleistocene age in Sample 103-639B-1R, CC, and Pliocene for Samples 103-639C-1R, CC, and 103-639C-2R-1, 0-1 cm.

Much of the section at Hole 639D was washed through. A mud-line core (Sample 103-639D-1R, CC) is dated as early Pleistocene. Several cores of dolomite (from Samples 103-639D-2R, CC, to 103-639D-4R-1, 9 cm; lithologic Unit IV) were recovered and contain no identifiable fossils. Below this, the limestone of Unit V (Samples 103-639D-4R, 9 cm, to 103-639D-13R, 36 cm) contains moderately preserved, sporadic benthic foraminiferal assemblages of Tithonian age (as revealed in prepared samples and thin sections). Nannofossils, radiolarians, and a few recovered calpionellids also indicate a Tithonian age.

Holes 639E and 639F recovered hard limestone and dolomite. Thin sections reveal a few Tithonian benthonic foraminifers.

The integrated paleontological evidence, therefore, suggests that the marlstone sediments of lithologic Unit III above the dolomite are Lower Cretaceous, early Valanginian in age, whereas the limestone sediments beneath the dolomite are Tithonian in age.

Foraminifers

Hole 639A

Core-catcher samples and specific intervals from Hole 639A were examined for benthic and planktonic foraminiferal content. Samples 103-639A-1R, CC, and 103-639A-2R, CC, belong to lithologic Unit I (see "Sediment Lithology" section, this chapter) and consist of gray nannofossil ooze and marl. Their contained foraminifers are abundant, well preserved, and dominated by planktonics. The presence of *Globorotalia truncatulinoides* together with *Neogloboquadrina pachyderma, N. dutertrei,* and *Globigerina bulloides* indicates a Quaternary age (N22/23 of Blow, 1969, and Berggren, 1983). Low-latitude warmer water taxa such as *Sphaeroidinella dehiscens, Globigerinoides trilobus,* and *Pulleniatina* sp. are absent. Sample 103-639A-3R, CC, contains a sporadic, poorly preserved but distinctively late Miocene fauna (M12/13) including *G. paralenguaensis, G. lenguaensis, N. acostaensis,* and *Sphaeroidinellopsis seminulina*. Sediments of Pliocene age are not found in Hole 639A. The exact location of this apparent unconformity, better constrained by nannofossil assemblages (see following text), lies between Samples 103-639A-3R-3, 102 cm, and 103-639A-3R-4, 19 cm.

Underlying the late Miocene nannofossil ooze are sediments of lithologic Unit III (see "Sediment Lithology" section, this chapter), consisting of pale-yellow nannofossil marl interbedded with clasts and layers of limonite-stained fine-grained sandstone. Sample 103-639A-4R, CC, within this unit is barren, but Sample 103-639A-5R-1, 75-79 cm, contains a sporadic, poorly preserved benthic foraminiferal fauna having Valanginian-age taxa. Thus, a substantial unconformity exists between Cores 103-639A-3R and 103-639A-5R and corresponds to the lithological change between Units I and III. The occurrence of *Lenticulina nodosa nodosa* further indicates an early Valanginian age (Moullade, 1983) although this species (*sensu* Aubert and Bartenstein, 1979) has been described from younger sediments. The overall character of the assemblage is, however, Valanginian and indicates a bathyal environment; important species include *L. subangulata, Glomospirella gaultina, Spirillina minima, Ammodiscus cretaceus*, and various trochamminid and nodosariid species together with fragments of *Bathysiphon* species. A more distinct early Valanginian age is indicated by the sporadic, poorly preserved fauna recovered from Samples 103-639A-6R, CC; 103-639A-7R, CC; and 103-639A-8R, CC. In particular, the occurrence of *Dorothia* cf. *kummi* (*sensu* Moullade), *D.* cf. *hauteriviana*, and *D. hechti* suggests an early Valanginian age according to Moullade (1979). Other species include *L. gibba, Tritaxia pyramidata, Patellina subcretacea, Trocholina* spp. (very poorly preserved), *Miliammina* spp., and various nodosariids.

The hard, dolomitized nature of sediments encountered below Sample 103-639A-8R, CC, to total depth (Sample 103-639A-10R, CC) precludes recovery of foraminiferal faunas.

Hole 639B

Four cores were recovered from Hole 639B. Sample 103-639B-1R, CC, contains an abundant, well-preserved planktonic foraminiferal fauna and is assigned a Pleistocene age on the basis of the occurrence of *Globorotalia truncatulinoides, G. inflata,* and *Neogloboquadrina pachyderma*. The remaining cores from this hole contain the same dolomitized sediments as encountered in Hole 639A and did not allow foraminiferal determination.

Hole 639C

Two cores were recovered from Hole 639C. Samples 103-639C-1R, CC, and 103-639C-2-1R, 0-1 cm, both reveal a sporadic, poorly preserved planktonic foraminiferal fauna of early-middle Pliocene character. Important species include *Globorotalia puncticulata, G. crassaformis,* and *G. venezuelana*. No other foraminiferal faunas were recovered from this hole; two samples (103-639C-2R-1, 117-122 cm, and 103-639C-2R-2, 23-28 cm) taken from the brown clay contain Eocene ichthyoliths (P. Doyle, pers. comm., 1985).

Hole 639D

Thirteen cores were recovered from Hole 639D, of which Core 103-639D-1W was a wash core. Only Samples 103-639D-5R, CC, and 103-639D-6R-2, 149-150 cm, allowed processing for foraminifers; the rest consist of highly dolomitized sediments or hard limestone. Foraminifers recovered from these samples were few and only moderately preserved. Sample 103-639D-5R, CC, revealed no age-diagnostic foraminifers, although *Trochammina* sp., *Lenticulina* sp., *Epistomina* sp., and *Haplophragmoides* sp. are present. Thin sections from higher up the hole (Samples 103-639D-4R-1, 31-34 cm, and 103-639D-5R-2, 75-77 cm) show the presence of *Anchispirocyclina lusitanica*, an important marker in sediments of Tithonian age of the Atlantic margin, North America (Ascoli et al., 1984) and Africa (Hottinger, 1967). Bassoullet and Fourcade (1979) also restrict this species to the Tithonian in the Tethyan region. Other species include *Trocholina alpina-T. elongata* and *Pseudocyclammina lituus*. Similarly, *A. lusitanica* dominates Sample 103-639D-6R-2, 149-150 cm, indicating a Tithonian age, and occurs with *Everticyclammina* sp., *Triplasia* sp., *Lituola* sp., *Pseudolamarckina* sp., and *Paalzowella feifeli*. The species *A. lusitanica* persists downhole and is recognized in thin sections (Samples 103-639D-7R-1, 29-30 cm; 103-639D-9R-1, 7-10 cm; 103-639D-10R-1, 128-130 cm; 103-639D-11R-1, 70-72 cm; 103-639D-12R-1, 27-31 cm; 103-639D-12R-3, 56-57 cm; 103-639D-13R-1, 117-120 cm; 103-639D-13R-2, 72-76 cm; 103-639D-13R, CC). Thus, the oldest sediments cored at Hole 639D seem to be Tithonian in age. Nannofossil and calpionellid data (see following text) also indicate a Tithonian age for sediments recovered from Hole 639D.

Hole 639E

Only thin sections were examined from this hole. Sample 103-639E-1R-1, 43-45 cm, contains *Anchispirocyclina lusitanica*, indicating a Tithonian age. This species was also observed in

Samples 103-639E-1R-1, 64–67 cm, and 103-639E-1R, CC, together with *Pseudocyclammina lituus*.

Hole 639F

This hole (Sample 103-639F-1R-1, 67–69 cm) was barren of age-diagnostic foraminifers.

Nannofossils

Hole 639A

Pleistocene and middle Miocene nannofossil assemblages are present in the clayey nannofossil ooze and marl in the upper part of Hole 639A, lithologic Unit I (see "Sediment Lithology" section, this chapter). A nearly complete Pleistocene section containing well-preserved nannofossil assemblages lies unconformably on top of poorly preserved assemblages of middle Miocene age; this unconformity is located between Samples 103-639A-3R-3, 102 cm, and 103-639A-3R-4, 19 cm. Nannofossils are abundant throughout lithologic Unit I, and trace amounts of reworked nannofossils, mainly Eocene in age, occur in the Miocene sediment.

The interval from Samples 103-639A-1R-1, 113 cm, to 103-639A-3R-3, 102 cm, includes the *Emiliania huxleyi* Zone to the *Calcidiscus macintyrei* Zone described by Gartner (1977). *Emiliania huxleyi*, identified by the shipboard scanning electron microscope, is present in Sample 103-639A-1R-1, 113 cm, but not in 103-639A-1R, CC. Most of the Pleistocene sediment is placed in the late Pleistocene *Gephyrocapsa oceanica* Zone. Early Pleistocene nannofossil assemblages are present in only two core sections (103-639A-3R-2 and 103-639A-3R-3). Beneath lower Pleistocene sediment, middle Miocene assemblages of the *Discoaster hamatus* Zone, CN-7 (Okada and Bukry, 1980) were recovered from Samples 103-639A-3R-4, 19 cm, and 103-639A-4R-1, 1 cm. Middle Miocene sediments unconformably overlie Lower Cretaceous strata.

Poorly preserved Lower Cretaceous nannofossil assemblages of Valanginian age occur in the pale-yellow to light-gray marl/marlstone of lithologic Unit III (see "Sediment Lithology" section, this chapter). The abundance of nannofossils varies from rare to common. Nannoconids are the predominant forms observed within these assemblages, especially in Samples 103-639A-7R-1, 16 cm, to 103-639A-7R, CC. Species occurring throughout lithologic Unit III include *Nannoconus steinmanni, Cruciellipsis cuvillieri, Speetonia colligata*, and *Calcicalathina oblongata. Tubodiscus verenae* was found in several samples in Core 103-639A-4R. The presence of this species and of *C. oblongata* indicate an age no older than Valanginian. *Parhabdolithus infinitus* is present in the upper part of Unit III and has its lowest occurrence in Sample 103-639A-6R-1, 117–118 cm. According to Roth (1983), Thierstein (1976), and Wind and Čepek (1979), this species is first observed in lower upper Valanginian sediment. *Ruciniolithus wisei*, a form restricted to the upper Berriasian and lower Valanginian and normally having its uppermost occurrence immediately below the *P. infinitus* datum (Čepek, 1978; Roth, 1983), was not observed. Although perhaps indicating a post-early Valanginian age for the marl/marlstone, the absence of this form may be due to ecological restriction. Thus, at present, this section is assigned to the *Calcicalathina oblongata* Zone (CC-3) of Sissingh (1977). The base of this zone was calibrated to the upper part of the lower Valanginian in the hypostratotype locality (Busnardo et al., 1979).

Lithologic Unit IV, a vuggy fractured dolomite, which occupies the interval from Sample 103-639A-8R, CC, 7 cm, to the total depth of the hole, is barren of nannofossils.

Hole 639B

Abundant and well-preserved nannofossils of the *Gephyrocapsa oceanica* Zone (Gartner, 1977), late Pleistocene in age, were found in Sample 103-639B-1R, CC. The remaining three cores from this hole recovered dolomite and do not contain any preserved nannofossils.

Hole 639C

Two cores were recovered from Hole 639C. Core 103-639C-1R contains abundant and well-preserved nannofossils of the *Discoaster asymmetricus* Subzone (CN-11b), late–early Pliocene age. Samples 103-639C-2R-1, 35 cm, and 103-639C-2R-2, 38 cm, contain barren brown clay.

Hole 639D

Of the 13 cores recovered from Hole 639D, only Core 103-639D-1R contains Cenozoic nannofossils, which occur in the clayey nannofossil ooze and marl of lithologic Unit I (see "Sediment Lithology" section, this chapter). In Sample 103-639D-1R, CC, nannofossils are common, poorly preserved, and indicate a Pleistocene age. This same sample is dated as late Pliocene on the basis of the planktonic foraminifers. Nannofossil assemblages in this sample do not contain gephyrocapsids or discoasters, whereas *Coccolithus pelagicus* is abundant. Thus, a cold-water assemblage may be indicated, perhaps explaining the absence of discoasters in a sample from upper Pliocene sediment.

The remaining 12 cores from Hole 639D contain mostly brownish gray dolomite and light brownish gray limestone, corresponding to lithologic Units IV and V, respectively (see "Sediment Lithology" section, this chapter). As at all other holes drilled at Site 639, the dolomite is barren. The limestone, first encountered in Sample 103-639D-4R-1, 9 cm, is composed of skeletal wackestone, packstone, and fossiliferous biomicrite intercalated with marlstone. Within this marlstone, rare and poorly preserved nannofossils occur. Sample 103-639D-5R, CC, contains few species, all of which are long ranging (Early Jurassic to Early Cretaceous). Thus, a specific age cannot be assigned to this sample. Sample 103-639D-6R-2, 100 cm, contains *Polycostella beckmannii* and small nannoconids, indicating a late Tithonian age (*Polycostella beckmannii* Subzone of Roth et al., 1983). Similar assemblages occur in Samples 103-639D-6R-2, 139 cm; 103-639D-7R, CC; and 103-639D-10R, CC. No nannofossils were recovered from Cores 103-639D-11R to 103-639D-13R.

Hole 639E

All sediment that was recovered from Hole 639E is barren of nannofossils.

Hole 639F

All sediment that was recovered from Hole 639F is barren of nannofossils.

Radiolarians

Hole 639A

Radiolarian (and calpionellid) preparations were made for all core-catcher samples and for an additional 40 samples from Hole 639A. Samples from Cenozoic lithologic Unit I (see "Sediment Lithology" section, this chapter) are barren of radiolarians and other siliceous microfossils. Samples from the marl/marlstone of lithologic Unit III contain few to common, poorly preserved radiolarians. In general, they are preserved in pyrite, owing to the oxidation of the pelagic sediments of lithologic Unit III (see "Sediment Lithology" section, this chapter); however, faunas are recrystallized in limonite, precluding a taxa determination. Additionally, a significant proportion of the specimens are flattened. Sample 103-639A-8R, CC, contains a moderately rich fauna, which allows the distinction of several genera having their acme in the Upper Jurassic/Lower Cretaceous and including *Sethocapsa, Mirifusus, Obesacapsula, Podobursa, Ho-*

moeoparonella/Paronella. Strewn-slide preparations made for the calpionellid study show a considerable amount of juvenile radiolarians (preserved in silica, calcite, and limonite). Thin sections 103-639A-7R-2, 38–40 cm; 103-639A-8R-1, 3–5 cm; and 103-639A-8R-2, 37–40, made from "calpionella"-rich micrites contain, concentrated in places (bioturbation?), radiolarians preserved in limonite.

Hole 639B

One sample from 103-639B-1R, CC, was prepared for siliceous microfossils. Both the 45–63-μm sieve fraction and the fraction coarser than 63 μm are barren of siliceous microfossils.

Hole 639C

Preparations were made from Samples 103-639C-1R-1, 148 cm; 103-639A-1R, CC; and 103-639A-2R-1, 0–2 cm. The 45–63-μm sieve fraction and the fraction coarser than 63 μm are barren of siliceous microfossils.

Hole 639D

Sample preparations were made for all core-catcher samples from Hole 639D. An additional sample was obtained from Sample 103-639D-5R-1, 43 cm. All samples are barren of radiolarians and other siliceous microfossils.

Table 3. Calpionellids, Holes 639A and 639D. F = few; R = rare.

Calpionellids \ Sample	103-639A-5R-1, 18–20 cm	103-639A-5R-1, 88–90 cm	103-639A-6R-2, 113–118 cm	103-639A-7R-1, 56–58 cm	103-639A-7R-2, 38–40 cm	103-639A-7R-3, 9–12 cm	103-639A-7R,CC (14–15 cm)	103-639A-8R-1, 3–5 cm	103-639A-8R-2, 37–40 cm	103-639A-8R,CC	103-639D-5R-1, 105–108 cm
SEM										X	
Strewn slide	X	X	X							X	
Thin section				X	X	X	X	X	X		X
Calpionellites darderi	R	R	F	R	R		R	R	R	R	
Tintinnopsella carpathica	F	R	R		R	R	F	R		R	
Calpionella alpina		F	F	F	R	R	F	F	F	F	R
C. elliptica	R		R	F	R		R			F	
Remaniella(?) sp.					R		R			R	
Calpionellopsis oblonga					R						
Crassicollaria massutiniana											R
C. brevis											R
	Calpionellites E Zone (e. Valanginian)										*Crassicollaria* A Zone (l. Tithonian)

Calpionellids

Rare to common, poorly to moderately well-preserved calpionellids were observed in two holes at Site 639 (Holes 639A and 639D).

Hole 639A

Calpionellids occur in Cores 103-639A-5R to 103-639A-8R in the marl/marlstone of lithologic Unit III (see "Sediment Lithology" section, this chapter). Calpionellids found in the 44–100-μm fraction were extracted from these sediments by usual preparation techniques and mounted on strewn slides. These microfossils were also studied in thin sections, and one moderately well-preserved assemblage (Sample 103-639A-8R, CC) was observed with the shipboard scanning electron microscope.

All samples yielded basically the same assemblage, which includes *Calpionella alpina, C. elliptica, Tintinnopsella carpathica*, and *Calpionellites darderi* (Table 3). In a few samples, very rare specimens, tentatively attributed to the genus *Remaniella* and to the species *Calpionellopsis oblonga*, were also found. A significant proportion of the specimens can be defined only as "undifferentiated calpionellids," owing to their poor preservation. Such specimens show only remains of the lorica (often totally or partly reduced to an internal mold) and lack the more delicate apical part (= collar), the shape of which would permit a better identification. Increasing dolomitization (as seen by appearance of dolomite rhombs in the micritic matrix) in samples from Cores 103-639A-5R through 103-639A-8R also affected calpionellids. As a result, crystal overgrowth of dolomite precludes the exact determination of large parts of the faunal assemblages.

The occurrence of *Calpionellites darderi* limits Cores 103-639A-5R through 103-639A-8R to the late-early Valanginian *Calpionellites* E Zone (Remane, 1978), an age assignment consistent with the foraminiferal and calcareous nannofossil data. *T. carpathica, Remaniella,* and *Calpionellopsis* have also been reported as occurring in the early Valanginian (Remane, 1978). *Calpionella alpina* is mainly a late Tithonian–Berriasian species, which according to Remane (1978) becomes rare near its uppermost occurrence in the lowest Valanginian. Nevertheless, this taxon represents a relatively important component of the Valanginian calpionellid fauna in Hole 639A. More striking is the occurrence of a certain amount of specimens that we attribute to *C. elliptica*, a species known to be extinct at the early/late Berriasian boundary (Remane, 1978). Similar abnormal calpionellid highest occurrences were depicted in DSDP Site 416 in the Moroccan Basin (Vincent et al., 1979) and were interpreted as resulting from reworking by turbidites. In Hole 639A, no evidence appears of either abnormal occurrences or of reworking among the foraminiferal and nannofossil faunas from the same levels, though turbid flows are suggested for the deposition of at least part of lithologic Unit III (see "Sediment Lithology" section, this chapter).

In Hole 639A, the Valanginian calpionellids occur in fine-grained, micritic sediments, which includes sparse and small crystals of dolomite. Contemporaneous foraminifers (this chapter) in the same interval indicate a deep, at least bathyal, environment.

Hole 639D

The oldest level containing calpionellids is in Hole 639D. Thin sections made from Sample 103-639D-5R-1, 105–108 cm, yielded rare and moderately well-preserved specimens (*Calpionella alpina, Crassicollaria massutiniana*, and *C. brevis*); strewn slides prepared from Sample 103-639D-5R, CC, contain very poorly preserved undifferentiated calpionellids. The assemblage indicates a late Tithonian age, more precisely the middle part of the late Tithonian (*Crassicollaria* A Zone).

Calpionellids from the upper Tithonian beds of Hole 639D are scattered in a coarser but still relatively fine-grained bioclastic matrix, which includes scarce and much larger bioclasts and shallow-water benthic macroforaminifers. The occurrence of calpionellids indicates at least the possibility of communication with the open sea, assuming that the shallow-water biogenic component represents the *in-situ* fauna (see "Sediment Lithology" section, this chapter).

Hole 639F

Two thin sections (Samples 103-639F-1R-1, 67–69 cm; 103-639F-1R, CC) prepared from a micritic limestone contain rare and poorly preserved undifferentiated calpionellids. Two of the better-preserved specimens, however, can be identified as *Tintinnopsella carpathica* and *Crassicollaria* sp., suggesting a possible late Tithonian (*Crassicollaria* A Zone) age for this core.

PALEOMAGNETICS

Every core of Mesozoic sediments was sampled for magnetostratigraphy. Whole-core analyses were run on several Neogene and Mesozoic cores, but the results, when compared with later analyses of washed and cut half-rounds, indicate pervasive rust-flake contamination (see discussion in the "Explanatory Notes" chapter, this volume). The discrete samples collected were generally too weak for analysis on board. Select split-core analyses indicate that the natural remanent magnetization (NRM) is predominantly normal magnetic polarity, presumably indicating an overprint of the present field. The oriented discrete sampling consists of the following: 3 samples of Late Cretaceous(?) brown clay, 25 samples of lower Valanginian marl, 2 samples of Berriasian(?) dolomite, 58 samples of Tithonian shallow-water limestone, and 9 samples of the various sediments and volcanics in Holes 639E and 639F.

All samples were analyzed on a cryogenic magnetometer at the University of Wyoming paleomagnetics laboratory (see the "Paleomagnetics" section, Site 638 chapter, for a description of the procedures).

Brown Clay (Late Cretaceous[?]; Core 103-639C-2R)

The three samples of brown clay from an 80-cm interval yielded normal polarity upon progressive thermal demagnetization. No polarity chron assignment is possible from such a short section.

Lower Valanginian Marl (Cores 103-639A-5R through 103-639A-8R)

These samples underwent a detailed progressive thermal demagnetization through either 500°C (nine steps) or 600°C (ten steps). Magnetic polarity was generally evident by 150°C, and stable characteristic directions were generally maintained from 300° to 500°C. Intensities of characteristic magnetization averaged about 2×10^{-7} emu/cm^3 (= 2×10^{-4} A/m).

The lower part of Cores 103-639A-6R through 103-639A-8R show reversed polarity (Fig. 18). The age is late early Valanginian (Calpionellid Zone E). The polarity chron assignment is M13 because the base of Calpionellid Zone E is known to be near the top of chron M14 (Ogg, in press; J. E. T. Channell, pers. comm., 1986). The lower part of chron M13 is absent; the immediately underlying dolomite has normal polarity but is not considered to be chron M14n (early Valanginian) in age.

The lowest sample of Core 103-639A-5R is reversed, which could represent poor recovery of the short polarity chron M12A (nomenclature of Harland et al., 1982).

Dolomite (Berriasian[?]; Cores 103-639A-8R and 103-639A-10R)

Only two pilot samples were analyzed — one each by progressive thermal and progressive alternating field (AF) demagnetization. Thermal demagnetization (Sample 103-639A-8R-2, 89 cm) yielded a stable normal polarity through 450°C. At 500°C and above, unstable magnetization was observed. AF demagnetization yielded an indeterminant result of a stable steep downward direction of magnetization.

Shallow-Water Limestone (Tithonian; Cores 103-639D-5R through 103-639A-13R)

Lithologic Unit V is predominantly gray, bioclastic-rich, pelletal oncolitic limestone. The magnetic intensities were weak; NRM intensities averaged about 2×10^{-7} emu/cm^3 (= 2×10^{-4} A/m). Characteristic directions were generally obtained between 200°C and 350°C, intensities typically being less than 5×10^{-8} emu/cm^3.

Nearly all samples displayed normal polarity; two showed narrow reversed-polarity zones (Fig. 19). The dominance of normal polarity is consistent with the middle Tithonian age. The identification of Calpionellid Zone A in Core 103-639D-5R suggests that the short reversed-polarity zone in Core 103-639D-6R is either M19 or $M20_{n-1}$, according to the late Tithonian studies of Ogg (1981; Ogg and Lowrie, 1986). The poorly documented reversed-polarity interval of Cores 103-639D-8R through 103-639D-9R is possibly polarity chron M20 or M21. The magnetostratigraphy interpretation suggests that the abundant reversed-polarity intervals typical of the Kimmeridgian and earliest Tithonian (polarity chrons M22 and older) were not penetrated by the drilling.

Sediments and Volcanic Rocks from Holes 639E and 639F

The Tithonian and pre-Tithonian sedimentary, igneous, and metamorphic rocks of Holes 639E and 639F were poorly sampled and lack biostratigraphy; therefore, the mixed polarity results are not useful for magnetostratigraphy.

ORGANIC GEOCHEMISTRY

Organic Carbon Analysis

Twenty-four samples were taken at Site 639 for organic carbon and nitrogen determination using the Perkin-Elmer elemental analyzer. Results of the organic carbon percentage on a dry-sediment weight basis and percentage of carbonate are listed in Table 4. Because of technical problems, reliable determination of elemental nitrogen was not possible.

In general, preservation of organic matter at Site 639 is poor. A few exceptions are observed in samples collected within the upper few meters of the sediment/water interface. Bacterial degradation of organic matter is high in the early stages of burial; therefore, high organic matter concentration in the upper few meters is not unusual.

Rock-Eval Analysis

Samples collected at Site 639 are extremely organic carbon lean; therefore, reliable Rock-Eval analysis was impossible.

Organic Carbon Isotope Analysis

Organic carbon isotope values are listed in Table 5.

INORGANIC GEOCHEMISTRY

Interstitial-Water Chemistry

Eight sediment samples were taken from rotary-drilled cores recovered at Site 639. Of these eight samples, five were taken immediately from the core while "on-deck" as whole-rounds, whereas the other three samples were obtained from a 10-cm interval of the working half of the core immediately after the designated core section was split (Table 6). The sampling strategy was to obtain one sample from each core in the upper 50 m of Hole 639A and in decreasing frequency below 50 m. This strategy was followed if at least 1.5 m of sediment was recovered in the designated core. For example, in Core 103-639A-4R, insufficient sediment was recovered; consequently, no sample was taken. No samples were taken from cores containing dolomite (lithologic Unit IV; see "Sediment Lithology" section, this chapter) or limestone (lithologic Unit V). In Hole 639B, only the first mud-line core provided sufficient and appropriate sediment for extraction of interstitial water. All subsequent drill holes at this site (Holes 639C through 639F) were washed down to the upper region of the dolomite and, therefore, did not provide appropriate sediment for extraction of interstitial water.

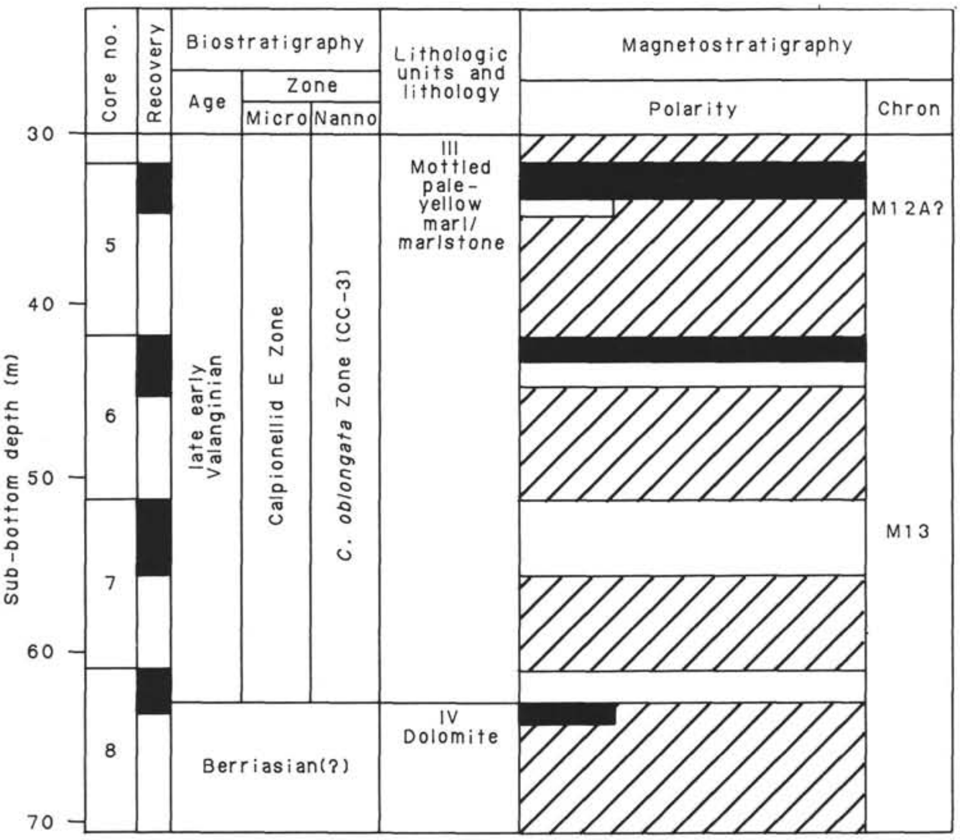

Figure 18. Magnetostratigraphy and tentative assignment of polarity chrons of Hole 639A. Black shading is normal-polarity zones, and white is reversed polarity. Diagonal pattern indicates gaps in recovery or intervals of indeterminant or unreliable polarity. Half bar represents a single sample having a polarity interpretation opposite that of the adjacent samples or indicates that only one sample was available from the core. Assignment of magnetic polarity chrons is the best current guess based upon the biostratigraphy given in this site chapter and published magnetic polarity time scales. Complete tables of paleomagnetic data and polarity interpretations will be given in Part B of the Leg 103 volumes.

The eight sediment samples were squeezed aboard ship to obtain the interstitial water from the sediment. The water samples were analyzed for pH, alkalinity, chlorinity, salinity, calcium, and magnesium. One of the three samples taken from the working half of the core (Sample 103-639A-3R-2, 140–150 cm; 14.9–15.0 m sub-bottom depth) yielded insufficient interstitial water for alkalinity and pH measurement. The same analytical methods used at Sites 637 and 638 were employed for the samples recovered at Site 639. The primary standard used for calibration of the water analysis is IAPSO standard seawater, and surface-seawater samples retrieved by a bucket overboard were used for comparison with the interstitial-water samples from each drill hole.

The results listed in Table 6 and graphed in Figure 20 show very little variation in the values with increasing depth. Alkalinity slightly decreases in the upper 33.4 m of Hole 639A and increases at 43.0 m (Sample 103-639A-6R-1, 140–150 cm), abruptly decreasing at 52.6 m sub-bottom depth (Sample 103-639A-7R-1, 140–150 cm). The alkalinity value of Sample 103-639B-1R-1, 0–10 cm, near the sediment/water interface, is lower than the alkalinity value for the shallowest sample from Hole 639A. The second sample from Hole 639B (Sample 103-639B-1R-5, 140–150 cm) at 7.4 m sub-bottom depth has an alkalinity value similar to that obtained from the sample at 6.7 m sub-bottom depth in Hole 639A (Sample 103-639A-2R-3, 140–150 cm). The increase and abrupt drop in alkalinity in Sample 103-639A-6R-1, 140–150 cm, and Sample 103-639A-7R-1, 140–150 cm, may be associated with the increasing lithification of the marl in Core 103-639A-7R by a drop in the carbon dioxide content and precipitation of a carbonate mineral (calcite? and/or dolomite?) in Core 103-639A-7R.

The salinity and chlorinity values correlate in the sense that both shift in the same direction in Holes 639A and 639B. No significant downhole trends of a progressive increase or decrease in the salinity or chlorinity values appear.

Calcium and magnesium values at Site 639 show weak trends downhole. Calcium values increase, while the magnesium values generally decrease with increasing sub-bottom depth (Figure 21). In Cores 103-639A-5R, 639A-6R, and 639A-7R, the calcium values are significantly higher than the calcium values of the overlying interstitial-water samples (Table 6). The magnesium values also fluctuate in these three lower samples. Changes in the calcium and magnesium values are attributed to the increasing lithification of the marl and the precipitation of dolomite identified in smear slides (see "Sediment Lithology" section, this chapter). The downhole decrease in magnesium in the interstitial waters may also be the result of its uptake in the detrital clay minerals.

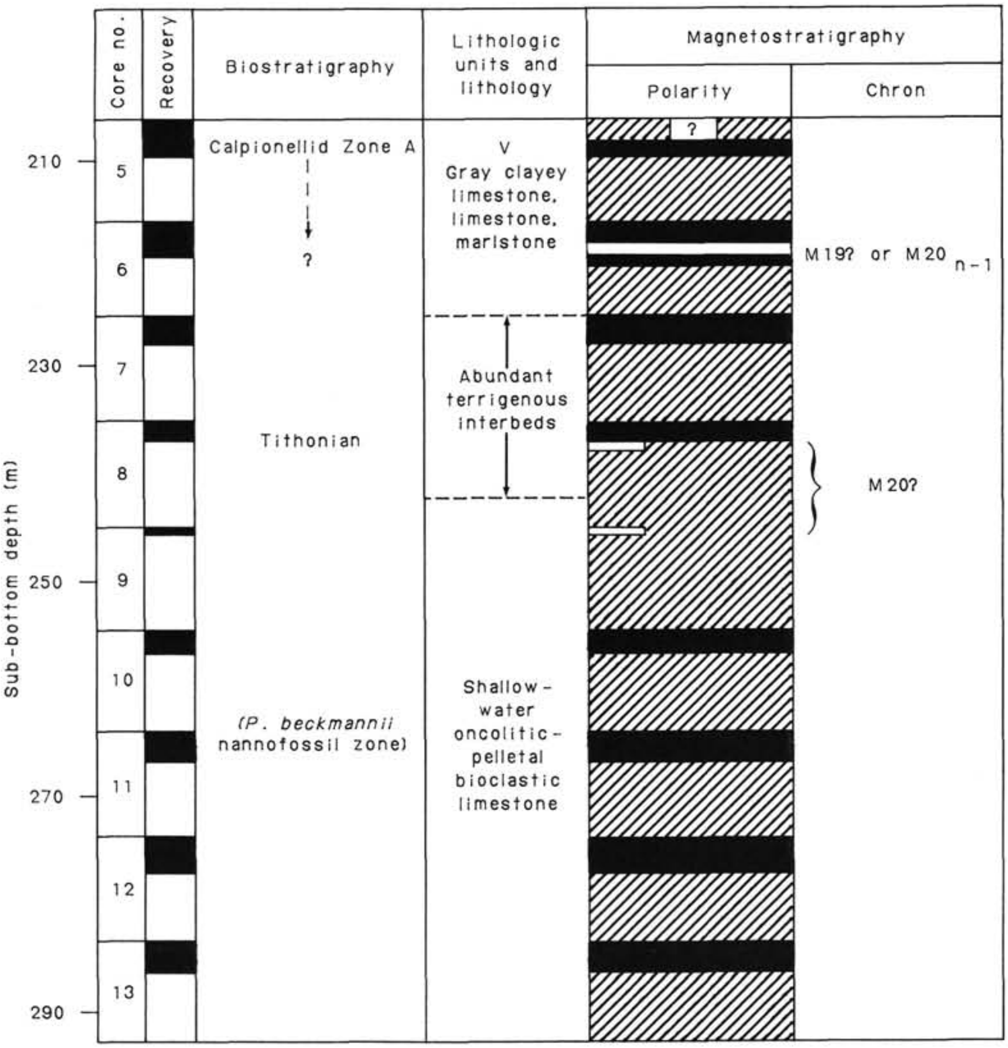

Figure 19. Magnetostratigraphy and tentative assignment of polarity chrons of Hole 639D. Black shading is normal-polarity zones, and white is reversed polarity. Diagonal pattern indicates gaps in recovery or intervals of indeterminant or unreliable polarity. Half bar represents a single sample having a polarity interpretation opposite that of the adjacent samples or indicates that only one sample was available from the core. Assignment of magnetic polarity chrons is the best current guess based upon the biostratigraphy given in this site chapter and published magnetic polarity time scales. Complete tables of paleomagnetic data and polarity interpretations will be given in Part B of the Leg 103 volumes.

Calcium Carbonate

Approximately 50 samples were analyzed for percentage carbonate, and the results, listed in Table 7, reflect the differences among the assigned lithologic units (see "Sediment Lithology" section, this chapter).

In lithologic Unit I, composed of clayey nannofossil ooze, nannofossil marl, and calcareous clay, the carbonate ranges from 9% to 98% of the dried-sediment weight. In Hole 639A, the sediments assigned to lithologic Unit I (0–21.6 m sub-bottom depth) are pelagic carbonates deposited above the carbonate compensation depth (CCD), but they contain clay-rich intervals that might be a response to Pliocene–Pleistocene glaciation. Lithologic Unit II, composed of brown clay, was recovered only in Hole 639C at 95.0 to 96.8 m sub-bottom depth and contains no carbonate in the dried-sediment sample. Lithologic Unit III, composed of marl/marlstone, was recovered only in Hole 639A from 21.6 to 70.3 m sub-bottom and has carbonate values ranging from 42% to 74% of the dried-sediment weight. One anomalous value of 0% carbonate was recorded in Sample 103-639A-4R-1R, 17–19 cm, at the top of Unit III. This clay was interpreted by the sedimentologists as possibly being a residual weathering product (see "Sediment Lithology" section, this chapter). Lithologic Unit IV, recovered in Holes 639A through 639D, is composed of dolomite having carbonate values of 96% to 100% of the dried-sediment weight. Unit V, composed of clayey limestone, marlstone, and sandstone, was recovered from Hole 639D from 199 to 293.1 m sub-bottom depth. The carbonate values range from 20% (silty clay) to 94% (oncolitic limestone) of the dried-sediment weight. In Hole 639E, dolomite and clayey limestone were also recovered. The dolomite (Sample 103-639E-2R-1, 56–62 cm) contains 98% carbonate of the dried-sediment weight, and the clayey limestone (Sample 103-639E-1R-1, 51–53 cm) contains 82% carbonate of the dried-sediment weight. In the bottom of Hole 639E and Hole 639F, altered volcanics and metamorphosed rocks were recovered. A quartzite (Sample 103-639E-3R-1, 19–24 cm) and rhyolite (Sample 103-639E-3R, CC, 2–5 cm) from Hole 639E were analyzed for car-

Table 4. CHN summary, Site 639.

Sample (interval in cm)	Sub-bottom depth (m)	Organic carbon (%)	Inorgan. carbon (%)	Lithology
103-639A-1R-1, 63-65	0.21	0.32	20	Calcareous clay
103-639A-1R-2, 67-69	0.73	0.17	80	Clayey nannofossil ooze
103-639A-2R-1, 15-19	2.45	0.23	9	Olive-gray clay
103-639A-3R-1, 105-107	13.05	0.17	74	Clayey nannofossil ooze
103-639A-3R-4, 105-108	17.55	0.03	61	Nannofossil ooze
103-639A-4R-1, 47-49	21.97	0.02	0	Clay
103-639A-5R-2, 94-95	34.34	0.02	49	Nannofossil marl
103-639A-6R-2, 123-126	44.34	0.04	60	Nannofossil marl
103-639A-7R-2, 60-62	53.30	0.05	52	Marlstone
103-639A-8R-1, 27-29	61.07	0.03	74	Clayey limestone
103-639A-8R-2, 28-30	62.58	0.04	64	Marlstone
103-639A-9R-1, 12-14	70.55	0.02	97	Dolomite
103-639B-1R-3, 63-64	3.63	0.91	3	Olive-gray clay
103-639B-1R-5, 52-54	6.52	0.20	68	Clayey nannofossil ooze
103-639C-1R-2, 52-54	80.02	0.12	72	Clayey nannofossil ooze
103-639C-2R-1, 48-50	91.28	0.02	0	Brown clay
103-639C-2R-2, 4-6	92.34	0.02	0	Varigated brown-pink clay
103-639D-5R-1, 52-53	207.02	0.02	20	Calcareous silty clay
103-639D-5R-1, 125-127	207.75	0.15	87	Clayey limestone
103-639D-6R-1, 77-79	216.77	0.07	90	Clayey limestone
103-639D-7R-1, 48-50	225.80	0.03	55	Marlstone
103-639D-7R-2, 85-86	227.95	0.04	39	Marlstone
103-639D-8R-1, 40-42	235.60	0.05	76	Clayey limestone
103-639D-10R-1, 61-63	254.11	0.05	62	Marlstone

Table 5. Organic carbon isotope values, Site 639.

Sample (interval in cm)	Sub-bottom depth (m)	Age	Organic carbon (%)	$CaCO_3$ (%)	$\delta^{13}C$
103-639A-1R-2, 67-69	0.73	Pleistocene	0.17	80	−24
103-639A-2R-1, 15-19	2.45	Pleistocene	0.23	9	−24
103-639A-4R-1, 47-49	21.97	Valanginian	0.02	0	−25.5
103-639A-7R-2, 60-61	53.3	Valanginian	0.05	52	−23.8
103-639B-1R-3, 63-64	3.63	?	0.91	3	−25.6
103-639D-7R-2, 85-86	227.95	Tithonian	0.04	39	−25.2
103-639D-8R-1, 40-42	235.6	Tithonian	0.05	76	−25.3

Table 6. Shipboard interstitial-water analyses, Site 639.

Sample (interval in cm)	Sub-bottom depth (m)	pH	Alkalinity (meq/kg)	Salinity (‰)	Chlorinity (‰)	Ca^{++} (mmol/L)	Mg^{++} (mmol/L)
103-639A-1R-4, 140-150	2.0-2.1	7.26	3.82	34.8	19.30	10.15	54.61
[a]103-639A-2R-3, 140-150	6.7-6.8	7.29	3.79	35.2	19.38	10.28	54.89
[a]103-639A-3R-2, 140-150	14.9-15.0	[b]	[b]	33.9	18.77	9.73	52.08
103-639A-5R-1, 140-150	33.3-33.4	7.28	3.45	35.0	19.50	12.47	52.98
[a]103-639A-6R-1, 140-150	43.0-43.1	7.84	4.03	33.7	18.56	13.44	48.65
103-639A-7R-1, 140-150	52.6-52.7	7.54	3.07	34.8	19.29	14.27	50.81
103-639B-1R-1, 0-10	0.0-0.1	7.45	3.44	35.0	19.42	10.23	54.71
103-639B-1R-5, 140-150	7.4-7.5	7.29	4.21	34.5	18.99	9.62	54.39

[a] Sediment sample taken only from working half of core immediately after section was split.

[b] Insufficient interstitial water, extracted from sediment obtained from working half of core, for alkalinity and pH measurement.

bonate content. The quartzite contains 4% carbonate of the dried-powdered weight; the rhyolite has 3% carbonate of the dried-powdered weight. A pisolite-bearing metamorphosed claystone (Sample 103-639E-3R-1, 24-27 cm) and a metamorphosed granule conglomerate (Sample 103-639E-4R, CC, 0-4 cm) were analyzed for carbonate content and were found to contain no carbonate.

PHYSICAL PROPERTIES

Physical-property measurements were made on sediments and sedimentary rocks from Site 639, according to the procedure described in previous site chapters, except as noted in the following text. Unsplit sediment cores were analyzed on the Gamma Ray Attenuation Porosity Evaluator (GRAPE), allowed to warm to room temperature for 4 hr, measured for thermal conductivity, and then split. After being split, sediment from the upper part of Hole 639A (Cores 103-639A-2R through 103-639A-4R, 2-32 m sub-bottom), Hole 639B (Core 103-639B-1R, 0-7 m sub-bottom), and Hole 639C (Core 103-639C-1R; 78-91 m sub-bottom) were analyzed on the vane-shear-strength apparatus. Sedimentary rock was analyzed on the GRAPE after removal from the core liner and measurement of the diameter of individual rock pieces. Sediments and sedimentary rocks from throughout the holes of Site 639 were measured for compressional seis-

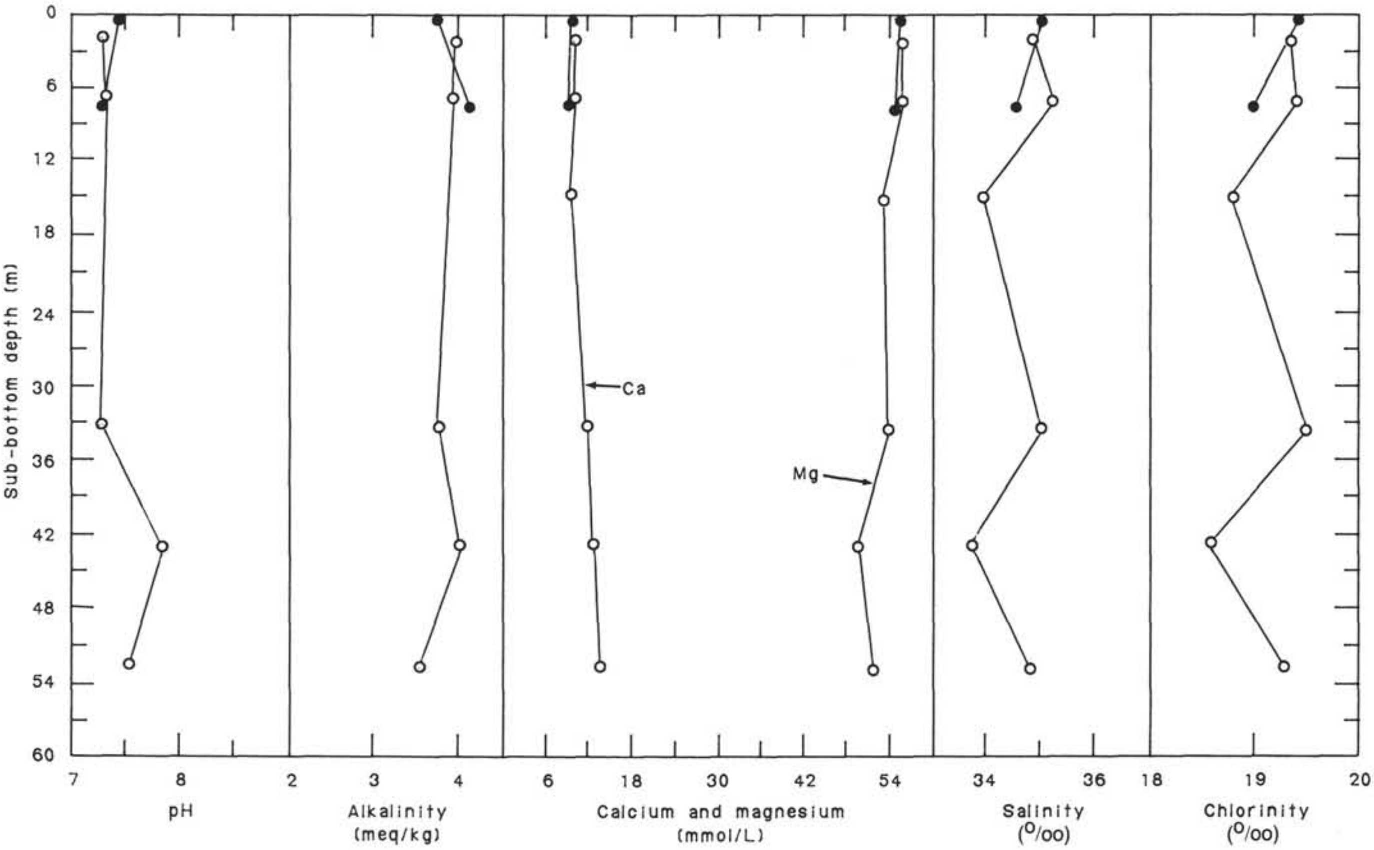

Figure 20. Summary of interstitial-water data, Site 639. Data from Hole 639A are plotted as open symbols, whereas data from Hole 639B are plotted as solid symbols. All data are given in Table 6.

mic velocity on the Hamilton Frame velocimeter. Index properties (bulk and grain density, water content, and porosity), as calculated on the basis of weights obtained from a triple-beam balance and volumes obtained using the shipboard Penta-Pycnometer densitometer, were measured for the same samples used for seismic-velocity measurements. A second bulk-density value for these same samples was also measured in special 2-min GRAPE analyses. Index-property samples were analyzed for carbonate content using the carbonate bomb (see "Inorganic Geochemistry" section, this chapter; Müller and Gastner, 1971).

Thermal Conductivity

Thermal-conductivity measurements were made on sediment from Cores 103-639A-1R through 103-639A-8R (0–70 m sub-bottom), Core 103-639B-1R (0–7 m sub-bottom), Cores 103-639C-1R and 103-639C-2R (78–100 m sub-bottom) in Neogene ooze and underlying undated mud, and Core 103-639D-5R (207–216 m sub-bottom) in a marl interval below dolomite (Fig. 22A). Except two anomalously high near-surface values from Hole 639A, the thermal conductivity of Neogene ooze (lithologic Unit I; see "Sediment Lithology" section, this chapter) is low, ranging from 2.35 to as high as 2.72×10^{-3} cal $\times$ $°C^{-1}$ $\times$ cm^{-1} $\times$ s^{-1} (calories/degree Celcius-centimeter-second). Such few data points per hole limit reliable observation of trends; nevertheless, thermal-conductivity values do seem to increase with greater depth of burial in the Neogene ooze.

Thermal-conductivity measurements in the Lower Cretaceous marl of lithologic Unit III were made on sediment from Cores 103-639A-5R through 103-639A-8R (32–70 m sub-bottom) and from Core 103-639C-2R (91–100 m sub-bottom). This material has a higher thermal conductivity, ranging from 2.64 to 4.28×10^{-3} cal $\times$ $°C^{-1}$ $\times$ cm^{-1} $\times$ s^{-1} and averaging 3.41×10^{-3} cal $\times$ $°C^{-1}$ $\times$ cm^{-1} $\times$ s^{-1}; values increase with greater burial depth.

The single analysis of marl interbedded in dolomite from Core 103-639D-5R yields a moderate thermal-conductivity value of 3.61×10^{-3} cal $\times$ $°C^{-1}$ $\times$ cm^{-1} $\times$ s^{-1}.

Vane Shear

Vane-shear-strength measurements were made on sediments from the Neogene lithologic Unit I (see "Sediment Lithology" section, this chapter) in Cores 103-639A-2R through 103-639A-4R (2–32 m sub-bottom), Core 103-639B-1R (0–7 m sub-bottom), and Core 103-639C-1R (78–91 m sub-bottom); below this unit, drilling biscuits began to appear in the recovered material, and measurements were halted. Shear strength, low near the sediment/water interface, ranges from 3.3 to 6.6 kPa (kiloPascals) from 0 to 15 m sub-bottom (Fig. 22B). This may reflect drilling disturbance in the upper core, as may a similarly low value of 4.0 kPa measured in the single analysis from Hole 639C in Sample 103-639C-1R-2, 45 cm (79.95 m sub-bottom). Shear strength increases with depth at Hole 639A to 24.25 kPa in Sample 103-639A-3R-4, 70 cm (17.20 m sub-bottom) and to 35.33 kPa in Sample 103-639A-4R-1, 22 cm (21.72 m sub-bottom). The underlying sediment was too stiff to analyze without damaging the vane-shear-strength apparatus.

Compressional Seismic Velocity

Compressional seismic velocity was measured on sediments and sedimentary rocks over the entire depths of Holes 639A through 639F (Fig. 22C). The Neogene ooze (lithologic Unit I) generally increases in seismic velocity from 1.4 to 1.6 km/s in

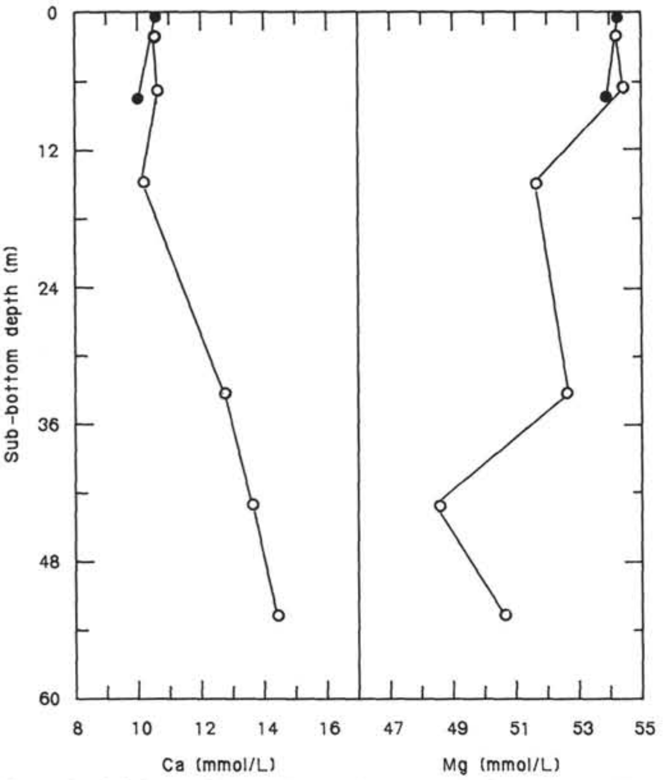

Figure 21. Calcium and magnesium cation concentrations in interstitial-water samples, Site 639. Data from Hole 639A are plotted as open symbols, whereas data from Hole 639B are plotted as solid symbols. All data are given in Table 6.

Cores 103-639A-1R through 103-639A-3R (0–22 m sub-bottom) and yields a seismic velocity of about 1.4 km/s in two samples from Core 103-639B-1R (0–7 m sub-bottom), of 1.6 km/s in Core 103-639C-1R (78–91 m sub-bottom), and of 1.4 km/s in the wash core through Neogene material at Hole 639D (Core 103-639D-1W, 0–178 m sub-bottom). Two low values in Core 103-639A-2R probably reflect severe drilling disturbance and possibly gas, as discussed in the Site 638 "Physical Properties" section (this volume). Reported velocities in the upper two cores of Hole 639A reflect a precision of ±0.05 km/s; below this and in all other cores at Site 639, precision is ±0.02 km/s.

The stiff brown mud of lithologic Unit II ("Sediment Lithology" section, this chapter) was analyzed for seismic velocity in Core 103-639C-2R (91–100 m sub-bottom); measured velocity is 1.6 km/s.

The stiff Lower Cretaceous marl (lithologic Unit III) in Cores 103-639A-4R through 103-639A-8R (22–70 m sub-bottom) shows an increase in seismic velocity from 1.7 to 2.2 km/s, one hard sample measuring 2.6 km/s in Core 103-639A-8R.

Below lithologic Unit III in Hole 639A, lithologic Unit I in Holes 639B and 639D, and lithologic Unit II in Hole 639C, a strong velocity contrast is generated by the extremely high velocities measured in the dolomite that composes lithologic Unit IV. Dolomite seismic velocities range from 5.9 to 6.9 km/s, averaging 6.5 km/s. The high velocities measured in unfractured laboratory samples may represent exaggerated values relative to those that would be calculated from seismic stratigraphic studies or measured during logging, given that the dolomite samples recovered contain numerous vugs and were evidently fractured and cemented during several episodes of brecciation and vein filling. The size of the dolomite samples measured in the laboratory is too small to take into account the widespread vugs and large-scale fractures, which would lower the average seismic velocity of the formation as a whole. On the other hand, dolomite fracturing may be largely confined to the faulted surface drilled at Site 639; thus, laboratory values may well represent *in-situ* values.

Fossiliferous limestone, clayey limestone, and marlstone were recovered below the dolomite, and their physical properties were measured in Hole 639D and at the top of Hole 639E (Cores 103-639D-4R through 103-639D-13R, 199–293 m sub-bottom, lithologic Unit V; Core 103-639E-1R, 199–209 m sub-bottom, part of lithologic Unit VI). These layers range in seismic velocity from a low of 3.0 km/s (marlstone; Sample 103-639D-10R-1, 61–63 cm; 255.11 m sub-bottom) to a high of 5.7 km/s (well-lithified limestone; Sample 103-639D-5R-2, 105–107 cm; 209.05 m sub-bottom). Silicified limestone from Sample 103-639D-12R-1, 80–82 cm; 284.2 m sub-bottom) yields a high velocity of 6.0 km/s. Seismic velocity in this unit reflects the nature of the lithology rather than the depth of burial. Higher seismic velocities (4.4–5.7 km/s) are observed in limestone, whereas lower velocities (3.0–4.0 km/s) correspond to clayey limestone.

Seismic velocity of 12 samples of widely varying lithology from Holes 639E and 639F, all denoted as lithologic Unit VI, was measured; results are listed in Table 8. Recovery in these holes was low, and the relationships of the different rock types is unclear (see "Sediment Lithology" and "Basement Rocks" sections, this chapter).

Index Properties

Gravimetric results of bulk-density and porosity analysis from Site 639 are plotted against depth in Figures 22D and 22E, respectively. In lithologic Unit I, bulk density increases from 1.6 to 1.7 g/cm^3, and porosity decreases from 72% to 62% in Cores 103-639A-1R through 103-639A-3R (0–22 m sub-bottom). A bulk density of 1.6 g/cm^3 occurs in the two samples of Unit I measured in Hole 639B (Core 103-639B-1R; 0–7 m sub-bottom), 1.8 g/cm^3 in Core 103-639C-1R (78–91 m sub-bottom), and 1.7 g/cm^3 in a single sample taken from the wash core, Core 103-639D-1W (washed 0–178 m sub-bottom, cored 178–180 m sub-bottom).

Bulk density of the stiff brown mud of lithologic Unit II in Core 103-639C-2R (95–97 m sub-bottom) is 2.0 g/cm^3, and porosity is 50%.

The Lower Cretaceous marl of lithologic Unit III increases in bulk density from 2.0 to 2.4 g/cm^3 in Cores 103-639A-4R through 103-639A-8R (22–70 m sub-bottom), with a corresponding decrease in porosity from 48% to 26%.

Bulk density of the dolomite in Cores 103-639A-9R and 103-639A-10R is 2.79 g/cm^3 (2-min GRAPE), about the same as that measured in the three cores containing dolomite in Hole 639B (Cores 103-639B-2R through 103-639B-4R; 64–80 m sub-bottom; 2.81 g/cm^3, 2-min GRAPE) and in the dolomite from Core 103-639D-3R (187–197 m sub-bottom; 2.85 g/cm^3, 2-min GRAPE). Dolomite porosity is generally low, ranging from 2% to 9%. The limestone and clayey limestone from Cores 103-639D-4R through 103-639D-13R (199–293 m sub-bottom) ranges from 2.51 to 2.69 g/cm^3 in bulk density (2-min GRAPE); porosity ranges from 9% to 16%. The single sample of silicified limestone from Sample 103-639D-12R-1, 80–82 cm (284.2 m sub-bottom), has a bulk density of 2.69 g/cm^3 (2-min GRAPE) and a measured porosity of 1%. As with seismic velocity, bulk-density and porosity values do not follow a depth-related trend.

Two-minute GRAPE analyses on the same samples corroborate these bulk-density measurements, yielding values that are generally within 5% of the gravimetrically obtained bulk-density measurements except in lithified samples. Gravimetric bulk-density results from these samples are generally too high, yielding bulk-density values that exceed the density of pure dolomite or calcite. We attribute this discrepancy to the small sample size used in analysis of the dolomite and limestone for gravimetric

Table 7. Carbonate-bomb data, Site 639.

Sample (interval in cm)	Sub-bottom depth (m)[a]	Carbonate (%)	Lithology[b]
103-639A-1R-1, 63–65	0.21	20	Calcareous clay
103-639A-1R-2, 67–69	0.73	80	Clayey nannofossil ooze
103-639A-2R-1, 15–19	2.45	9	Olive-gray clay
103-639A-2R-1, 73–75	3.03	87	Clayey nannofossil ooze
103-639A-3R-1, 105–107	13.05	74	Clayey nannofossil ooze
103-639A-3R-2, 105–107	14.55	88	Clayey nannofossil ooze
103-639A-3R-3, 105–107	16.05	76	Clayey nannofossil ooze
103-639A-3R-4, 105–107	17.55	61	Nannofossil marl
103-639A-4R-1, 17–19	21.67	0	Clay
103-639A-5R-1, 100–102	32.90	42	Nannofossil marl
103-639A-5R-2, 94–95	34.34	49	Nannofossil marl
103-639A-6R-1, 123–124	42.83	57	Nannofossil marl
103-639A-6R-2, 123–126	44.33	60	Nannofossil marl
103-639A-7R-1, 77–78	51.97	54	Marl
103-639A-7R-1, 94–96	52.14	56	Marl
103-639A-7R-2, 60–61	53.30	52	Marlstone
103-639A-7R-3, 35–37	54.55	68	Marlstone
103-639A-8R-1, 27–29	61.07	74	Clayey limestone
103-639A-8R-1, 98–100	61.78	56	Marlstone
103-639A-8R-2, 28–30	62.58	64	Marlstone
103-639A-9R-1, 12–14	72.63	97	Dolomite
103-639A-10R-1, 45–47	80.55	100	Dolomite
103-639A-10R-2, 115–117	82.75	96	Dolomite
103-639B-1R-1, 71–72	0.71	55	Nannofossil marl
103-639B-1R-1, 101–102	1.01	23	Calcareous clay
103-639B-1R-3, 63–64	3.63	3	Olive-gray clay
103-639B-1R-3, 100–105	4.00	70	Clayey foraminiferal–nannofossil ooze
103-639B-1R-5, 52–54	6.52	68	Clayey nannofossil ooze
103-639B-2R-1, 67–69	64.17	100	Dolomite
103-639B-3R-1, 44–45	66.94	100	Dolomite
103-639B-4R-1, 31–33	76.31	100	Dolomite
103-639C-1R-2, 52–54	80.02	72	Clayey nannofossil ooze
103-639C-2R-1, 48–50	91.28	0	Brown clay
103-639C-2R-2, 4–6	92.34	0	Varigated brown and pinkish clay
103-639D-1W-1, 40	178.0	15	Calcareous clay
103-639D-3R-1, 82–84	188.12	96	Dolomite
103-639D-5R-1, 52–53	207.02	20	Calcareous silty clay
103-639D-5R-1, 125–127	207.75	87	Clayey limestone
103-639D-5R-2, 105–107	209.05	90	Clayey limestone
103-639D-6R-1, 77–70	216.77	90	Clayey limestone
103-639D-7R-1, 48–50	266.08	55	Marlstone
103-639D-7R-2, 85–86	227.95	39	Marlstone
103-639D-8R-1, 40–42	235.60	76	Clayey limestone
103-639D-9R-1, 37–39	245.27	90	Clayey limestone
103-639D-10R-1, 61–63	254.11	62	Marlstone
103-639D-11R-1, 22–24	265.82	98	Oncolitic limestone
103-639D-12R-1, 80–82	274.60	63	Marlstone
103-639D-13R-2, 139–141	286.29	94	Oncolitic limestone
103-639E-1R-1, 51–53	199.40	82	Clayey limestone
103-639E-2R-1, 56–62	209.66	98	Dolomite
103-639E-3R-1, 19–24	218.79	4	Quartzite
103-639E-3R-1, 24–27	218.84	0	Pisolite-bearing metamorphosed claystone
103-639E-3R, CC, 2–5	219.00	3	Rhyolite
103-639E-4R, CC, 0–4	228.20	0	Metamorphosed granule conglomerate

[a] Sub-bottom depths are calculated by the standard ODP method (see "Explanatory Notes" chapter, this volume). Sub-bottom depth indicates only the relative position of the rocks from within the cored interval because of the inherent problems of low recovery and addition of spacers between the rocks.

[b] Lithologic names are those used on visual core description forms.

analysis; because of low recovery, sampling of these lithologies was restricted. Because 2-min GRAPE analysis does not destroy samples as gravimetric analysis does (during carbonate-content analysis subsequent to gravimetric measurement), we were able to take samples large enough for accurate measurement.

Table 8 lists the bulk density and porosity of 12 samples taken from the widely varying lithologies recovered from Holes 639E and 639F. Sampling of these holes was restricted because of low recovery; in several samples, analysis was limited to seismic velocity and 2-min GRAPE bulk-density measurements on thin-section billets. The thin-section billet samples lack porosity data.

Figure 23 shows sediment and sedimentary-rock velocity plotted against bulk density of Site 639 materials. As in previous sites, sediments in area A (unlithified mud, marl, and ooze) show a positive correlation of more gentle slope than the material in area B, which encircles lithified material (dolomite, limestone, and clayey limestone).

Acoustic Impedances and Predicted Reflectors

Average bulk density and seismic velocity between the lithologic units of Site 639 change rapidly, implying a high reflectivity at unit interfaces. Figure 22F shows acoustic impedance (the product of compressional velocity and bulk density) plotted against sub-bottom depth. We calculated the reflectivity (R) between adjacent lithologic units using the equation

$$\frac{V_{p1}\rho_{b1} - V_{p2}\rho_{b2}}{V_{p1}\rho_{b1} + V_{p2}\rho_{b2}}$$

where V_p is compressional velocity and ρ_b is bulk density; the resulting reflectivities are listed beside the lithologic unit boundaries shown in Figure 22C.

Table 9 shows the average velocities and bulk densities of the lithologic units used to calculate impedances and reflectivities at Site 639; the strongest reflector is that between lithologic Unit IV (the dolomite) and lithologic Unit I, although any reflector between the dolomite or limestone and overlying unlithified sediment shows a high reflectivity. The velocity and density inversion between dolomite and underlying limestone also produces a significant impedance contrast, but seismic-reflection detection of the interface is not expected through the thick, high-impedance dolomite unit. Although none of the holes drilled at Site 639 recovered lithologic Unit V limestone juxtaposed against lithologic Unit I Neogene ooze, this juxtaposition may occur farther downslope. Thus, we calculated a reflectivity for this and other contacts not actually encountered during drilling; Table 9 also lists these hypothetical contacts and associated reflectivity coefficients.

Summary

Thermal conductivity of unlithified sediments from Site 639 in Neogene ooze show low values, averaging around 2.53×10^{-3} cal × $°C^{-1} \times cm^{-1} \times s^{-1}$ and possibly increasing with depth. Values of Lower Cretaceous marl increase with depth from 2.64 to 4.28×10^{-3} cal × $°C^{-1} \times cm^{-1} \times s^{-1}$. The single measurement on the marl that interbeds the dolomite yields a moderate thermal-conductivity value of 3.61×10^{-3} cal × $°C^{-1} \times cm^{-1} \times s^{-1}$. As mentioned in previous site reports, the increase in thermal conductivity is probably most closely related to the downhole decrease in porosity.

Vane-shear-strength measurements on Neogene sediments yields low values (3.3–6.6 kPa) in the upper 15 m of Hole 639A; below this depth, values are moderately low (35 kPa). The underlying sediment is too stiff to measure without damaging the shipboard vane-shear-strength apparatus.

Compressional seismic velocity generally increases with depth in unlithified sediments of Site 639. Neogene nannofossil ooze increases from 1.4 to 1.6 km/s from 0 to 22 m sub-bottom (Cores 103-639A-1R through 103-639A-3R); Lower Cretaceous marl beneath this ooze increases in seismic velocity from 1.7 to 2.2 km/s (Cores 103-639A-4R through 103-639A-8R). Below Neogene ooze and Lower Cretaceous marl, lithified dolomite and limestone create a strong velocity contrast. Compressional seismic velocity of dolomite varies little from an average of 6.5 km/s. Limestone values span a broader range from 3.0 to 5.7 km/s; lower velocities correspond to clayey limestones. The velocities measured in the dolomite may be higher than those measured during logging because they are derived from laboratory samples too small to average in the effects of widespread vugs and fractures in the dolomite formation, features which would lower the average formation velocity.

Bulk density and porosity in unlithified sediments of Neogene lithologic Unit I act as expected of near-surface sediments that have no burial history. Bulk density increases from 1.6 to 1.7 g/cm^3, and porosity decreases from 72% to 62% in Cores 103-639A-1R through 103-639A-3R (0–22 m sub-bottom). The stiff brown mud of lithologic Unit II has a bulk density of 2.0 g/cm^3 and a porosity of 50% in the single sample measured from this unit. In Hole 639A, Lower Cretaceous marl (lithologic Unit III) shows an increase in bulk density and a decrease in porosity with burial depth from 2.0 to 2.4 g/cm^3 and 48% to 26%, respectively. Some of this increase may be due to slight dolomitization of the marlstone near the contact with the underlying dolomite. The dolomite of Unit IV has a porosity range from 2% to 9% and an average bulk density of 2.8 g/cm^3 with little variation. The limestone and clayey limestone of Unit V ranges in bulk density from 2.5 to 2.7 g/cm^3 and in porosity from 9% to 16%; a single silicified limestone sample from Unit V (Core 103-639D-12R) has a bulk density of 2.7 g/cm^3 and porosity of 1%.

The porosity–depth values of Neogene nannofossil ooze in Hole 639A correspond closely to the empirical curves published by Bryant et al. (1981) for sediment containing 60%–80% clay-sized sediment and 75% carbonate, indicating that the sediment has never been buried more deeply. Lithologic Units II and III are characterized by an abrupt decrease in porosity. Empirical porosity–depth curves of fine-grained carbonate and terrigenous sediment mixtures of analogous composition compared to data from lithologic Units II and III (Bryant et al., 1981) imply that the Lower Cretaceous marl/marlstone (lithologic Unit III) occupied a significantly greater burial depth than that at which it is currently found. However, signs of cementation increasing downhole in lithologic Unit III present a serious complication, as discussed in the following text. The 50% porosity of the single sample of stiff brown mud of lithologic Unit II indicates an earlier burial depth of about 150 m, whereas the 29%–48% porosity range of lithologic Unit III marl/marlstone indicates a 500- to 2000-m burial depth. Empirical bulk-density–depth curves of fine-grained terrigenous and calcareous sediments published by Hamilton (1976) indicate a burial depth of around 400 m for the mud of lithologic Unit II and a previous burial depth of greater than 1 km for lithologic Unit III. There is disagreement on the exact depths indicated by these two comparisons, but both clearly imply that sediment compaction occurred in response to a greater overburden than currently exists at Site 639. The difference in previous overburden between lithologic Units II and III is at least a factor of 5 by both methods of empirical comparison; lithologic Unit II has been buried by much less overburden than has Lower Cretaceous lithologic Unit III.

This information may aid in identifying the age of lithologic Unit II. Barren of biostratigraphically significant fossils, lithologic Unit II overlies Lower Cretaceous lithologic Unit III and underlies Pliocene ooze at Site 639. The same brown mud is found in slumped Miocene beds in Core 103-638B-18R (see Site 638 chapter, this volume). The difference between estimated previous overburden (about 150 m) and current burial depth (about 100 m in Hole 639A) of lithologic Unit II is much less than the difference between estimated overburden (about 500–2000 m) and current burial depth (about 30–60 m in Hole 639A) of lithologic Unit III. Although Unit II overlies Lower Cretaceous Unit III, it may never have been buried as deeply and may thus be much younger.

One complication in the porosity-overburden relationship is the presence of pore-filling cement. Smear-slide descriptions of calcite-cemented clumps of sediment and dolomite rhombs in increasing abundance downsection in lithologic Unit III imply that the rapid decrease in porosity over a depth of 50 m is a function of both compaction and cementation. The porosity gradient from 48% to 26% for about 40 m is much steeper than that illustrated by Hamilton (1976) or Bryant et al. (1981). We suspect that this is due to prelithification by precipitation of calcite and dolomite in pore spaces, causing greater bulk density and lower porosity downhole, all with little effect on seismic velocity.

Although the presence of precipitated carbonate in the lower part of lithologic Unit III heightens the porosity gradient, porosity and bulk-density values (48% and 2.2 g/cm^3) at the top

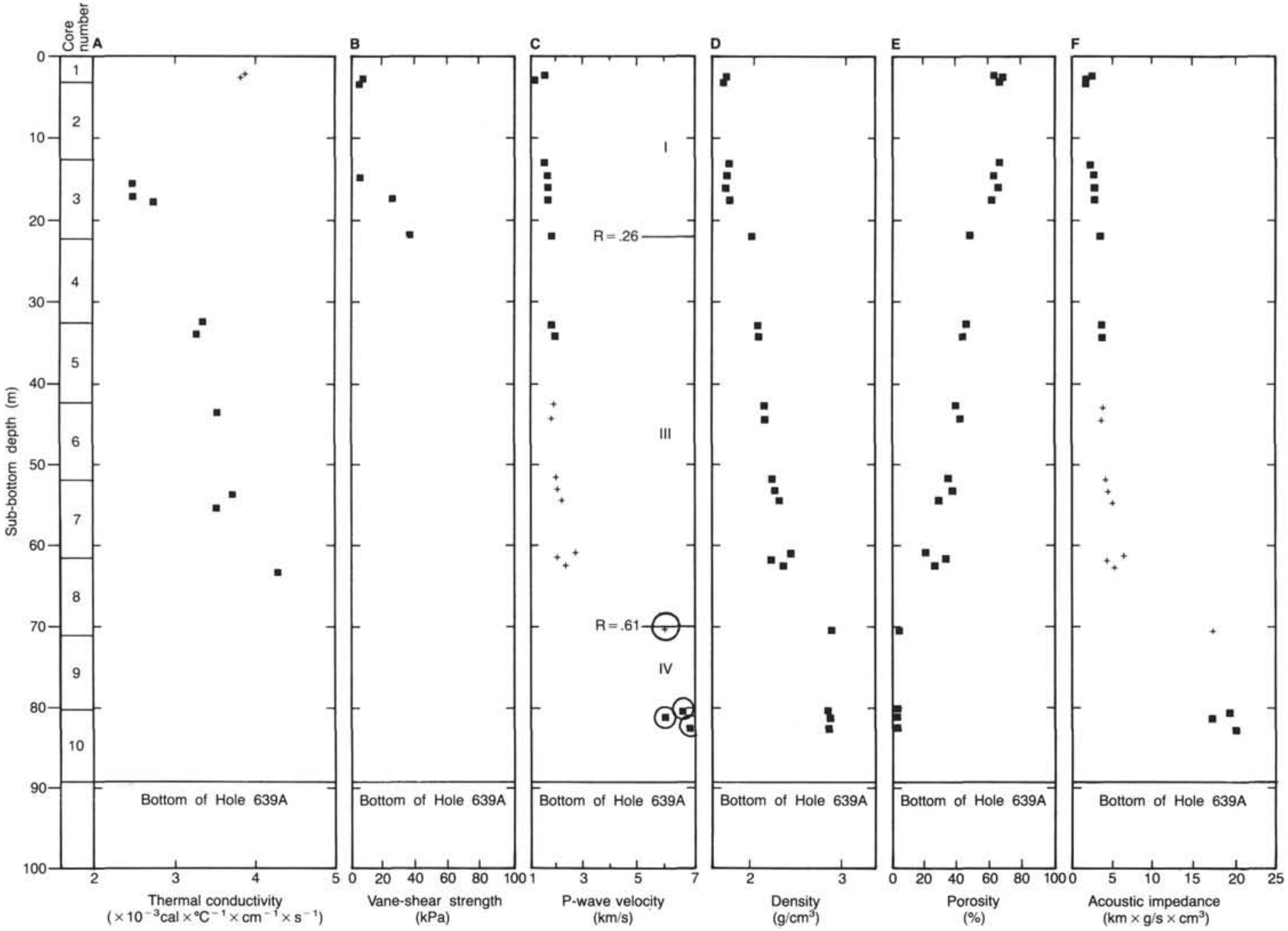
Core number
A
B
C
D
E
F
1
2
3
4
5
6
7
8
9
10
Sub-bottom depth (m)
0
10
20
30
40
50
60
70
80
90
100
I
R = .26
III
R = .61
IV
Bottom of Hole 639A
Thermal conductivity (× 10⁻³cal × °C⁻¹ × cm⁻¹ × s⁻¹)
2
3
4
5
Vane-shear strength (kPa)
0
20
40
60
80
100
P-wave velocity (km/s)
1
3
5
7
Density (g/cm³)
2
3
Porosity (%)
0
20
40
60
80
100
Acoustic impedance (km × g/s × cm³)
0
5
10
15
20
25

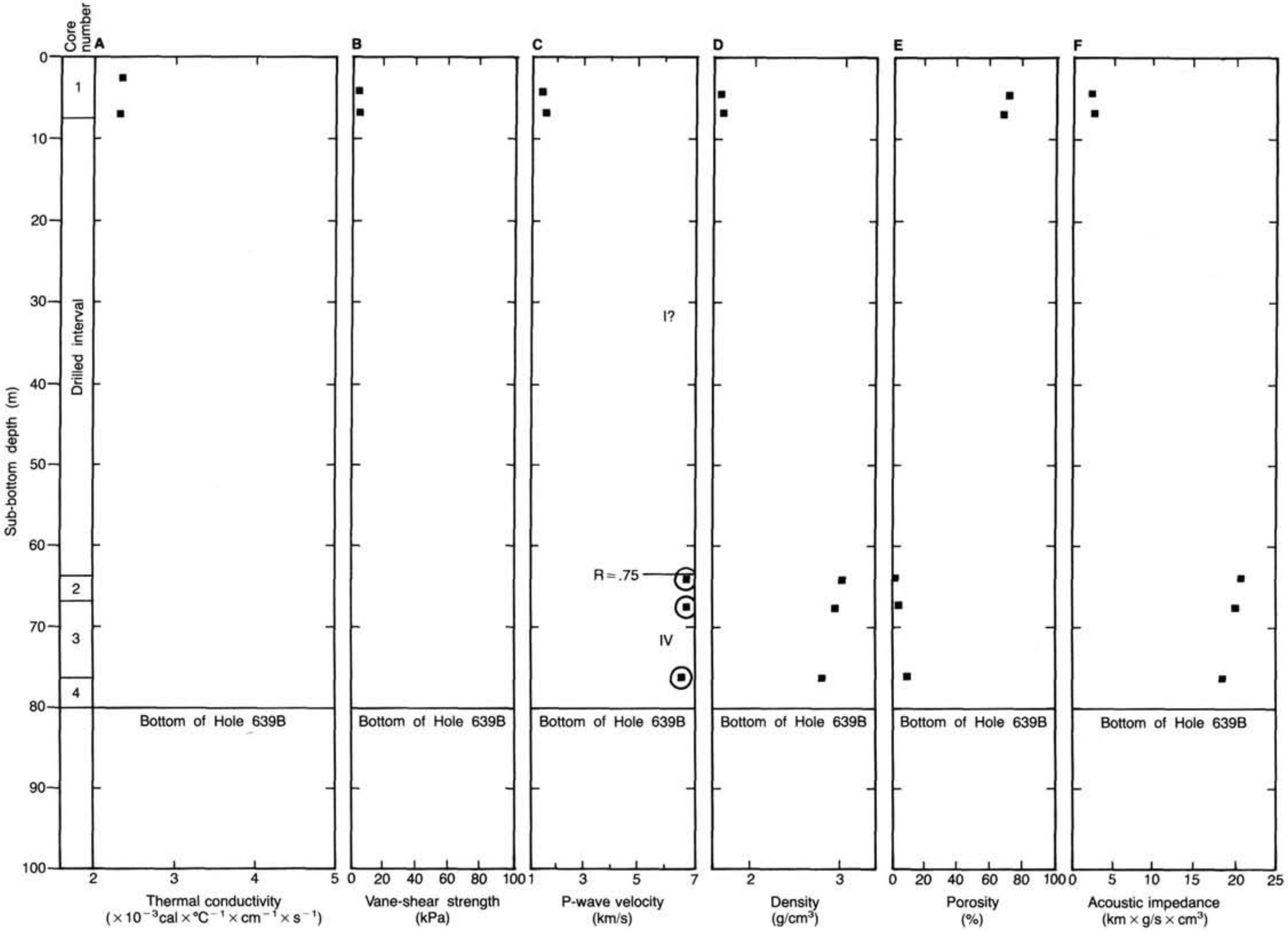

Figure 22. Physical-property measurements on sediments and sedimentary rocks from Site 639 plotted against sub-bottom depth. Lithologic units as described in the "Sediment Lithology" section (this chapter) are indicated on the right side of the column containing compressional seismic-velocity data. A. Thermal-conductivity values (× 10^{-3} cal × $°C^{-1}$ × cm^{-1} × s^{-1}). B. Vane-shear strength (kiloPascals). C. Compressional seismic velocity (kilometers per second). Square data points indicate velocities measured in the plane of the core diameter and parallel to the cut face of the core (b-direction); crosses indicate velocities measured perpendicular to the plane of the core diameter (a-direction). Dolomite data points are encircled, and limestone data points are enclosed by squares. Numbers next to the data points in Holes 639E and 639F correspond to numbers of samples described in Table 8. D. Bulk density (grams per cubic centimeter). E. Porosity (percent). F. Acoustic impedance (compressional seismic velocity × bulk density; g-km/cm^3-s).

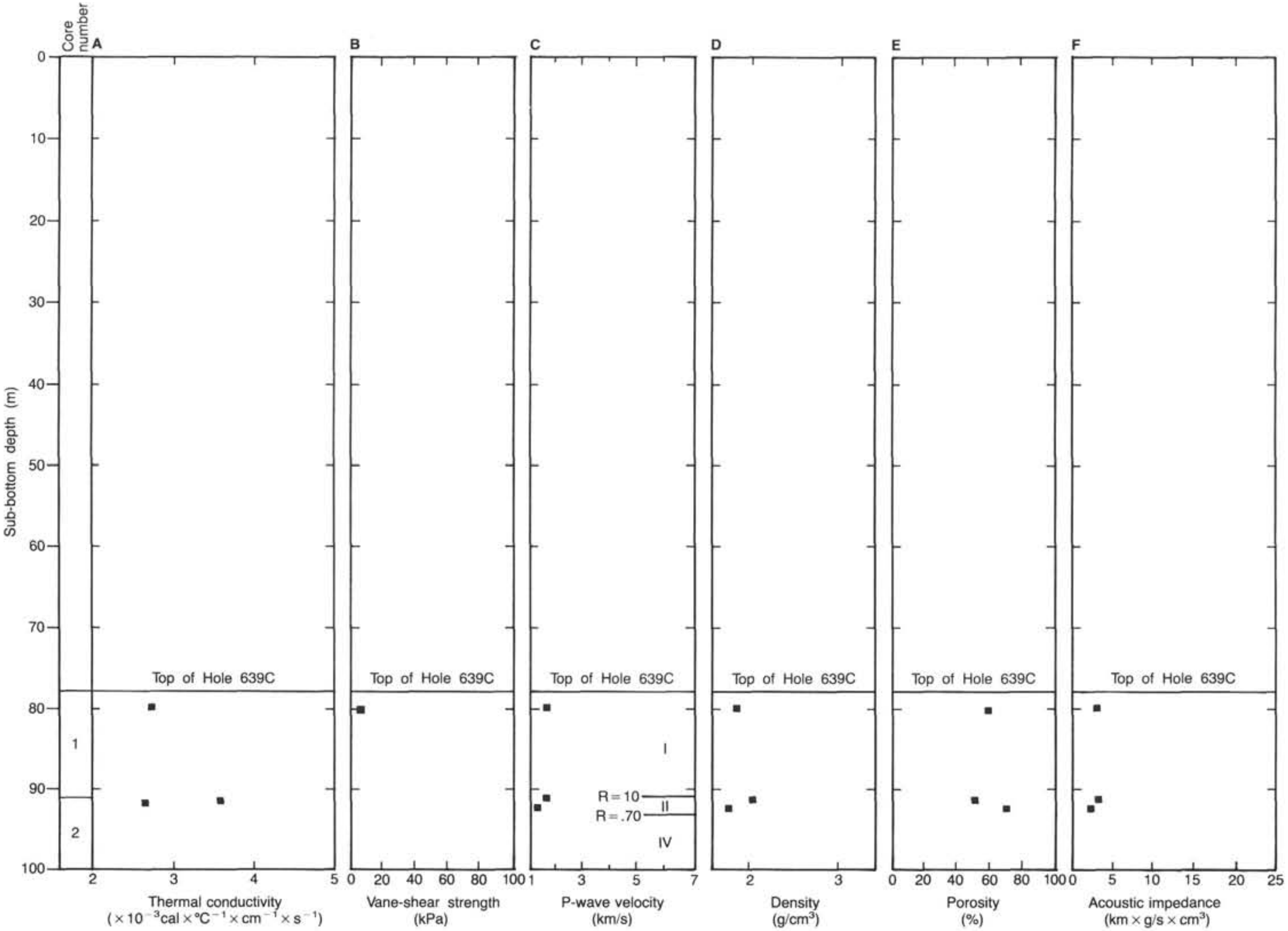
Core number
A
B
C
D
E
F
Sub-bottom depth (m)
0
10
20
30
40
50
60
70
80
90
100
1
2
Top of Hole 639C
I
R = 10
II
R = .70
IV
2
3
4
5
Thermal conductivity
(× 10⁻³cal × °C⁻¹ × cm⁻¹ × s⁻¹)
0
20
40
60
80
100
Vane-shear strength
(kPa)
1
3
5
7
P-wave velocity
(km/s)
2
3
Density
(g/cm³)
0
20
40
60
80
100
Porosity
(%)
0
5
10
15
20
25
Acoustic impedance
(km × g/s × cm³)

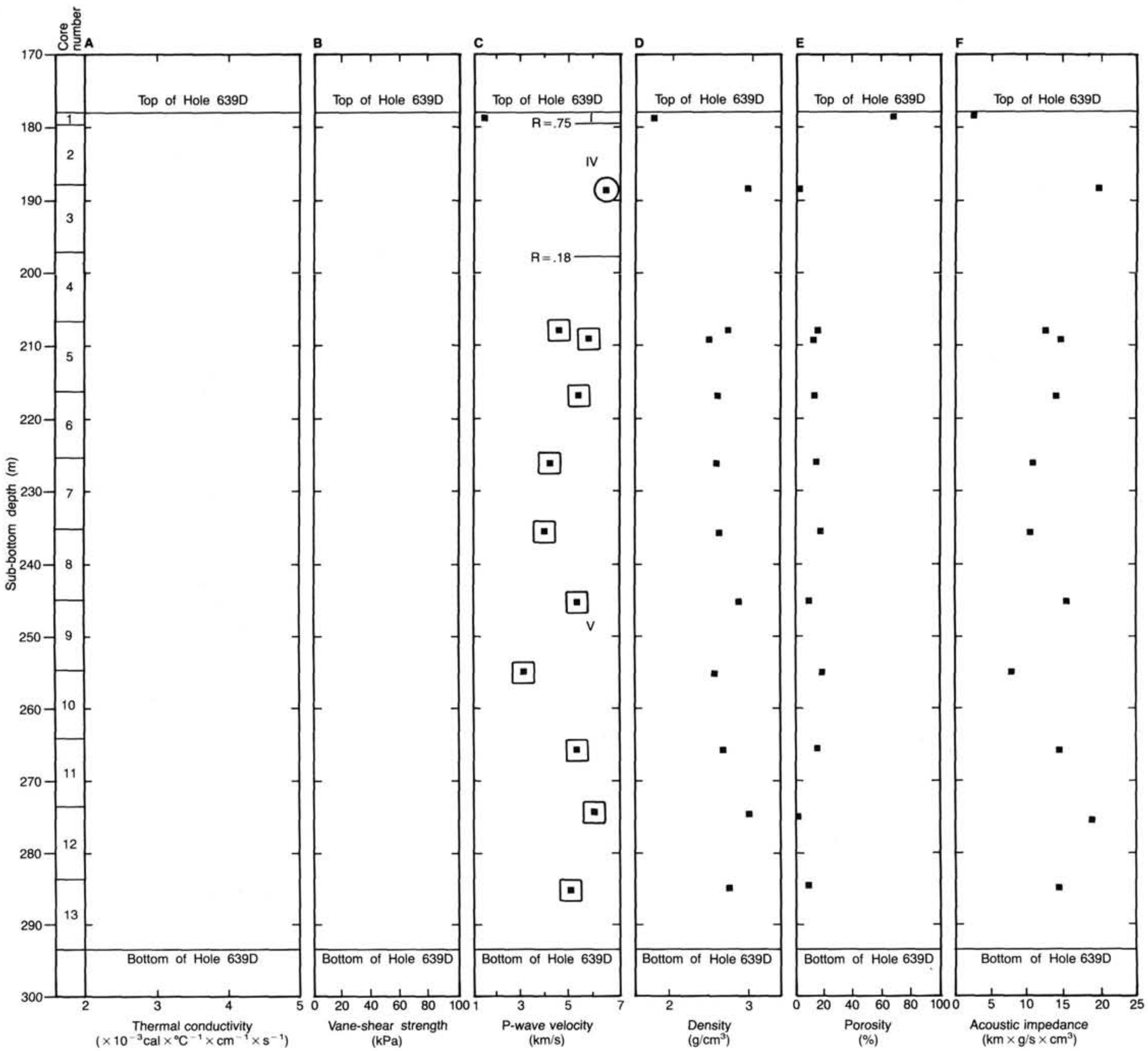

Figure 22 (continued).

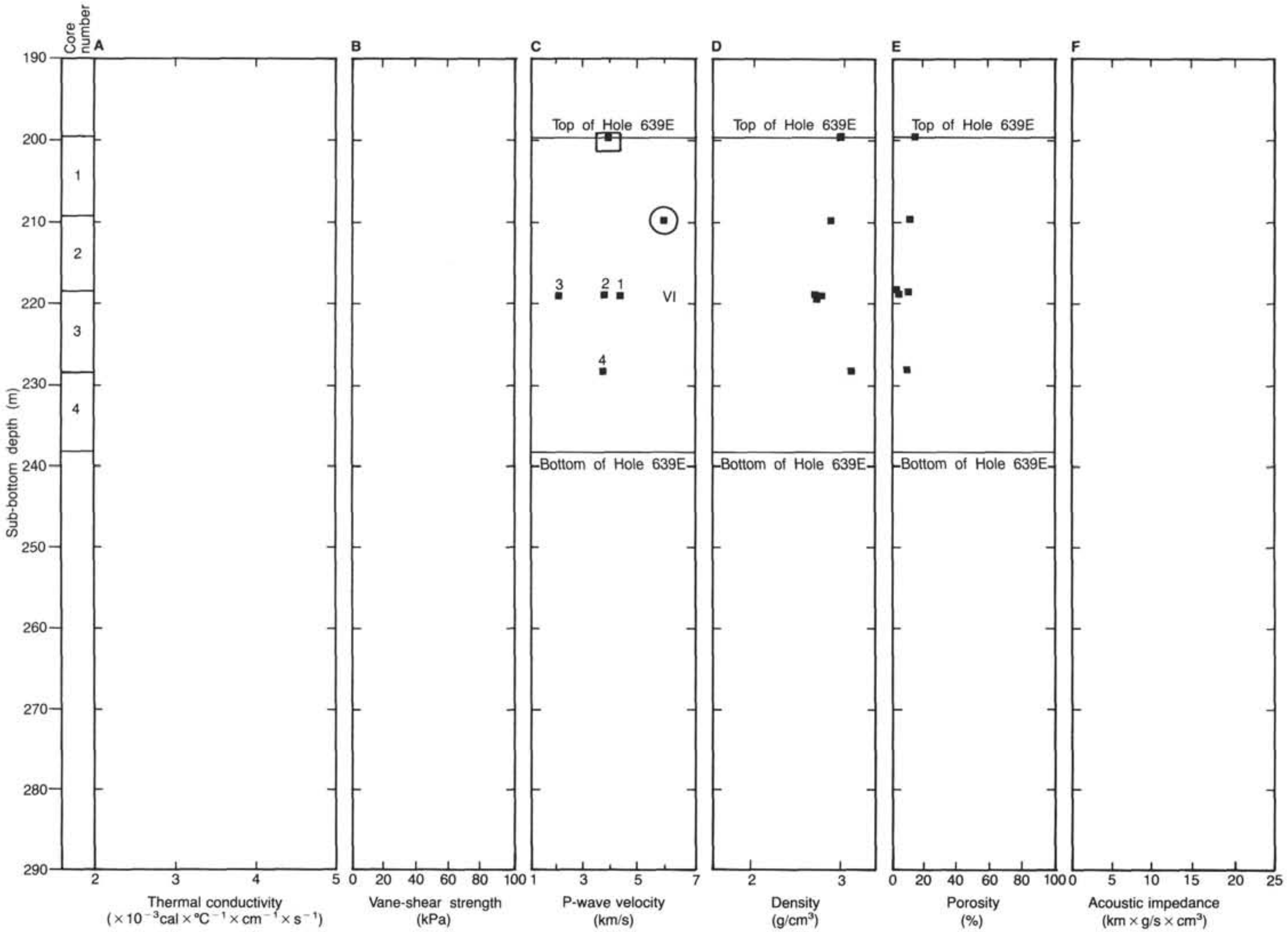
Core number
A
B
C
D
E
F
Sub-bottom depth (m)
190
200
210
220
230
240
250
260
270
280
290
1
2
3
4
Top of Hole 639E
Bottom of Hole 639E
3
2
1
VI
4
2
3
4
5
Thermal conductivity
(× 10⁻³cal × °C⁻¹ × cm⁻¹ × s⁻¹)
0
20
40
60
80
100
Vane-shear strength
(kPa)
1
3
5
7
P-wave velocity
(km/s)
2
3
Density
(g/cm³)
0
20
40
60
80
100
Porosity
(%)
0
5
10
15
20
25
Acoustic impedance
(km × g/s × cm³)

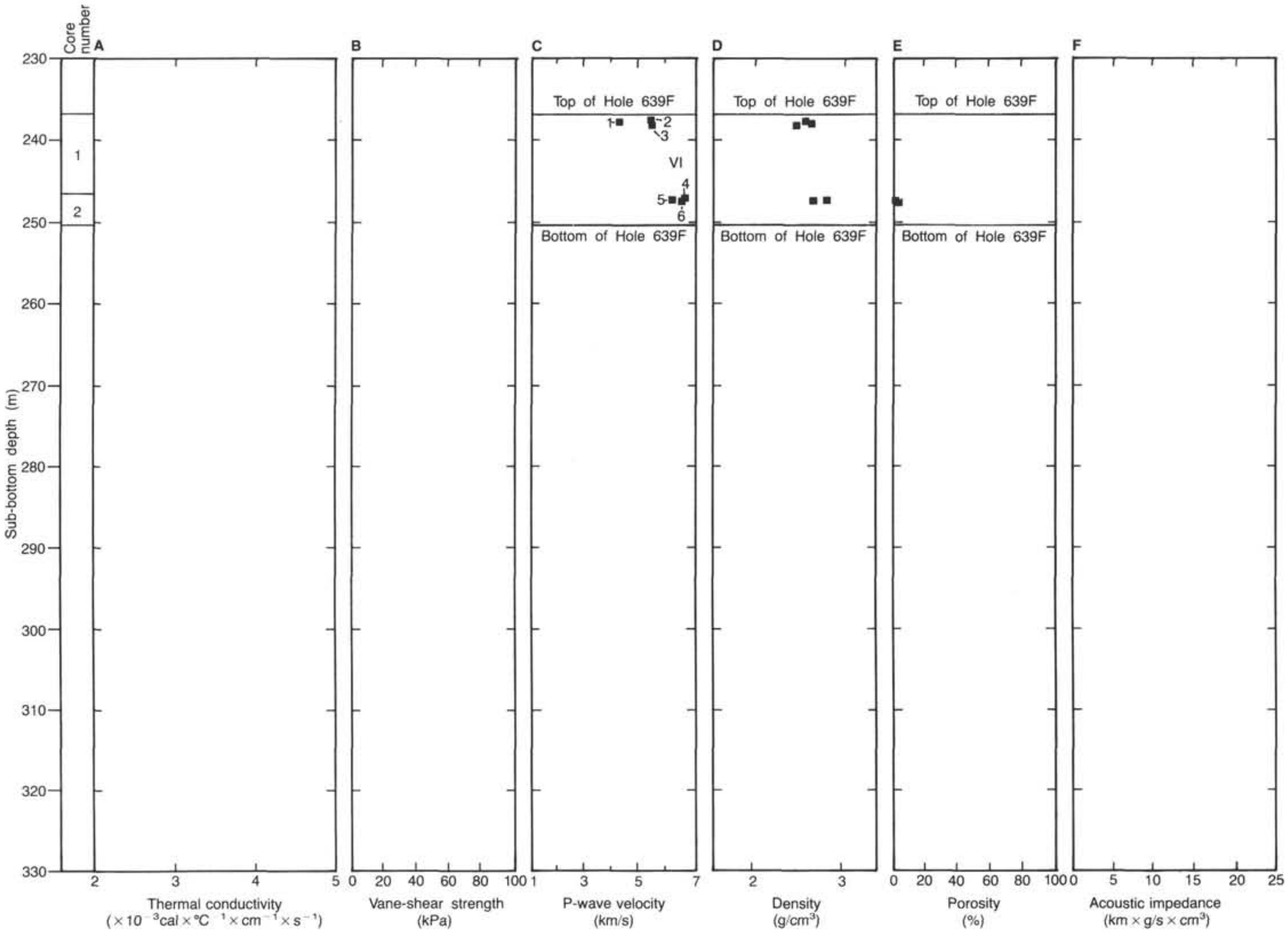

Figure 22 (continued).

Table 8. Compressional seismic velocity (V_p; km/s), bulk density (ρ_b; g/cm^3), porosity (%), and lithology of samples from Holes 639E and 639F. Bulk density is from 2-min GRAPE analysis; porosity values are based on gravimetric analysis. Numbers in parentheses before ODP sample numbers refer to numbered data points in Figure 22C.

Sample (interval in cm)	Sub-bottom depth (m)	V_p	ρ_b	Porosity[a]	Lithology
103-639E-1R-1, 53–55	199.40	3.78	2.64	12.3	Clayey limestone
103-639E-2R-1, 56–62	209.66	5.86	2.64	10.2	Vuggy dolomite
(1) 103-639E-3R-1, 19–24	218.79	4.24	2.69	1.6	Siliceous quartzite breccia
(2) 103-639E-3R-1, 24–27	218.84	3.65	2.75	8.5	Pisolite-bearing metaclaystone
(3) 103-639E-3R,CC (2–5)	219.00	1.94	2.48	3.1	Altered rhyolite/dacite
(4) 103-639E-4R,CC (0–4)	228.20	3.62	2.77	7.6	Metagranule conglomerate
(1) 103-639F-1R-1, 2-5	237.80	5.36	2.63	—	Laminated metaclayey sandstone
(2) 103-639F-1R-1, 10–12	237.90	4.22	2.71	—	Metasiltstone/sandstone
(3) 103-639F-1R-1, 37–40	238.17	5.37	2.52	—	Brecciated dolomite
(4) 103-639F-2R,CC (1–4)	247.31	6.58	2.76	1.2	Black quartz sandstone
(5) 103-639F-2R,CC (9–11)	247.39	6.13	2.54	0.8	Altered rhyolite/dacite
(6) 103-639F-2R,CC (18–20)	247.48	6.49	2.65	3.6	Altered rhyolite/dacite

[a] — Not determined.

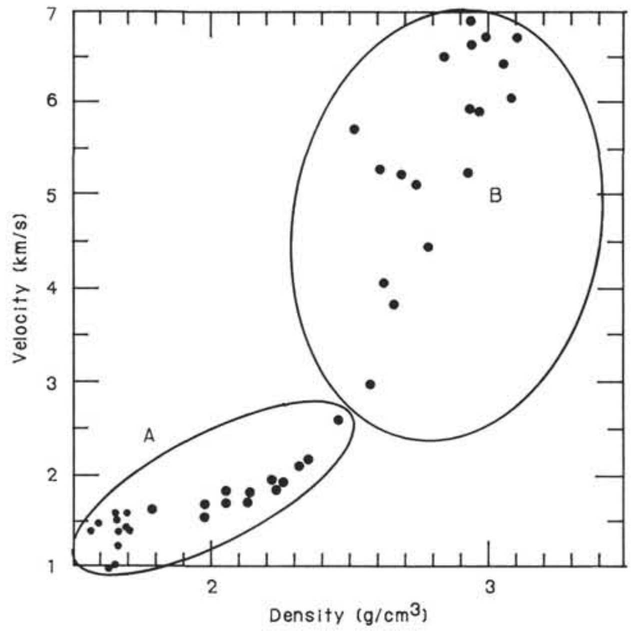

Figure 23. Bulk density plotted against compressional seismic velocity for samples from Holes 639A through 639D. Area A = unlithified material; Area B = lithified material.

Table 9. Average compressional seismic velocities (V_p) and bulk densities (ρ_b) used to calculate lithologic unit acoustic impedance ($V_p\rho_b$) and reflectivity (R) between lithologic units. Bulk density of Units IV and V based on 2-min GRAPE results.

		V_p	ρ_b	$V_p\rho_b$	R
Unit I	Neogene nannofossil ooze	1.5	1.7	2.6	0.10 (I/II) 0.26 (I/III) 0.75 (I/IV) 0.66 (I/V)
Unit II	Brown mud	1.6	2.0	3.2	0.16 (II/III) 0.70 (II/IV) 0.60 (II/V)
Unit III	Lower Cretaceous marl	2.0	2.2	4.4	0.61 (III/IV) 0.48 (III/V)
Unit IV	Dolomite	6.5	2.8	18.2	0.18 (IV/V)
Unit V	Limestone	4.7	2.7	12.7	

of lithologic Unit III still suggest an overburden of approximately 500 m, about three times greater than the overburden inferred for lithologic Unit II.

Density and porosity in lithologic Units IV and V do not follow depth-related trends.

Reflection coefficients calculated for acoustic contrasts between the lithologic units of Site 639 show strong reflectors between any combination of lithified units (lithologic units IV or V) against unlithified units (lithologic Units I, II, or III). A reflector generated at such a contact would probably result in the acoustic basement reflection, so the high impedance value of the thick Unit IV probably prevents detection of deeper acoustic-impedance contrasts, such as that between lithologic Unit IV and Unit V.

AGE-VS.-DEPTH CURVE

No age-vs.-depth curve was prepared for Site 639 because age control is so uncertain, even in the intervals that were continuously cored.

LOGGING RESULTS

Introduction

Geophysical logs were obtained at Hole 639D in three different runs using both Schlumberger and L-DGO tools. The first run recorded Schlumberger long-spaced sonic, dual-induction, gamma-ray, and caliper logs from 180 to 238 mbsf. The second run comprised Schlumberger lithodensity, neutron, and natural gamma-ray spectrometry tools run from 168 to 264 mbsf. The L-DGO multichannel sonic tool was run third from 168 to 245 mbsf. None of the runs successfully reached total depth (293 mbsf) because of impassable bridges at 238, 264, and 245 mbsf, respectively.

The borehole was drilled with a 9⅞-in. bit and filled with 9.7 lb/gal fresh gel mud. The 5-in. (outer diameter) drill pipe and 8¼-in. (outer diameter) drill collars were pulled up to 180 and 168 mbsf before logging. Logs were recorded as the tools were pulled uphole. Between the first and second run, a successful wiper trip enabled the succeeding tools to pass deeper into the hole.

Log Analysis

Three log-lithologic units were determined from the tool responses over the logged interval. These units are identified by distinct changes in the logs shown in Figs. 24 and 25. The ranges of these values are summarized in Table 10. Poor hole conditions, owing to wall rugosity and wash-out, prevented reliable log data in several intervals. These intervals are apparent in the logs where DT, ILD, SFLU, RHOB, and PEF values are low and NPHI readings are high.

Log-lithologic Unit A has gamma-ray values ranging from 10 to 37 API units (Fig. 24), probably corresponding to two sediment types of differing clay content. Clay-rich intervals have higher bulk-density, gamma-ray, and resistivity readings than do clay-poor intervals. The clay-poor intervals are probably washed out.

Log-lithologic Unit B has relatively constant gamma-ray values but large variations in sonic velocity, bulk density, and resistivity logs (Fig. 24). High velocity, density, and resistivity values and low porosity and photoelectric values correspond to dolomite intervals (Table 10). Elsewhere, low velocity, density, and resistivity values probably correspond to wash-outs or chalk intervals having similar log responses to the clay-poor intervals in Unit A.

Log-lithologic Unit C is divided into three subunits (Fig. 25). The clay content in these subunits is generally higher than in Unit A or B. The log data are reliable only in intervals where the borehole is narrow. Subunit C1 is severely washed out, but the gamma-ray log suggests a mostly calcareous mineralogy that includes one clay-rich layer between 204 and 208 mbsf. At the bottom of Subunit C1 (214 and 216 mbsf), a thick limestone layer has bulk-density and sonic velocity values of 2.65 g/cm^3 and 3.7 km/s, respectively. Subunit C2 is heterogeneous. The log responses suggest an alternating sequence of clay-rich and clay-poor layers of differing densities (Fig. 25). Subunit C3 has low gamma-ray readings of 20 API units, bulk-density values between 2.2 to 2.5 g/cm^3, and photoelectric-effect values of about 4.5 barns/electron, suggesting a primarily calcareous mineralogy.

Lithostratigraphic Correlation

The three log-lithologic units correlate reasonably well with the lithostratigraphic units described from the recovered cores (see "Sediment Lithology" Section, this chapter). This correlation is summarized in Table 11. In log Unit A, low gamma-ray values generally correspond to nannofossil ooze and chalk of lithologic Unit I. High gamma-ray values may represent calcareous clay intervals that were not recovered in Cores 103-639D-1R and 103-639D-2R.

Log Unit B correlates with the fractured and brecciated dolomite of lithologic Unit IV. Low log values probably correspond to intervals of nannofossil ooze and chalk that respond like Unit A chalk.

Log Subunit C1 corresponds to the upper part of the lithologic Unit V limestone. High gamma-ray values between 207 and 208 mbsf probably correspond to the marl recovered in Core 103-639D-5R, and low gamma-ray values to the skeletal-peloidal limestone identified in the rest of the subunit. Subunit C2 correlates with the clay-rich limestone, marl, clay, and sandstone sequence in the middle part of lithologic Unit V. In this interval, high gamma-ray and low density values correspond to marl and clay, and low gamma-ray and high density values to sandstone and limestone. Subunit C3 correlates with the oncolitic, skeletal-peloidal limestones in the lower part of lithologic Unit V.

SEISMIC STRATIGRAPHY

Because reflectors on the seismic line surveyed by the *JOIDES Resolution* are obscure, we used multichannel line GP-101, which is located less than 1 km north of Site 639, to project Holes 639A through 639F for seismic stratigraphic correlations, keeping the same distances from the nearby ridgecrest (Fig. 26) as on the *JOIDES Resolution* line.

At Site 639, seismic reflections from the seafloor and within the Neogene sequence cross hyperbolic traces of wave diffractions from the slopes of the ridge. Nevertheless, reflector R4 (Fig. 26), which lies beneath the Valanginian sandstone drilled at Site 638, clearly correlates with the top of the dolomite at Hole 639A, agreeing well with the physical-property studies (this chapter) that show a strong impedance contrast and reflectivity coefficient between lithologic Unit IV (dolomite) and overlying strata.

No coherent reflectors occur below reflector R4, now identified as the top of the carbonate platform, probably because the strong impedance contrast at R4 so attenuates sound energy that deeper reflectors are effectively masked. A weak and discontinuous reflector, labeled R5 on Figure 26, possibly corresponds to the top of crystalline basement.

SUMMARY AND CONCLUSIONS

Objectives

The plan at Site 639 was to core the entire sedimentary section below the level of the Lower Cretaceous syn-rift turbidite sandstone unit in which coring had ended at Site 638. Correlations between the sequence drilled at Site 638 and the seismic-reflection records had shown that a thickness of probably less than 100 m of syn-rift sediments separated the bottom of Hole 638C from the top of the strong seismic reflector identified as the top of an extensive carbonate platform, thought to represent the top of the pre-rift sequence. Dredge hauls about 6 km northwest and 13 km northeast of Site 638 had recovered pieces of limestone that indicated an age somewhere in the interval of Kimmeridgian–Berriasian for at least part of the sequence (Mougenot et al., 1985; Dupeuble et al., this volume), but we wanted to drill the complete sequence in stratigraphic order, with no gaps, and to continue coring into the basement rocks beneath the sedimentary column.

The following questions were to be answered:

1. What syn-rift sediments lie below the lowest level cored in Hole 638C? Are these deep-water turbidites, or does some kind of transitional facies exist between the turbidites and the presumably shallow-water carbonates below?
2. What is the nature of the contact at the top of the carbonate rocks? Was the platform gradually or suddenly drowned? Does an unconformity exist? Does a hardground, soil, or karstic surface occur?
3. What is the thickness and stratigraphy of the carbonate rocks, as indicated by lithology, age, and depositional environments? Are they, for example, *in-situ* platform strata, or might they have been resedimented in deeper water?
4. What underlies the carbonate strata? The red sandstone in one of the dredge hauls suggests a possible Triassic age, and the variety of metamorphic and igneous rocks in the same dredge suggests a complex basement geology.

Operational Obstacles and Their Effect on Strategy

Hole 639A was sited to give us answers to these aforementioned questions by providing one continuous sequence of cores, from the Valanginian syn-rift strata through the platform and

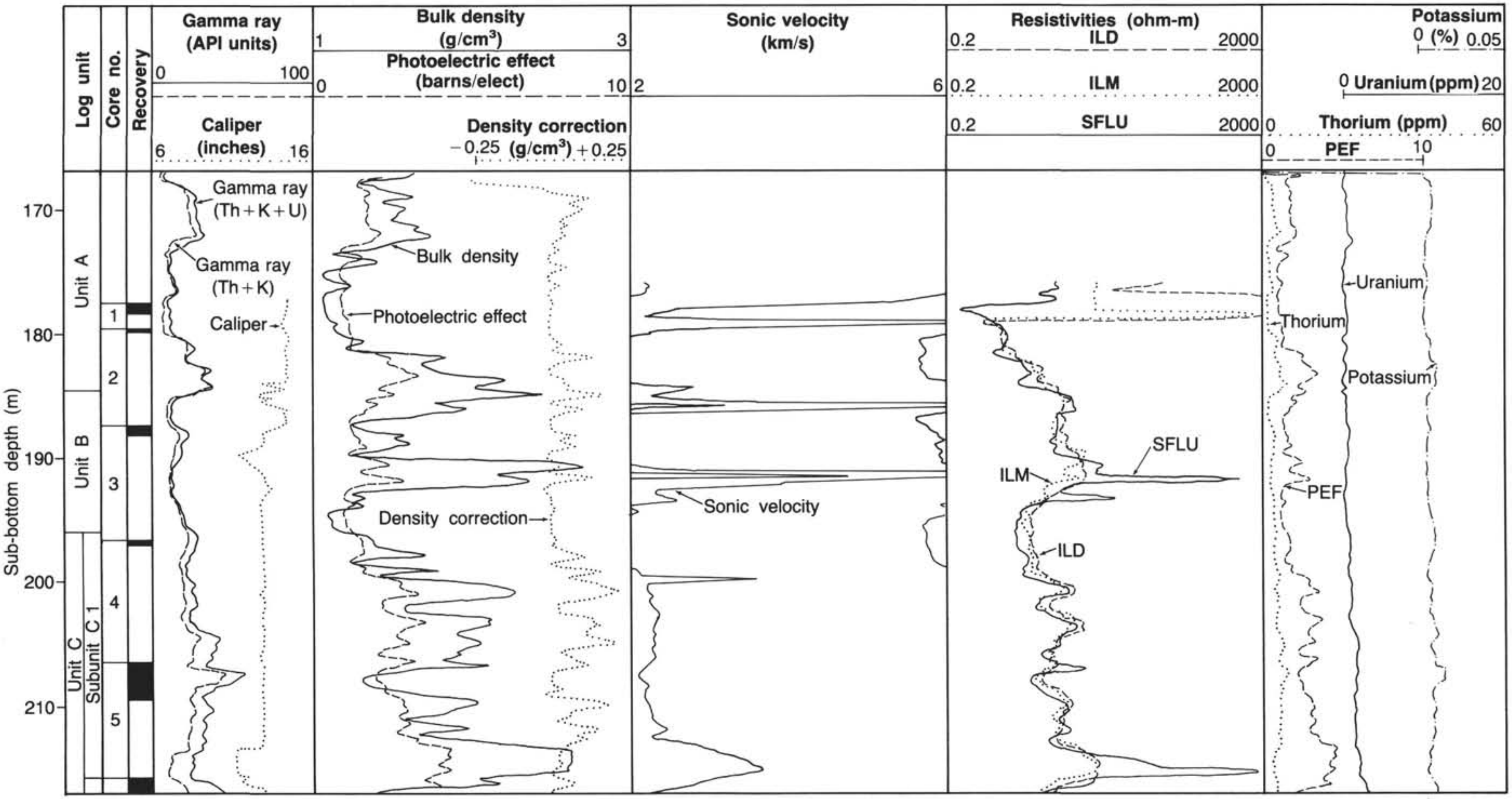

Figure 24. Composite logs and core recovery in log-lithologic Units A and B, Hole 639D. See text for description of logs.

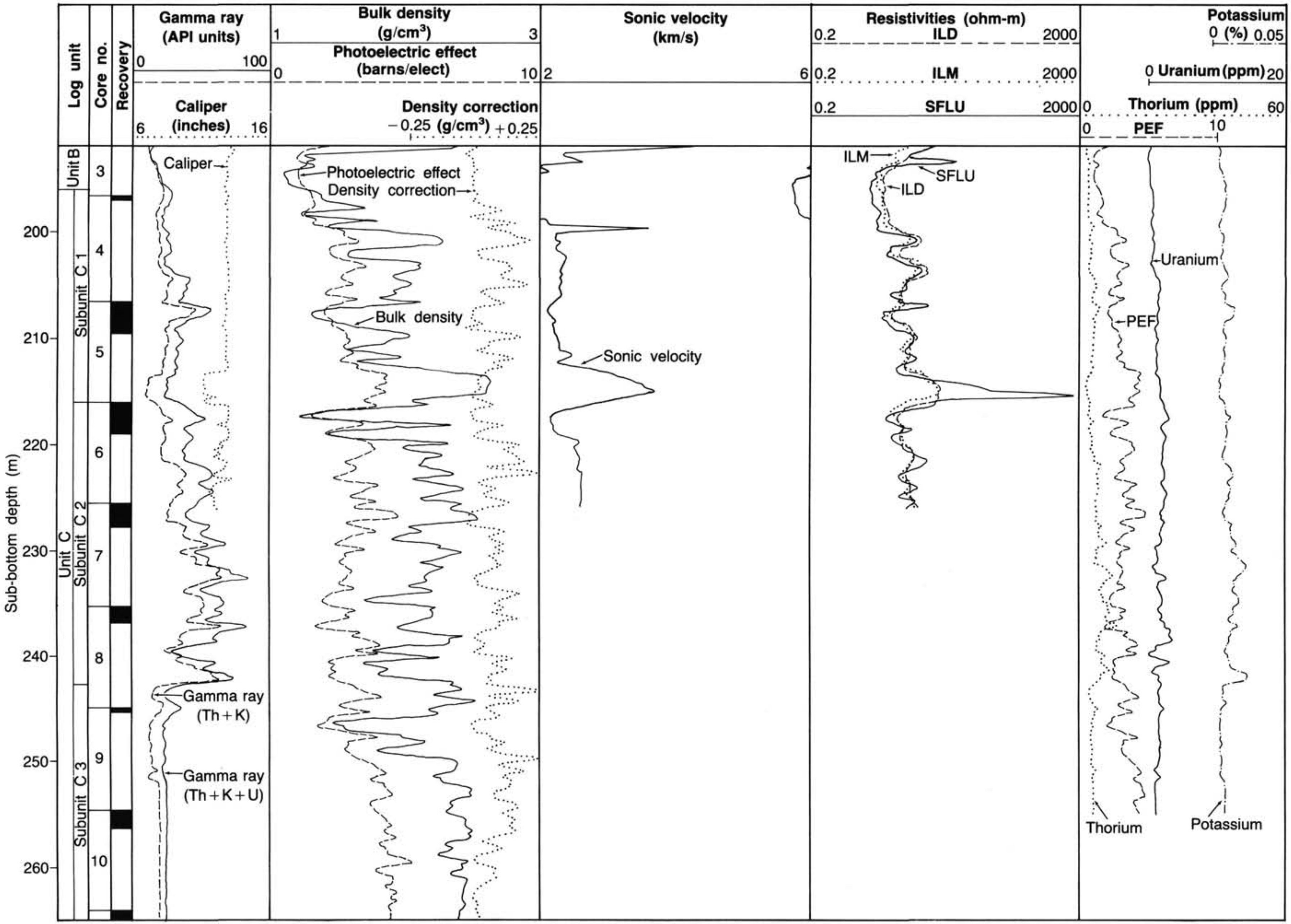

Figure 25. Composite logs and core recovery in log-lithologic Unit C, Hole 639D. See text for description of logs.

Table 10. Minimum/maximum values in log-lithologic units. GR = gamma ray (API units); VEL = sonic velocity (km/s); ILD = deep induction (ohmm); SFLU = spherical focused induction (ohmm); RHOB = bulk density (g/cm^3); PEF = photoelectric effect (barns/electron); POTA = potassium (% wt); THOR = thorium (ppm); URAN = uranium (ppm); NPHI = neutron porosity (%).

	Unit A	Unit B	Subunit C1	Subunit C2	Subunit C3
Depth	168–184.5	184.5–196	196–216	216–242.5	242.5–264
GR	10/37	10/22	20/56	38/85	20/35
VEL	1.7/2.8	1.8/7	2.0/3.7	No data	No data
ILD	1/5	2/10	3/15	No data	No data
SFLU	0.8/8	1.4/1000	2.1/1500	No data	No data
RHOB	1.1/1.8	1.1/2.7	1.3/2.65	1.7/2.55	1.5/2.5
PEF	1/3.3	1/2.8	1.5/4.2	2/4.6	2/4.5
POTA	0.001/0.01	0.002/0.007	0.001/0.012	0.001/0.02	0.001/0.003
THOR	1/5	1/3	2/3	3/10	1/3
URAN	0/1	0/0.5	1/2	1/3	1/2
NPHI	52/72	9/68	6/65	15/60	21/39

any underlying strata and into the basement, but technical drilling obstacles prevented our carrying out this simple, straightforward plan. We were forced to abandon Hole 639A after coring easily through the Neogene and Lower Cretaceous rocks when drilling conditions in the underlying fractured and vuggy dolomite became impossible. The dolomite is apparently too fractured and the fractured blocks are too loosely bonded together to maintain a firm hole for drilling. Pieces of dolomite, therefore, fell into the hole and lodged firmly against the drill collars, which are only about 3 cm smaller in diameter than the hole drilled by the bit. When enough of these pieces fall into the annulus between pipe and wall, the pipe will neither rotate nor move up or down. Since the amount of "overpull" allowed is about 40 or 50 tons beyond the total weight of the drill string suspended from the derrick, and since the pipe cannot be freed without exceeding this force, the only recourse was to lower a charge of explosives into the pipe to cut it off slightly above the problem area.

We then sited Hole 639B about 200 m west of Hole 639A, in the hopes that this location would be far enough west to be below the base of the dolomite, but we met dolomite there also, with the same results. This drilling obstacle blocked us throughout the entire campaign of drilling at Site 639, which eventually required six holes, located progressively farther west, to sample the entire section, Even then, only partial coverage of the complete stratigraphic section was cored, and of even that thickness only a tiny proportion was actually recovered as core.

Stratigraphy

From the bits and scraps recovered from the six holes, we pieced together a composite picture of the stratigraphic section at Site 639, which is portrayed in cross section in Figure 1. The cross section in Figure 27 shows an alternative interpretation that minimizes the stratigraphic thicknesses at Site 639 by taking into account the regional dip estimated from seismic-profile data and by postulating faults that steepen dips and repeat the section at Site 639. The details of the lithology, biostratigraphy, and physical properties of the sequence cored at each one of the six holes are shown in Figure 28.

The following paragraphs describe the stratigraphic section as inferred from the cored material, starting with the basement rocks and proceeding upward. For each unit, we also attempt an environmental reconstruction, as far as shipboard data will permit.

Basement Rocks

In the lowest part of the final core of Hole 639F and in the lowest part of the next-to-last core of Hole 639E, six pieces of silicic volcanic rock as much as 8 cm long were recovered. Only one small piece of rock (a fragment of conglomerate) was recovered in the final core from Hole 639E. We suspect that this piece was cored after having fallen into the hole from above while the pipe was being pulled up about 10 m off the bottom during the retrieval of the preceding core. We, thus, regard the pieces of volcanic rock as possible *in-situ* samples of basement rock, while recognizing the other possibility that the pieces may be from cobbles or boulders in a conglomerate and not from the basement itself.

The pieces, which are pinkish and similar in texture and mineral composition, consist of about 20% phenocrysts of alkali feldspar (~15%), quartz (2%–3%), muscovite and biotite, and altered mafic minerals (probably originally hornblende, plus accessory zircon, rutile [in biotite], magnetite, and apatite). The groundmass contains spherulites, interpreted either as a primary quench texture consisting of alkali feldspar and quartz or as secondary rosettes of alteration phases. In the groundmass are also fine-grained quartz, feldspar, and chloritized mica, perhaps representing altered glass. Phenocrysts are euhedral albitic plagioclase and probably sanidine, micas, and quartz as well.

The rocks are probably rhyolite or rhyodacite, and may be either volcanic or hypabyssal. Spherulites and altered minerals might indicate alteration under low-temperature, possibly hydrothermal conditions.

Possible Conglomerate Unit

Above the rhyolitic pieces in Cores 103-639E-3R, 103-639F-1R, and 103-639F-2R are many angular to subrounded (by drilling?) pieces of a great variety of rock types, including metagraywacke, metamorphic pisolitic argillite, metaconglomerate, which represent greenschist facies conditions, and mylonitic quartzite breccia. If these are *in-situ* samples of the basement, they were metamorphosed differently from the rhyolitic rocks. The variety of rock types suggests that they may be clasts in a layer of conglomerate or breccia resting depositionally on the basement. We attribute occurrence of supposed clasts from this conglomerate

Table 11. Preliminary correlation between log-lithologic and lithologic units at Hole 639D.

Log unit	Lithologic unit	Cores	Lithology
A	Unit I	103-639D-1W	Nannofossil ooze, marl, calcareous clay
B	Unit IV	103-639D-2R to 103-639D-3R	Brecciated dolomite, nannofossil ooze
C1	Upper Unit V	103-639D-4R to 103-639D-5R	Clay-rich, skeletal-peloidal limestone
C2	Middle Unit V	103-639D-6R to 103-639D-8R	Clay-rich limestone, marl, sandstone
C3	Lower Unit V	103-639D-9R to 103-639D-13R	Oncolitic, skeletal-peloidal limestone

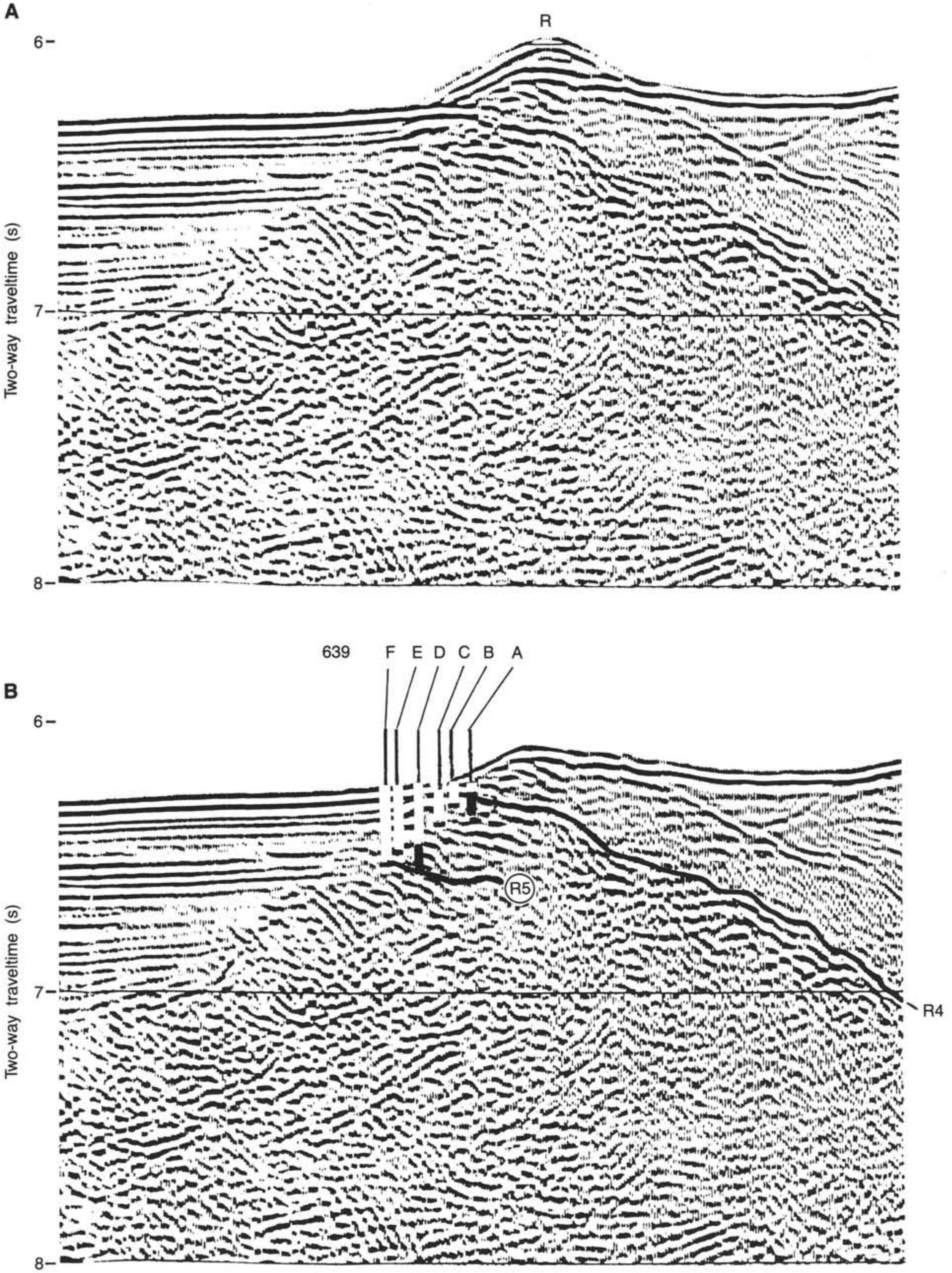

Figure 26. A. Section of IFP seismic line GP-101 (courtesy of L. Montadert). R = location of ridge top. B. The same section, but with diffractions removed from ridge R, showing the projected position of Holes 639A through 639F. For each hole, the Neogene section is shown in white and Mesozoic rocks in black. R4 = seismic reflector correlated with the top of the dolomite (lithologic Unit IV). R5 = top (?) of crystalline basement. Location of seismic profile shown in Figure 2.

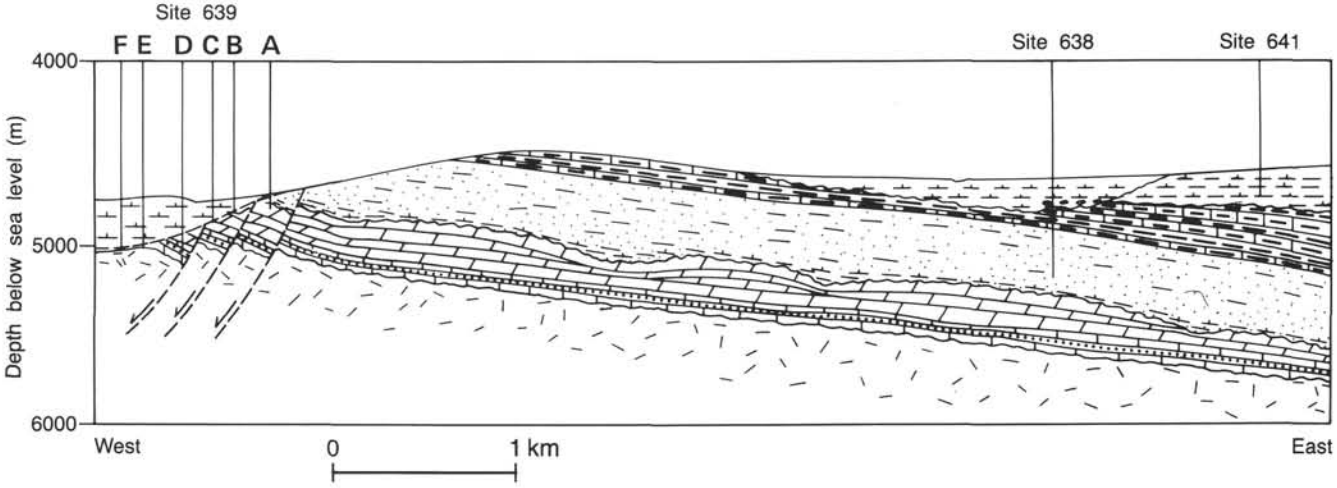

Figure 27. Geologic cross section through Sites 639, 638, and 641, as interpreted from drilling and seismic data. The faulting shown at Site 639 is schematic, and the irregular upper surface of the dolomite can also be interpreted as resulting from offsets by normal faults.

in Core 103-639F-2R, considerably lower than the top of basement (Fig. 1), to the clasts having been carried downslope as talus after deposition of the entire pre- and syn-rift sequence and tilting of the beds but before deposition of the Cenozoic deposits.

Limestone Unit (Lithologic Unit V in "Sediment Lithology" Section, This Chapter)

From Hole 639D, the cores consist of a sequence of limestone beds estimated to be at least 95 m thick (Fig. 1) interstratified with marlstone and with lesser intervals of sandstone and claystone, capped by about 18 m of fractured dolomite, probably in a talus unit. A 1-m interval of lithologically similar limestone occurs in Hole 639E, immediately beneath the Cenozoic sediments, where it is interpreted as being part of a rock slide (Fig. 1). We thus do not recognize any conformable contact between the limestone unit and the underlying or overlying units, and the true thickness must be estimated from indirect evidence. The position of the base of the unit is constrained only by the discovery of the metamorphic and igneous rock fragments in Hole 639E and by the position of the deepest sample from Hole 639D.

The position of the contact with the overlying dolomite is limited only by the position of the dolomite sampled in Hole 639C (assuming that the dolomite sample is in place and not part of a rock slide). Clues suggest that the contact may be located near Hole 639C: the slope changes somewhere between Holes 639C and 639D, and, given that the dolomite crops out on a steep slope between Holes 639B and 639C, whereas the limestone at Hole 639D underlies a gentle slope, the contact is plausibly placed at this change. The source of the limestone in the rock slide in Hole 639E, which requires an outcrop of limestone somewhere upslope, is problematic. The underlying dolomite slide breccia covers the outcrop at Hole 639D; hence, the source is farther up the slope, as suggested in Figure 1.

The limestone cored in Hole 639D is divided, on the basis of the lithology of the core material and of the characteristics seen on the downhole logs, into three informal subunits:

1. A lower interval about 42 m thick (stratigraphic) of oncolitic limestone, having skeletal-peloidal packstone to wackestone texture and abundant (~10%) oncoids in a finer grained peloidal matrix. Fossils include mollusks, ostracodes, and large benthic foraminifers, in particular *Anchispiracyclina lusitanica*, which is limited to the Tithonian. The somewhat impoverished fauna, the abundance of oncoids, and the lack of clastic detritus suggest a low-energy, fairly shallow-water environment, such as a shelf lagoon.
2. A middle unit of clayey limestone and sandstone, 25 m thick (stratigraphic). The limestone includes skeletal wackestone and fossiliferous mudstone, with large, agglutinated benthic foraminifers, mollusks, ostracodes, echinoderm debris, and rare oncoids. Marlstone and calcareous clay have coarse laminations of current-sorted benthic foraminifers. Sandstone beds are massive, poorly sorted, and as much as 15 cm thick. The sandstone is quartzose but contains feldspar and rounded carbonate bioclasts. Downhole logs show a possible cyclic repetition of about six sandstone-claystone-limestone sequences, each about 4 or 5 m thick. The clastic sediment suggests an environment near a stream mouth or tidal channel, but the poor core recovery makes precise determination of the depositional setting of this subunit difficult. The occurrence of clastic sediment near the top of the Jurassic section is widespread in Portugal and in offshore Canada and is commonly treated as signaling a regional regression.
3. An upper subunit of clayey limestone, about 17 m thick. The limestone is mainly skeletal-peloidal packstone and wackestone, and in some places the skeletal debris constitutes floatstone. Fossils include solitary corals (one of which is in an upright, growth position), both siliceous and calcareous sponges, mollusk fragments, serpulids, echinoderm debris, and large, agglutinated benthic foraminifers, identified as mainly *Anchispiracyclina lusitanica*. A few samples contain poorly preserved, recrystallized calpionellids. Minor interbeds of marlstone, calcareous silt, and claystone occur near the base of the subunit, suggesting a gradational contact with the middle subunit. The abundance of skeletal debris and the presence of calpionellids suggest an open, shallow-water-shelf depositional environment, perhaps near a bioherm.

Dolomite (Lithologic Unit IV in "Sediment Lithology" Section, This Chapter)

Dolomite occurs in every hole drilled at Site 639, but only in Holes 639A, 639B, and 639C do we think that the dolomite is more or less *in situ*. In the other holes, the dolomite has been transported as talus or rock slides. Even where the dolomite is in place, it is pervasively fractured, and only small fragments were generally recovered in the cores: we have only about 6 m of recovered samples from about 45 m of *in-situ* dolomite cored.

Because of incomplete coring, we know neither whether other types of lithology are interbedded with the dolomite nor the total thickness of the unit. Neither the upper nor lower contact with adjacent units was recovered intact in the cores. Assuming that no faulting occurred, the minimum thickness of the dolomite is about 215 m, measured from the highest sample recovered from Hole 639A to the lowest sample in Hole 639C. As discussed in the section on the thickness of the underlying limestone, we surmise that the limestone/dolomite contact is near Hole 639C, and the contact with the overlying Valanginian marlstone is within the interval cored in Core 103-639A-8R, probably near the bottom of the interval, judging by the performance of the drill string at the time the core was cut.

Dolomite is similar wherever it was cored in any of the six holes at Site 639. It consists mainly of a mosaic of fine- to coarse-grained subhedral crystals of dolomite. The porosity ranges from about 6% to 9% and is both intercrystalline and vuggy. Drusy dolomite crystals generally line the vugs, which tend to be somewhat elongate and crudely aligned within the rock. The dolomite is also cut by numerous fractures of two kinds: some are partly or completely filled with veins of coarse-grained dolomite, and some are entirely or partly filled with internal sediment consisting of yellowish dolomicrite containing debris of broken dolomite crystals. The dolomite in Holes 639D, 639E, and 639F is the most intensely fractured and veined; a connection may exist between this intense fracturing and the occurrence of the dolomite in these three holes as parts of talus deposits or rock slides.

The main types of dolomite are (1) light-gray grainstone and packstone and (2) dark grayish brown skeletal wackestone. Fossils still recognizable in the first type include echinoderm debris and gastropods; in the second type are echinoderm fragments, various gastropods and pelecypods, oncoids, and intraclasts. From this information, we infer that the depositional environment of the dolomite was probably shallow, in water of normal salinity, and perhaps included local bioherms.

The diagenetic history of the dolomite has been complex, and preliminary shipboard study of thin sections provides insufficient data to construct an unambiguous account. A tentative sequence of events is as follows:

1. Filling of primary voids in original limestone with penecontemporaneous calcite cement and internal sediment. Some dissolution.
2. Brittle fracturing and sparry calcite filling fractures.
3. Pervasive dolomitization.
4. Further dolomitization but along pathways, about which some divergence of opinion remains among the shipboard scientific party. This subject is discussed in several chapters in Part B of the Leg 103 volume.

No age can be assigned to the dolomite unit, other than that it is bracketed between the underlying Tithonian limestone and the overlying upper Valanginian marlstone; no age-diagnostic fossils were recognized in the dolomite.

Marlstone, Marl, and Minor Amounts of Sandstone (Lithologic Unit III in "Sediment Lithology" Section, This Chapter)

In Hole 639A below the Neogene ooze and resting on the dolomite is a stratigraphic thickness of about 36 m of pale-yellow to light-gray nannofossil and calpionellid marlstone and marl, mottled in pale brownish and pinkish shades. Near the top of the cored interval are thin layers of arkosic sandstone interbedded in the marl. The sequence doubtless continues upward into the Valanginian sandstone strata in which drilling terminated in Hole 638C, but we have no precise way of knowing how much section, if any, was missed in the drilling of the two holes. From the arguments presented in the "Seismic Stratigraphy" section in Site 638 chapter (this volume), we estimate that only tens of meters separate the bottom of Hole 638C and the top of the carbonate platform, and the 36 m drilled at Hole 639A probably nearly fills that gap.

Most of the marl and marlstone is massive, without primary sedimentary structures. A few burrows occur, and color banding defines bedding in some intervals. Calcite-filled fractures cut the strata at many places, and limonite stains and iron/manganese spots and streaks indicate highly oxidized sediments.

The induration is greatest in the lower part of the sequence, and scattered small dolomite rhombs appear in smear slides from the lower 10 m.

Sandstone beds in the upper half of the sequence are laminated and have a mineralogy similar to the Valanginian sandstone sampled in Hole 638C. One piece shows water-escape structures.

The change in environment at the dolomite/marlstone contact is abrupt, and we were disappointed that the contact itself was not sampled in a core. One of the important objectives of Leg 103 was to sample the strata near this contact to document the history of drowning of the platform. The relative abundance of nannofossils and of calpionellids, together with the lack of any traces of a benthic fauna of larger invertebrates in the lower part of the marlstone sequence, suggests an accumulation site below the photic zone, in somewhat pelagic conditions.

The appearance of sandstone in the upper part of the sequence probably signals the first turbidity currents and suggests subsidence to even greater depths. The subsidence rate during the accumulation of the first few tens of meters of Valanginian marlstone and sandstone greatly exceeded the sedimentation rate; alternatively, the major subsidence preceded the accumulation of marlstone, during a time when no sediments were deposited.

Possible Talus and Rock-Slide Deposits

The highly fractured and veined pieces of dolomite in Holes 639D, 639E, and 639F and the limestone above the dolomite in Hole 639E are regarded as materials dislodged from the slopes above, where *in-situ* dolomite and limestone occur, and transported down to their present positions by talus falls and rock slides, as shown on Figure 1. For these rocks to represent *in-situ* strata requires complicated stratigraphic and structural conditions, and we prefer the resedimentation hypothesis because of its relative simplicity. In Hole 639F, we also include the pieces of metamorphic and sedimentary rock above the rhyolitic pieces. The talus hypothesis explains the severe fracturing of the dolomite and the inversion of the expected stratigraphic order of dolomite and limestone. This hypothesis also may help explain the technical difficulties we had in trying to drill this material. We think that perhaps even the dolomite that we regard as *in-situ*, in Holes 639A, 639B, and 639C may be unstable partly because of fractures developed within incipient or potential slide masses on the steep submarine escarpment that marked the outcrop of the dolomite before burial beneath Cenozoic sediments.

Brown Clay (Lithologic Unit II in "Sediment Lithology" Section, This Chapter)

In Hole 639C, just above the fractured dolomite, is about 1.9 m of diffusely laminated brown clay, variegated in shades of pink and yellow. Patches of olive-colored silt and limonite-stained sand are present in the clay. The clay is devoid of fossils.

We do not know whether the brown clay occurs in any other hole at Site 639. The strategy at subsequent holes was to wash through the soft sediments until a hard layer was encountered; hence, no coring was intentionally done in soft sediments. Nev-

Hole 639A Location: 42°08.6′N, 12°14.9′W Water depth: 4735 m below derrick floor (4725 mbsl)

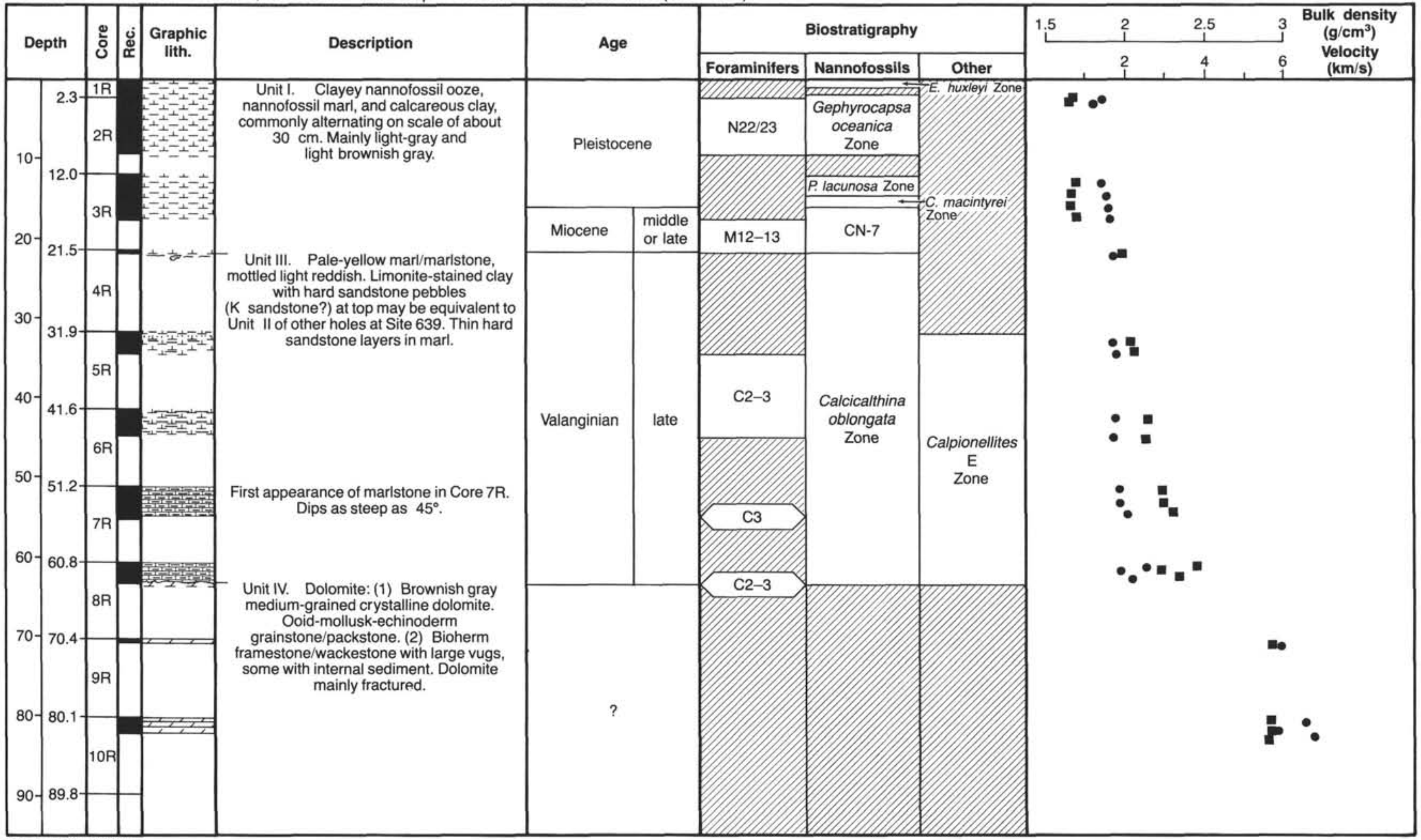

Unit I. Clayey nannofossil ooze, nannofossil marl, and calcareous clay, commonly alternating on scale of about 30 cm. Mainly light-gray and light brownish gray.

Unit III. Pale-yellow marl/marlstone, mottled light reddish. Limonite-stained clay with hard sandstone pebbles (K sandstone?) at top may be equivalent to Unit II of other holes at Site 639. Thin hard sandstone layers in marl.

First appearance of marlstone in Core 7R. Dips as steep as 45°.

Unit IV. Dolomite: (1) Brownish gray medium-grained crystalline dolomite. Ooid-mollusk-echinoderm grainstone/packstone. (2) Bioherm framestone/wackestone with large vugs, some with internal sediment. Dolomite mainly fractured.

Total depth 89.8 m

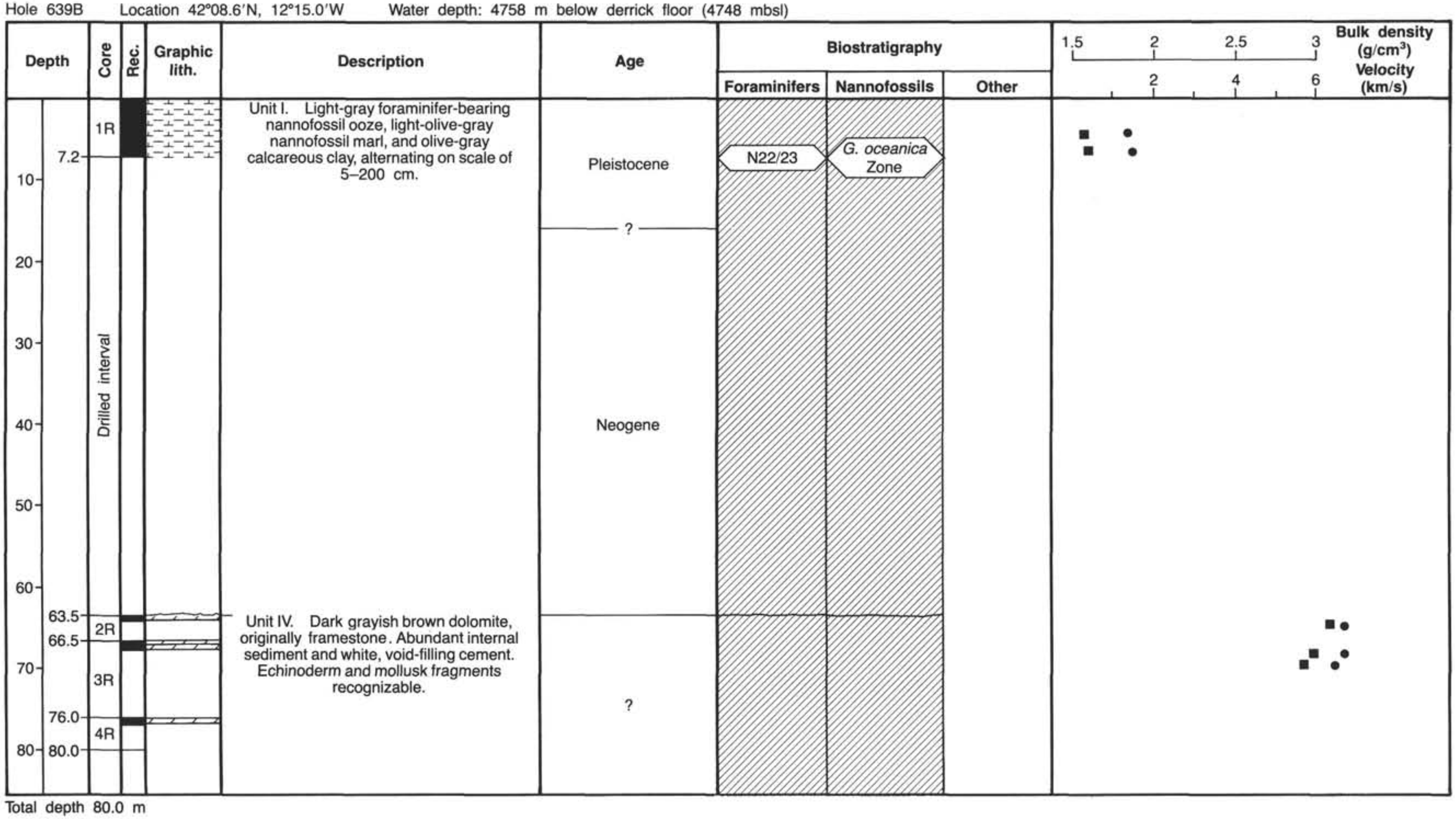

Figure 28. Summary logs, Site 639. Dots indicate velocity data points; squares indicate bulk-density data points.

Hole 639C Location: 42°08.6′N, 12°15.1′W Water depth: 4792 m below derrick floor (4782 mbsl)

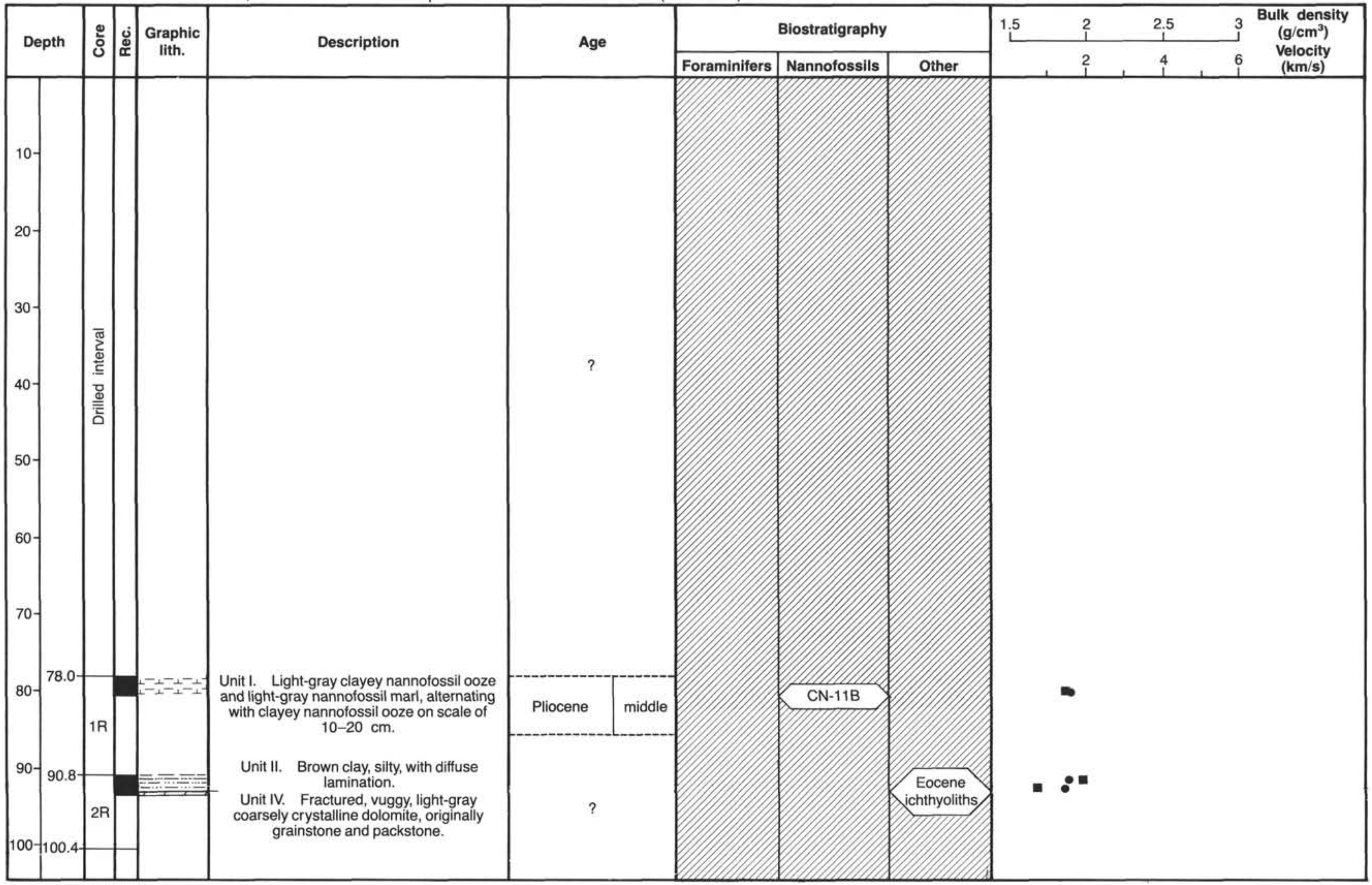

Total depth 99.8 m

Hole 639D Location: 42°08.6′N, 12°15.3′W Water depth: 4753 m below derrick floor (4743 mbsl)

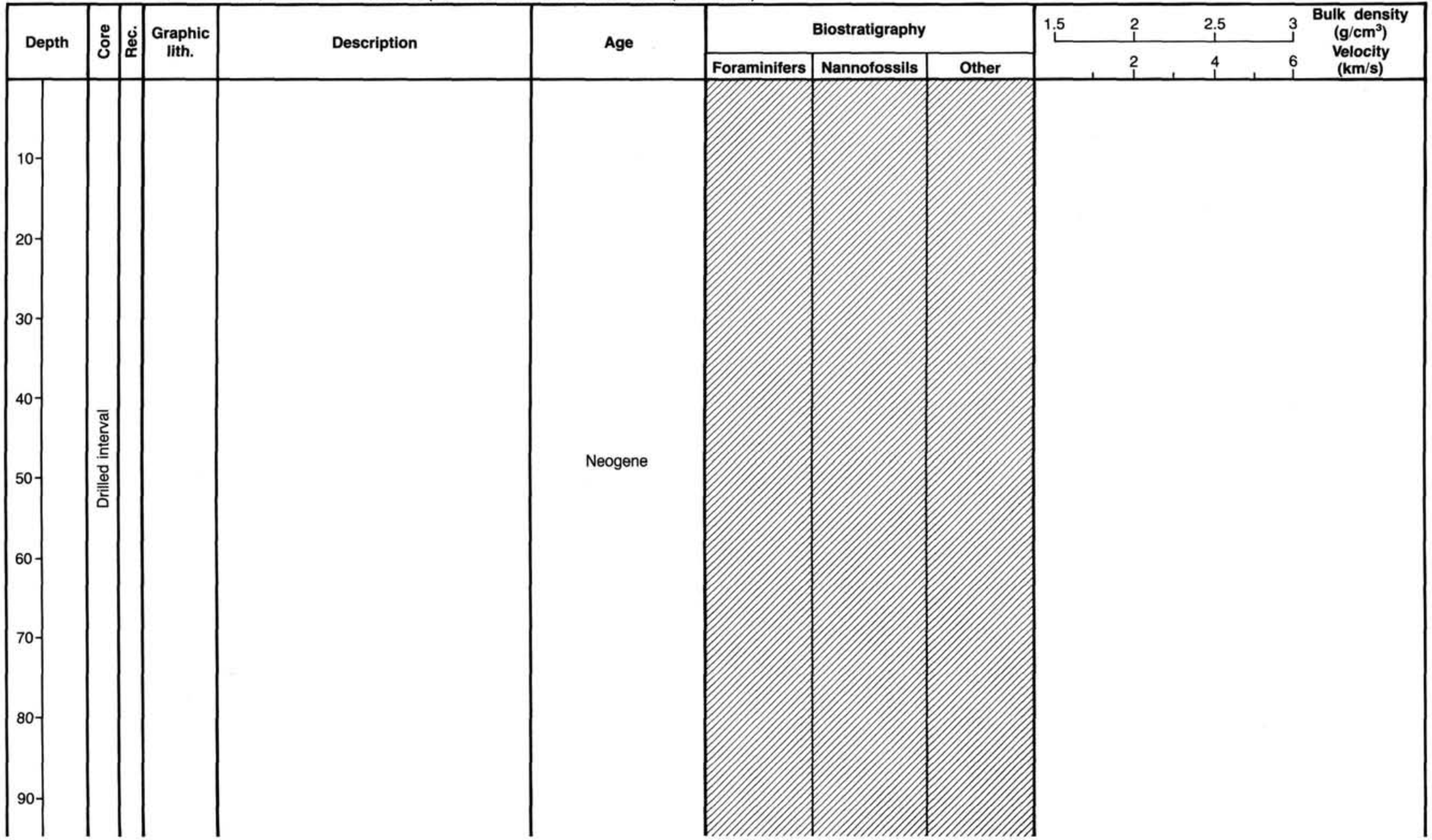

Figure 28 (continued).

Hole 639D (continued)

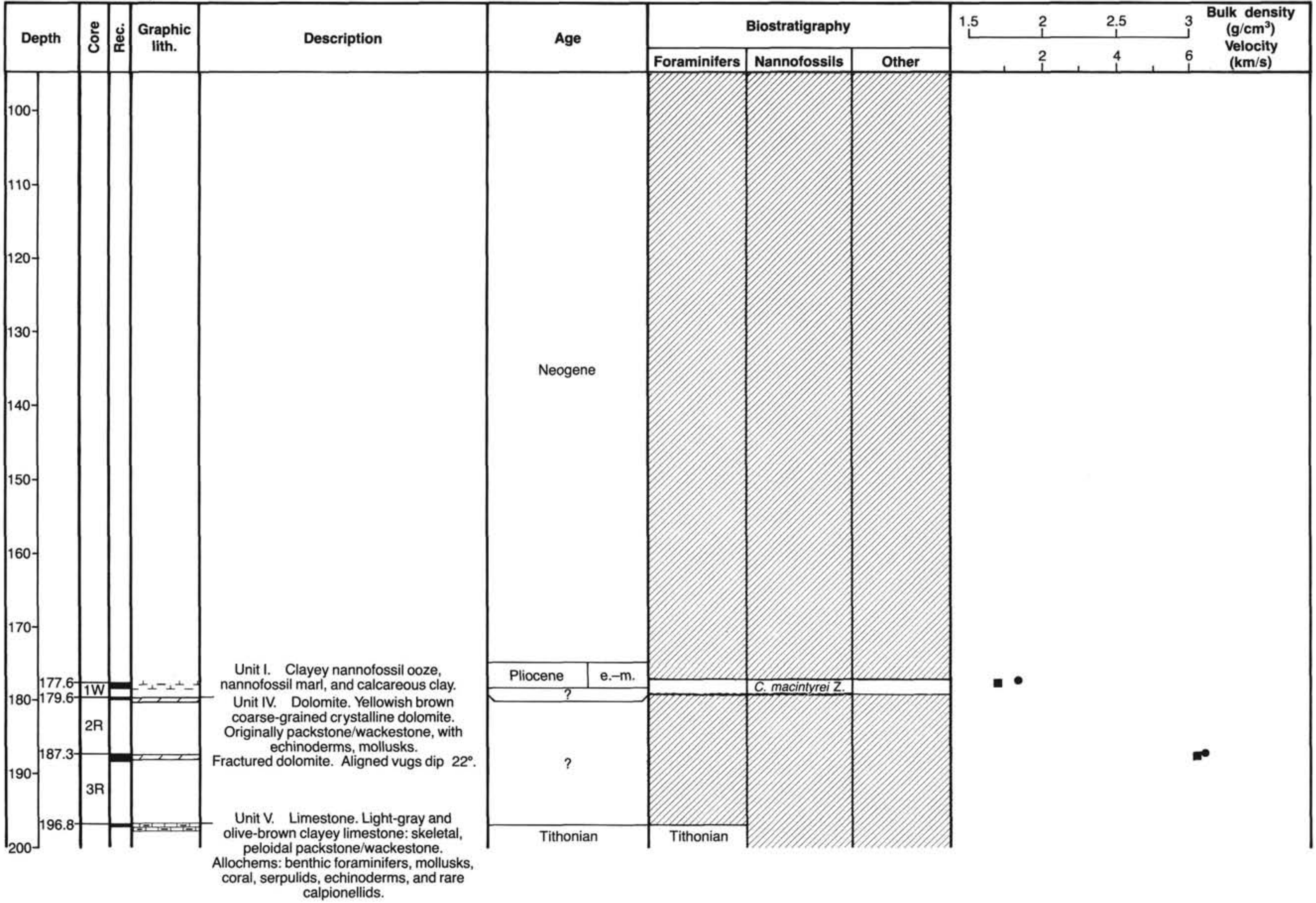

Unit I. Clayey nannofossil ooze, nannofossil marl, and calcareous clay.

Unit IV. Dolomite. Yellowish brown coarse-grained crystalline dolomite. Originally packstone/wackestone, with echinoderms, mollusks.

Fractured dolomite. Aligned vugs dip 22°.

Unit V. Limestone. Light-gray and olive-brown clayey limestone: skeletal, peloidal packstone/wackestone. Allochems: benthic foraminifers, mollusks, coral, serpulids, echinoderms, and rare calpionellids.

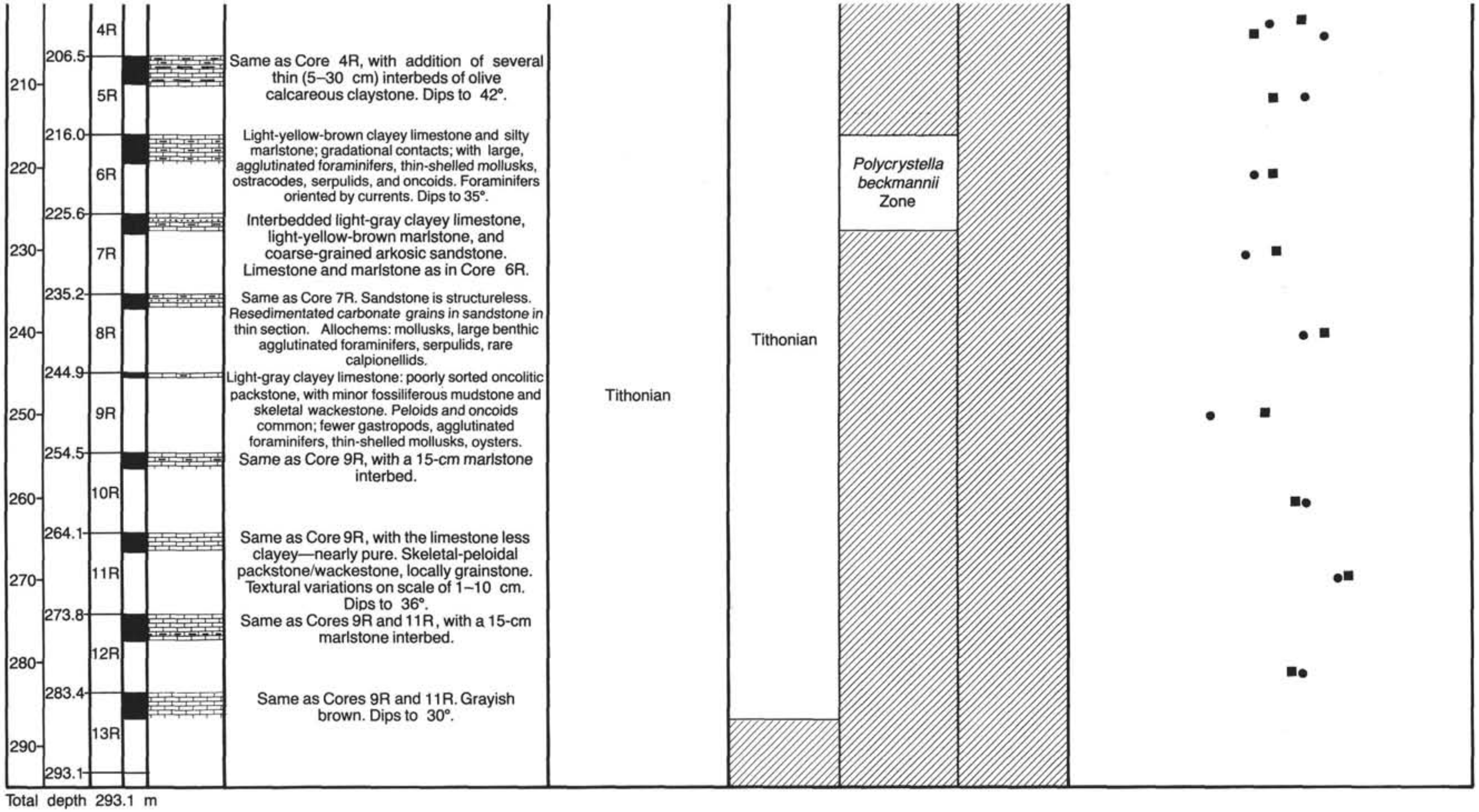

Same as Core 4R, with addition of several thin (5–30 cm) interbeds of olive calcareous claystone. Dips to 42°.

Light-yellow-brown clayey limestone and silty marlstone; gradational contacts; with large, agglutinated foraminifers, thin-shelled mollusks, ostracodes, serpulids, and oncoids. Foraminifers oriented by currents. Dips to 35°.

Interbedded light-gray clayey limestone, light-yellow-brown marlstone, and coarse-grained arkosic sandstone. Limestone and marlstone as in Core 6R.

Same as Core 7R. Sandstone is structureless. Resedimentated carbonate grains in sandstone in thin section. Allochems: mollusks, large benthic agglutinated foraminifers, serpulids, rare calpionellids.

Light-gray clayey limestone: poorly sorted oncolitic packstone, with minor fossiliferous mudstone and skeletal wackestone. Peloids and oncoids common; fewer gastropods, agglutinated foraminifers, thin-shelled mollusks, oysters.

Same as Core 9R, with a 15-cm marlstone interbed.

Same as Core 9R, with the limestone less clayey—nearly pure. Skeletal-peloidal packstone/wackestone, locally grainstone. Textural variations on scale of 1–10 cm. Dips to 36°.

Same as Cores 9R and 11R, with a 15-cm marlstone interbed.

Same as Cores 9R and 11R. Grayish brown. Dips to 30°.

Figure 28 (continued).

Hole 639E Location: 42°08.6′N, 12°15.4′W Water depth: 4770 m below derrick floor (4760 mbsl)

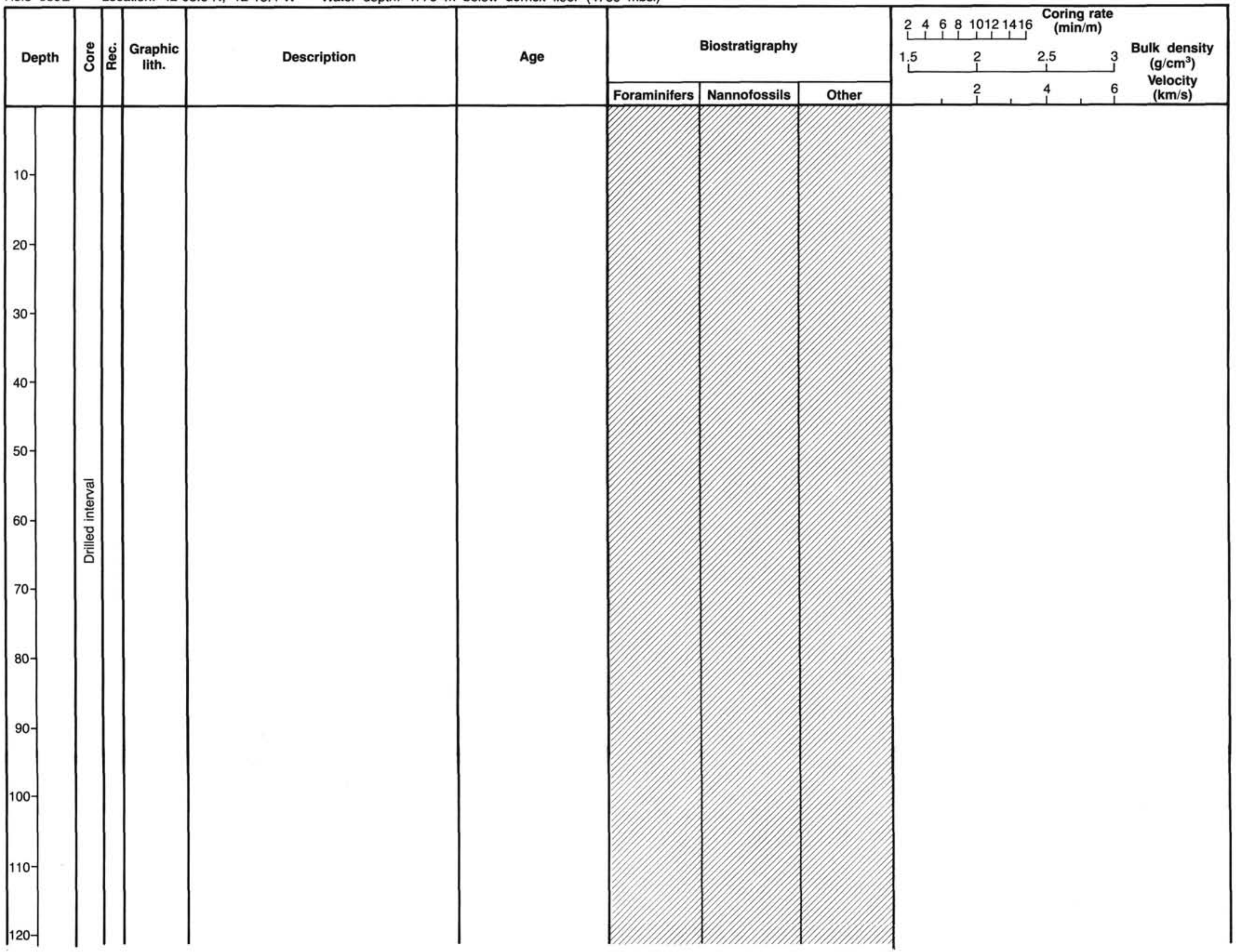

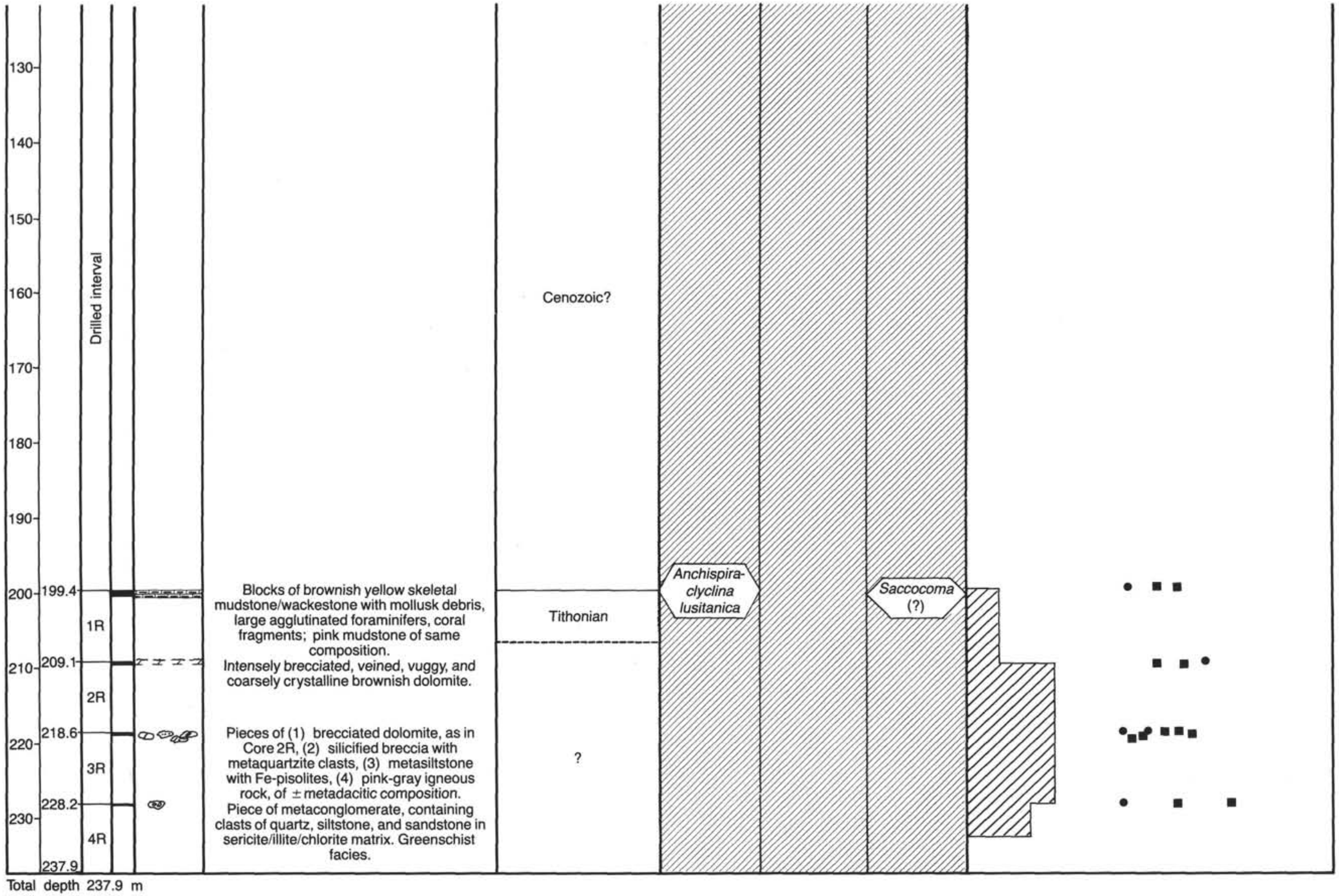

Blocks of brownish yellow skeletal mudstone/wackestone with mollusk debris, large agglutinated foraminifers, coral fragments; pink mudstone of same composition.

Intensely brecciated, veined, vuggy, and coarsely crystalline brownish dolomite.

Pieces of (1) brecciated dolomite, as in Core 2R, (2) silicified breccia with metaquartzite clasts, (3) metasiltstone with Fe-pisolites, (4) pink-gray igneous rock, of ± metadacitic composition.

Piece of metaconglomerate, containing clasts of quartz, siltstone, and sandstone in sericite/illite/chlorite matrix. Greenschist facies.

Figure 28 (continued).

Hole 639F Location: 42°08.6′N, 12°15.5′W Water depth: 4771 m below derrick floor (4761 mbsl)

Depth	Core	Rec.	Graphic lith.	Description	Age	Biostratigraphy			Coring rate (min/m) 2 4 6 8 10 12 14 16 Bulk density (g/cm³) 1.5 2 2.5 3 Velocity (km/s) 2 4 6
						Foraminifers	Nannofossils	Other	
10									
20									
30									
40									
50									
60									
70									
80									
90									
100									
110									
120									

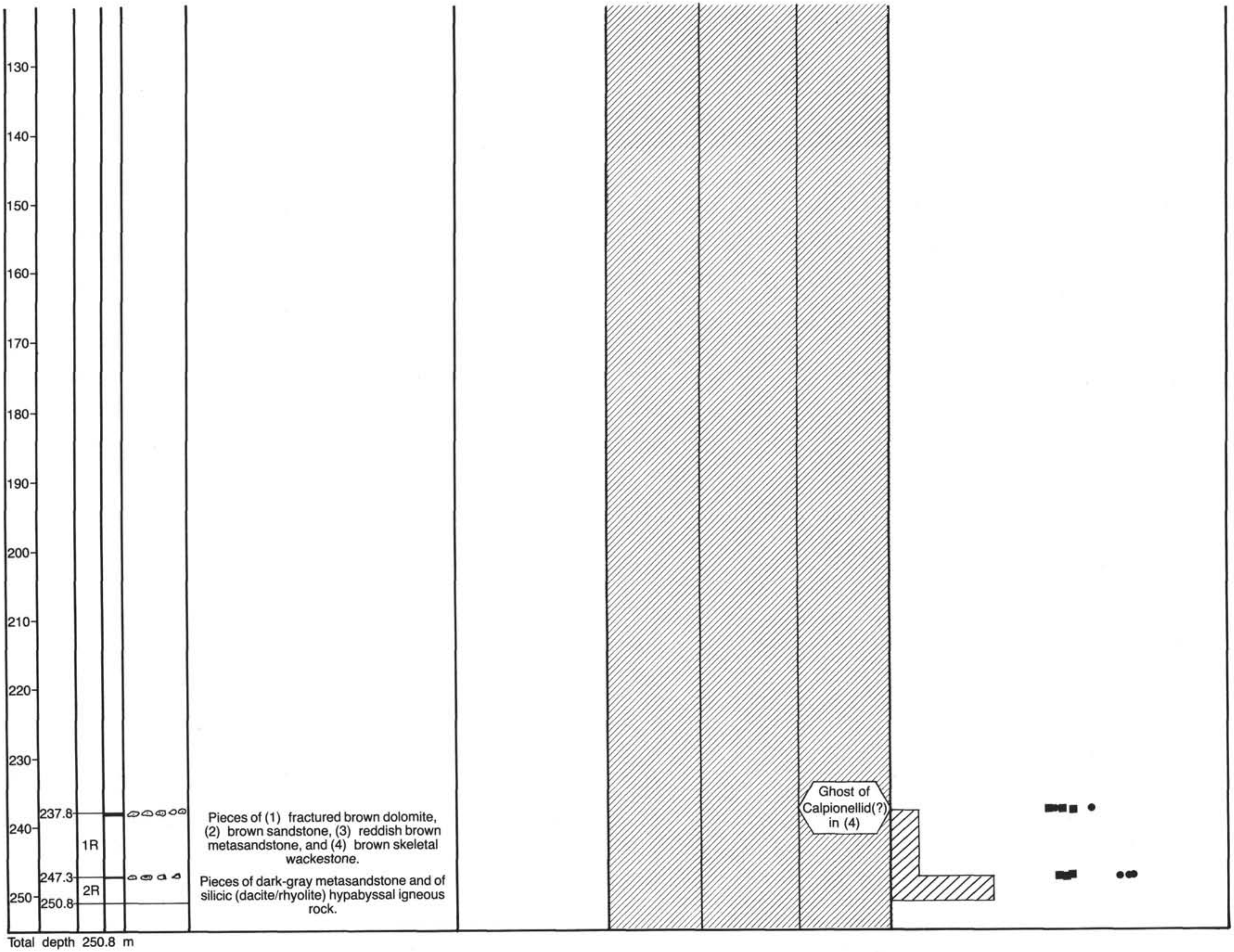

Figure 28 (continued).

ertheless, a highly oxidized zone occurs at the contact between Neogene ooze and Valanginian marl in Hole 639A and includes a weathered pebble of sandstone. This may be the lateral equivalent of the brown clay.

The brown clay is similar in both lithology and stratigraphic position to the brown clay cored at Site 637; we suspect that it may be the equivalent of Upper Cretaceous/Paleogene barren brown clay known at many drilling sites in the North Atlantic. The clay, not entirely barren of fossils and containing small amounts of dissolution-resistant fish debris, was dated by P. Doyle (pers. comm., 1985) as late or middle Eocene.

Neogene Ooze and Clay (Lithologic Unit I in "Sediment Lithology" Section, This Chapter)

The Neogene section was sampled only in Holes 639A and 639C. In Hole 639A, a thickness of about 16 m of Pleistocene clayey nannofossil ooze and calcareous clay overlies a few meters of middle Miocene ooze. In Hole 639C, a few meters of middle Pliocene ooze was cored at a depth of 78 mbsf, immediately above the barren brown clay that overlies dolomite.

The thickness of the Neogene section, best estimated on the cross section through the drill sites (Fig. 1), ranges from about 22 m in Hole 639A to about 238 m in Hole 639F. According to the flat appearance of reflectors in the upper part of the sedimentary column seen on seismic-reflection profiles near the site, the sequence includes turbidite layers, probably much like those cored at Site 637 (Site 637 chapter, this volume). The average rate of sedimentation at Site 639C, where middle Pliocene ooze occurs at 78 mbsf, was about 25 m/m.y., which is about half the average rate for the same time interval at Site 637.

Conclusions and Regional Considerations

Drilling at Site 639 gives us reasonably satisfactory answers to most of the questions posed at the beginning of this summary:

1. The syn-rift sediments below the level reached in Hole 638C consist of marl interbedded with turbidite sandstone, passing downward gradually into marl and marlstone, suggesting less clastic and more pelagic conditions, perhaps at somewhat shallower depths than represented by the turbidites in Hole 638C. No gradual transition to the shallow-water environments inferred for the dolomite was cored.

2. No satisfactory answer was obtained about the exact nature of the contact between dolomite and the overlying syn-rift sequence. The contact is abrupt at the scale of a few meters and represents a major shift in environments.

3. The estimated thickness of the pre-rift carbonate sequence, assuming no faults, as shown in Figure 1, is about 480–500 m, consisting of limestone about 265 m thick overlain by dolomite about 215 m thick. On the other hand, according to the thickness estimated from study of the seismic profile (Fig. 27), the combined thickness of the limestone and dolomite may be only about 300 m. The limestone was deposited in relatively shallow-water conditions, ranging from a fairly open shelf, possibly with bioherms, to a more near-shore environment, near a stream mouth or tidal channel where clay and coarse sand could be deposited. The dolomite probably represents shallow-water normal-salinity conditions and may include biohermal deposits. Intense dolomitization and fracturing of the dolomite makes environmental inferences especially risky.

4. We infer that a conglomerate or breccia layer may lie between the carbonate beds and basement rock. The layer contains a great variety of low-grade metamorphic rocks of sedimentary origin. Silicic volcanic or hypabyssal rocks of rhyolitic or rhyodacitic composition may be a part of the basement.

A question raised by the drilling at Site 639 is whether the dolomite is a local phenomenon, related to special diagenetic conditions near the up-tilted edge of the fault block, or whether the dolomitization extends over a wide region. Limestone similar to the limestone cored at Site 639 was dredged on the steep escarpments near Site 639, but no dolomite was collected in the dredges (Mougenot et al., 1985). Apart from drilling at another location, the only practical way to address this question is to describe and sample the nearby escarpments from a submersible.

Finding Tithonian limestone resting either directly on basement rock or on a thin basal conglomerate that rests, in turn, on basement implies that this region remained a structural high, possibly even a source of sediments, until late into the Jurassic. Whatever depositional basin there might have been offshore from mainland Galicia would of necessity have been located nearer the present coast because little room is available for a basin between Site 639 and the edge of the ocean. This implies that the locus of maximum thinning and rifting of the crust, where the first oceanic crust was later emplaced, was in a region that had been a structural high until the latest part of the Jurassic and not in a region with a history of rifting, subsidence, and sedimentation.

REFERENCES

Ascoli, P., Poag, C. W., and Remane, J., 1984. Microfossil zonation across the Jurassic-Cretaceous boundary on the Atlantic Margin of North America. *In* Westermann, E., (Ed.) *Jurassic Cretaceous Biochronology and Paleogeography of North America*. Geol. Assoc. Can. Spec. Pap. 27, 31–48.

Aubert, J., and Bartenstein, M., 1979. *Leutuculina (L) nodosa*. Additional observations in the world-wide Lower Cretaceous. *Bull. Cent. Rech. Pau.*, 10:1–33.

Bassoullet, J. P., and Fourcade, E., 1979. Repartition des principes Foraminifères du Jurassique Mésogéen. *Soc. Geol. Fr., C. R. Somm.*, 2: 69–71.

Berggren, W. A., 1983. Correlation of Atlantic, Mediterranean, and Indo-Pacific Neogene stratigraphies: geochronology and chronostratigraphy. *IGCP Project 114: Intern. Workshop of Pacific Neogene Biostrat.* (Osaka and Kobe, Japan), Nov. 24-29, 1981.

Blow, W. H., 1969. Late Middle Eocene to Recent planktonic foraminiferal biostratigraphy. *In* Broenniman, P., and Renz, H. H. (Eds.), *Proceedings, First International Conference on Planktonic Microfossils*: Leiden (Brill), 1:199–422.

Bryant, W. R., Bennett, R. H., and Katherman, C. E., 1981. Shear strength, consolidation, porosity, and permeability of oceanic sediments. *In* Emiliani, C. (Ed.), *The Sea*, New York (John Wiley), 7: 1555–1616.

Busnardo, R., Thieuloy, J. P., and Moullade, M., (Eds.) 1979. *Hypostratotype Mésogéen de l'étage Valanginian.* Les Stratotypes français. *C. N. R. S.*, 6:110–126.

Čepek, P., 1978. Mesozoic calcareous nannoplankton of the eastern North Atlantic, Leg 41. *In* Lancelot, Y., Siebold, E., et al., *Init. Repts. DSDP*, 41: Washington (U.S. Govt. Printing Office), 667–687.

Eliuk, L. S., 1978. The Abenaki Formation, Nova Scotia Shelf, Canada—a depositional and diagenetic model for a Mesozoic carbonate platform. *Can. Pet. Geol. Bull.*, 26:424–514.

Gartner, S., 1977. Calcareous nannofossil biostratigraphy and revised zonation of the Pleistocene. *Mar. Micropaleont*, 2:1–25.

Hamilton, E. L., 1976. Variations of density and porosity with depth in deep-sea sediments. *J. Sed. Pet.*, 46:280–300.

Harland, W. B., Cox, A. V., Llewellyn, P. G., Pickton, C. A. G., Smith, A. G., and Walters, R., 1982. *A Geologic Time Scale:* Cambridge (Cambridge Univ. Press), 1–131.

Hottinger, L., 1967. Foraminifères imperfores du Mésozoique Morocain. *Notes Memoires Serv. Géol. Maroe*, 209:1–168.

Jansa, L. F., 1981. Mesozoic carbonate platforms and banks of the eastern North American margin. *In* Cita, M. B., and Ryan, W. B. F. (Eds.), Carbonate platforms of the passive-type continental margins, present and past. *Mar. Geol*, 44:97–117.

Jansa, L. F., and Wiedmann, J., 1982. Comparison of the northwest African and northeast American margins. *In* von Rad, U., et al. (Eds.), *Geology of the Northwest African Continental Margin*: Berlin (Springer-Verlag), 215–269.

Mougenot, D., Capdevila, R., Palain, C., Dupeuble, P. A., and Mauffret, A., 1985. Nouvelles données sur les sediments ante-rift et le socle de la merge continentale de Galice. *Acad. Sci. Paris, C. R.*, 301(II):323-328.

Moullade, M., 1979. Les Foraminifères du Valanginien hypostratotypiques. *In* Busnardo, R., Thieuloy, J. P., Moullade, M. (Eds.), *Hypostratotype Mésogéen de l'étage Valanginien*: Les Stratotypes Français, *C. N. R. S.*, 6:110-126.

________, 1983. The value of deep smaller benthic foraminifera in the biostratigraphy and analysis of Mesozoic oceanic paleoenvironments. *Benthos '83*: Second International Symposium Benthic Foraminifera, Pau, 429-464.

Müller, G., and Gastner, M., 1971. The "Karbonate-Bombe," a simple device for determination of the carbonate content in sediments, soils, and other materials. *Neues. Jahrb. Mineral. Monatsch.*, 10:466-469.

Ogg, J. G., 1981. Sedimentology and paleomagnetism of Jurassic pelagic limestones ("Ammonitico Rosso" facies) [Ph.D. dissert.]. Scripps Inst. Ocean., San Diego.

________, in press. Early Cretaceous magnetic polarity time scale and the magnetostratigraphy of DSDP Sites 603 and 534, western Central Atlantic. *In* Van Hinte, J., Wise, S., et al., *Init. Repts. DSDP*, 93: Washington (U.S. Govt. Printing Office).

Ogg, J. G., and Lowrie, W., 1986. Magnetostratigraphy of the Jurassic-Cretaceous boundary. *Geology*, 14:547-550.

Okada, H., and Bukry, D., 1980. Supplementary modification and introduction of code numbers to the low latitude coccolith biostratigraphic zonation. *Mar. Micropaleont.* 5:321-325.

Remane, J., 1978. Calpionellids. *In* Haq, B. U., and Boersma, A. (Eds.), *Introduction to Marine Micropaleontology*: New York (Elsevier), 161-170.

Roth, P. H., 1983. Jurassic and Lower Cretaceous calcareous nannofossils in the western North Atlantic (Site 534). Biostratigraphy, preservation, and some observations on biogeography and paleoceanography. *In* Sheridan, R. E., Gradstein, F. M., et al., *Init. Repts. DSDP.*, 76: Washington, (U.S. Govt. Printing Office), 587-621.

Roth, P. H., Meed, A. W., and Watkins, D. K., 1983. Jurassic calcareous nannofossil zonation, an overview with new evidence from Deep Sea Drilling Project Site 534. *In* Sheridan, R. E., Gradstein, F. M., et al., *Init. Repts. DSDP.*, 76: Washington (U.S. Govt. Printing Office), 573-579.

Sissingh, W., 1977. Biostratigraphy of Cretaceous calcareous nannoplankton. *Geol. Mijnbouw*, 56:37-65.

Thierstein, H. R., 1976. Mesozoic calcareous nannoplankton biostratigraphy of marine sediments. *Mar. Micropaleont.*, 1:325-362.

Vincent, E., Lehmann, R., Sliter, W. V., and Westberg, M. J., 1979. Calpionellids from the Upper Jurassic and Neocomian of Deep Sea Drilling Project Site 416, Moroccan Basin, eastern North Atlantic. *In* Winterer, E. L., and Hinz, K., et al., *Init. Repts. DSDP*, 50: Washington (U.S. Govt. Printing Office), 439-461.

Wind, F. H., and Čepek, P., 1979. Lower Cretaceous calcareous nannoplankton from DSDP Hole 397A (northwest African margin). *In* von Rad., U., Ryan, W. B. F., et al., *Init. Repts. DSDP*, 47 (Pt. A): Washington (U.S. Govt. Printing Office), 221-256.

Ziegler, P. A., 1975. Geologic evolution of North Sea and its tectonic framework. *Amer. Assoc. Petr. Geol. Bull.*, 59(7):1073-1097.

________, 1982. *Geologic Atlas of Western and Central Europe*: International Petroleum Maatschappis, B. V., Amsterdam (Elsevier).

SITE 639 HOLE A CORE 1 R CORED INTERVAL 4724.5-4726.8 mbsl; 0.0-2.3 mbsf

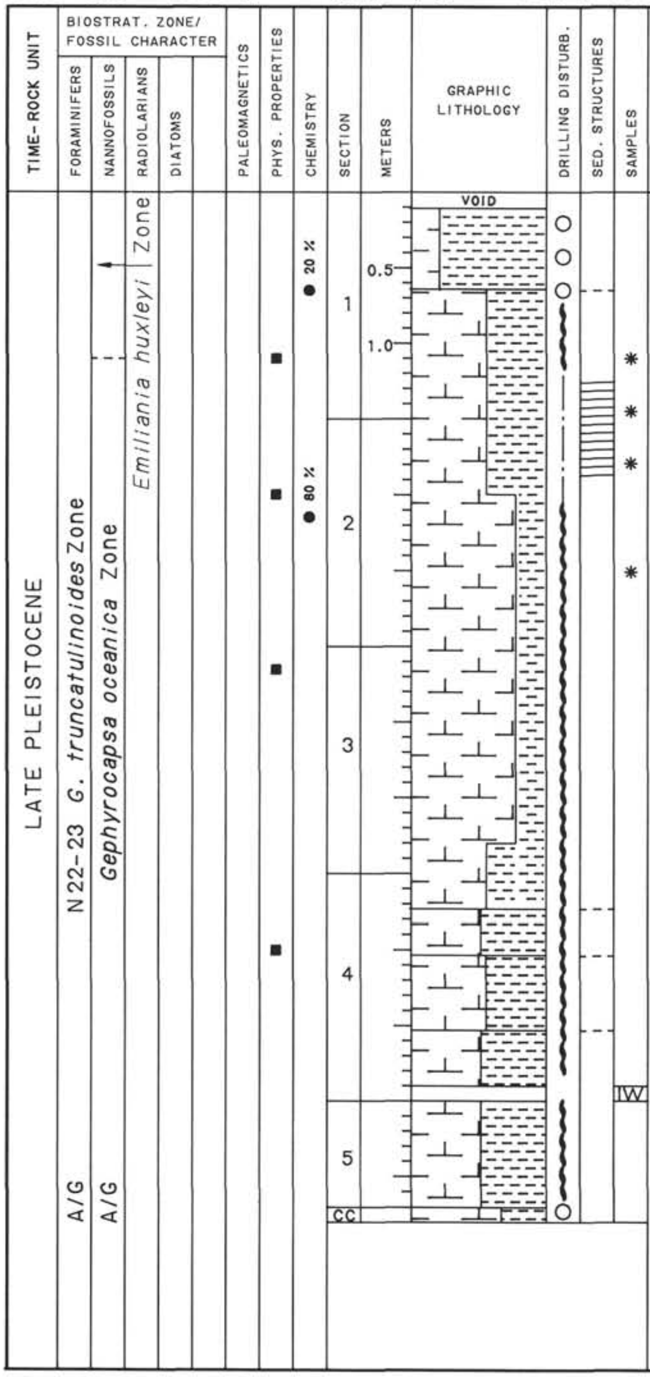

LITHOLOGIC DESCRIPTION

LIGHT GRAY CLAYEY NANNOFOSSIL OOZE, LIGHT BROWNISH GRAY NANNOFOSSIL MARL and GRAYISH BROWN CALCAREOUS CLAY.

The core consists of alternations of white, light gray, gray, olive gray and very pale brown (5Y8/1, 5Y7/1, 5Y6/1, 5Y6/2, 10Y7/3) clayey nannofossil ooze, light brownish gray (2.5Y6/2) nannofossil marl, and grayish brown (2.5Y5/2) calcareous clay. All lithologies are highly mixed by drilling except for relatively pure intervals of calcareous clay in Section 2, 55 cm to Section 3, 10 cm. Any primary sedimentary structures were destroyed by drilling except for some faint lamination in Section 1, 135-150 cm. Purplish streaks of Fe/Mn oxide are present in Section 3, 80 and 90 cm.

SMEAR SLIDE SUMMARY (%):

	1,109 D	1,143 D	2,25 D	2,100 D
TEXTURE:				
Silt	8	5	5	5
Clay	92	95	95	95
COMPOSITION:				
Quartz	Tr	10	1	Tr
Feldspar	–	Tr	Tr	–
Mica	Tr	2	Tr	Tr
Clay	10	25	30	5
Volcanic Glass	–	Tr	–	–
Calcite/Dolomite	Tr	Tr	Tr	–
Accessory Minerals: (Opaques, Fe Oxides, Zeolites?)	Tr	Tr	1	Tr
Foraminifers	7	1	5	5
Nannofossils	83	62	63	90
Sponge Spicules	Tr	–	–	–

PHYSICAL PROPERTIES DATA:

	1,111	2,50	3,16	4,50
V_p (c)	–	–	1.41	–
ρ_b	1.59	–	1.67	–
T_c	–	3.88	–	3.83

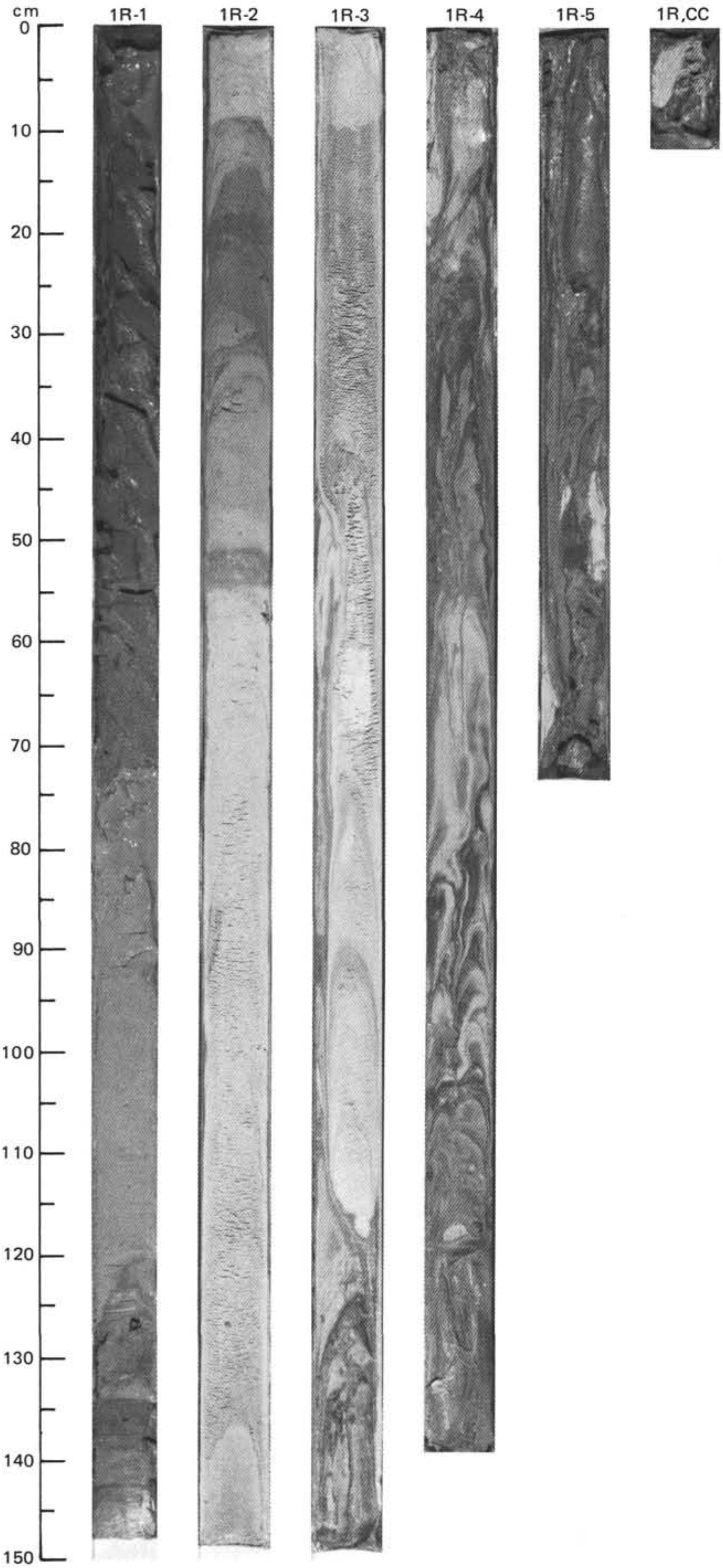
cm
0
10
20
30
40
50
60
70
80
90
100
110
120
130
140
150
1R-1
1R-2
1R-3
1R-4
1R-5
1R,CC

SITE 639 HOLE A CORE 2 R CORED INTERVAL 4726.8-4736.5 mbsl; 2.3-12.0 mbsf

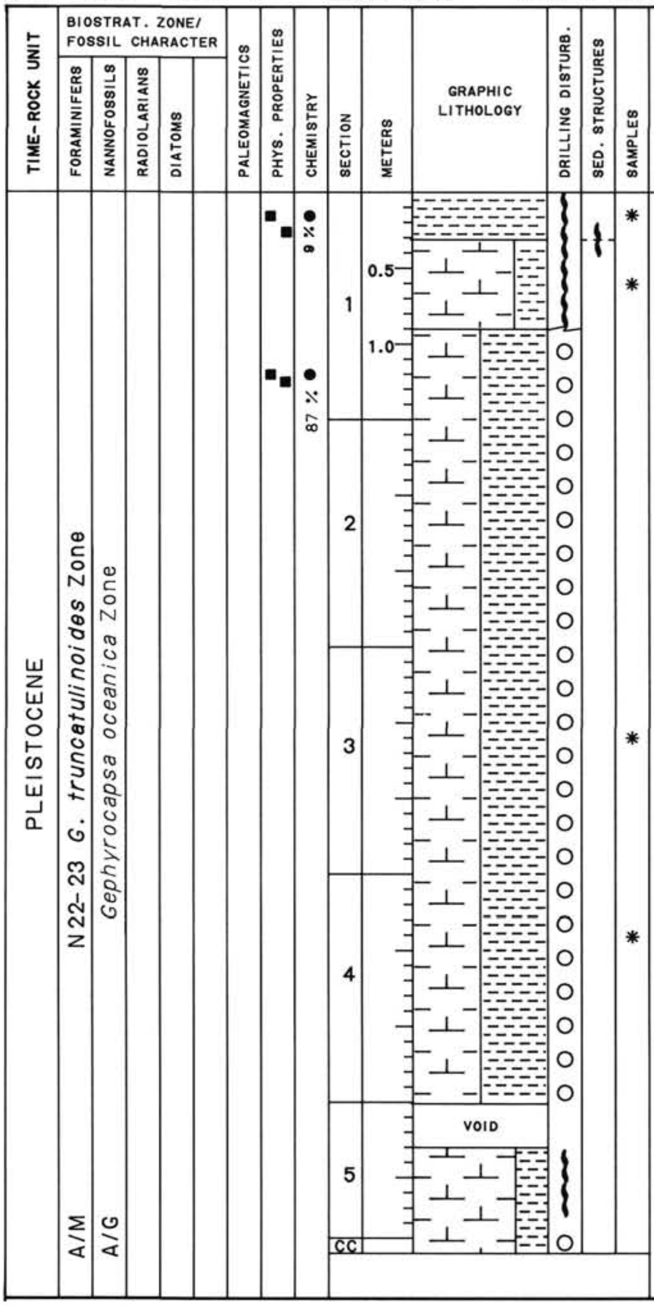

LITHOLOGIC DESCRIPTION

LIGHT BROWNISH GRAY NANNOFOSSIL MARL and LIGHT GRAY CLAYEY NANNOFOSSIL OOZE.

The core is dominantly a gray to light brownish gray (2.5Y5/2, 10YR6/1) soupy nannofossil marl. In addition, less disturbed intervals of grayish brown (2.5Y5/2) clay occur in Section 1, 0-27 cm and of white to light gray (5Y8/1, 10YR7/1) clayey nannofossil ooze in Section 1, 35-90 cm and in Section 5, 30-88 cm. Primary sedimentary structures are not observed.

SMEAR SLIDE SUMMARY (%):

	1,20 D	1,60 D	3,65 D	5,40 D
TEXTURE:				
Sand	–	–	–	3
Silt	10	7	3	–
Clay	90	93	97	97
COMPOSITION:				
Quartz	25	Tr	Tr	–
Mica	Tr	–	Tr	–
Clay	73	20	17	7
Volcanic Glass	Tr	–	–	–
Accessory Minerals:				
Zeolites	2	–	–	–
Opaques, Fe Oxides	–	Tr	Tr	–
Foraminifers	–	7	3	3
Nannofossils	Tr	73	80	90

PHYSICAL PROPERTIES DATA:

	1,16	1,24	1,70	1,74
V_p (c)	1.03	–	–	1.00
ρ_b	1.66	–	–	1.64
γ	–	6.57	4.53	–

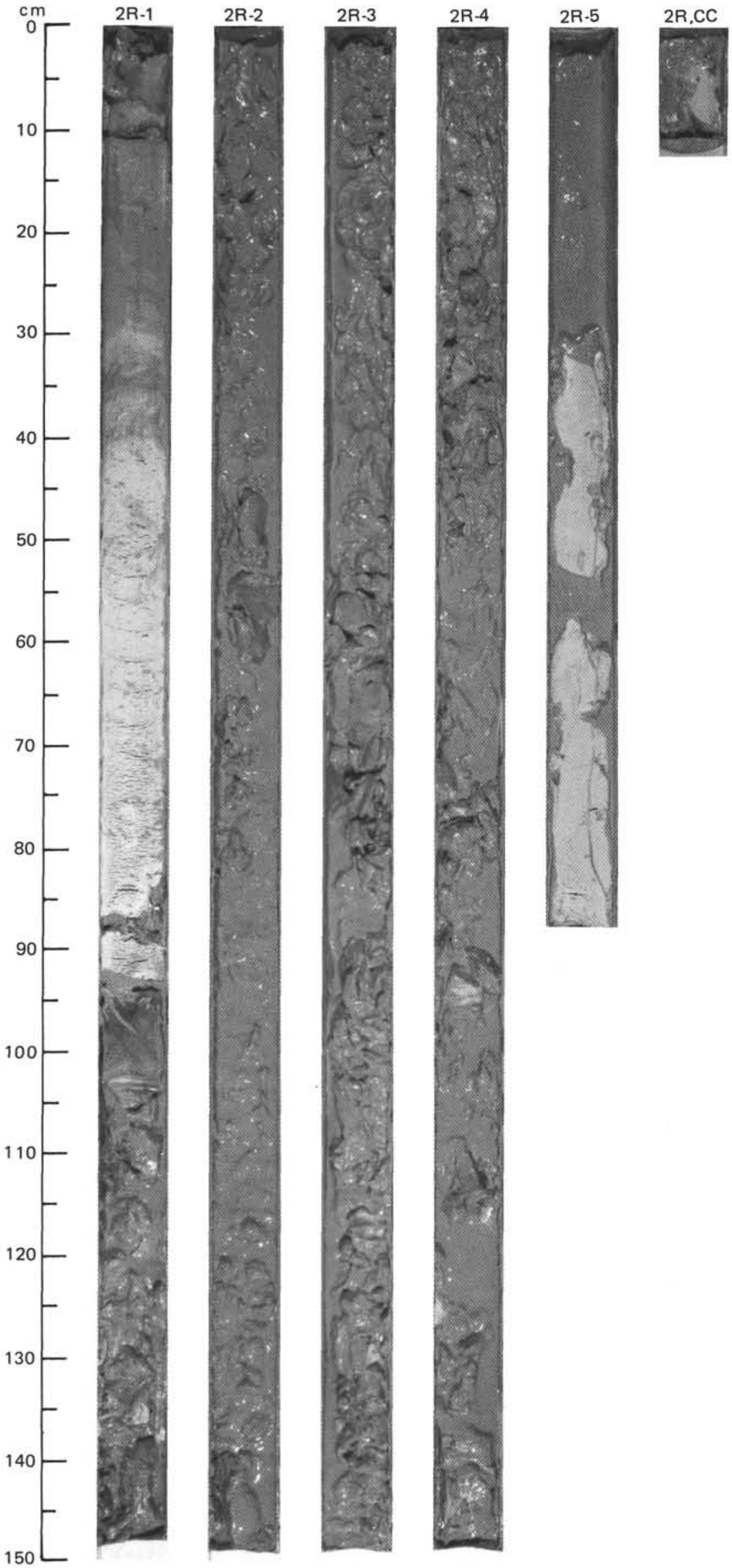
cm
0
10
20
30
40
50
60
70
80
90
100
110
120
130
140
150
2R-1
2R-2
2R-3
2R-4
2R-5
2R,CC

SITE 639 HOLE A CORE 3 R CORED INTERVAL 4736.5-4746.0 mbsl; 12.0-21.5 mbsf

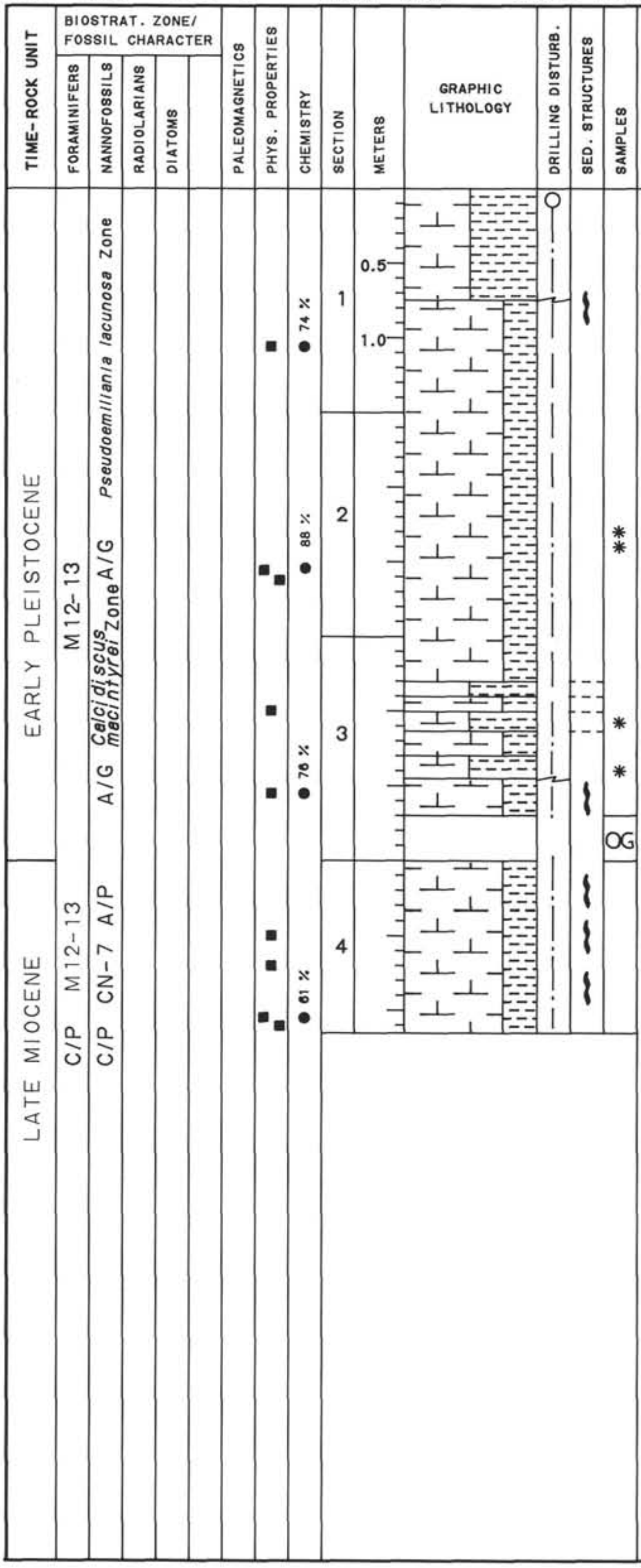

LITHOLOGIC DESCRIPTION

LIGHT GRAY CLAYEY NANNOFOSSIL OOZE and OLIVE GRAY NANNOFOSSIL MARL

The core dominantly consists of white, grayish white and light brownish gray (5Y8/1, 5Y7/1, 2.5Y7/2 to 8/2) clayey nannofossil ooze with alternations of light olive and olive gray (5Y6/2, 5Y7/2) nannofossil marl. Nannofossil marl occurs in Section 1, 5-40 cm and in Section 3, 33-42, 55-65, and 85-95 cm. Primary sedimentary structures are not observed except for vague alternation on a scale of 10-15 cm of lighter and darker shades of brownish gray clayey nannofossil ooze in Section 4 and in the upper part of Section 3. Dark bands, blebs and specks of an Fe/Mn precipitate are present throughout. A pyrite-stained burrow is present in Section 1, 86 cm.

SMEAR SLIDE SUMMARY (%):

	2,81 M	2,90 M	3,58 D	3,90 M
TEXTURE:				
Sand	–	–	–	37
Silt	13	–	5	8
Clay	87	100	95	55
COMPOSITION:				
Quartz	Tr	Tr	2	10
Feldspar	–	–	Tr	Tr
Mica	Tr	Tr	Tr	Tr
Clay	–	40	60	10
Accessory Minerals:				
Pyrite	10	–	Tr	Tr
Zircon, Opaques	Tr	Tr	Tr	Tr
Glauconite	–	–	–	Tr
Foraminifers	3	Tr	3	35
Nannofossils	87	60	35	45
Fish Remains	–	Tr	–	–

PHYSICAL PROPERTIES DATA:

	1,106	2,106	2,110	3,50	3,106
V_p (c)	1.43	1.54	–	–	1.57
ρ_b	1.70	1.67	–	–	1.67
γ	–	–	4.89	–	–
T_c	–	–	–	2.48	–

	4,50	4,70	4,106	4,110
V_p (c)	–	–	1.57	–
ρ_b	–	–	1.70	–
γ	–	24.25	–	–
T_c	2.49	–	–	2.74

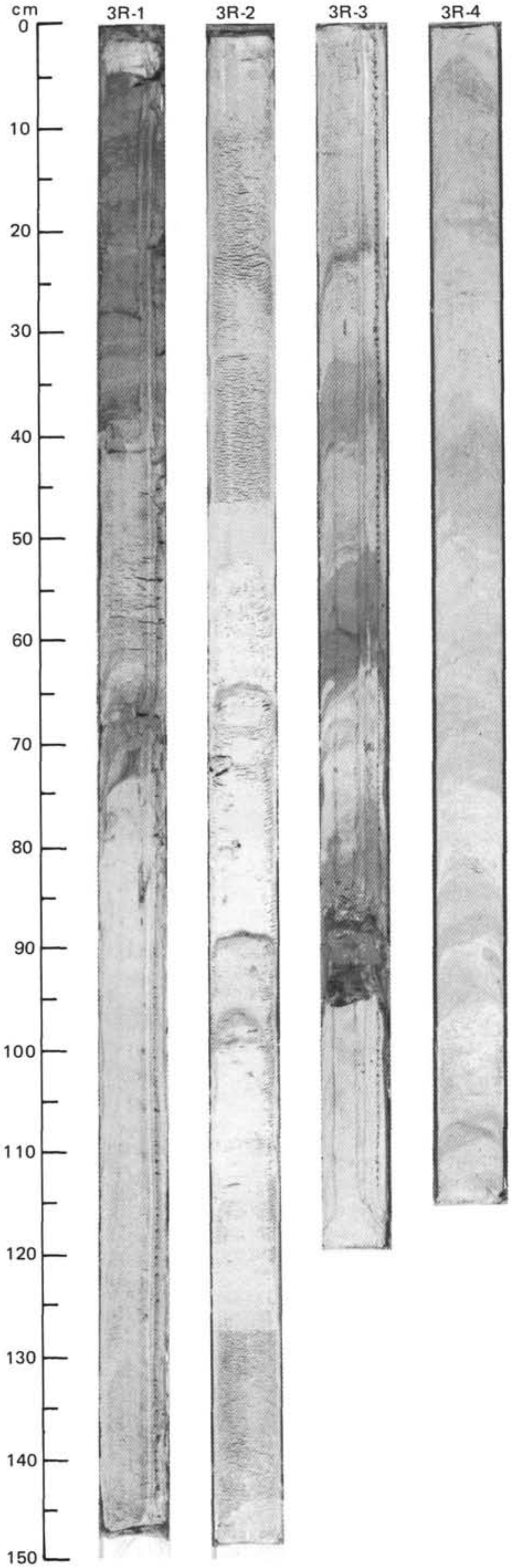
cm
0
10
20
30
40
50
60
70
80
90
100
110
120
130
140
150
3R-1
3R-2
3R-3
3R-4

SITE 639 HOLE A CORE 4 R CORED INTERVAL 4746.0-4756.4 mbsl; 21.5-31.9 mbsf

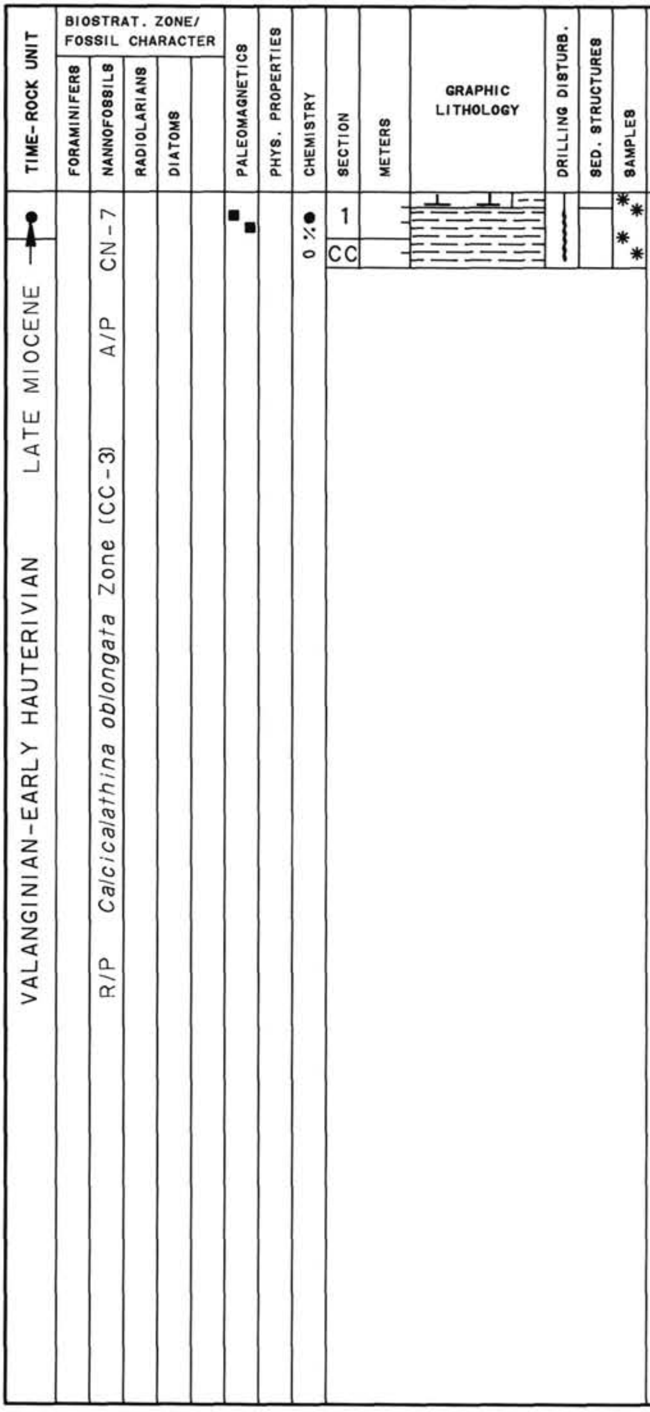

LITHOLOGIC DESCRIPTION

WHITE NANNOFOSSIL MARL IN CONTACT WITH LIMONITE-STAINED SILTY CLAY.

The core consists of gray (5Y7/1) clayey nannofossil ooze and white (5Y8/1) nannofossil ooze (Section 1, 0-10 cm) overlying an olive yellow (5Y6/6) limonite-stained silt to silty clay containing limonite-stained, pebble-sized sandstone clasts (Section 1, 10-24 cm). The contact between the ooze and the limonitic sediment is sharp with no evidence of mixing or erosion. The limonitic sediment, in turn, overlies a gray (2.5Y5/1) clay which in the CC encloses limonite-stained silty clay and sandstone clasts and a gray sandstone clast which is very similar to the Valanginian sandstone recovered at Site 638. It is possible that the gray material is contamination from material drilled at the previous site that was stuck in the drill collars. A second possibility is that the gray material is a slump deposit. Recovery is poor and drilling disturbance is considerable.

SMEAR SLIDE SUMMARY (%):

	1,2	1,8	1,27	CC
	D	D	D	D
TEXTURE:				
Silt	10	10	20	80
Clay	90	90	80	20
COMPOSITION.				
Quartz	–	–	5	70
Mica	–	–	2	–
Clay	20	5	85	–
Accessory Minerals	–	–	1	Tr
Zeolites	Tr	–	–	–
Pyrite	–	–	2	–
Limonite	–	–	–	30
Foraminifers	Tr	–	–	–
Nannofossils	80	95	–	–
Plant Debris	–	–	5	–

PHYSICAL PROPERTIES DATA:

	1,18	1,22
V_p (c)	1.70	–
ρ_b	1.98	–
γ	–	35.33

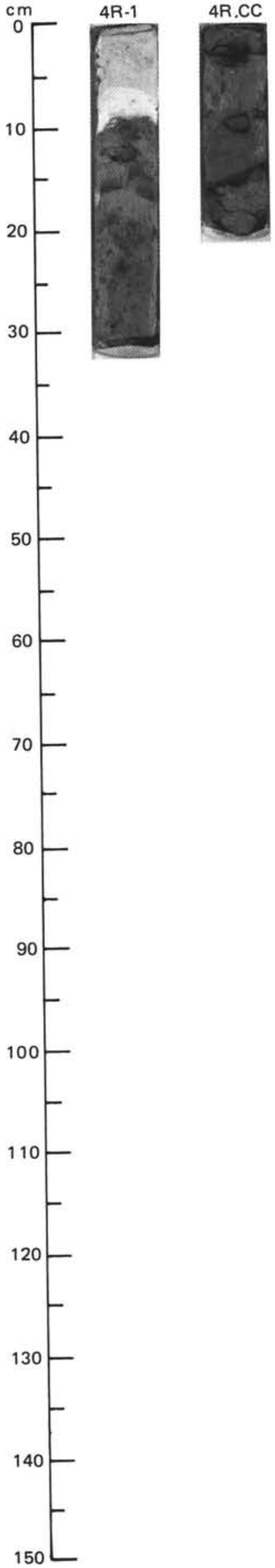
cm
4R-1
4R,CC
0
10
20
30
40
50
60
70
80
90
100
110
120
130
140
150

SITE 639 HOLE A CORE 5 R CORED INTERVAL 4756.4-4766.1 mbsl; 31.9-41.6 mbsf

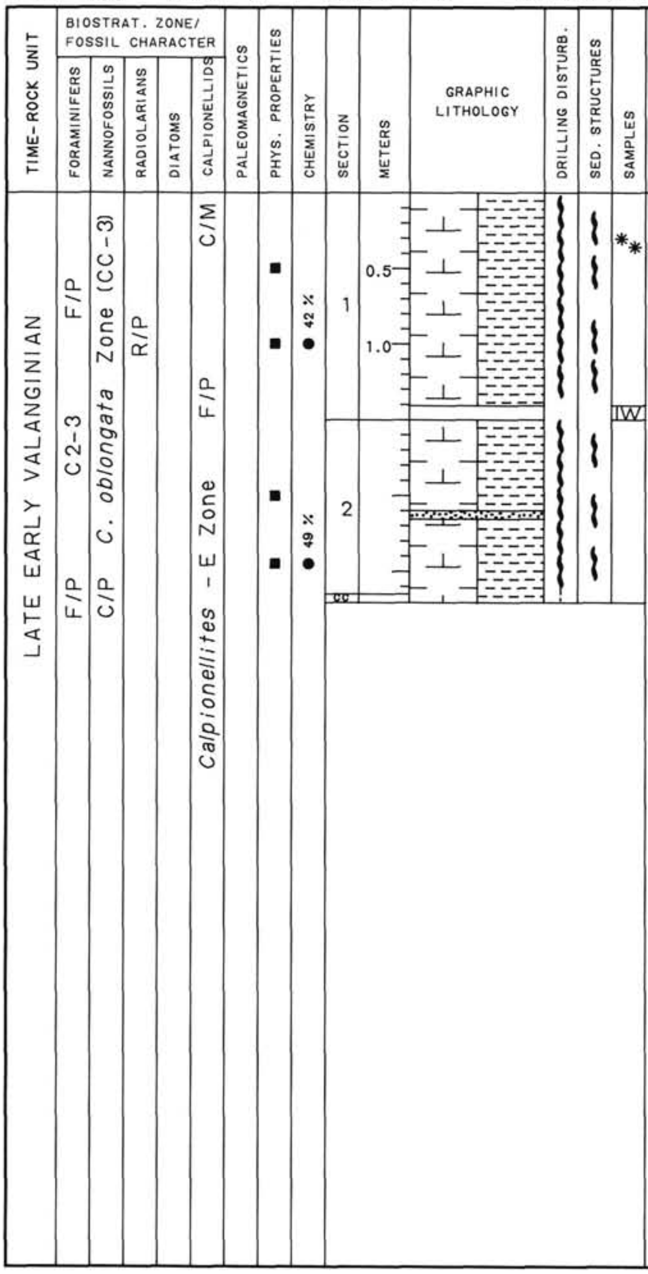

LITHOLOGIC DESCRIPTION

PALE YELLOW NANNOFOSSIL MARL.

The core consists of pale yellow to light gray (5Y7/3, 5Y7/2) nannofossil marl with scattered stringers and pieces of yellow (2.5Y5/4), limonite-stained, fine- to very fine- grained sandstone up to 4 cm thick (Section 2, 61-65 cm), but more commonly 1-10 mm thick. Locally associated with the sandstone are 5mm-thick layers of bioturbated light olive gray (5Y6/2) quartz-silt-bearing calcareous clay. The nannofossil marl has rare burrows which are filled with light olive gray calcareous clay. The sandstones seem to be true interbeds which are highly disturbed by drilling. Black specks of Fe/Mn precipitates are pervasive.

SMEAR SLIDE SUMMARY (%):

	1,33 D	1,35 M
TEXTURE:		
Silt	10	10
Clay	90	90
COMPOSITION:		
Quartz	–	10
Feldspar	Tr	Tr
Mica (Chlorite)	–	Tr
Clay	65	68
Calcite/Dolomite	10	–
Accessory Minerals:		
Glauconite	Tr	–
Nannofossils	25	15
Micritic Peloids	–	7

PHYSICAL PROPERTIES DATA:

	1,50	1,101	2,50	2,95
V_p (c)	–	1.75	–	1.84
ρ_b	–	2.06	–	2.07
T_c	3.36	–	3.28	–

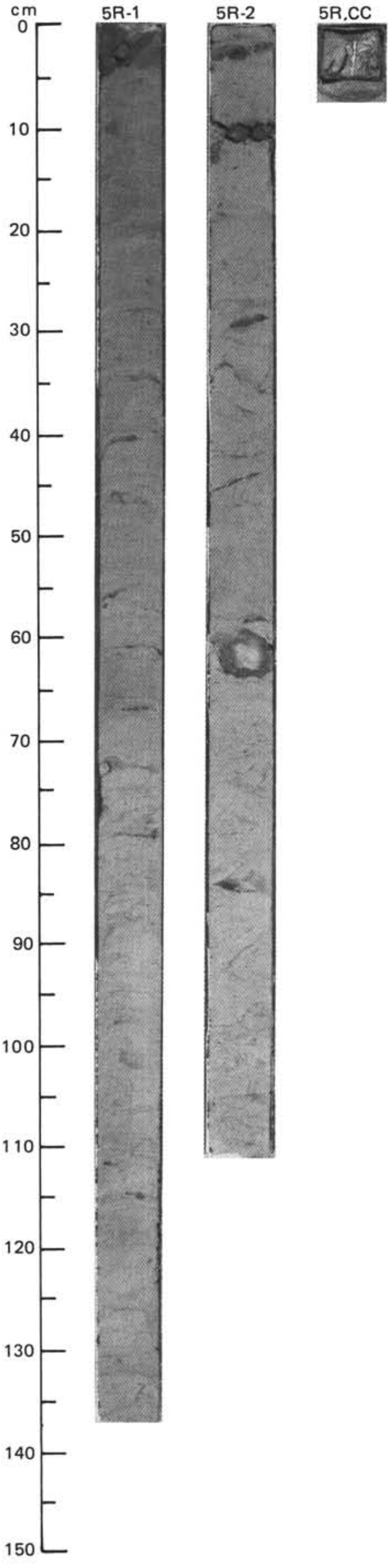
cm
0
10
20
30
40
50
60
70
80
90
100
110
120
130
140
150
5R-1
5R-2
5R,CC

SITE 639 HOLE A CORE 6 R CORED INTERVAL 4766.1-4775.7 mbsl; 41.6-51.2 mbsf

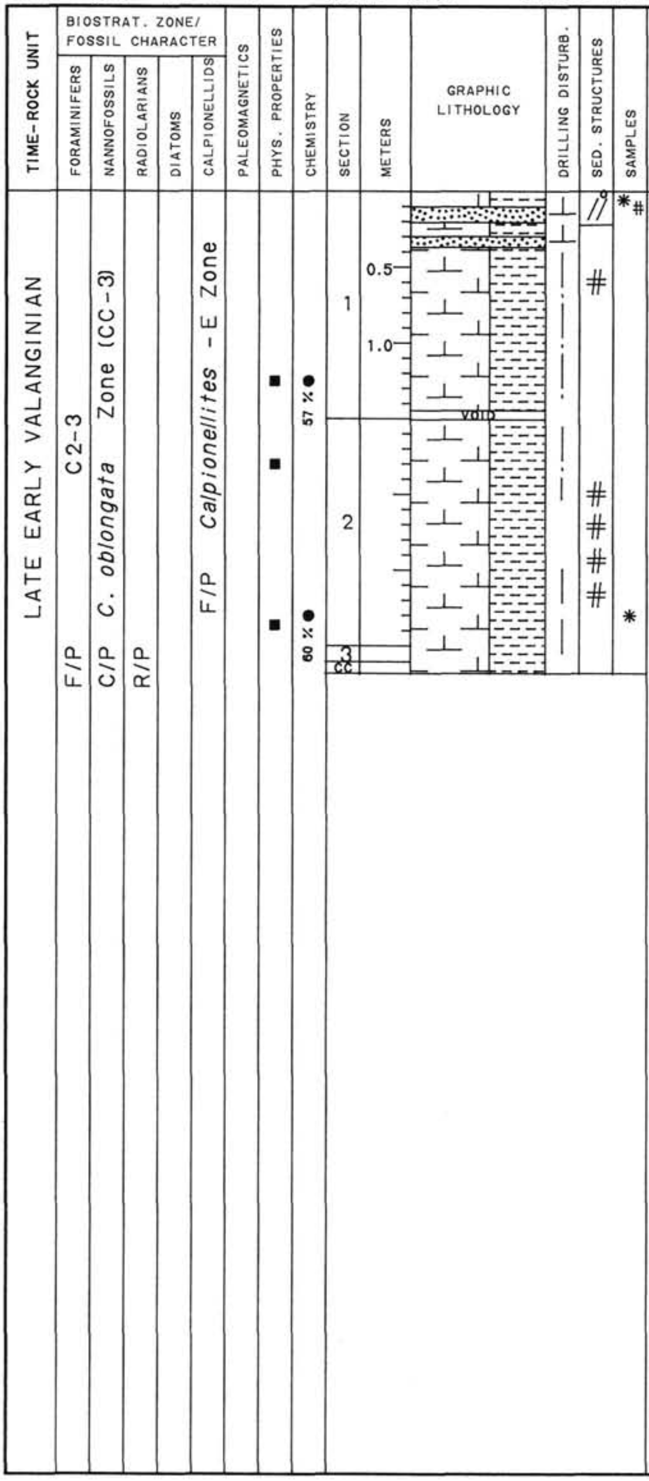

LITHOLOGIC DESCRIPTION

MOTTLED PALE YELLOW AND LIGHT REDDISH BROWN STIFF NANNOFOSSIL MARL.

The core consists dominantly of mottled pale yellow to light gray (5Y7/3, 2.5Y6/2, 2.5Y7/2) and light reddish brown to light brown (5YR6/4, 7.5YR6/4) stiff nannofossil marl. The pale yellow color is a diagenetic product localized along fractures, best seen in Section 2, 68-80 cm. Also, localized along fractures are : (a) yellowish brown (10YR5/8) limonite- and clay-bearing calcite in blades up to 5 mm long and in patches up to 2 cm across, (b) brownish yellow (10YR6/8) limonite stain and (c) black specks of Fe/Mn precipitate, mm across. The upper part of Section 1 contains two limonite-stained, yellowish brown (10YR5/4), fine-grained sandstone layers, 10 and 6 cm thick.

SMEAR SLIDE AND THIN SECTION SUMMARY (%):

	1,7 D	2,133 D	1,12-14 M
TEXTURE:			
Sand	10	–	90
Silt	–	10	10
Clay	90	90	–
COMPOSITION:			
Quartz	Tr	Tr	41
Feldspar	–	–	30
Mica	Tr	–	3
Clay	40	75	–
Calcite/Dolomite	–	5	–
Cement (Carbonate)	–	–	20
Accessory Minerals:			
Fe Oxide	1	–	1
Glauconite	–	–	Tr
Foraminifers	10	–	–
Nannofossils	49	15	–
Debris (Organic)	–	–	2
Micrite size particles	–	5	–
Bioclasts	–	–	2

PHYSICAL PROPERTIES DATA:

	1,124	2,31	2,135
V_p (a)	1.81	–	1.73
ρ_b	2.15	–	2.14
Tc	–	3.53	–

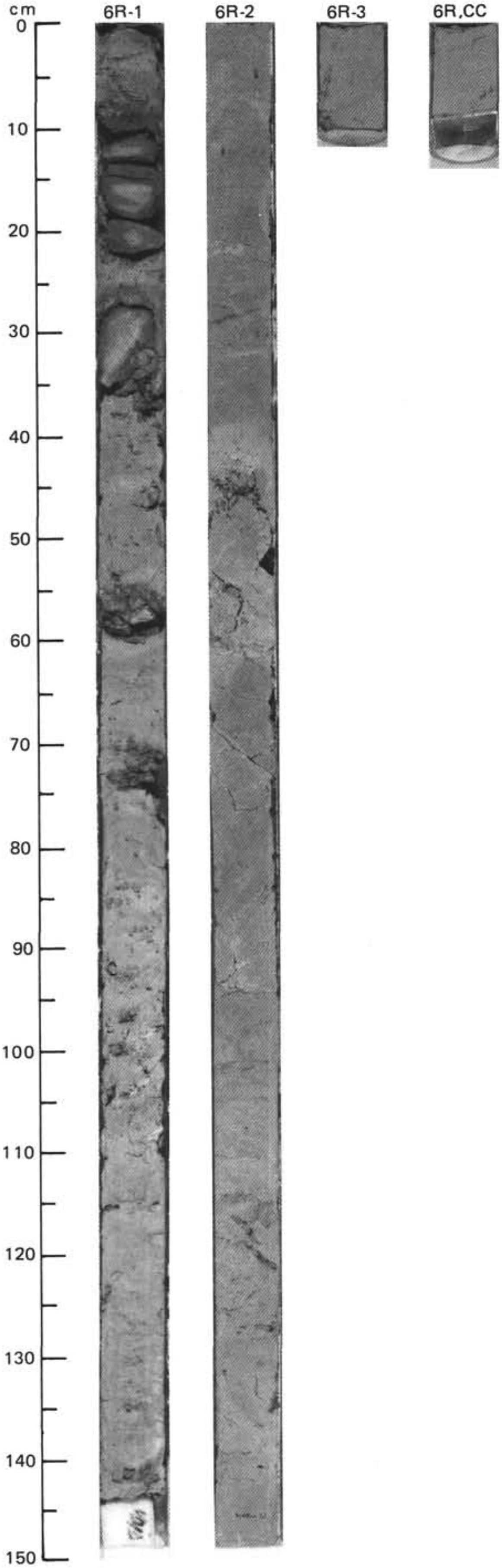
cm
0
10
20
30
40
50
60
70
80
90
100
110
120
130
140
150
6R-1
6R-2
6R-3
6R,CC

SITE 639 HOLE A CORE 7 R CORED INTERVAL 4775.7-4785.3 mbsl; 51.2-60.8 mbsf

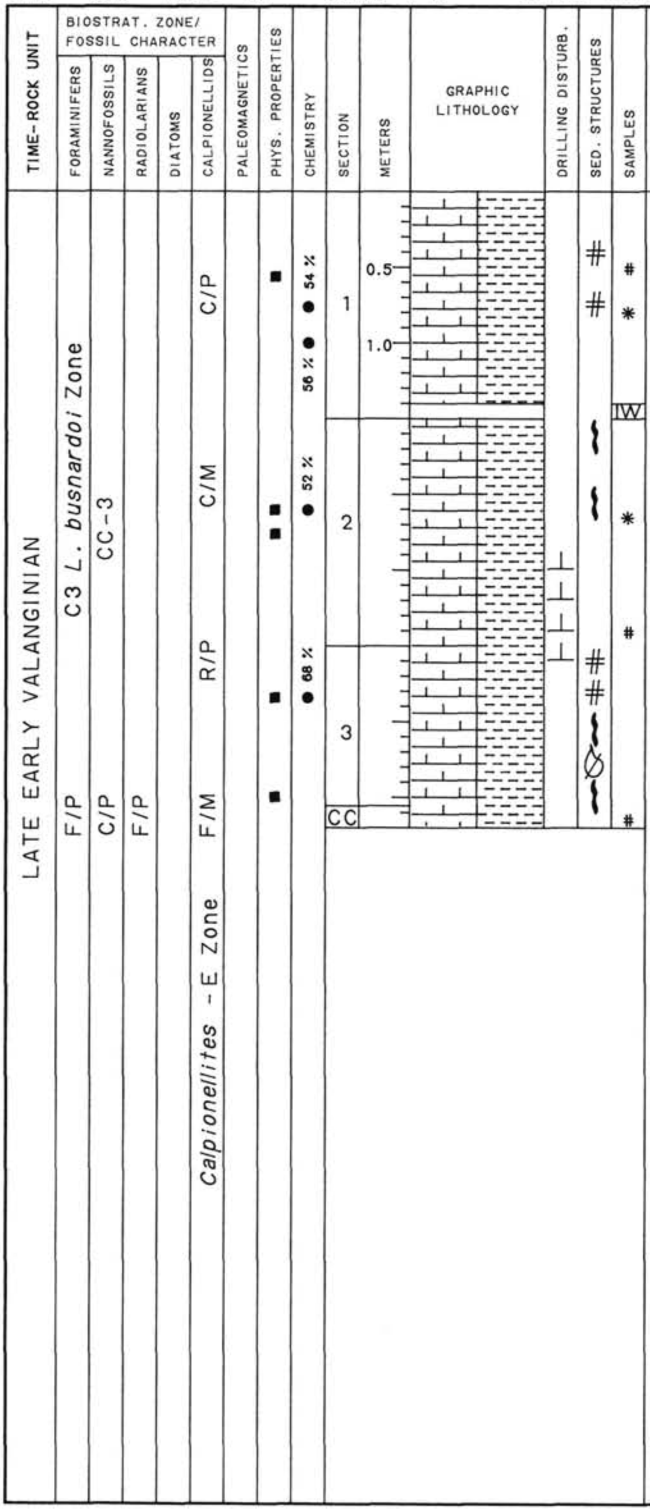

LITHOLOGIC DESCRIPTION

MOTTLED PALE YELLOW NANNOFOSSIL MARLSTONE.

The core consists of homogeneous mottled pale yellow (5Y7/3) and pinkish gray (5YR7/2) marlstone with 10-20 cm thick intervals of stiff marl. Recognizable trace fossils are rare; two Fe/Mn stained rings in Section 2, 48-52 cm, may envelope a large burrow. Mollusc molds and shells are present (Section 2, 147 cm). Fractures are present which are either stained by limonite or lined with a yellowish brown (10YR5/8) sparry calcite up to 5 mm thick. Limonite micronodules (Section 2, 11 cm) and radial dendritic patterns of Fe/Mn precipitate up to 6 mm across are also observed. Primary sedimentary structures are lacking, and drilling cakes and fractures are common.

SMEAR SLIDE AND THIN SECTION SUMMARY (%):

	1,82 D	2,65 D	1,56-58 D	2,38-40 D	CC,14-15
TEXTURE:					
Silt	5	20	–	10	3
Clay	95	80	100	90	97
COMPOSITION:					
Quartz	–	1	–	Tr	Tr
Feldspar	–	Tr	–	–	–
Mica	Tr	Tr	–	–	–
Clay	78	69	40	25	35
Calcite/Dolomite rhombs	2	15	4	5	20
Cement Spar Calcite	–	–	–	5	2
Accessory Minerals:					
Opaques (Hematite)	Tr	Tr	Tr	1	–
Foraminifers (Benthic)	–	–	Tr	Tr	–
Nannofossils	20	15	5	–	–
Radiolarians	Tr	Tr	–	Tr	Tr
Micrite	–	–	49	64	40
Calpionellids	–	–	2	5	Tr
Ostracodes	–	–	Tr	–	–
Crinoids	–	–	–	Tr	–
Bioclasts	–	–	–	–	3

PHYSICAL PROPERTIES DATA:

	1,55	2,61	2,77	3,36	3,89
V_p (a)	1.87	1.93	–	2.11	–
ρ_b	2.24	2.26	–	2.32	–
T_c	–	–	3.72	–	3.52

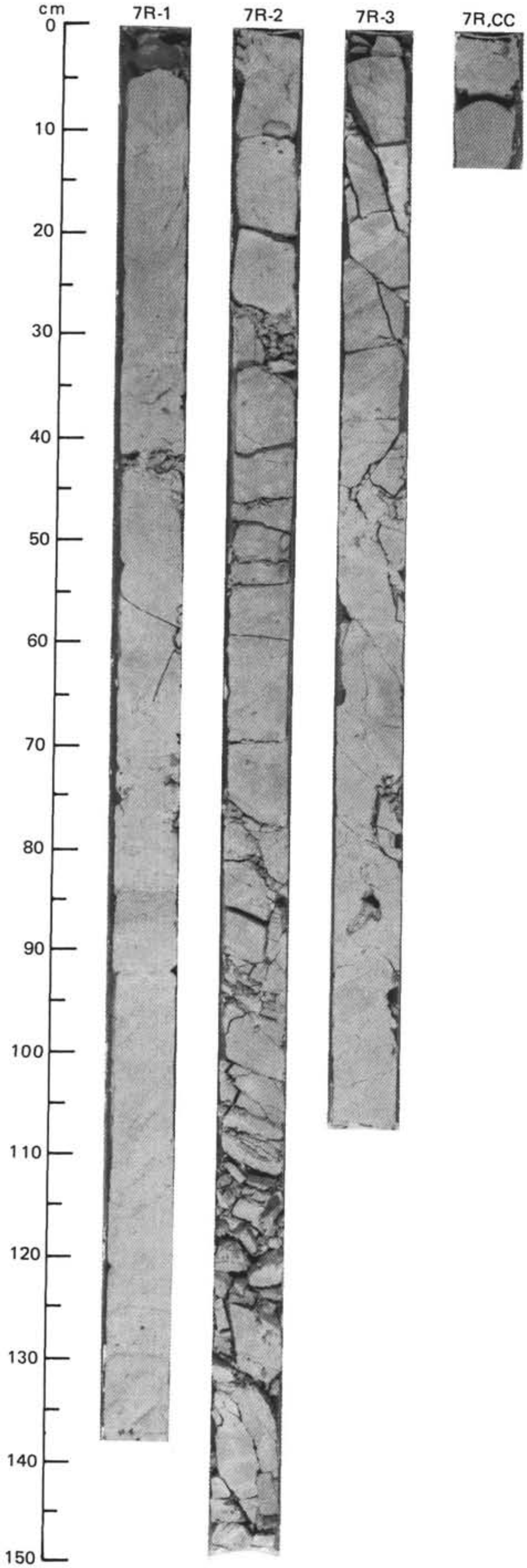
cm
0
10
20
30
40
50
60
70
80
90
100
110
120
130
140
150
7R-1
7R-2
7R-3
7R,CC

SITE 639 HOLE A CORE 8 R CORED INTERVAL 4785.3-4794.9 mbsl; 60.8-70.4 mbsf

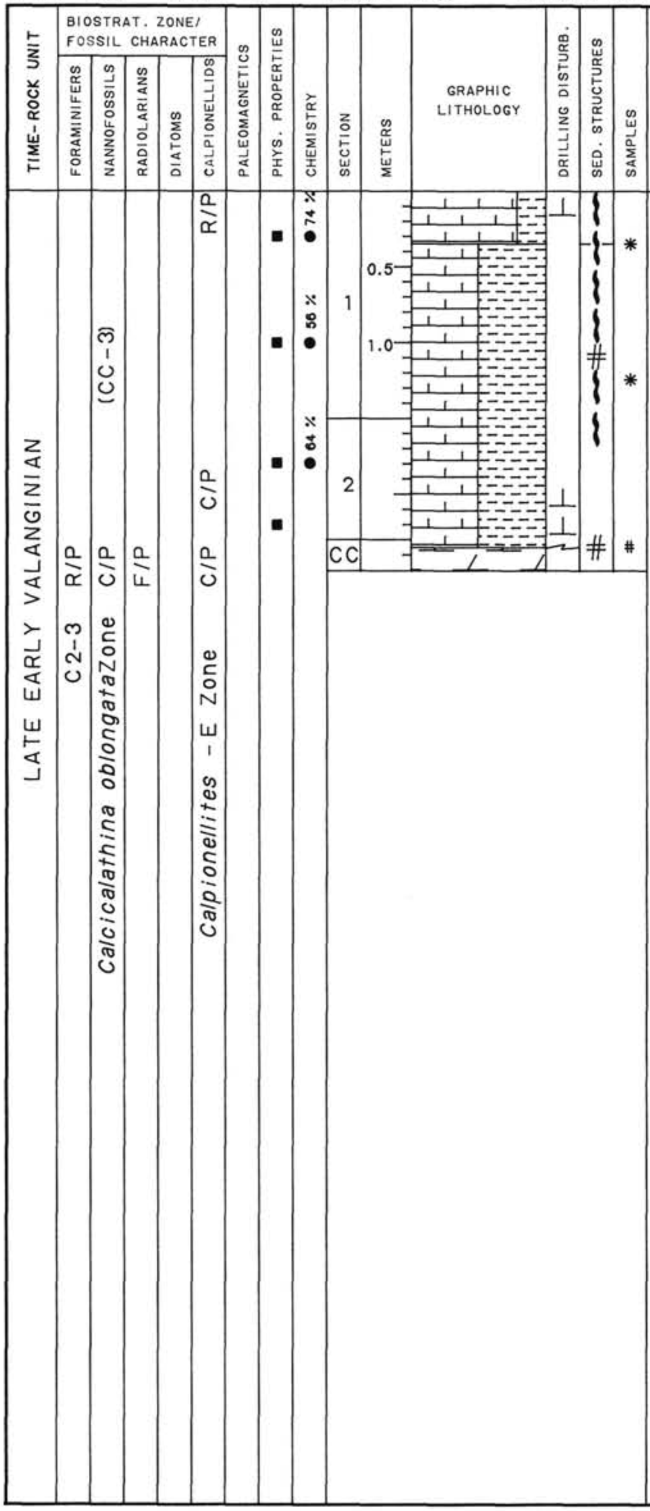

LITHOLOGIC DESCRIPTION

HOMOGENEOUS PALE YELLOW MARLSTONE IN CONTACT WITH LIGHT YELLOWISH BROWN DOLOMITE

Sections 1 and 2 of the Core consist of very uniform pale yellow (5Y 7/3) marlstone which has an apparent dip of 30 degrees. Homogeneity is broken only by (a) rare olive yellow (2.5Y6/6) limonite-stained trace fossils oriented parallel to bedding varying in size from 5 x 20 mm to 1 x 10 mm, (b) Fe/Mn dendritic precipitates concentrated along fractures (Section 1, 112 cm), (c) a loose purplish vein? quartz pebble 1 x 0.5 cm in Section 1, 10 cm and (d) minor very pale brown (10YR7/3) clayey limestone in Section 1, 8-22 cm.

The CC contains a 15 cm long piece of light yellowish brown (2.5Y 6/4), medium-grained dolomite which becomes fine grained in the lowermost 5 cm. Fractures in the dolomite are filled with a dolomicritic sediment. The contact between the dolomite and the marlstone was not recovered.

SMEAR SLIDE AND THIN SECTION SUMMARY (%):

	1,124	CC, 8-11	1,35
	D	D	D
TEXTURE:			
Silt	7	–	8
Clay	93	–	92
COMPOSITION:			
Quartz	Tr	–	Tr
Clay	40	–	30
Calcite	4	–	5
Dolomite	–	95	–
Pore Space	–	5	–
Accessory Minerals:			
Glauconite and bituminous residues and opaques	–	Tr	3
Foraminifers	–	–	Tr
Nannofossils	18	–	–
Radiolarians	–	–	Tr
Micrite	38	–	49
Calpionellids	–	–	3

PHYSICAL PROPERTIES DATA:

	1,28	1,99	2,29	2,70
V_p (a)	2.60	1.93	2.19	–
ρ_b	2.46	2.23	2.36	–
T_c	–	–	–	4.28

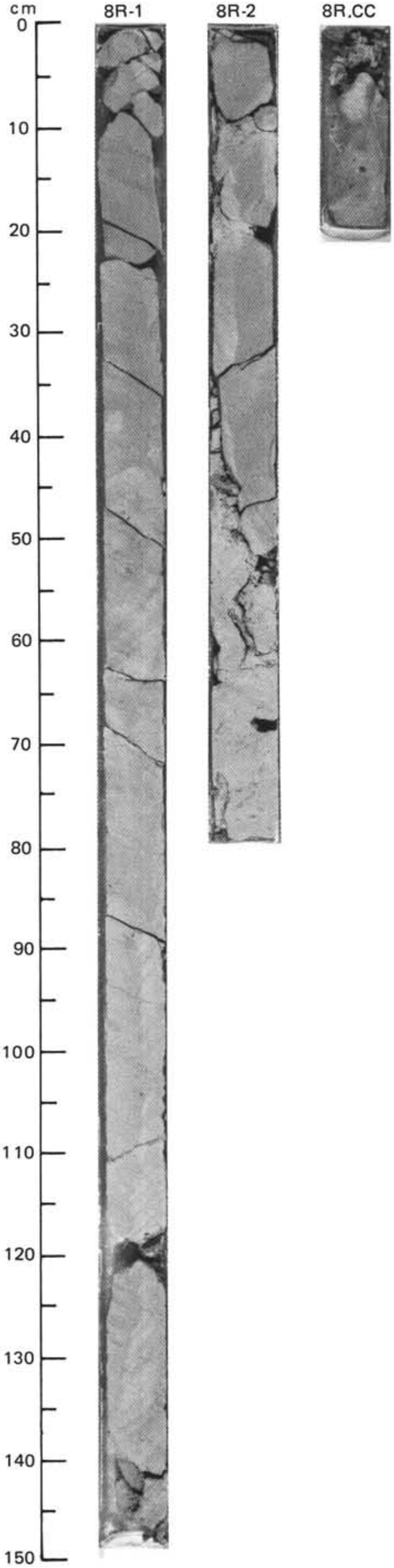
cm
0
10
20
30
40
50
60
70
80
90
100
110
120
130
140
150
8R-1
8R-2
8R,CC

SITE 639 HOLE A CORE 9 R CORED INTERVAL 4794.9–4804.6 mbsl; 70.4–80.1 mbsf

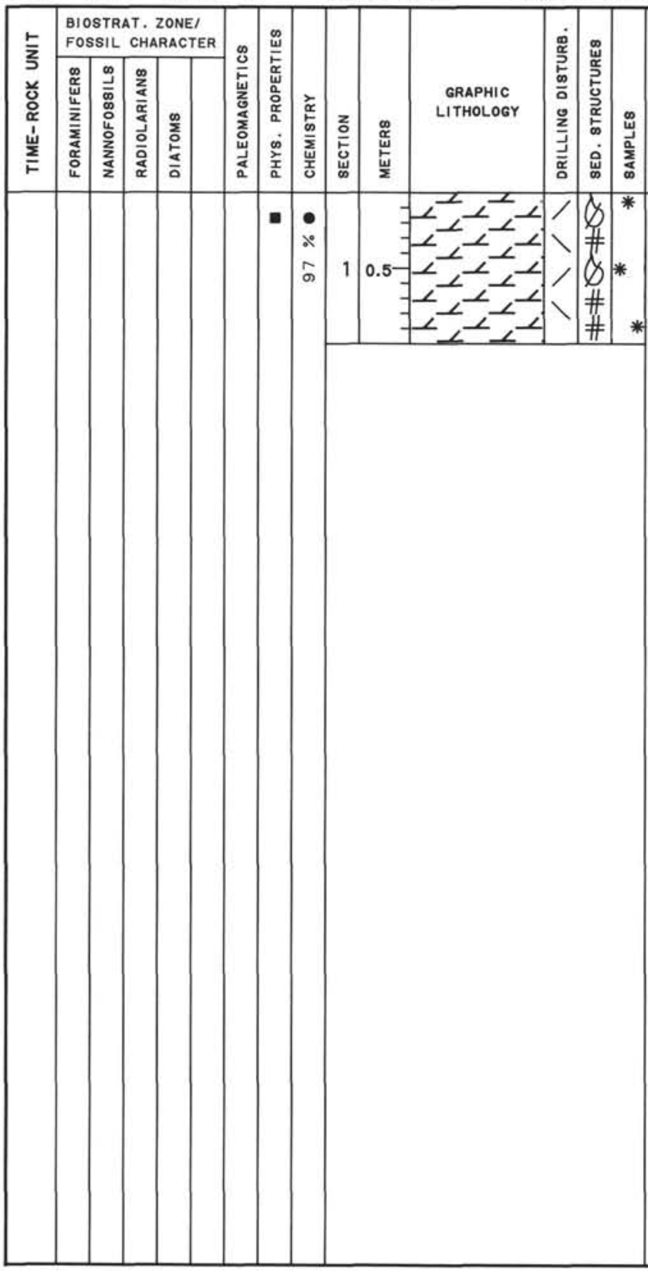

LITHOLOGIC DESCRIPTION

FRACTURED DOLOMITE

The core consists of 16 pieces, averaging 5 cm in diameter, of light brownish gray (2.5Y6.5/3), medium-grained, crystalline, sugary textured dolomite. Allochems and internal structure are difficult to recognize, but rounded ooids (?) up to 0.5 mm in diameter are observed, as well as less common echinoderm and mollusc debris (Section 1, 5-10 cm and 47-55 cm) and gastropod molds (up to 1 cm). Original texture was probably grainstone to packstone. Pre- dolomitization fractures filled with white spar, now dolomite, are common. These are thin, 1-2 mm thick, crosscutting veins at 67-72 cm and 80-101 cm. A final set of fractures is filled with yellowish (2.5Y8/6), very fine-grained dolomite sediment which contains sand-sized rhombs of dolomite (19-27 cm, 42-47 cm, and 86-92 cm). Vugs up to 1 cm across are present and are best developed at 86-92 cm. Thin sections show dolomite-crystal size to be rather uniform, averaging 300 microns. Single crystals commonly have rhombohedral-shaped, zoned cores of impurities. Locally centimeter or larger sized patches are cloudy with impurities.

THIN SECTION SUMMARY (%):

	1,4-9	1,52-54	1,94-98
	D	D	D
TEXTURE:			
(CM=Crystaline Mosaic)	CM	CM	CM
COMPOSITION:			
Dolomite	100	100	95
Cement	–	–	5

PHYSICAL PROPERTIES DATA:

	1,13
V_p (a)	5.90
ρ_b	2.96

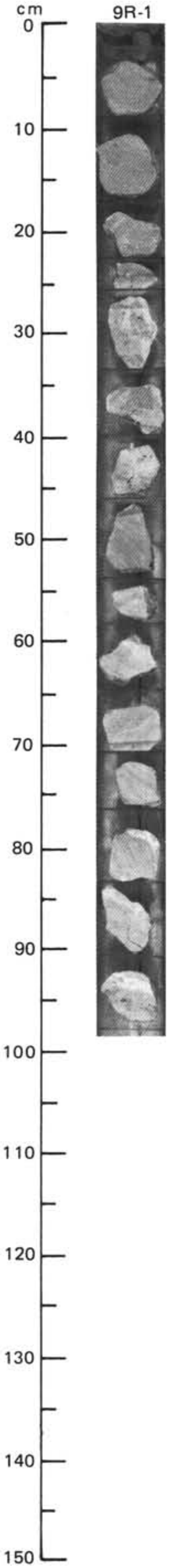
cm
9R-1
0
10
20
30
40
50
60
70
80
90
100
110
120
130
140
150

SITE 639 HOLE A CORE 10 R CORED INTERVAL 4804.6-4814.3 mbsl; 80.1-89.8 mbsf

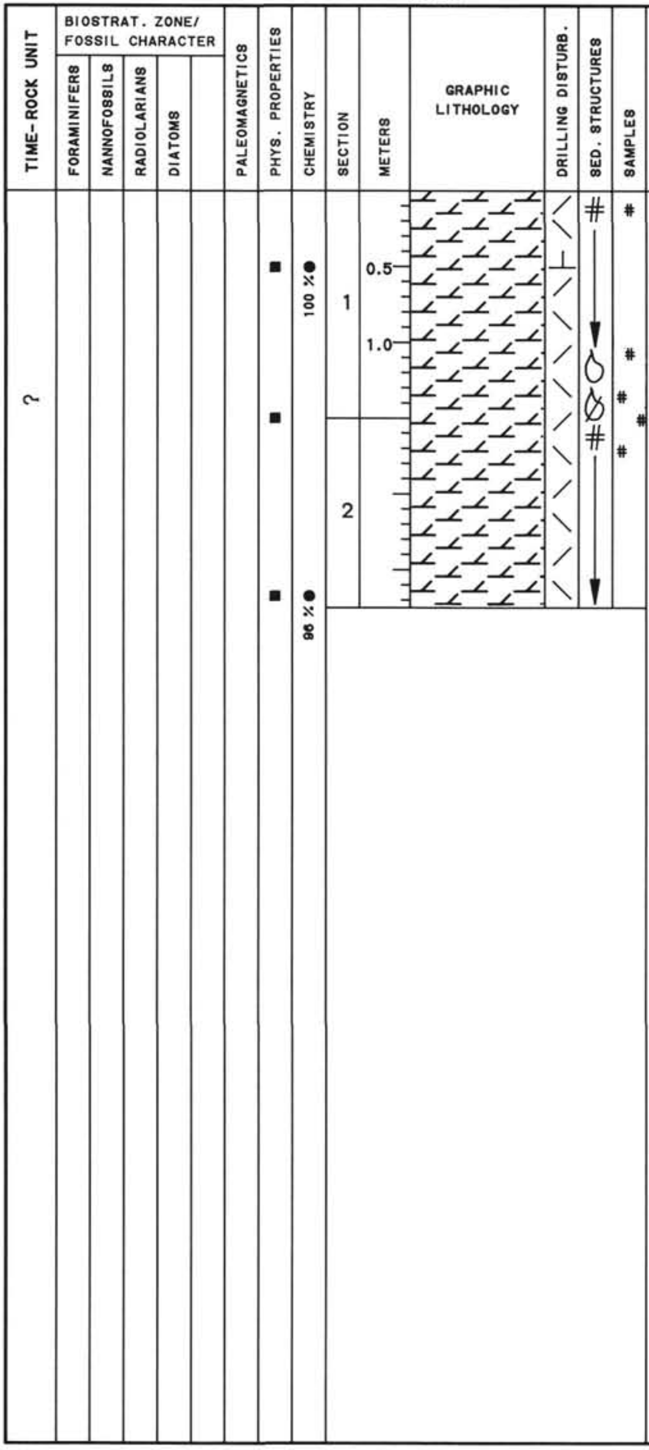

LITHOLOGIC DESCRIPTION

FRAMESTONE (?) DOLOMITE

The core consists of pieces of vuggy, light yellowish brown (2.5Y 6.5/4) medium- to coarse-grained, crystalline dolomite. Most allochems and internal structures cannot be identified, but skeletal grains (gastropods, bivalves, echinoderm debris), oncoide(?) and intraclasts(?) are observed. Original texture was probably a grainstone to packstone. Open vugs, up to 1.5 cm across, are common. Filled vugs and fractures are also abundant. Filling of large vugs, up to 5 cm across (best observed in Section 2, 17-23 cm), includes: (a) dark grayish brown (2.5Y4/2) geopetal, laminated, originally micritic, very fine-grained dolomitic internal sediment, (b) pale yellow (2.5Y7.5/4) internal sediment which has a dolomicrite to dolomicrospar matrix and laminations of sand- and silt-sized dolomite crystals and (c) baroque dolomite vug lining. Fractures include those which are filled with spar that is now dolomite (predolomitization fractures), and a set which cuts all fabric in the rock. The latter set is filled with a yellow (2.5Y8/6), dolomicrite to dolomicrosparite, locally laminated internal sediment. The fact that many of the recovered pieces are coated with this yellow material suggests the dolostone is rubbly and highly fractured here.

Thin section observation shows crystal size to average 300 microns, ranging from 15-800 microns. Single crystals commonly have cores of impurities which are zoned and rhombehedral shaped. Locally centimeter- or larger-size patches are cloudy with impurities.

THIN SECTION SUMMARY (%):

	1,15- 18 D	1,144- 116 D	1,143- 144 D	1,147- 149 D	2,16- 21 D
TEXTURE:					
(CM=Crystaline Mosaic)	CM	CM	CM	CM	CM
COMPOSITION:					
Clay	–	–	–	–	2
Dolomite	100	85	100	100	98
Pore Space	–	15	–	–	–

PHYSICAL PROPERTIES DATA:

	1,46	1,144	2,116
V_p (c)	6.62	5.91	6.85
ρ_b	2.94	–	–

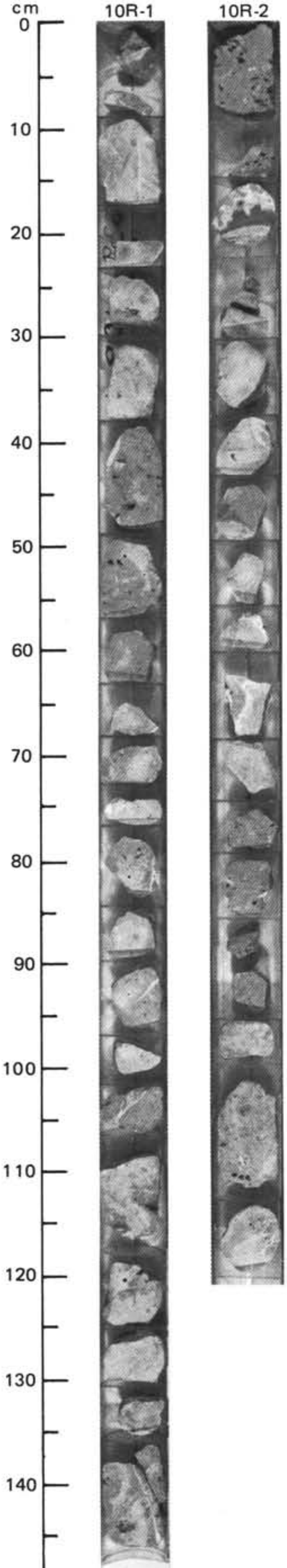
cm
0
10
20
30
40
50
60
70
80
90
100
110
120
130
140
150
10R-1
10R-2

SITE 639 HOLE B CORE 1 R CORED INTERVAL 4747.5-4754.5 mbsl; 0.0-9.7 mbsf

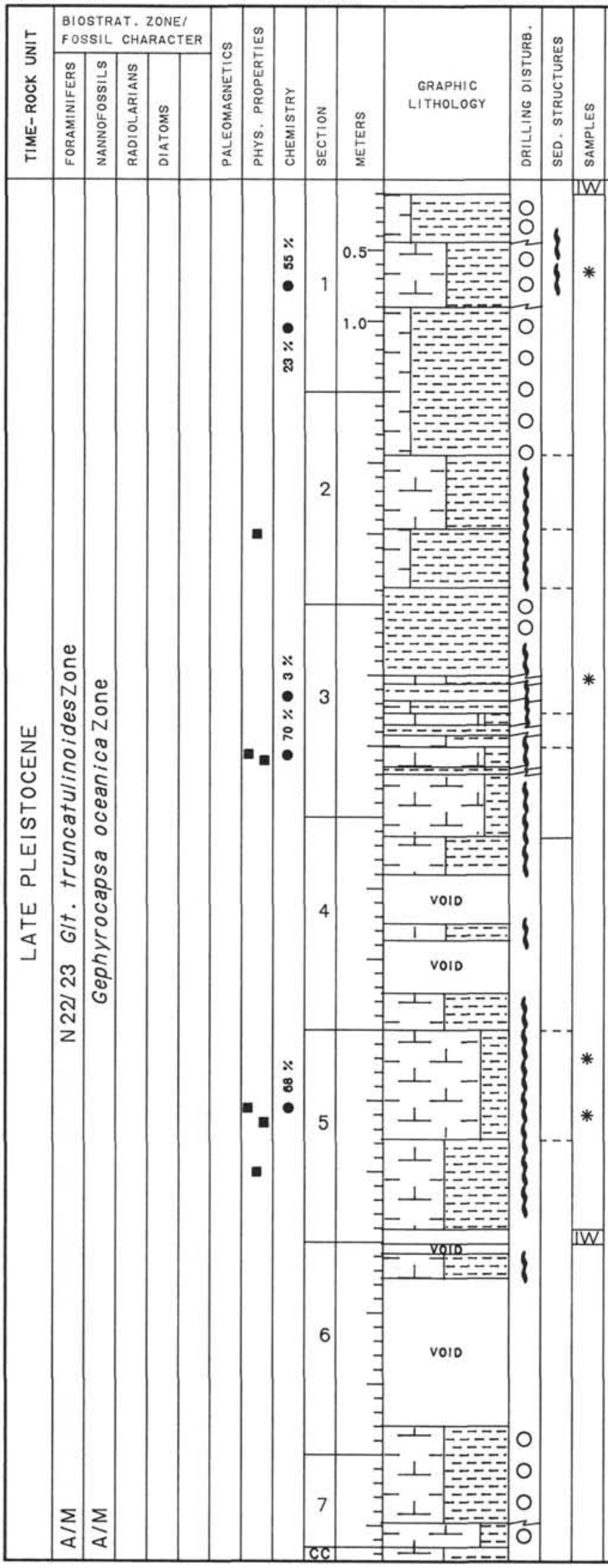

LITHOLOGIC DESCRIPTION

INTERBEDDED CLAYEY NANNOFOSSIL OOZE, NANNOFOSSIL MARL, CALCAREOUS CLAY and CLAY.

The core consists of alternating (on a scale of 5-200 cm) light gray (5Y7/1), locally foraminiferal-bearing, nannofossil ooze, light olive gray (5Y6/2) clayey nannofossil ooze, olive gray (5Y5/2) calcareous clay and lesser olive gray (5Y4/2) clay. Drilling disturbance is high, and no primary sedimentary structures are preserved except for some burrows (?) in Section 1. Foraminiferal silt occurs in Section 5 at 80-88 cm. Purplish-stained streaks from a Fe/Mn precipitate are common.

SMEAR SLIDE SUMMARY (%):

	1,70 D	3,60 D	5,22 D	5,60 D
TEXTURE:				
Silt	7	4	10	12
Clay	93	96	90	88
COMPOSITION:				
Quartz	Tr	4	–	–
Mica	Tr	2	–	–
Clay	40	82	30	30
Calcite/Dolomite	–	5	–	–
Accessory Minerals:				
Pyrite	–	–	–	Tr
Foraminifers	7	–	10	12
Nannofossils	53	3	60	58
Sponge Spicules	Tr	–	–	–
Plant Debris	Tr	4	–	–

PHYSICAL PROPERTIES DATA:

	2,100	3,103	3,109	5,53	5,64	5,100
V_p (c)	–	–	1.40	1.48	–	–
ρ_b	–	–	1.58	1.61	–	–
γ	–	3.28	–	–	3.85	–
T_c	2.35	–	–	–	–	2.35

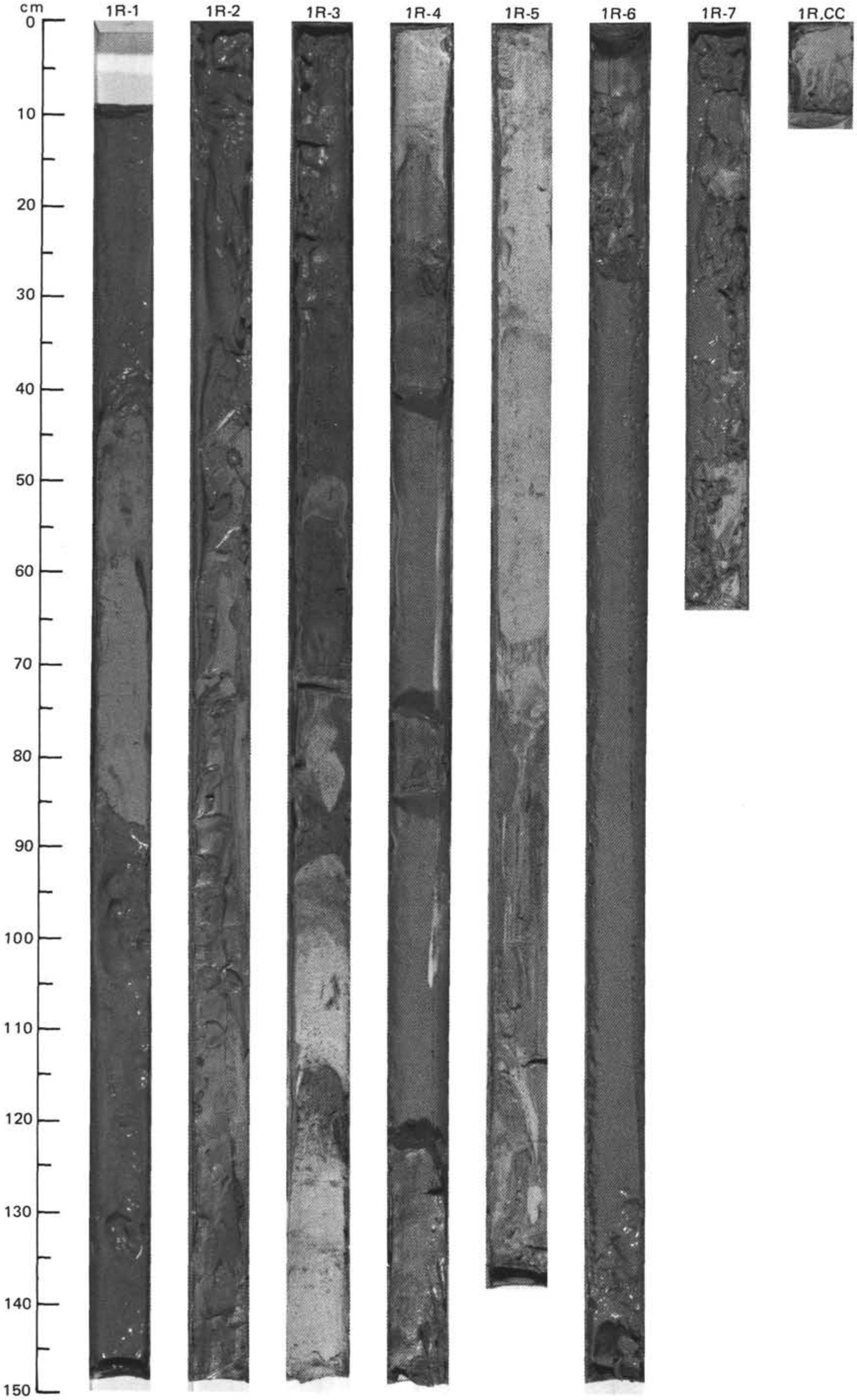
cm
0
10
20
30
40
50
60
70
80
90
100
110
120
130
140
150
1R-1
1R-2
1R-3
1R-4
1R-5
1R-6
1R-7
1R,CC

SITE 639 HOLE B CORE 2 R CORED INTERVAL 4811.0-4814.0 mbsl; 63.5-66.5 mbsf

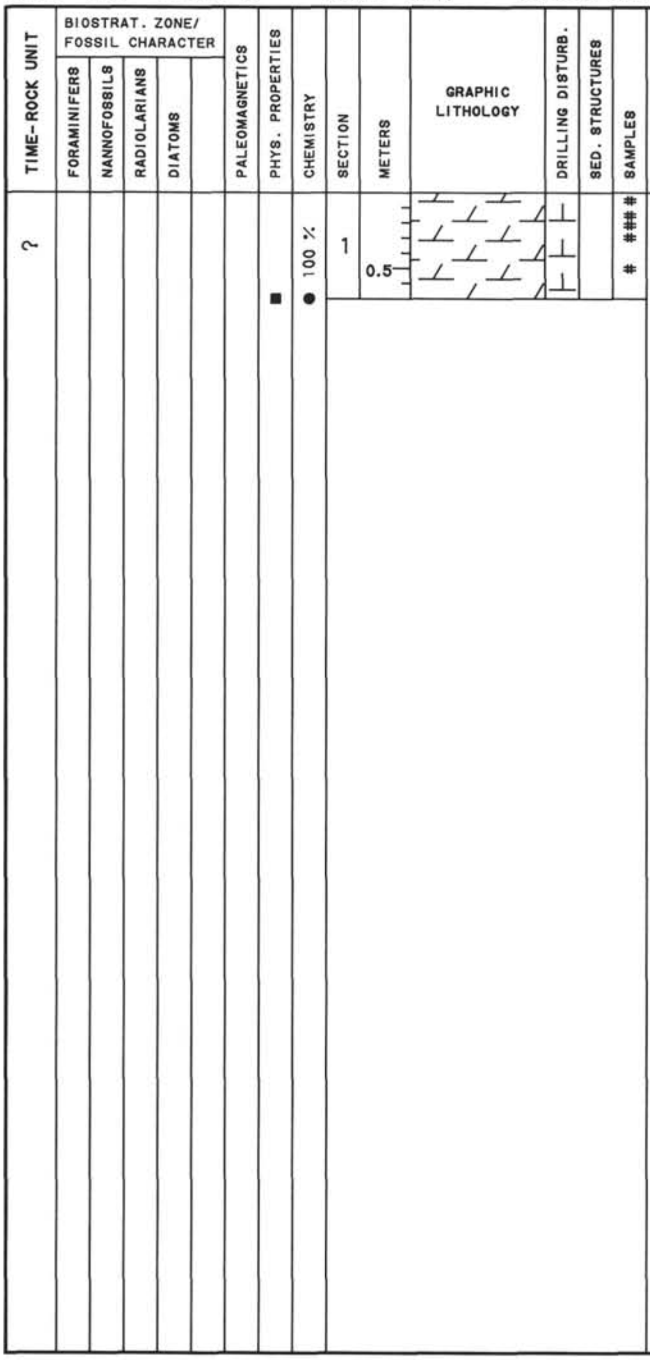

LITHOLOGIC DESCRIPTION

FRAMESTONE (?) DOLOMITE

The core consists of four pieces of dark grayish brown (10YR4/2), massive, dolomite to dolomitic limestone with white marbling. Parts of the rock may be a reefal (?) framestone. Intraclast breccia with clasts up to 7 cm long, one of which has spar-filled fractures and cement lining, occurs in Section 1 at 60-70 cm. Samples display a complex pattern of voids and void filling (on a cm or perhaps much larger scale). Some voids may be primary cavities of building organisms filled with: (a) coarse-grained sediment which includes intraclasts, cemented crusts and crystal debris in a yellow (10YR8/8) dolomicritic matrix, (b) peloidal packstone and (c) white coarse-grained sparry cement or peloidal packstone. Unoriented, plate- and tube-like, white, spar-filled structures (1 mm wide and varying in length from mm to several cm) are common throughout. Their origin remains undetermined.

Thin section observation shows echinoderm debris, bivalves, pelecypods, dasycladacean (?) algae, and unidentified tube-like structures (200 x 800 microns). Dolomite- crystal size averages 300 microns. Single crystals commonly have cores of impurities which are rhombohedral and zoned. Locally centimeter- or larger- size patches are cloudy with impurities.

THIN SECTION SUMMARY (%):

	1,0- 3 D	1,3- 5 D	1,27- 30 D	1,48- 50 M	1,23- 26 D
TEXTURE:					
(CM=Crystalline Mosaic)	CM	CM	CM	–	CM
COMPOSITION:					
Clay	–	–	–	8	–
Dolomite	100	100	100	92	100

PHYSICAL PROPERTIES DATA:

	1,68
V_p (c)	6.70
ρ_b	3.10

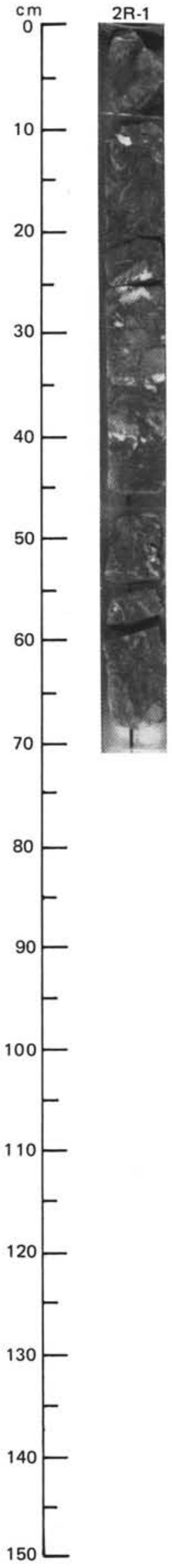
cm
2R-1
0
10
20
30
40
50
60
70
80
90
100
110
120
130
140
150

SITE 639 HOLE B CORE 3 R CORED INTERVAL 4814.0-4823.5 mbsl; 66.5-76.0 mbsf

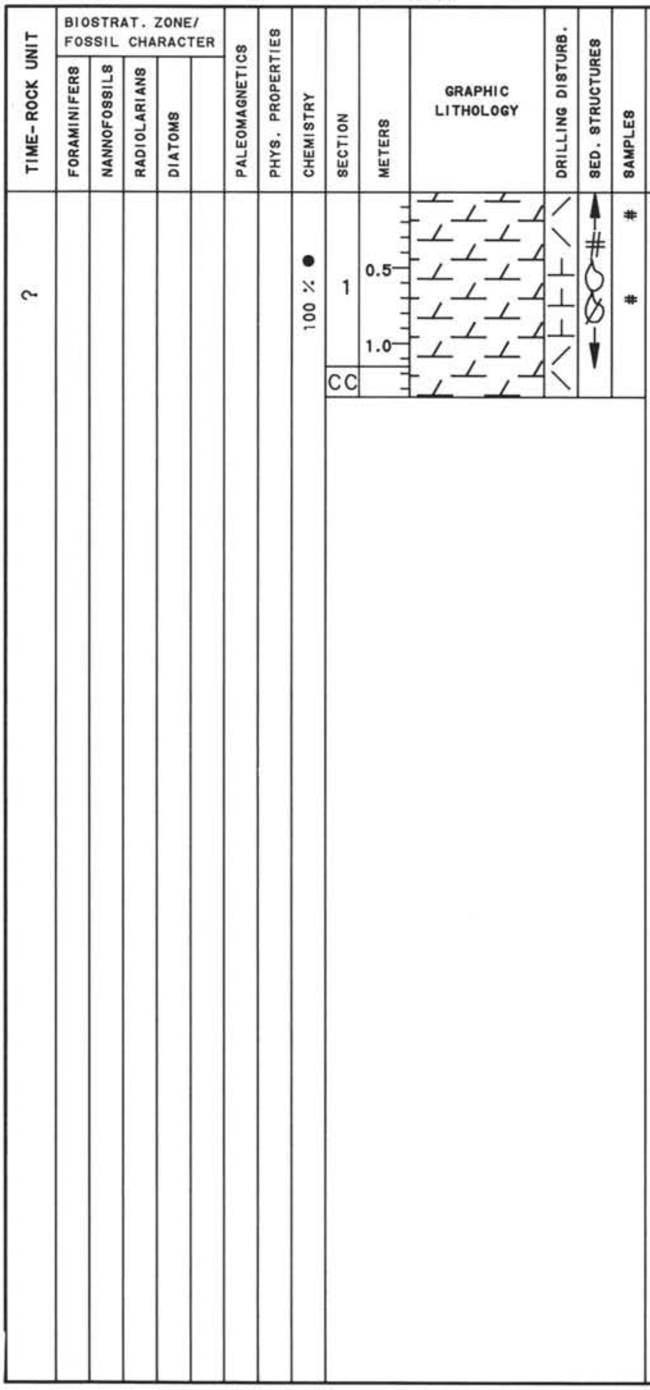

LITHOLOGIC DESCRIPTION

FRAMESTONE (?) DOLOMITE

The core consists of dark grayish brown (10YR4/2) dolomite to dolomitic limestone which may be a biohermal (?) framestone. Allochems and internal structure are generally not recognizable but gastropods and echinoderm debris can be identified. A complicated system of vugs, cavities and fractures filled with cements and internal sediment is present throughout. Laminated, light gray (10YR7/2), dolomicritic, geopetal fill is present in Section 1 at 10-16 cm and 52-65 cm. Colorless, isopachous, fibrous spar (now dolomite) occurs as: (a) linings in fractures, (b) filling of 'stromatactoid voids' and (c) filling of molds and vugs (Section 1, 106-113 cm). Late-stage fractures are filled with a yellowish (2.5Y8/6), slightly recrystallized, laminated, dolomicrite to dolomicrospar internal sediment which contains laminae of sand-sized dolomite rhombs. Thin sections show that a 2 mm wide border of the crystalline-dolomite mosaic adjacent to these fractures is free of impurities. Most allochems and internal structures cannot be identified, but fossil debris including gastropods, echinoderms, pelecypods(?), brachiopods(?), and algal filaments is observed. Plate- and tube-like, white, spar-filled structures (1 mm wide and varying in length from mm to cm) are common; their origin is not determined. Pale brown (10YR6/3), vuggy, medium-grained, crystalline dolomite occurs in Sections 1, 100-113 cm and Sections 2, 0-20 cm. These may have been grainstones with echinoderm and gastropod debris common.

THIN SECTION SUMMARY (%):

	1,20- 22 D	1,75- 79 D
TEXTURE:		
(CM=Crystalline Mosaic)	CM	CM
COMPOSITION:		
Dolomite	100	100

PHYSICAL PROPERTIES DATA:

	1,44
V_p (c)	6.71
ρ_b	2.99

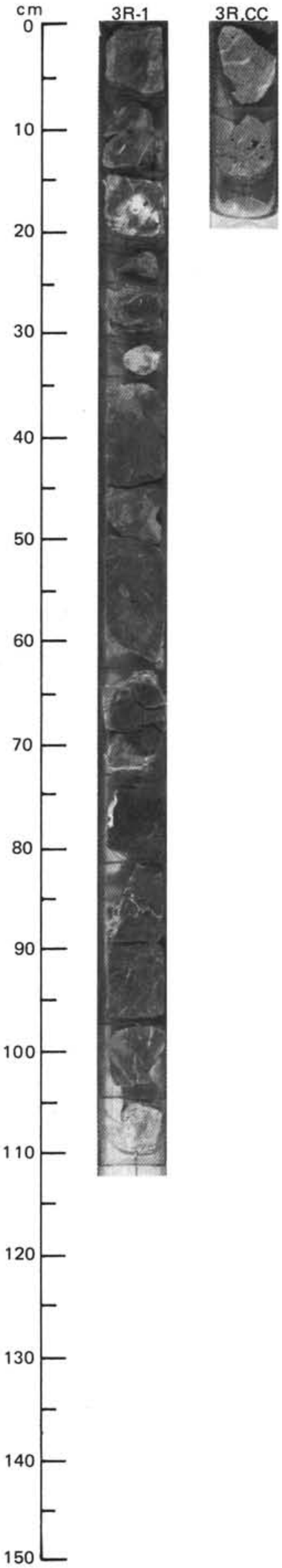
cm
3R-1
3R,CC
0
10
20
30
40
50
60
70
80
90
100
110
120
130
140
150

SITE 639 HOLE B CORE 4 R CORED INTERVAL 4823.5-4827.5 mbsl; 76.0-80.0 mbsf

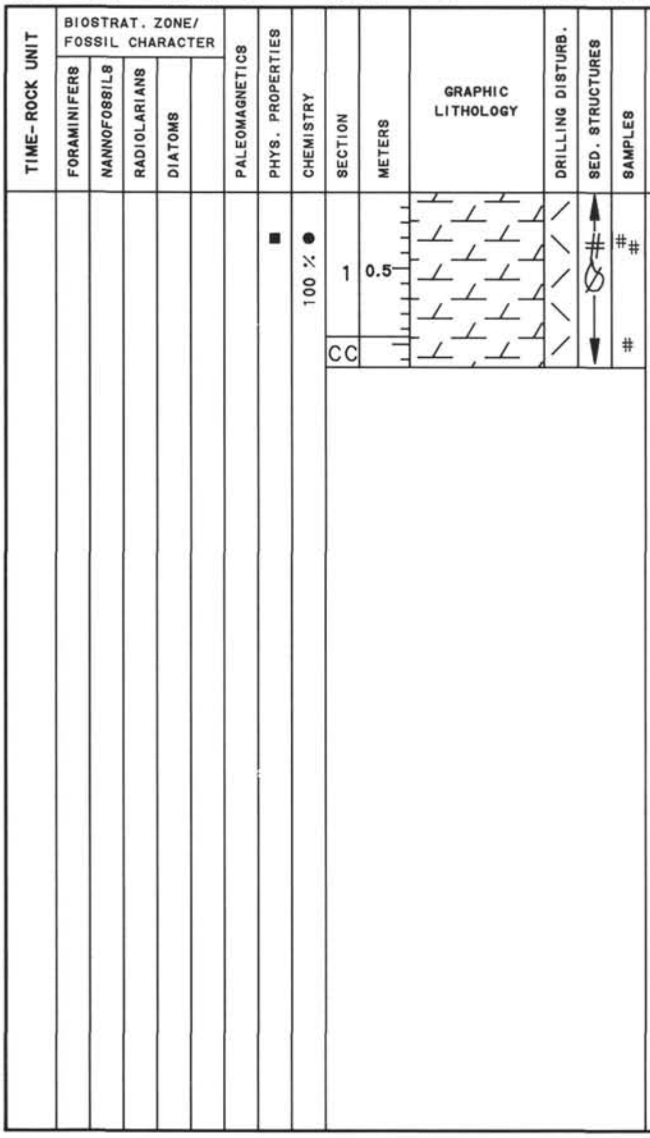

LITHOLOGIC DESCRIPTION

DOLOMITE

The core consists of generally small pieces (4 cm on average) of dolomite with continuous color gradations from dark grayish brown to light brownish gray to light gray (2.5Y4/2, 2.5Y6/3, 2.5Y7/2). Original texture varies from (a) grainstones which are generally light brownish gray to light gray, more extensively fractured and which contain echinoderm debris, to (b) wackestones which are dark brownish gray. Plate- and tube-like, white, spar-filled structures approximately 1 mm x 15 mm are common in the wackestones. Their origin in not known. Multiple periods of pre-dolomitization fracturing, dissolution and void filling by both cement and internal sediment are observed. The youngest system of fractures is filled with a light gray (10YR7/2) dolomicrite to dolomicrospar internal sediment which contains dolomite crystals up to sand size. Some fractures are filled with a dark, faintly rust-colored internal sediment (Section 1, 1-5 cm). Most allochems and internal structures cannot be identified.

THIN SECTION SUMMARY (%):

	1,29- 31 D	1,92- 95 D	1,33- 37 D
COMPOSITION:			
Dolomite	100	100	75
Pore Space	–	–	25

PHYSICAL PROPERTIES DATA:

	1,32
V_p (c)	6.50
ρ_b	2.84

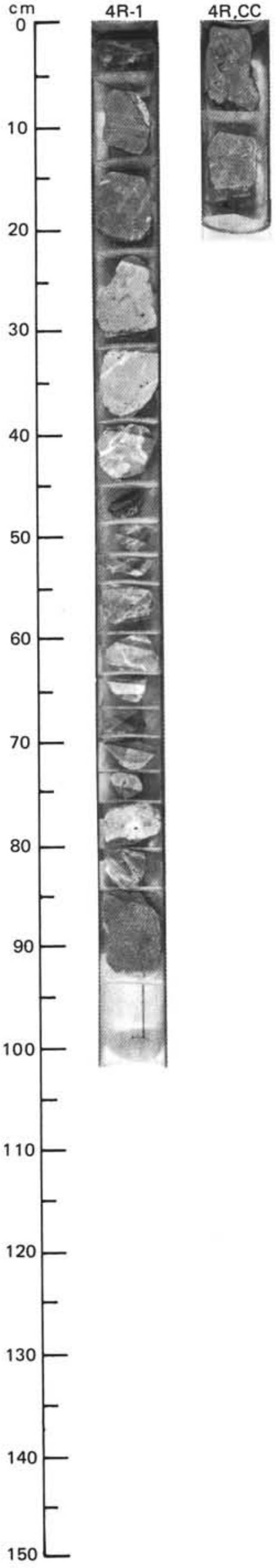
cm
0
10
20
30
40
50
60
70
80
90
100
110
120
130
140
150
4R-1
4R,CC

SITE 639 HOLE C CORE 1 R CORED INTERVAL 4859.5-4872.3 mbsl; 78.0-90.8 mbsf

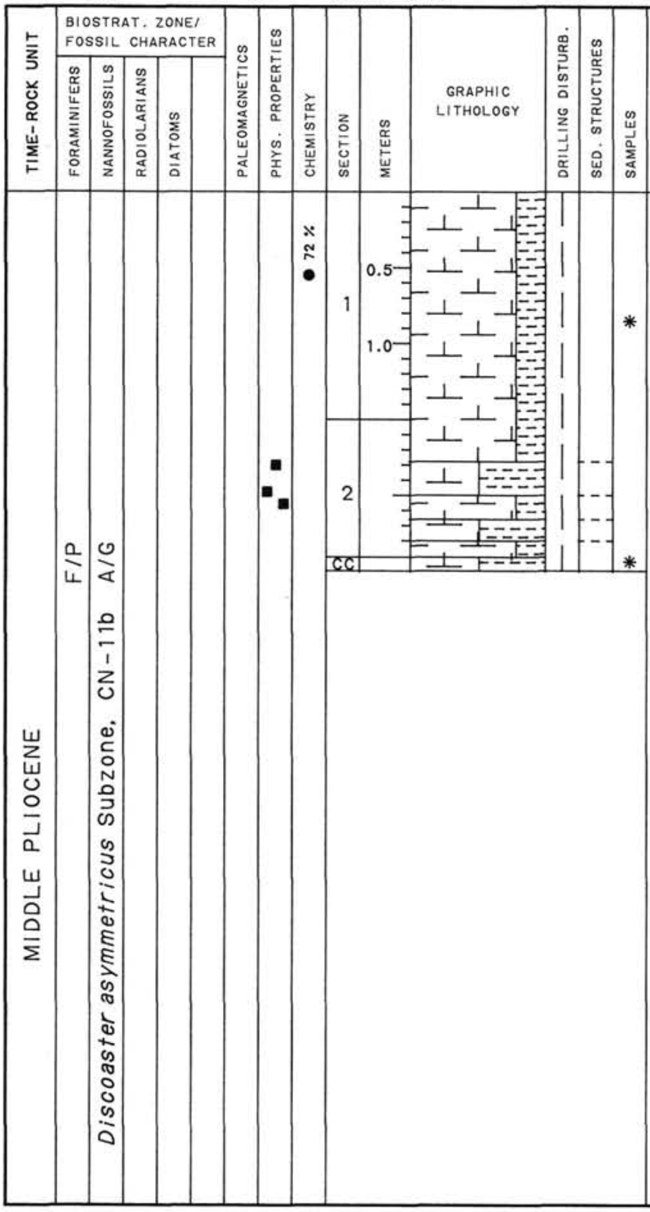

LITHOLOGIC DESCRIPTION

CLAYEY NANNOFOSSIL OOZE and NANNOFOSSIL MARL.

The core consists of stiff, white to light gray (5Y8/1-5Y7/1) clayey nannofossil ooze and light gray (5Y7/1) nannofossil marl. Section 1 is entirely clayey nannofossil ooze, whereas in Section 2, the two lithologies alternate on a 10-20 cm scale. Purplish streaks and bands 1-5 cm thick stained by Fe/Mn precipitates are present throughout.

SMEAR SLIDE SUMMARY (%).

	1,86 D	CC,1 D
TEXTURE:		
Silt	7	5
Clay	93	95
COMPOSITION:		
Mica	–	1
Clay	15	42
Calcite/Dolomite	–	5
Accessory Minerals:		
Opaques	–	2
Foraminifers	7	–
Nannofossils	78	50

PHYSICAL PROPERTIES DATA:

	2,30	2,45	2,53
V_p (c)	–	–	1.63
ρ_b	–	–	1.79
γ	–	3.96	–
T_c	2.719	–	–

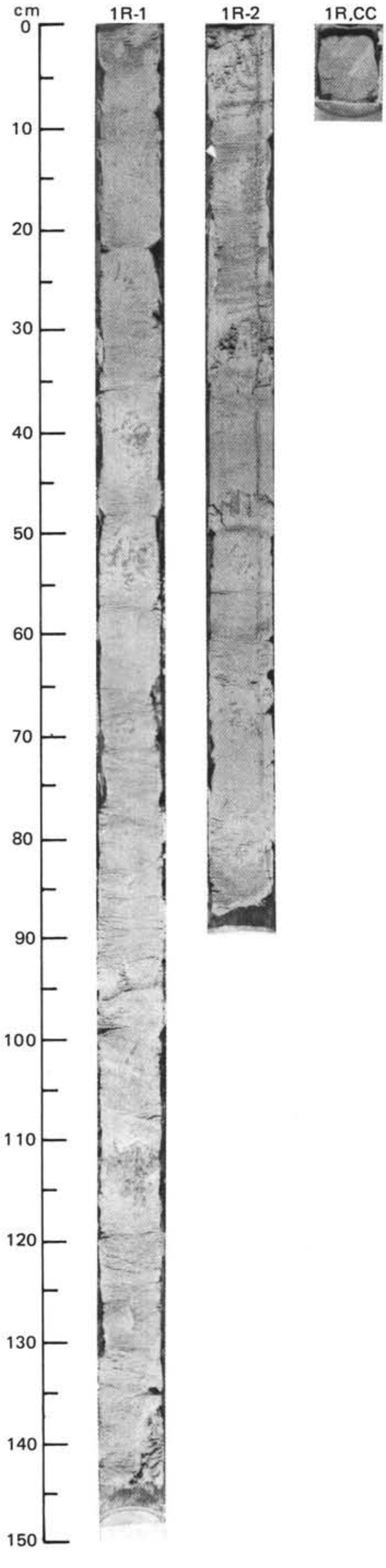
cm
0
10
20
30
40
50
60
70
80
90
100
110
120
130
140
150
1R-1
1R-2
1R,CC

SITE 639 HOLE C CORE 2 R CORED INTERVAL 4872.3-4881.9 mbsl; 90.8-100.4 mbsf

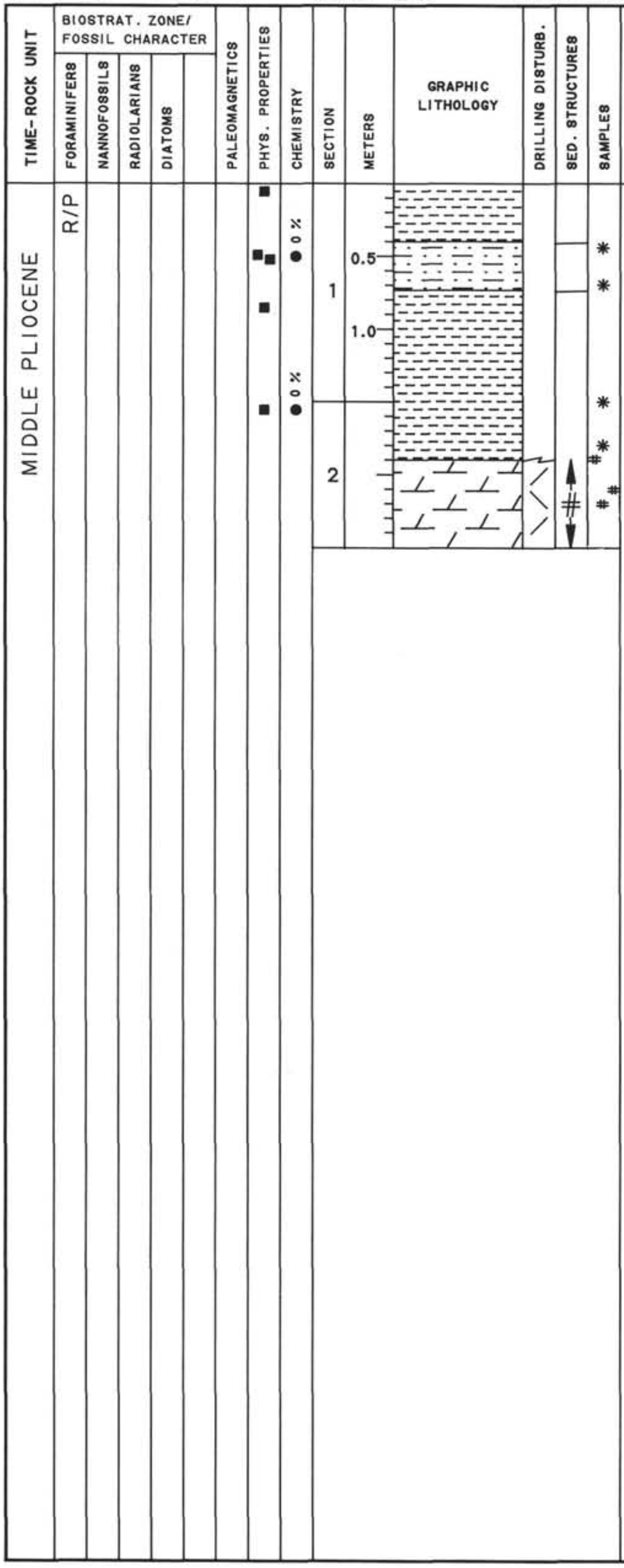

LITHOLOGIC DESCRIPTION

CLAY and CLAYEY SILT overlying DOLOMITE

The core consists of interlayered dark brown, brown, reddish brown and light reddish brown (5YR4/2, 10YR4/3, 2.5YR4/4 and 5YR6/4) clay, commonly variegated with pink and yellow shades and mottled with black (Mn-rich?) patches. The clay is extensively recrystallized. Pale olive (5Y6/4) clayey silt with limonite-stained sandy patches occur in Section 1 at 43-74 cm and 91-92 cm. Primary sedimentary structures are lacking.

The clay overlies (contact not recovered) a light gray (10YR7/2), vuggy, coarse-grained, crystalline dolosparite. The original texture was grainstone to packstone, and although most original allochems and internal structures are not recognizable, gastropods, thick-walled molluscs, a biserial foram and echinoderm debris are identified. Pre-dolomitization fractures with sparry cement are common, and at least one large cavity which is filled with void-filling cement and internal sediment is recognizable.

Thin section observation shows dolomite-crystal size to average 300 microns. Single crystals commonly have rhombohedral cores of impurities which are zoned. Irregular centimeter- or larger-size patches which are cloudy with impurities are common.

SMEAR SLIDE AND THIN SECTION SUMMARY (%):

	1,48	1,69	1,150	2,31	2,43	2,52	2,61-63
	D	M	D	M	D	D	D
TEXTURE:							
(CM=Crystalline Mosaic)	–	–	–	–	CM	CM	CM
Sand	Tr	–	–	–	–	–	–
Silt	10	50	5	15	–	–	–
Clay	90	50	95	85	–	–	–
COMPOSITION:							
Quartz	10	25	4	2	–	–	–
Feldspar	Tr	3	–	Tr	–	–	–
Rock Fragments	–	Tr	–	Tr	–	–	–
Mica	Tr	25	–	15	–	–	–
Clay	89	45	95	80	–	–	–
Calcite/Dolomite	–	–	Tr	Tr	100	100	100
Accessory Minerals:							
(Opaques, Zircon, Fe Ox)	1	–	1	3	–	–	–
Zeolites	Tr	–	–	–	–	–	–
Amph.,Pyrite,Opaques	–	5	–	–	–	–	–

PHYSICAL PROPERTIES DATA:

	1,5	1,49	1,52	1,85	2,5
V_p (c)	1.46	1.57	–	–	–
ρ_b	–	1.98	–	–	1.68
T_c	–	–	3.59	2.64	–

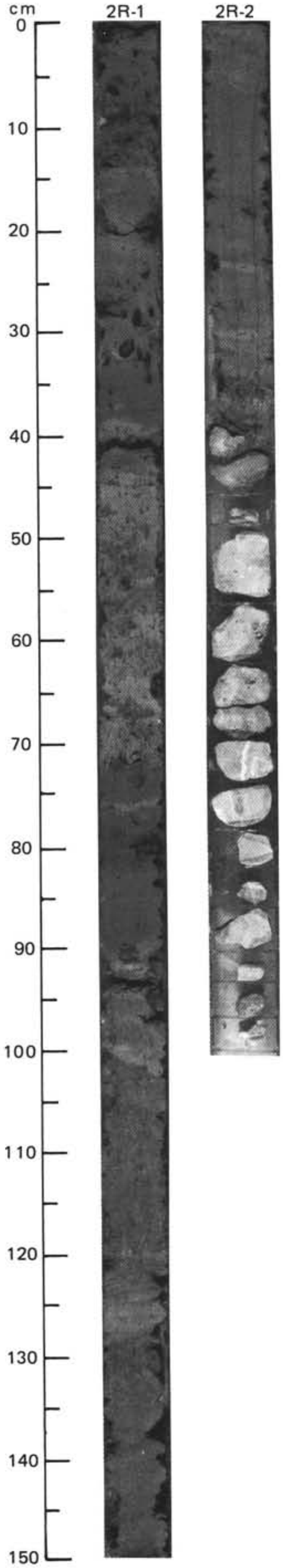
cm
0
10
20
30
40
50
60
70
80
90
100
110
120
130
140
150
2R-1
2R-2

SITE 639 HOLE D CORE 1 W CORED INTERVAL 4920.1-4922.1 mbsl; 177.6-179.6 mbsf

TIME-ROCK UNIT	BIOSTRAT. ZONE/ FOSSIL CHARACTER					PALEOMAGNETICS	PHYS. PROPERTIES	CHEMISTRY	SECTION	METERS	GRAPHIC LITHOLOGY	DRILLING DISTURB.	SED. STRUCTURES	SAMPLES
	FORAMINIFERS	NANNOFOSSILS	RADIOLARIANS	DIATOMS										
EARLY-MIDDLE PLIOCENE	A/M	*Calcidiscus macintyre* Zone ? C/P					■	● 15 %	1 CC	0.5	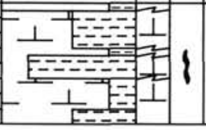			* *

CLAYEY NANNOFOSSIL OOZE, NANNOFOSSIL MARL and CALCAREOUS CLAY

The core consists of highly disturbed pieces (5-10 cm long) of stiff, light gray (5Y7/1) foraminiferal-bearing clayey nannofossil ooze, gray (5Y6/1) nannofossil marl and gray (5Y5/1) calcareous clay in subequal amounts. Except for large burrows (Section 1, 41-53 cm), primary structures are lacking. Dark purplish Fe/Mn-rich laminae are present.

SMEAR SLIDE SUMMARY (%):

	1,48 D	1,32 D
TEXTURE:		
Silt	3	10
Clay	47	90
COMPOSITION:		
Quartz	Tr	Tr
Mica	Tr	Tr
Clay	35	15
Accessory Minerals:		
(Opaques,Zeolites)	Tr	Tr
Foraminifers	3	10
Nannofossils	60	75
Fish Remains	–	Tr

PHYSICAL PROPERTIES DATA:

	1,41
V_p (c)	1.41
ρ_b	1.71

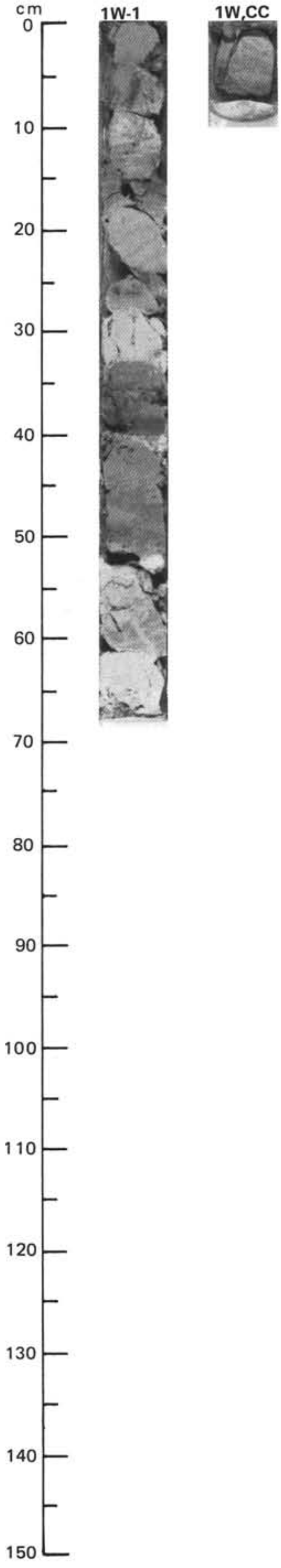
cm
0
10
20
30
40
50
60
70
80
90
100
110
120
130
140
150
1W-1
1W,CC

SITE 639 HOLE D CORE 2 R CORED INTERVAL 4922.1-4929.8 mbsl; 179.6-187.3 mbsf

TIME-ROCK UNIT	BIOSTRAT. ZONE/ FOSSIL CHARACTER					PALEOMAGNETICS	PHYS. PROPERTIES	CHEMISTRY	SECTION	METERS	GRAPHIC LITHOLOGY	DRILLING DISTURB.	SED. STRUCTURES	SAMPLES	LITHOLOGIC DESCRIPTION
	FORAMINIFERS	NANNOFOSSILS	RADIOLARIANS	DIATOMS											
?									CC			/	#	#	

DOLOMITE

The core consists of three pieces of yellowish brown to dark yellowish brown (10YR5/4 to 10YR4/4), coarse-grained, crystalline dolomite to dolomitic limestone. Tentative original texture is packstone to wackestone. Most allochems and internal structure cannot be identified, but echinoderm debris, bivalves, gastropods are observed. Fractures which are now filled with fibrous, drusy dolomite are common. Thin section observation shows pervasive irregular trails of inclusions. The trails commonly branch and join. Origin of this pattern is uncertain, but it may be biogenic.

THIN SECTION SUMMARY (%):

	2,CC 8-11 D
TEXTURE:	
(CM=Crystalline Mosaic)	CM
COMPOSITION:	
Dolomite	100

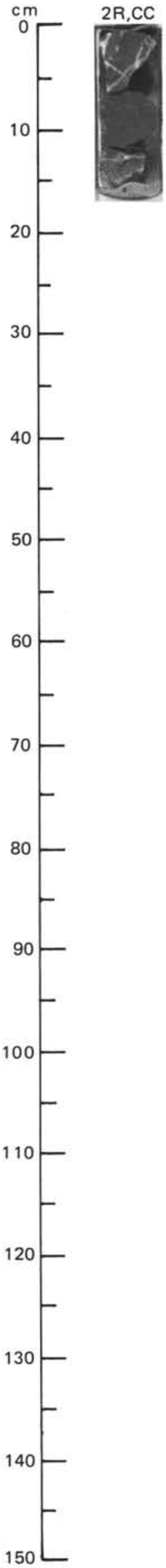
cm
2R,CC
0
10
20
30
40
50
60
70
80
90
100
110
120
130
140
150

SITE 639 HOLE D CORE 3 R CORED INTERVAL 4929.8-4939.3 mbsl; 187.3-196.8 mbsf

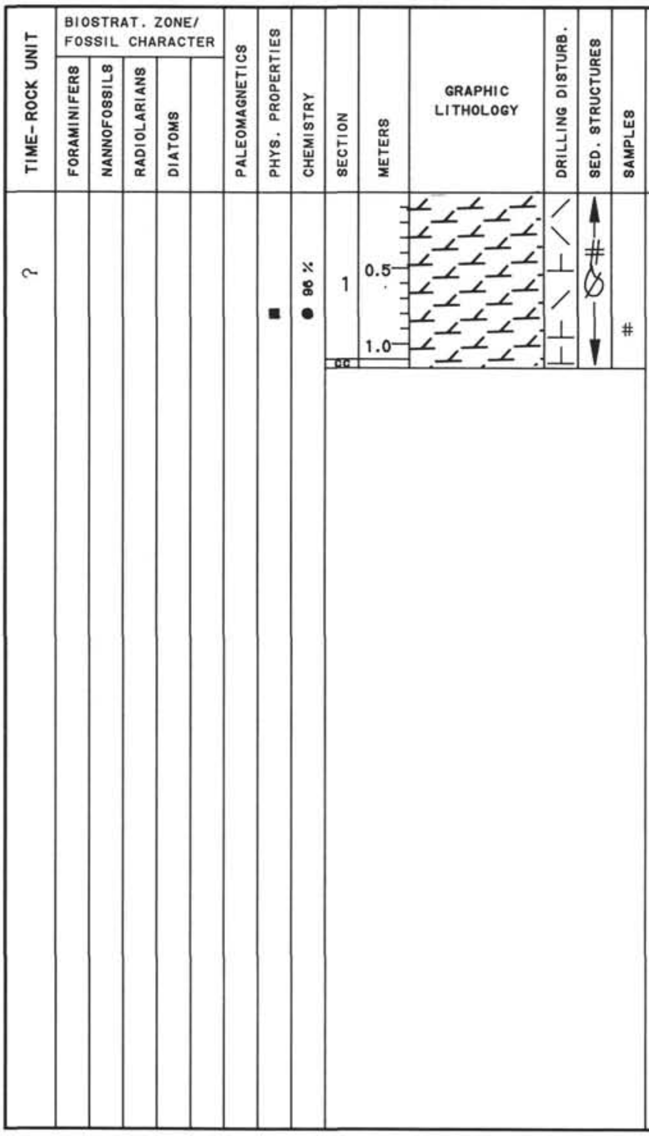

LITHOLOGIC DESCRIPTION

DOLOMITE

The core consists of pieces of grayish brown (2.5Y5/2), fine- to medium-grained, crystalline, locally vuggy dolomite. Original texture was dominantly grainstone to packstone with lesser amounts of wackestone. Most allochems and internal structure cannot be recognized, but echinoderm debris and gastropods are identified. Plates or filaments of probable biogenic origin are also present. Fractures filled with clear spar that is now dolomite are common (pre-dolomitization fractures). Intercrystal pores are lined with a limonitic stain. Vugs up to 8 mm across, partially filled with dolospar, are present throughout.

In thin section, dolomite crystals are generally subhedral. Single crystals commonly have rhombohedral-shaped cores of impurities which may contain up to 8 zonations. Maximum crystal size is 1200 microns and the average is 300 microns.

THIN SECTION SUMMARY (%):

	1,88-91
TEXTURE:	
(CM=Crystalline Mosaic)	CM
COMPOSITION:	
Dolomite	100

PHYSICAL PROPERTIES DATA:

	1,83
V_p (c)	6.49
ρ_b	3.05

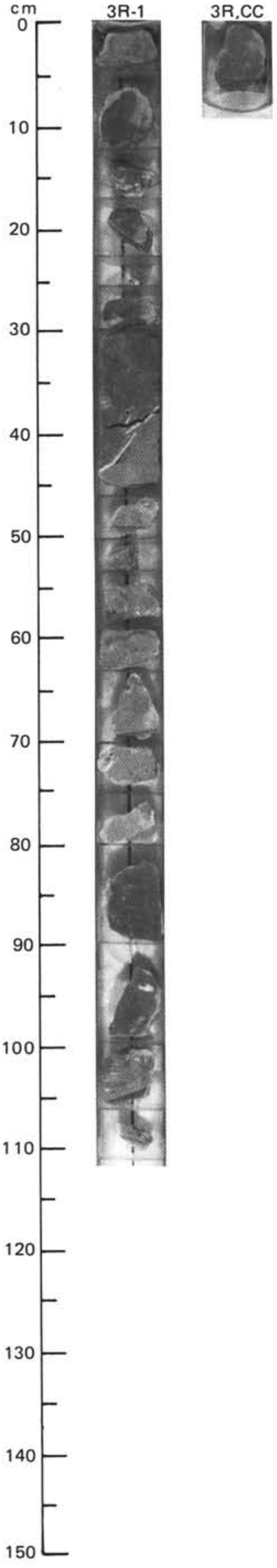
cm
0
10
20
30
40
50
60
70
80
90
100
110
120
130
140
150
3R-1
3R,CC

SITE 639 HOLE D CORE 4 R CORED INTERVAL 4939.3-4949.0 mbsl; 196.8-206.5 mbsf

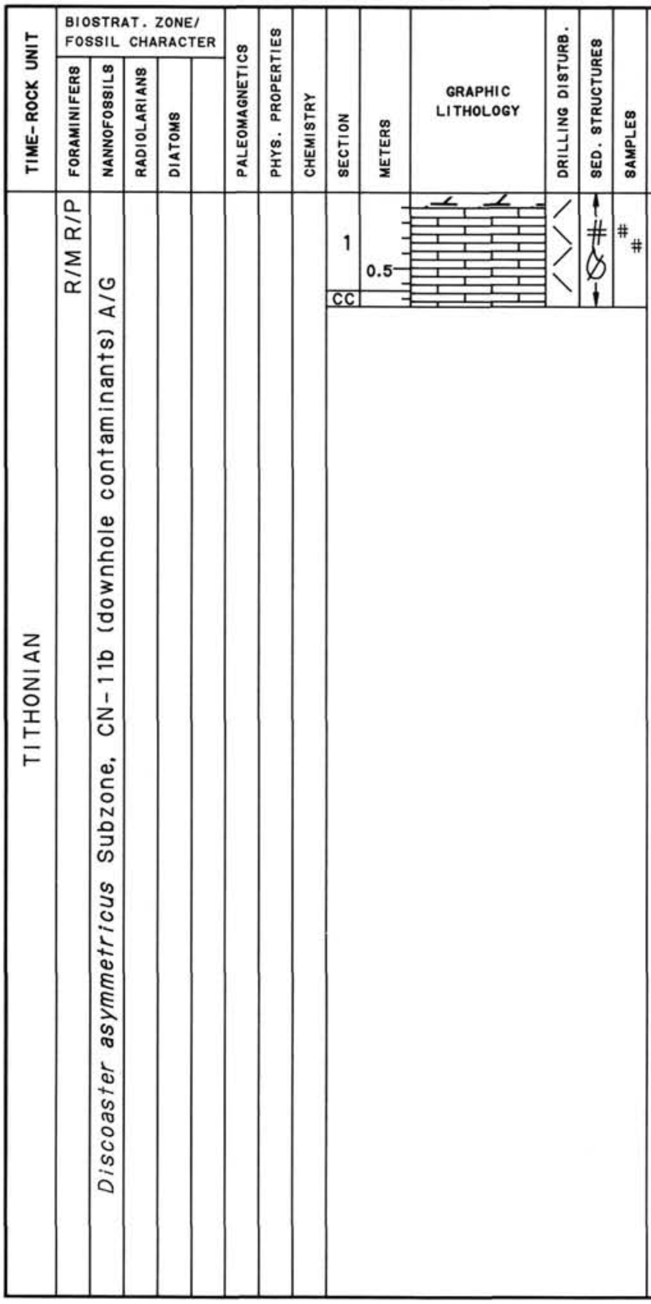

LITHOLOGIC DESCRIPTION

DOLOMITE and CLAYEY LIMESTONE

The core consists of one piece of light olive brown (2.5Y5/4), vuggy, medium-grained, crystalline dolomite (Section 1, 0-9 cm) overlying pieces of light gray, gray and light olive brown (2.5Y7/2, 2.5Y6/2, 2,5Y5/4; Section 1) and pinkish gray to dark reddish gray (5YR7/2, 5YR4/2; CC), slightly dolomitized (?) clayey limestone. The contact between dolomite and clayey limestone was not recovered. The clayey limestone is a skeletal, locally bioclastic, peloidal packstone to wackestone and locally a floatstone. Allochems include benthic foraminifera, encrusting bryozoa, pelecypods, gastropods, bivalves, brachiopods, serpulids, worm tubes, algae, sponges and debris of echinoderms, pelecypods and coral in a peloidal micrite matrix. Micrite is commonly recrystallized into neomorphic microspar. Small fractures and vugs (birds eye) filled and partially filled by sparry calcite are present. An encrusted surface occurs in the CC at 0-4 cm. Primary sedimentary structures are rare.

THIN SECTION SUMMARY (%):

	1,26-28 D	1,31-34 D	CC,7-9 D
TEXTURE:			
(CM=Crystalline Mosaic)	CM	CM	CM
Sand	50	81	70
Micrite/Cement	50	19	30
COMPOSITION:			
Sparry Calcite Cement	50	–	10
Foraminifers	5	–	Tr
Sponge Spicules	–	1	Tr
Pellets	10	40	20
Bioclasts	35	40	50
Micrite	–	19	20

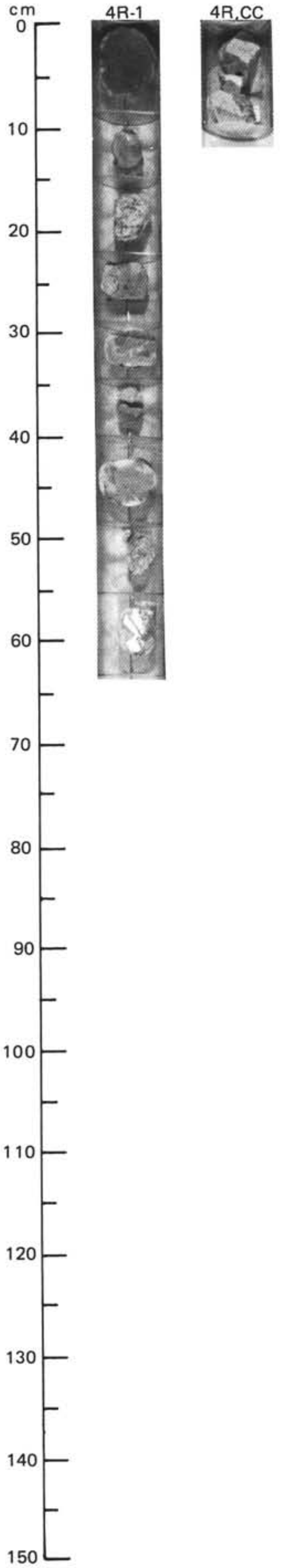
cm
0
10
20
30
40
50
60
70
80
90
100
110
120
130
140
150
4R-1
4R,CC

SITE 639 HOLE D CORE 5 R CORED INTERVAL 4949.0-4958.5 mbsl; 206.5-216.0 mbsf

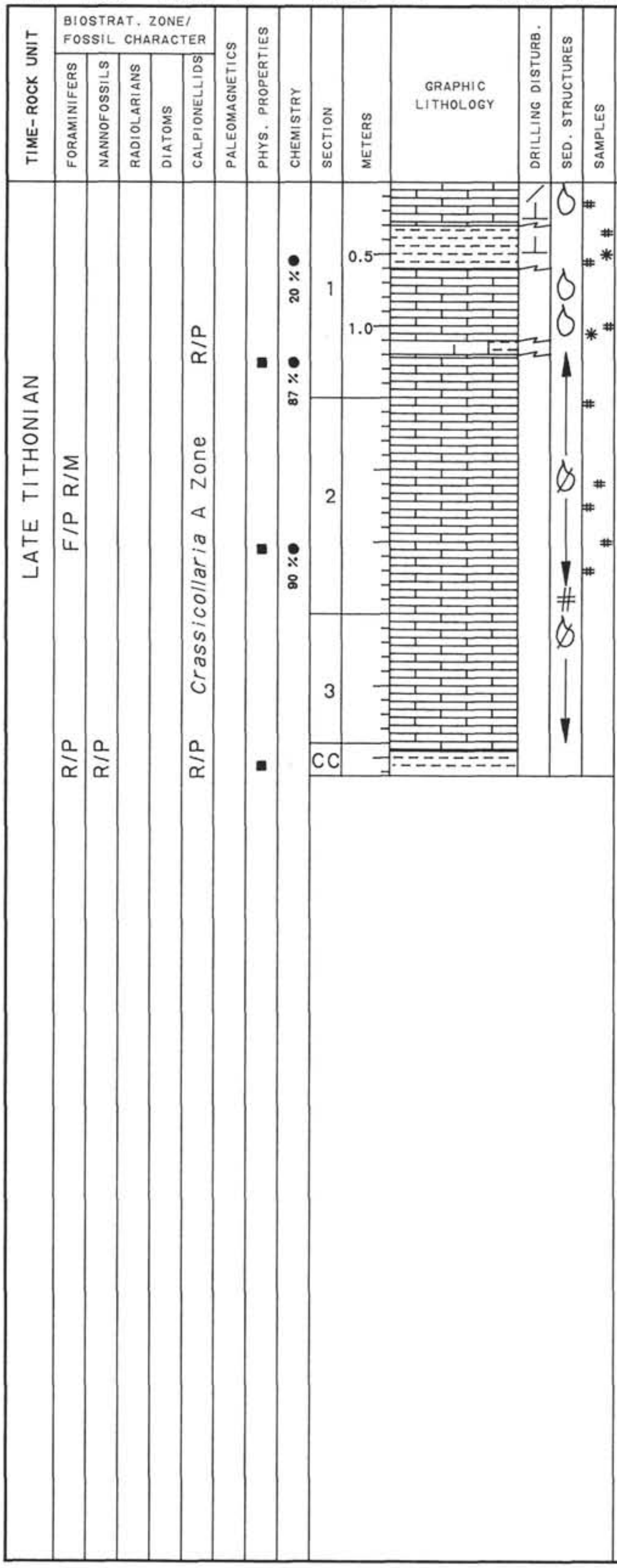

LITHOLOGIC DESCRIPTION

CLAYEY LIMESTONE.

The core consists of pieces of light gray, light brownish gray and light yellowish brown (2.5Y7/2, 2.5Y6/2, 10YR6/4) clayey limestone, interbedded with light olive brown to olive (2.5Y5/4, 5Y5/4) calcareous silt and silty clay in Section 1, 35-60 cm. The clayey limestone is dominantly skeletal, peloidal packstone to wackestone with lesser rudstone, chalk and fossiliferous mudstone (Section 1, 65-92 cm; CC, 5-20 cm). Allochems are highly diverse and include solitary corals, sponges, spongiomorph hydrozoa (?), serpulids, bivalves, gastropods, brachiopods, foraminifera, echinoderm debris, pelecypods, bryozoa, dascycladacean algae and calpionellids in a peloidal matrix. Skeletal debris is rudite to arenite size, and the larger bioclasts commonly have borings. Stylolites and calcite-filled fractures, both of which are limonite-stained and abundant, locally give a brecciated aspect. Quartz-filled vugs and veins are present in Section 2, structures are rare, and the nature of the contact between different-textured limestone are not clear because of the fragmentation of the core.

SMEAR SLIDE AND THIN SECTION SUMMARY (%):

	2,75-77 D	1,48 M	1,115 M	1,26-27 D	2,63-65 D	2,118 D	1,35-37 M
TEXTURE:							
(CM=Crystalline Mosaic)	CM	–	–	CM	CM	CM	CM
Sand	–	–	–	–	23	–	–
Silt	–	35	60	2	–	–	–
Clay/Micrite/Cement	–	65	40	98	77	–	–
COMPOSITION:							
Quartz	5	5	Tr	1	–	–	30
Feldspar	–	–	–	1	–	–	5
Mica	–	10	2	–	–	–	5
Clay	–	55	25	–	–	–	25
Calcite/Dolomite	–	25	70	–	–	–	35
Cement(Sparry Calcite)	25	–	–	–	3	–	–
Accessory Minerals	–	2	2	–	–	–	Tr
Foraminifers	3	–	–	1	1	Tr	–
Nannofossils	–	3	1	–	–	–	–
Pellets	10	–	–	5	20	15	–
Bioclasts	44	–	–	80	23	25	Tr
Micrite	15	–	–	12	38	60	–
Microsparite	–	–	–	–	15	–	–

PHYSICAL PROPERTIES DATA:

	1,126	2,106	CC,13
V_p (c)	4.43	5.72	–
ρ_b	2.79	2.52	–
T_c	–	–	3.61

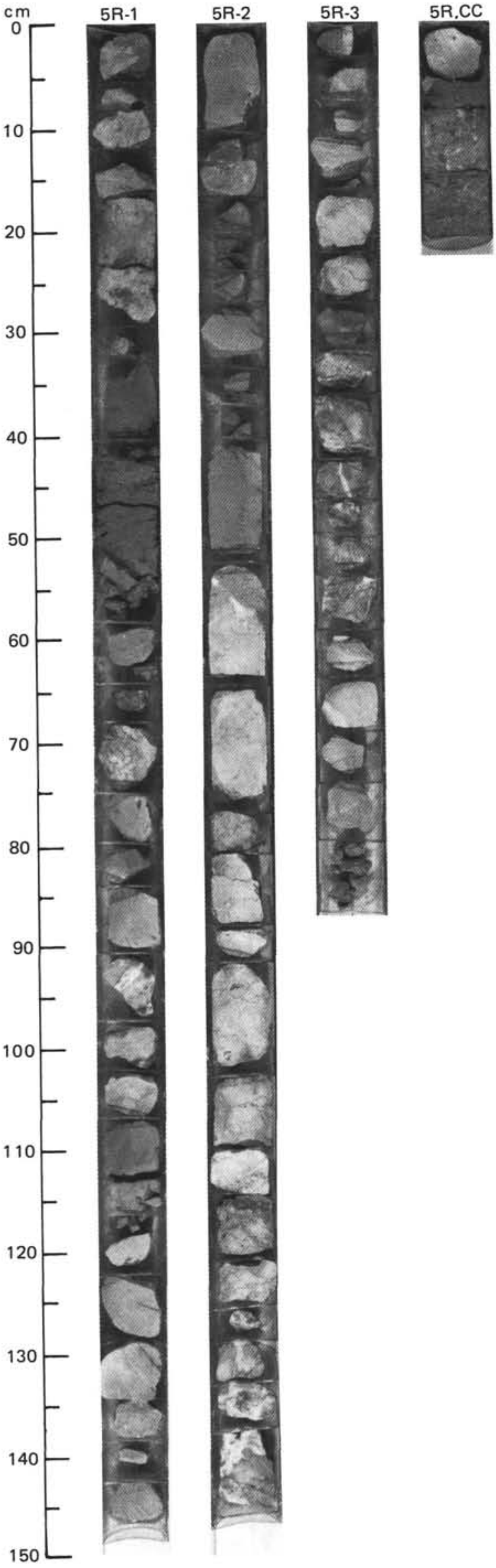
cm
0
10
20
30
40
50
60
70
80
90
100
110
120
130
140
150
5R-1
5R-2
5R-3
5R,CC

SITE 639 HOLE D CORE 6 R CORED INTERVAL 4958.5-4968.1 mbsl; 216.0-225.6 mbsf

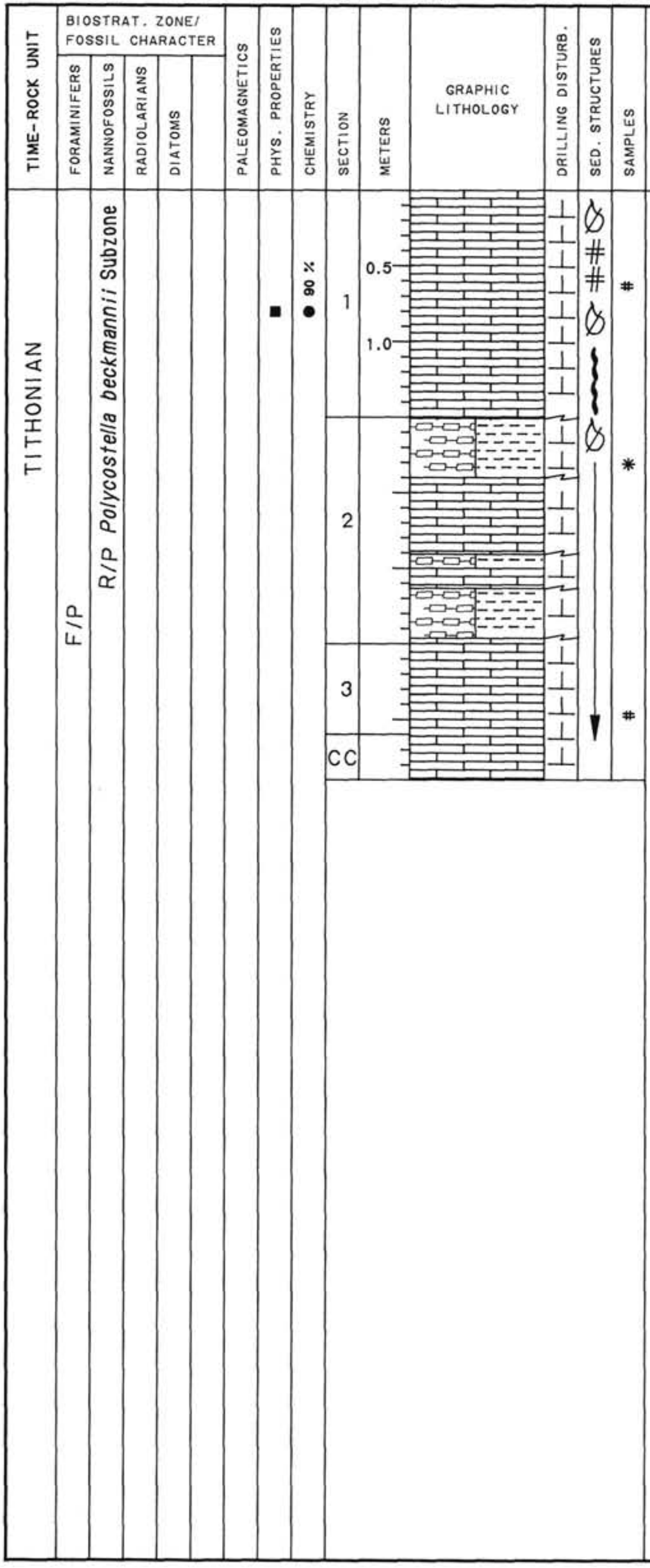

LITHOLOGIC DESCRIPTION

INTERBEDDED CLAYEY LIMESTONE and MARLSTONE.

The core dominantly consists of pieces of light yellowish brown and light olive yellowish brown (10YR6/4 and 2.5Y6/4 to 2.5Y6/5) clayey limestone which grades into intervals of light yellowish brown (2.5Y6/4) silty marl/marlstone, the thickest of which are found in Section 2, 0-41 cm and 118-144 cm. The clayey limestone dominantly has a wackestone texture with allochems of thin- and thick-walled molluscs (up to 3 cm in diameter), serpulid worm tubes, gastropods, large benthic foraminifera, ostracodes, rare small ammonites, pelecypods, echinoderms, peloids, and oncoids. Locally, the rock is a skeletal peloidal packstone. The silty marl/marlstone layers vary from 1 to 41 cm thick and commonly have 1 cm thick bands of large benthic foraminifera oriented parallel to bedding. Vertical, 2 mm-wide, calcite-filled fractures are common, as well as stylolites. Drusy calcite-lined vugs are present. Primary sedimentary structures are rare, and the nature of the contact between different lithologies is not clear because of the fragmental nature of the core.

SMEAR SLIDE AND THIN SECTION SUMMARY (%):

	2,28	1,60-66	3,48-51
	M	D	D
TEXTURE:			
(CM=Crystalline Mosaic)	–	CM	CM
Sand	–	–	60
Silt	40	–	5
Clay	60	–	35
COMPOSITION:			
Quartz	5	–	2
Mica	3	–	–
Clay	30	–	10
Calcite/Dolomite	60	–	–
Accessory Minerals: (Opaques, FeOxides)	1	–	5
Foraminifers	–	6	–
Nannofossils	1	–	–
Oncoids	–	4	50
Pellets	–	15	–
Bioclasts	–	40	3
Micrite	–	35	30

PHYSICAL PROPERTIES DATA:

	1,78
V_p (c)	5.29
ρ_b	2.62

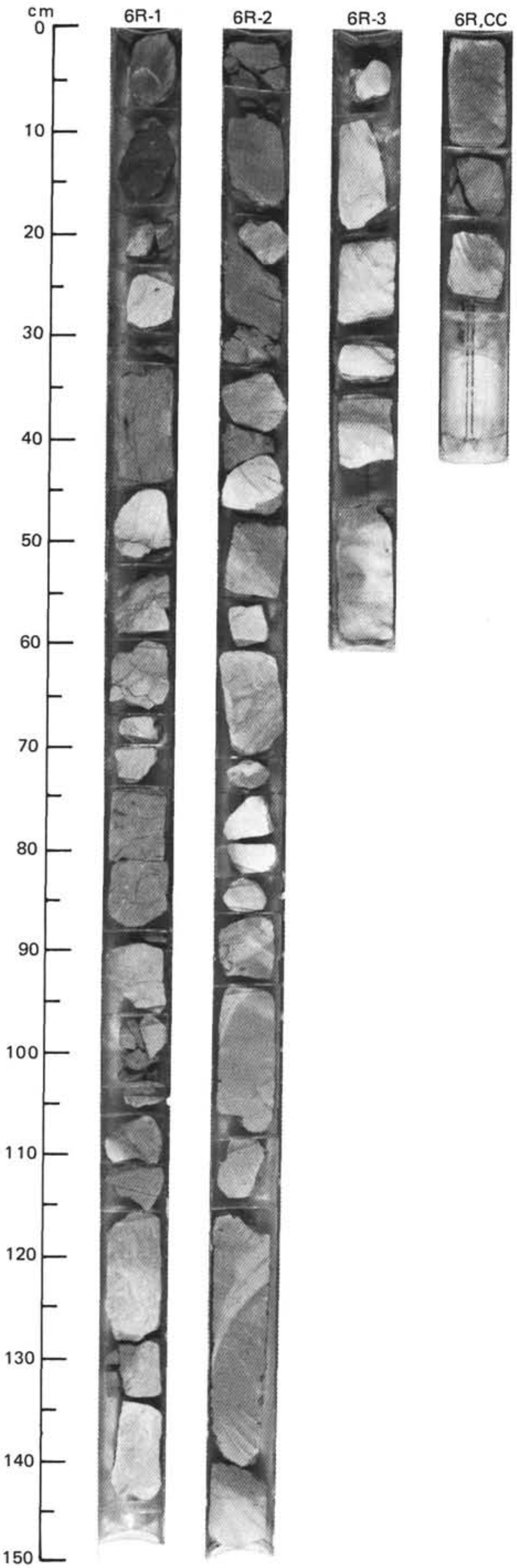
cm
0
10
20
30
40
50
60
70
80
90
100
110
120
130
140
150
6R-1
6R-2
6R-3
6R,CC

SITE 639 HOLE D CORE 7 R CORED INTERVAL 4968.1-4977.7 mbsl; 225.6-235.2 mbsf

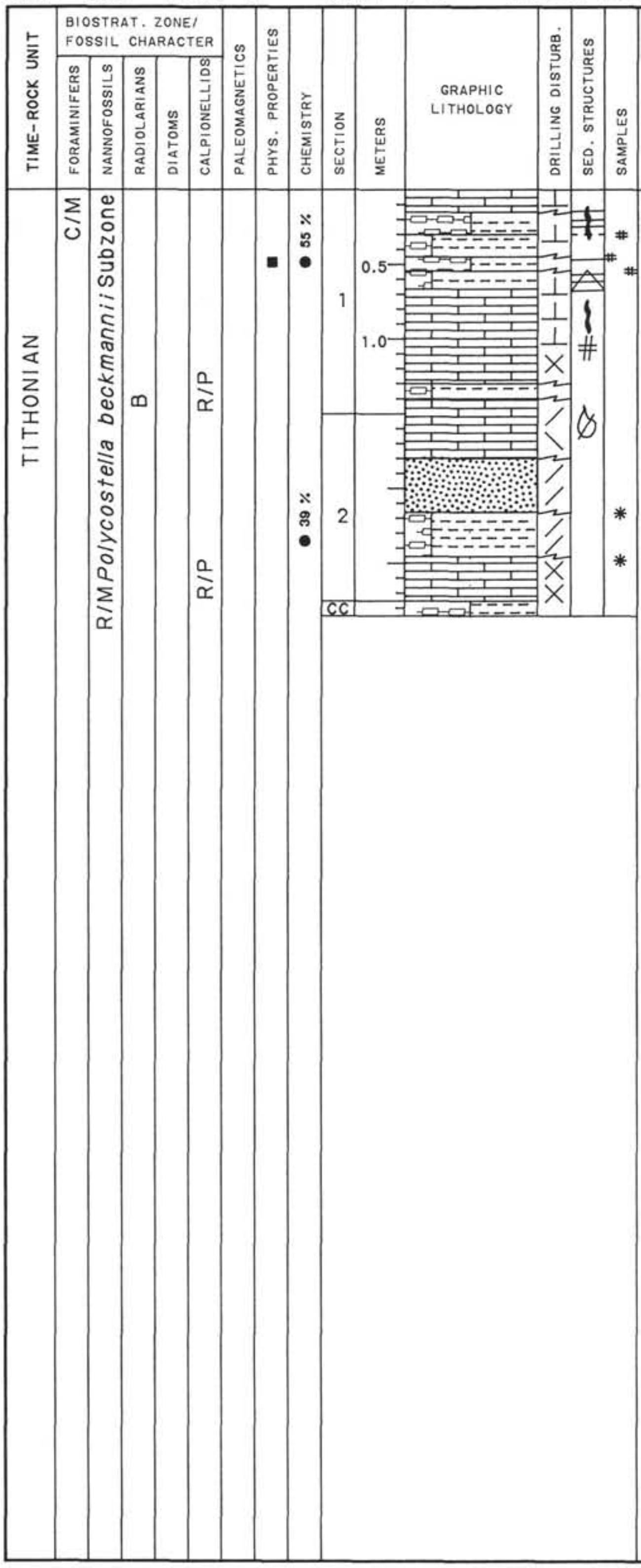

LITHOLOGIC DESCRIPTION

INTERBEDDED CLAYEY LIMESTONE, MARLSTONE, and COARSE-GRAINED SANDSTONE.

The core consists of alternating (on a scale of 5-15 cm in Section 1) light gray, light yellowish brown, and pale olive (2.5Y6/2, 2.5Y6/5, 5Y6/4) clayey limestone and quartz-silt-bearing light yellowish brown (2.5Y6/4) marl to calcareous clay. Brownish yellow (10YR6/8), poorly sorted, coarse-grained sandstone is interbedded in Section 2, 28-67 cm. Clayey limestone is dominantly fossiliferous mudstone containing thin-walled molluscs, with lesser grainstones to packstones containing oriented foraminifera, thin-walled molluscs and rare gastropods and intraclasts. The marl/marlstone commonly has current-sorted laminations of foraminifera which gradationally decrease in abundance upsection over an interval of 5-15 cm. Thin-walled molluscs are present in the upper parts of these intervals. The contact between the clayey limestone and marlstone/calcareous clay is gradational over 1-5 cm. Bioturbation is present, but its abundance is uncertain.

SMEAR SLIDE AND THIN SECTION SUMMARY (%):

	2,78	2,94	1,53	1,29-30	1,56-58
	D	M	D	D	D
TEXTURE:					
(CM=Crystalline Mosaic)	–	–	CM	CM	CM
Sand	–	–	7	60	–
Silt	25	20	77	21	9
Clay	75	80	16	19	91
COMPOSITION:					
Quartz	10	5	57	30	Tr
Feldspar	2	Tr	5	5	–
Mica	10	5	Tr	Tr	Tr
Calcite/Dolomite	5	15	1	–	5
Accessory Minerals	3	2	–	1	1
Pyr., Tourmaline	–	–	Tr	–	–
Foraminifers	–	–	–	–	Tr
Radiolarians	–	–	–	–	2
Intraclasts	–	–	22	20	–
Bioclasts	–	–	–	25	–
Micrite	–	–	–	14	61
Micritic-coated grains	–	–	–	Tr	–
Calpionellids	–	–	–	–	5

PHYSICAL PROPERTIES DATA:

	1,49
V_p (c)	4.05
ρ_b	2.62

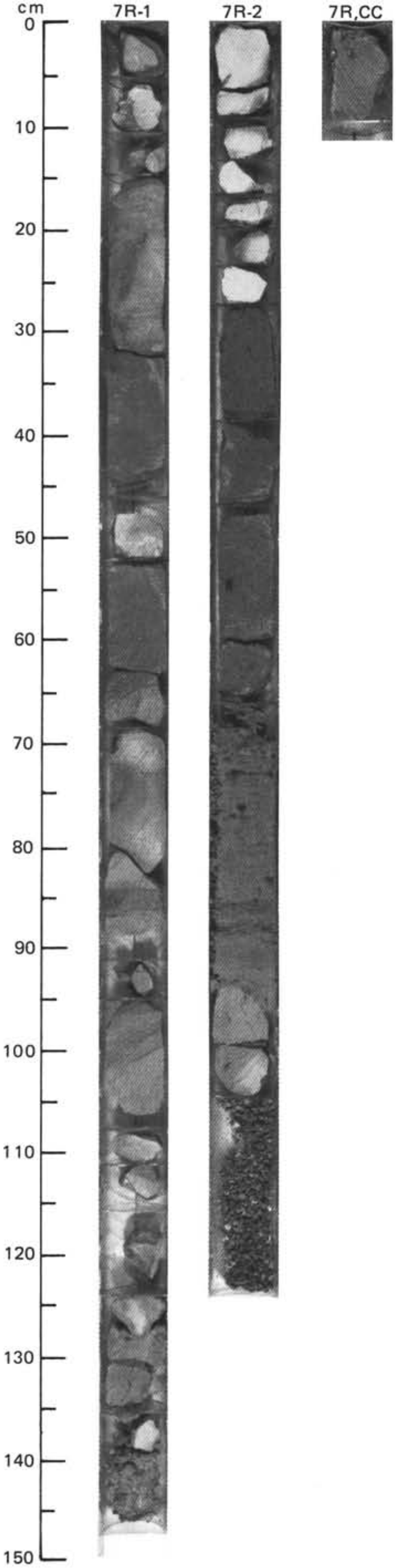
cm
0
10
20
30
40
50
60
70
80
90
100
110
120
130
140
150
7R-1
7R-2
7R,CC

SITE 639 HOLE D CORE 8 R CORED INTERVAL 4977.7-4987.4 mbsl; 235.2-244.9 mbsf

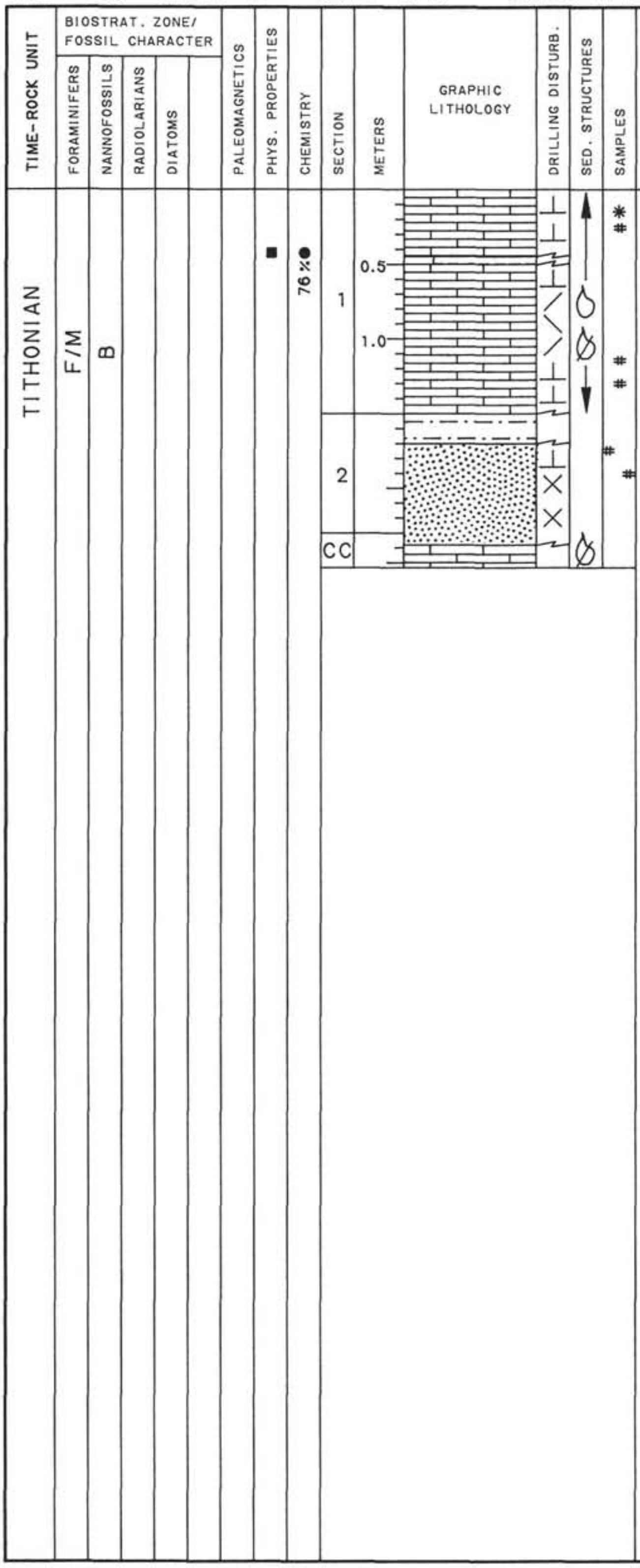

LITHOLOGIC DESCRIPTION

CLAYEY LIMESTONE, SANDSTONE and CALCAREOUS CLAY

The core consists of interbedded light reddish brown, very pale brown, and light gray (5YR6/3, 10YR7/3, 10YR7/2) clayey limestone and yellowish brown, dark yellowish brown and olive brown (10YR5/5, 10YR4/4, 2,5Y4/4) coarse- to fine-grained sandstone, pale olive (5Y6/4) siltstone and olive (5Y5/3) clay. Primary sedimentary structures other than bioturbation are not observed and the nature of contacts between the different lithologies is not clear due to the fragmented character of the core. Sandstone composition is very quartz-rich and locally foraminifera are common (Section 2, 63-68 cm). Clayey limestones vary from skeletal wackestones to oncolitic, peloidal, skeletal packstones. Skeletal allochems include molluscs, foraminifera, and trace calpionellids, pelecypods, coral and annelids. Several percent of quartz silt is ubiquitous. Limonite-stained, poorly developed, irregular stylolitic seams are common.

SMEAR SLIDE AND THIN SECTION SUMMARY (%):

	1,13 M	1,15-19 D	2,23-26 D	1,114-116 D	1,130-133 D	2,37-40 D
TEXTURE:						
(CM=Crystalline Mosaic)	–	CM	–	CM	CM	–
Sand	10	49	55	65	70	–
Silt	50	–	5	5	–	31
Clay/Micrite/Cement	40	51	40	30	30	69
COMPOSITION:						
Quartz	57	5	40	5	1	3
Feldspar	–	–	20	–	–	–
Rock Fragments	–	–	Tr	–	–	–
Mica	Tr	–	Tr	–	–	–
Clay	40	–	–	–	–	–
Calcite/Dolomite	1	–	30	–	–	1
Accessory Minerals:						
Opaques	2	2	Tr	–	–	–
Foraminifers	–	–	–	Tr	1	–
Radiolarians	–	–	–	–	–	2
Bioclasts	–	37	–	10	15	20
Incolites	–	5	–	20	25	–
Micrite	–	51	–	30	30	69
Intraclasts	–	–	10	–	–	–
Pellets	–	–	–	35	28	–
Quartz overgrowths	–	–	–	–	–	5

PHYSICAL PROPERTIES DATA:

	1,41
V_p (c)	3.85
ρ_b	2.66

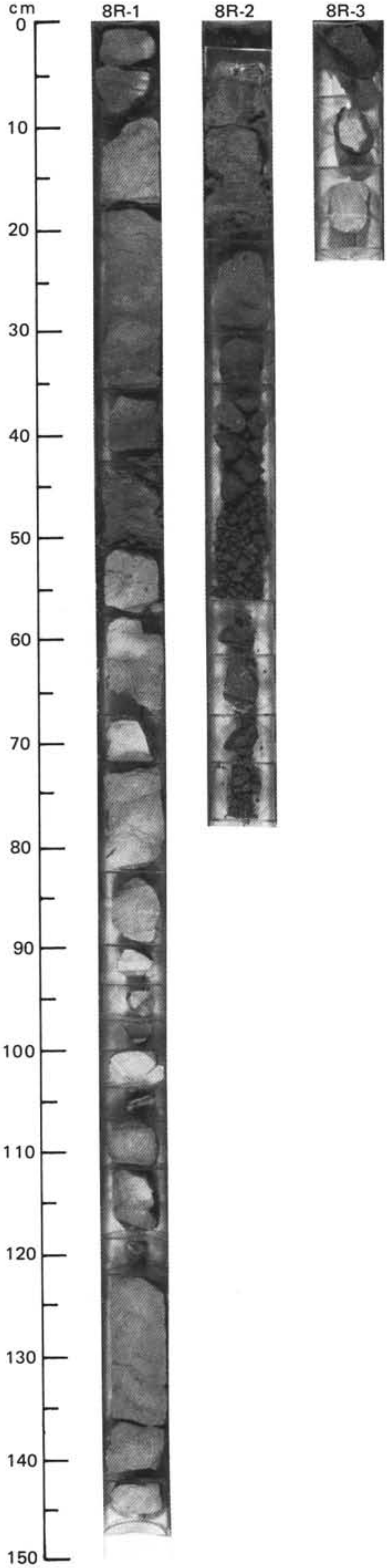
cm
8R-1
8R-2
8R-3
0
10
20
30
40
50
60
70
80
90
100
110
120
130
140
150

SITE 639 HOLE D CORE 9 R CORED INTERVAL 4987.4-4997.0 mbsl; 244.9-254.5 mbsf

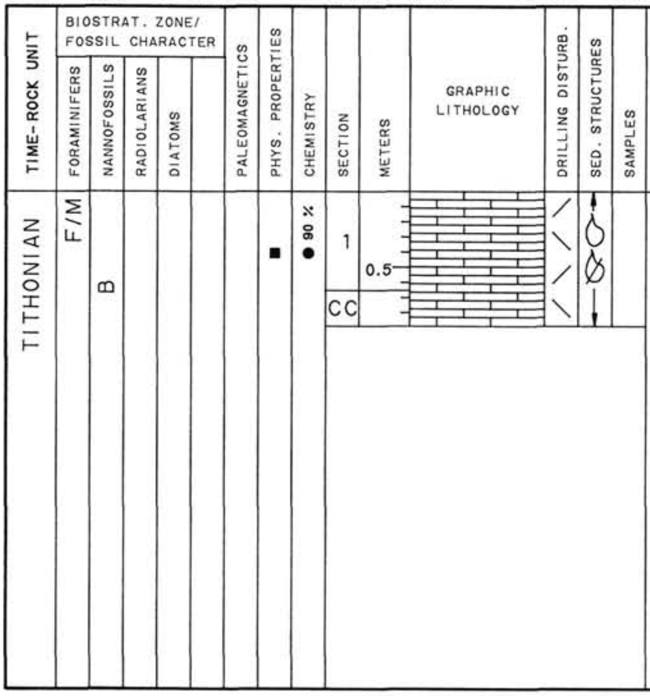

LITHOLOGIC DESCRIPTION

LIGHT GRAY CLAYEY LIMESTONE

The core consists of pieces of light gray to light brownish gray (5Y7/1, 10YR6/2) clayey limestone. The clayey limestone is dominantly a poorly sorted oncolitic, peloidal packstone with fossiliferous mudstone to skeletal wackestone in the CC. Allochems are dominantly peloids and oncoids (up to 7%; 4 mm average diameter), with lesser gastropods, foraminifers, and thin-walled molluscs. Thin, limonite-stained fractures and stylolites are common. The nature of contacts between different limestone textures is not clear due to the fragmented character of the core.

PHYSICAL PROPERTIES DATA:

	1,38
V_ρ (c)	5.24
ρ_b	2.93

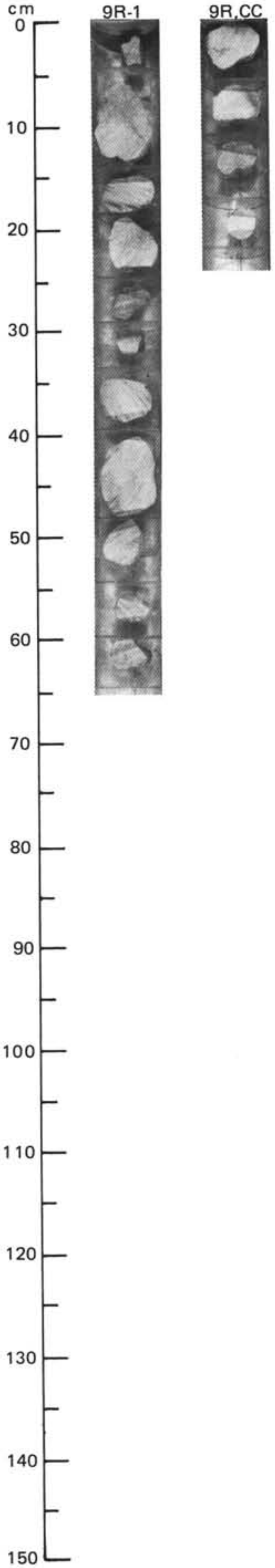
cm
0
10
20
30
40
50
60
70
80
90
100
110
120
130
140
150
9R-1
9R,CC

SITE 639 HOLE D CORE 10 R CORED INTERVAL 4997.0-5006.6 mbsl; 254.5-264.1 mbsf

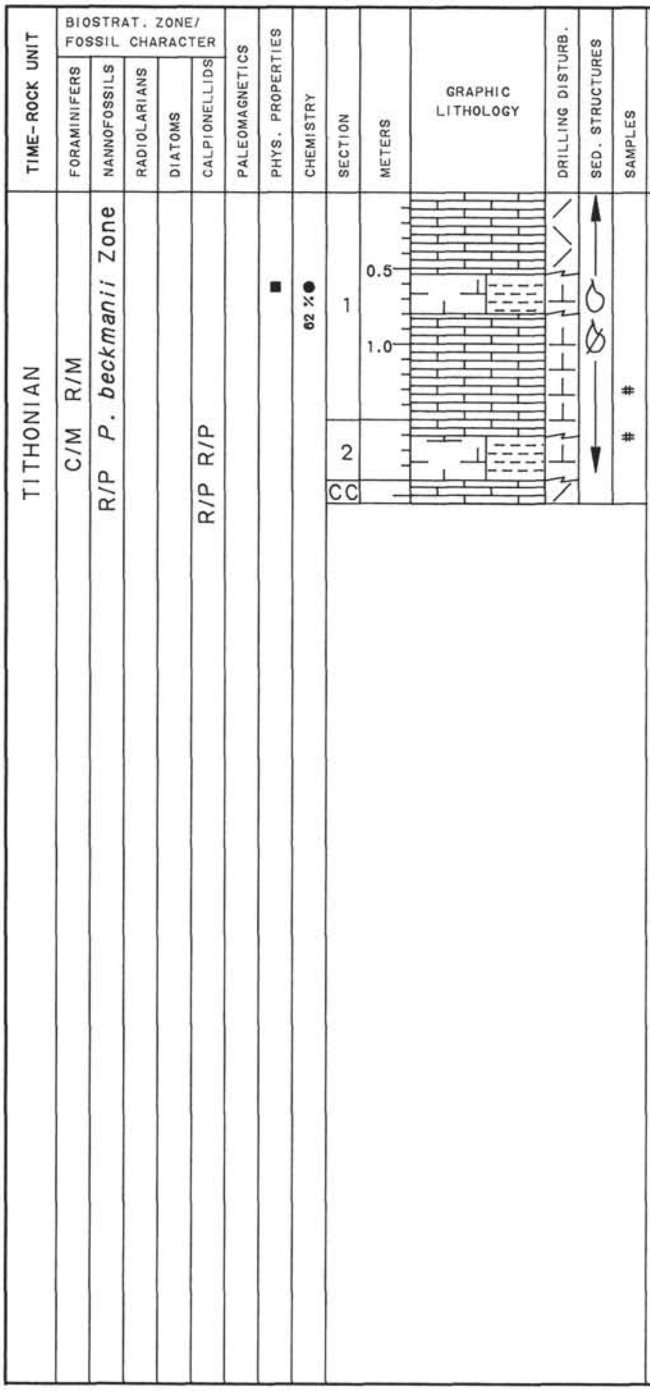

LITHOLOGIC DESCRIPTION

GRAY ONCOLITIC CLAYEY LIMESTONE and MARLSTONE

The core consists of pieces of gray to light olive gray (5Y5/1, 5Y6/2) clayey limestone interbedded with two 25 cm intervals of olive to pale olive (5Y5/4, 5Y6/3) marlstone. The clayey limestone is a poorly sorted skeletal peloidal packstone to wackestone with abundant (up to 10%) oncoids. Oncoids average 2 mm in diameter and the coatings vary from superficial to thick. Skeletal allochems include benthic foraminifers, oyster fragments with trace amounts of gastropods, ostracodes, pelecypods, echinoids, algae (?), and sponges/hydrozoa. Quartz is present in trace amounts. The interallochemical material is micrite locally recrystallized to microspar and spar. The marlstones have a bioturbated wackestone texture and contain foraminifera. The contacts between the various lithologies are not clear due to the fragmented nature of the core. Several yellow calcite-spar-filled veins are present.

THIN SECTION SUMMARY (%):

	2,9- 12 D	1,128- 130 D
TEXTURE:		
(CM=Crystalline Mosaic)	CM	CM
Sand	40	20
Silt	–	5
Clay	60	75
COMPOSITION:		
Quartz	Tr	–
Clay	–	3
Accessory Minerals	–	1
Foraminifers	2	5
Bioclasts	17	20
Micrite	82	70
Coated grains	–	1

PHYSICAL PROPERTIES DATA:

	1,62
V_p (c)	3.00
ρ_b	2.58

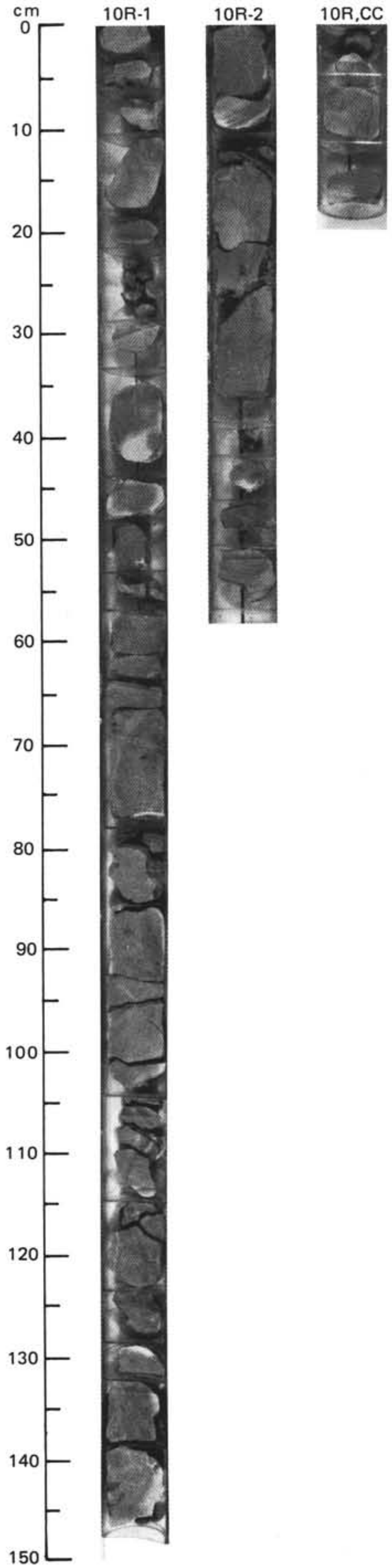
cm
0
10
20
30
40
50
60
70
80
90
100
110
120
130
140
150
10R-1
10R-2
10R,CC

SITE 639 HOLE D CORE 11 R CORED INTERVAL 5006.6–5016.3 mbsl; 264.1–273.8 mbsf

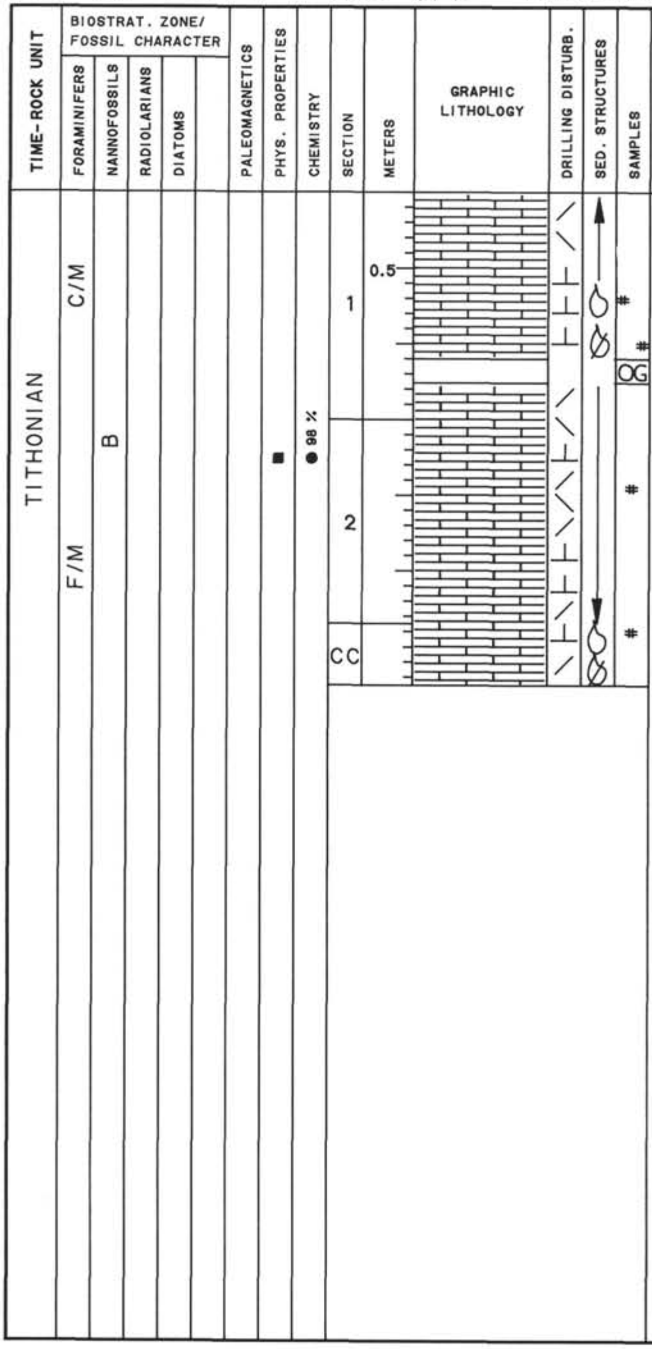

LITHOLOGIC DESCRIPTION

GRAY ONCOLITIC LIMESTONE

The core consists of pieces of gray to light gray (5Y5/1, 5Y7/1) limestone. The limestone is a poorly sorted skeletal peloidal packstone to wackestone (locally grainstone) with abundant (up to 10%) oncoids. Oncoids average 2 mm in diameter and the coatings vary from superficial to thick. Skeletal debris includes molluscs (bivalves and gastropods), foraminifera, and trace echinoderms and algae (?). Textural variation is gradational on a scale of 1-10 cm. Concentration of foraminifera occurs in abundant limonite-stained, clayey (?), irregular microstylolitic bands up to 3 cm thick. Limonite-stained hairline cracks and fractures are common throughout.

THIN SECTION SUMMARY (%):

	1,70- 76 D	1,95- 97 D	2,49- 51 D	CC,10- 13 D
TEXTURE:				
(CM=Crystalline Mosaic)	CM	CM	CM	CM
Sand	–	–	55	50
Silt	–	–	–	30
Clay	–	–	45	20
COMPOSITION:				
Clay	–	–	–	10
Accessory Minerals	–	–	–	Tr
Foraminifers	–	–	5	–
Sponge Spicules	–	–	5	–
Matrix(Micrite,pellets,etc.)	25	25	40	–
Oncoids	65	65	–	20
Bioclasts	5	5	5	30
Pressure solution zones	5	5	–	–
Micrite	–	–	45	10
Intraclasts	–	–	–	30

PHYSICAL PROPERTIES DATA:

	2,23
V_p (c)	5.24
ρ_b	2.69

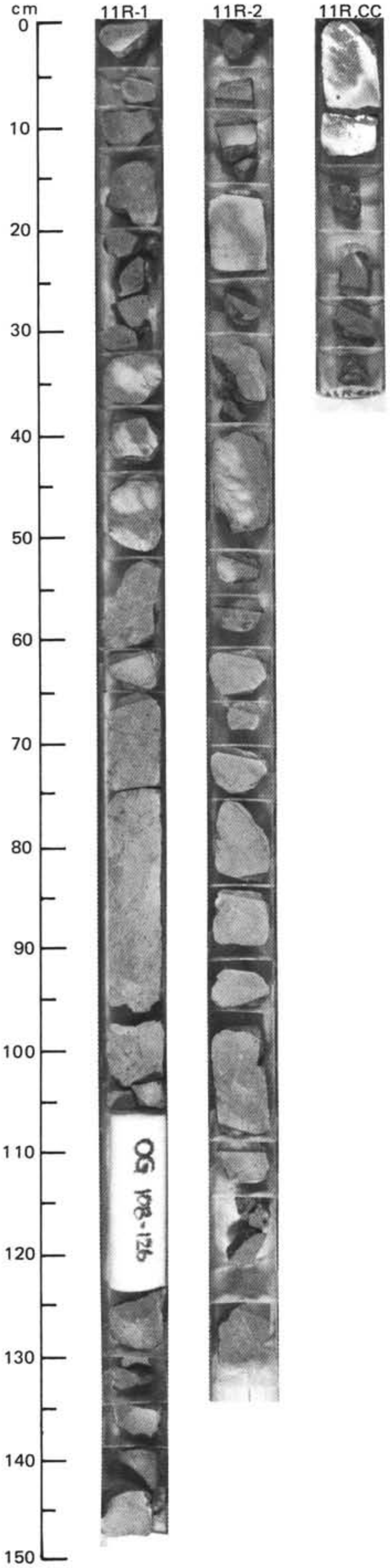
cm
0
10
20
30
40
50
60
70
80
90
100
110
120
130
140
150
11R-1
11R-2
11R,CC
OG 108-126

SITE 639 HOLE D CORE 12 R CORED INTERVAL 5016.3-5025.9 mbsl; 237.8-283.4 mbsf

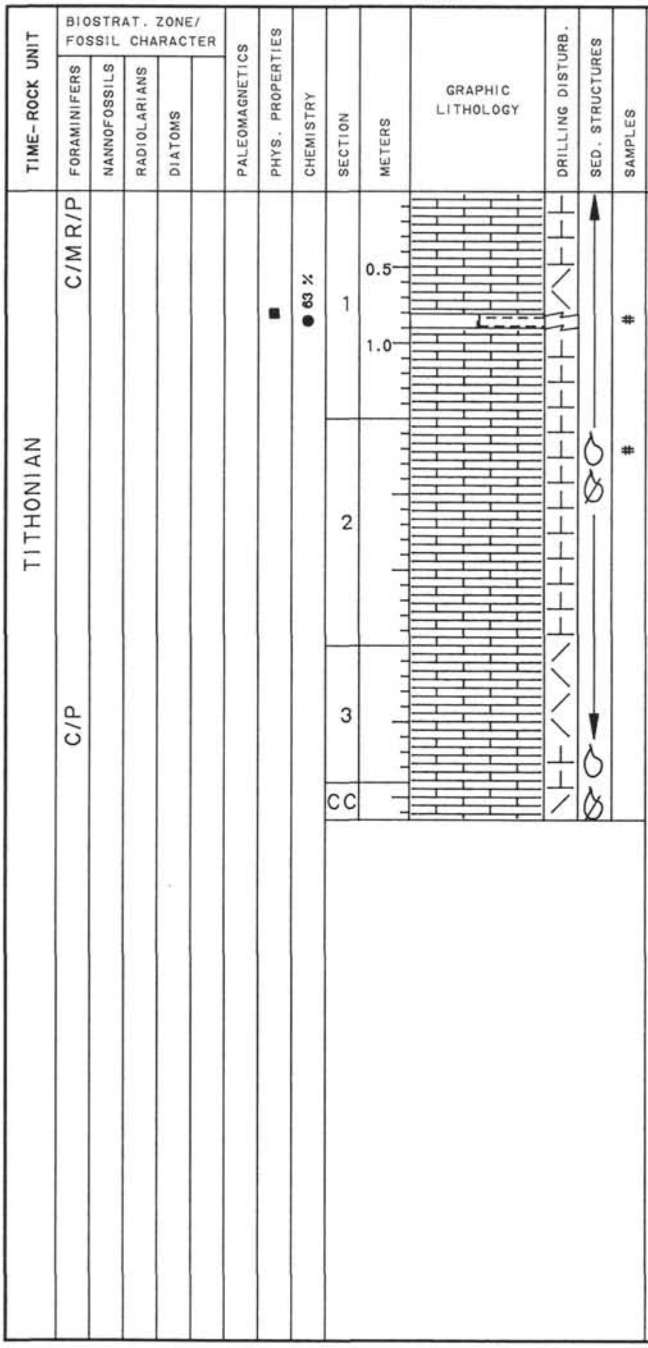

LITHOLOGIC DESCRIPTION

GRAY ONCOLITIC LIMESTONE.

The core consists of pieces of light gray, gray, and dark gray (10YR 7/1, 5Y5/1, 5Y4/1) limestone with an interbed of marlstone (Section 1, 78-92 cm). The limestone is dominantly a poorly sorted skeletal, peloidal packstone to grainstone with abundant (up to 10%) oncoids. Oncoids average 2 mm in diameter and coatings vary from superficial to thick. Locally the limestone is a grainstone or fossiliferous mudstone. Skeletal material includes thin-walled molluscs and foraminifers, many of which are broken. Textural variation is gradational on a scale of 1-10 cm. Microstylolitic bands up to 2 cm in thickness either parallel or oblique to the stratification are common. Concentrations of foraminifers and insoluble residue by dissolution creates a diagenetic packstone. The bands are stained yellow (10YR7/8).

THIN SECTION SUMMARY (%):

	1,81- 86 D	2,22- 27 D
TEXTURE:		
(CM=Crystalline Mosaic)	CM	CM
Sand	25	–
Silt	30	–
Clay	45	–
COMPOSITION:		
Clay	–	5
Foraminifers	20	–
Pellets	30	–
Bioclasts	5	10
Micrite	45	10
Oncoids	Tr	55
Intraclasts	–	20

PHYSICAL PROPERTIES DATA:

	1,81
V_p (c)	6.03
ρ_b	3.08

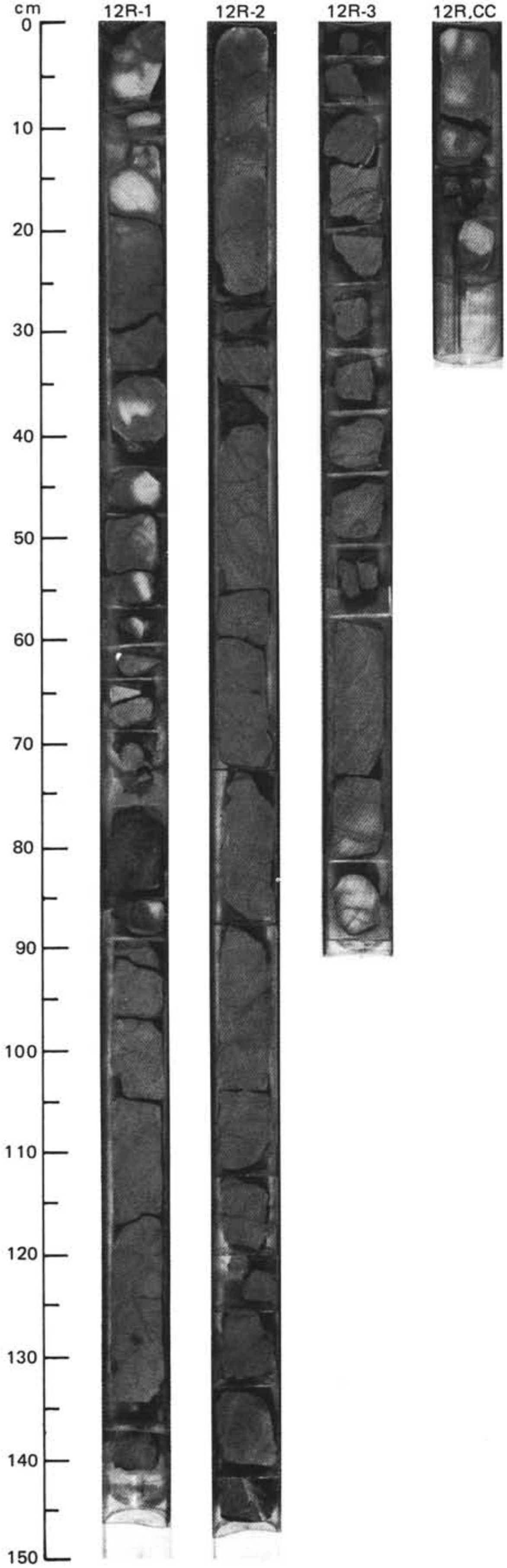
cm
0
10
20
30
40
50
60
70
80
90
100
110
120
130
140
150
12R-1
12R-2
12R-3
12R,CC

SITE 639 HOLE D CORE 13 R CORED INTERVAL 5025.9-5035.6 mbsl; 283.4-293.1 mbsf

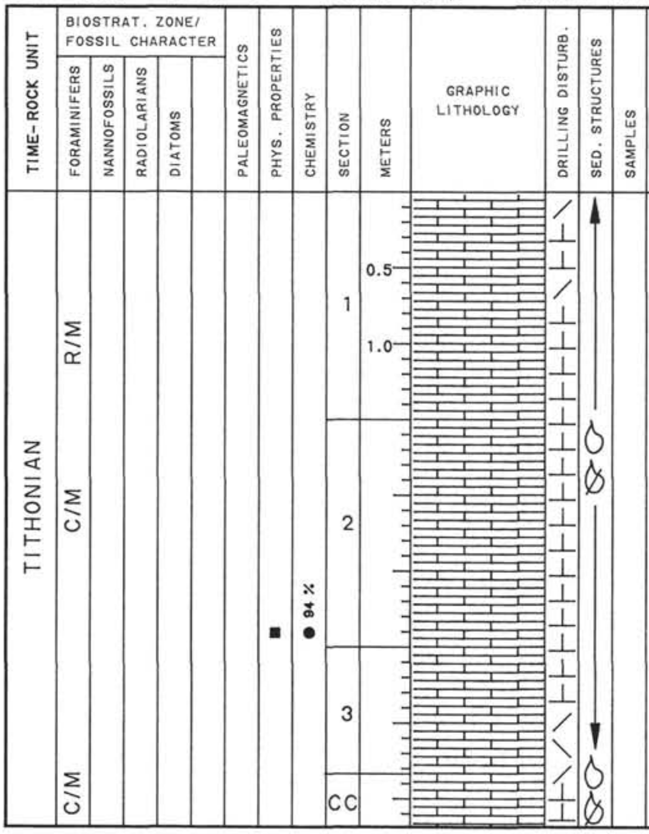

LITHOLOGIC DESCRIPTION

GRAYISH BROWN ONCOLITIC LIMESTONE

The core consists of rather uniform grayish brown (2.5Y5/2) limestone which is a poorly sorted skeletal peloidal packstone to wackestone with abundant (up to 10%) oncoids. The oncoids average 2 mm in diameter and the coatings vary from superficial to thick. Skeletal material includes thin-walled molluscs, foraminifers, and rare echinoderms, gastropod and pelecypod debris. The contact between packstone and wackestone commonly occurs across a stylolite. Vertical, 1 mm wide and up to 5 cm long, calcite-filled fractures are common. Irregular stylolitic seams, parallel or oblique to stratification and up to 2 cm wide, are common. The bands are stained yellowish-brown (10YR5/8), are clay-rich, and concentrate foraminifers creating a diagenetic packstone.

PHYSICAL PROPERTIES DATA:

	2,140
V_p (c)	5.12
ρ_b	2.74

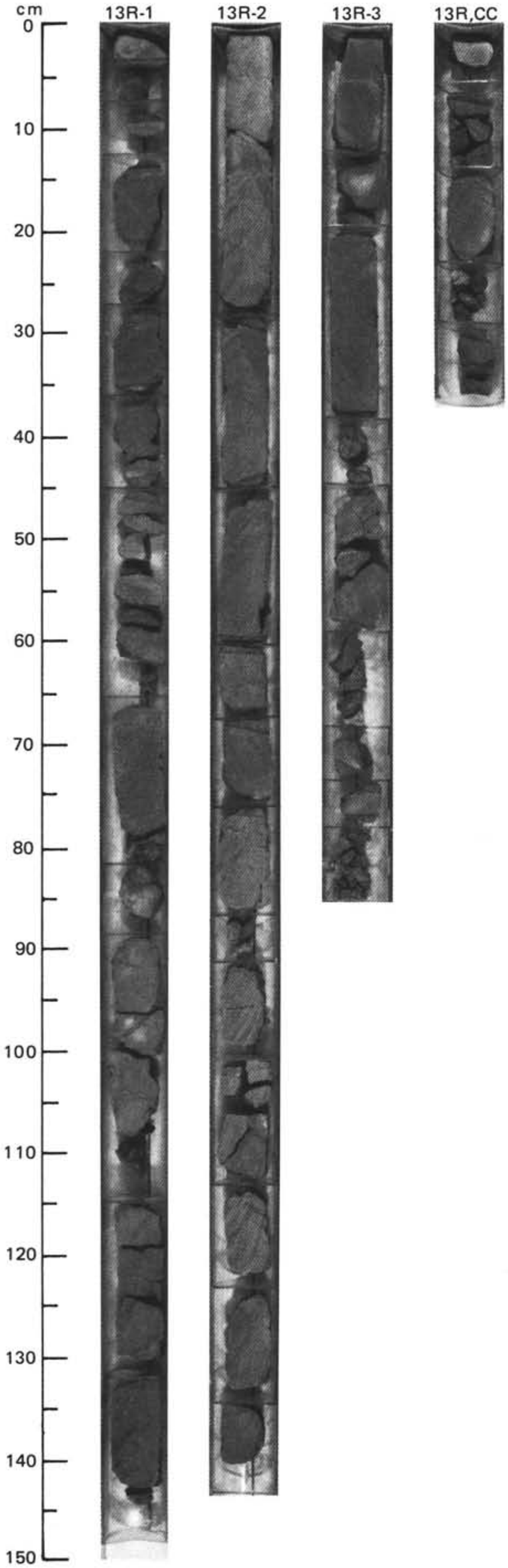
cm
0
10
20
30
40
50
60
70
80
90
100
110
120
130
140
150
13R-1
13R-2
13R-3
13R,CC

SITE 639 HOLE E CORE 1 R CORED INTERVAL 4958.9–4968.6 mbsl; 199.4–209.1 mbsf

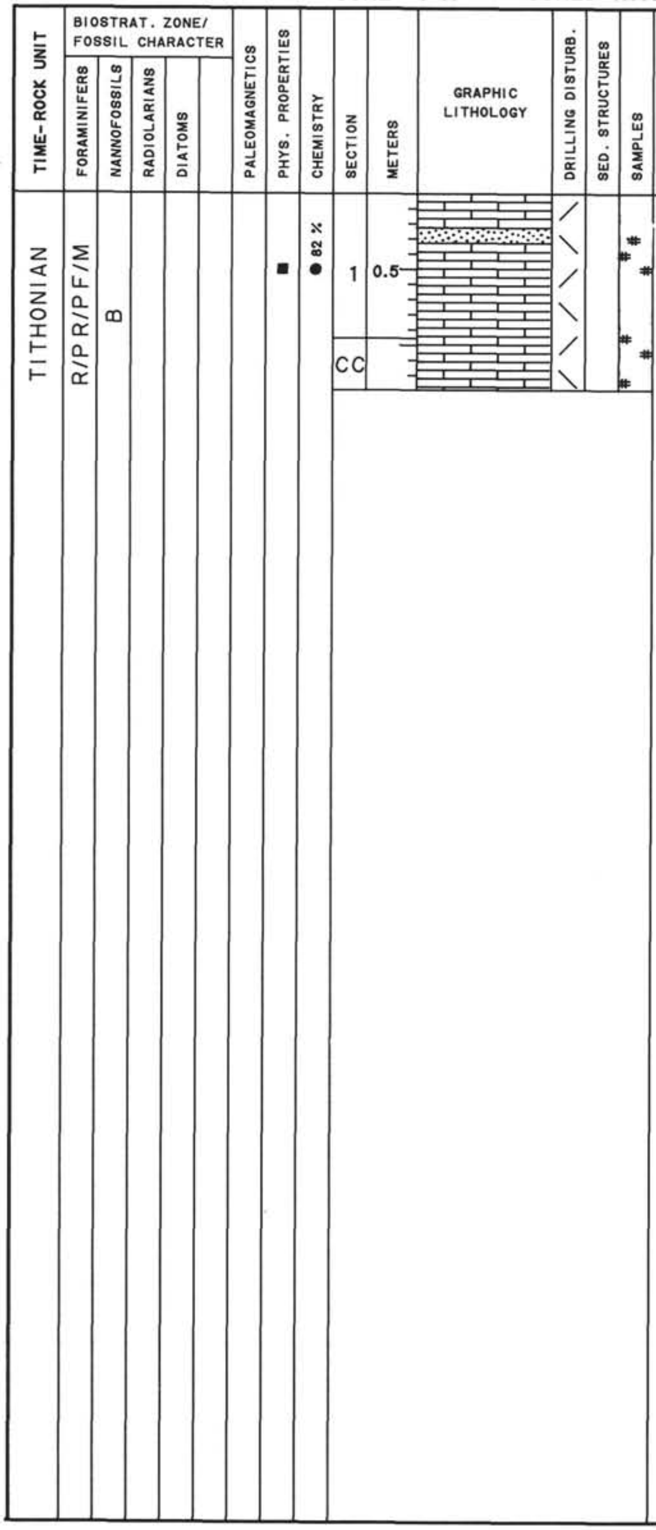

LITHOLOGIC DESCRIPTION

FOSSILIFEROUS LIME MUDSTONE

The core consists of disordered and unoriented pieces ranging from 1 to 6 cm across. Most pieces are brownish yellow (10YR 8/2, 10YR 6/6, 10YR 6/3) skeletal fossiliferous lime mudstone/wackestone. Biota includes molluscan debris, gastropods, large oyster fragments (up to few cm), rare large foraminifers, and one coral fragment. Minor variations in the limestone include a few pieces of pink mudstone (Section 1, 22-49 cm), skeletal-pelletal packstone to wackestone (Section 1, 0-5 cm), skeletal-oncolitic packstone, with large oyster fragments and yellow marly matrix (Section CC, 16-22 cm). Bioturbation is present, although not extensive (Section 1, 64-70 cm). Thin (up to 1 mm) calcite veins with random orientation occur in all pieces. A large (1 cm) vein filled with pelletal sediment and yellow limonite-stained, coarse sparry calcite occurs in Section 1, 24-29 cm. A piece of calcite-cemented, moderately sorted arkosic sandstone occurs in Sample CC, 27-31 cm. Some of the pink mudstone pieces are embedded in light yellowish brown (2.5Y 6/4) marl.

THIN SECTION SUMMARY (%):

	1,CC 9-12 D	1,CC 27-30 D	1,1 43-44 D	1,1 35 M
TEXTURE:				
Sand	10	60	23	–
Silt	–	–	Tr	4
Cement/Mic. Matrix	90	40	77	96
COMPOSITION:				
Quartz	Tr	45	1	3
Feldspar	–	15	Tr	–
Mica	–	–	–	Tr
Clay	–	–	25	40
Calcite/Dolomite (Micrite)	90	40	51	1
Accessory Minerals:				
FeOx	Tr	–	–	Tr
Apatite	10	–	20	–
Bioclasts	10	–	20	–
Oncoids	–	–	3	–
Micrite	–	–	–	2
Microspar	–	–	–	54

PHYSICAL PROPERTIES DATA:

	1,50
V_p	3.78
ρ_b	3.10

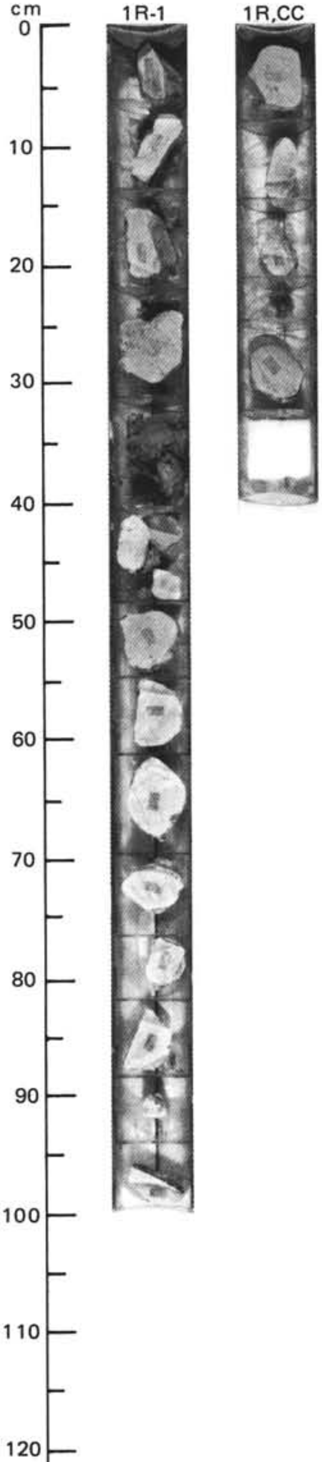
cm
1R-1
1R,CC
0
10
20
30
40
50
60
70
80
90
100
110
120
130
140
150

SITE 639 HOLE E CORE 2 R CORED INTERVAL 4968.6–4978.1 mbsl; 209.1–218.6 mbsf

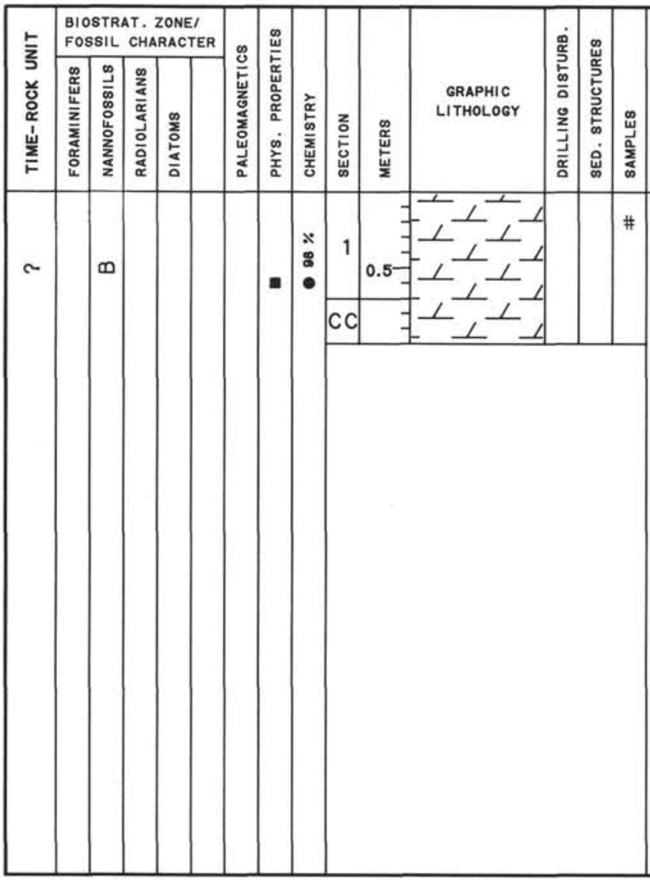

LITHOLOGIC DESCRIPTION

FRACTURED DOLOMITE

The core consists of unoriented pieces, 2-6 cm across, of grayish brown to brown (10YR 5/2 with shades of 10YR 5/3 to 6/3), fractured, coarse-grained crystalline dolomite. The original texture in most pieces (e.g. Section 1, 7-15 cm) is coarse-grained packstone/grainstone. The dolomite is intensely brecciated with a reticulate pattern of white, dolomite-filled veins (up to several mm thick), which make up as much as 50% of the rock. The dolomite has vuggy and intercrystalline porosity.

THIN SECTION SUMMARY (%):

	1,17-20
COMPOSITION:	
Dolomite	100

PHYSICAL PROPERTIES DATA:

	1,57
V_p	5.86
ρ_b	2.83

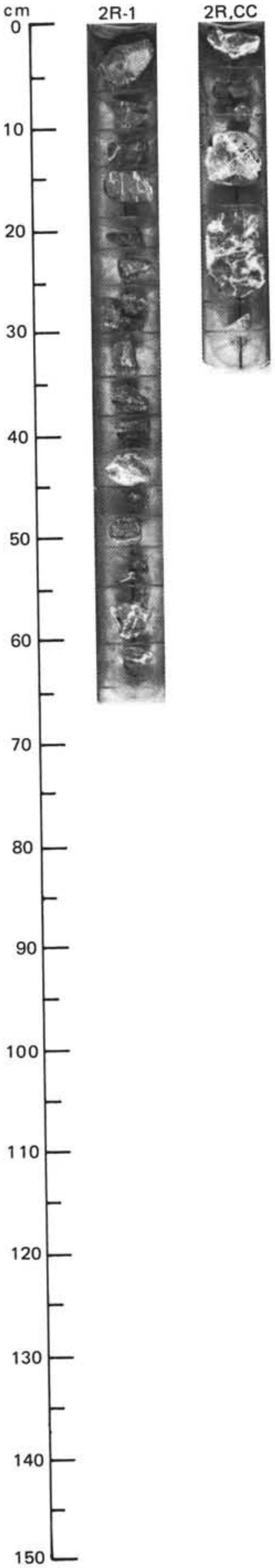
cm
0
10
20
30
40
50
60
70
80
90
100
110
120
130
140
150
2R-1
2R,CC

SITE 639 HOLE E CORE 3 R CORED INTERVAL 4978.1-4987.7 mbsl; 218.6-228.7 mbsf

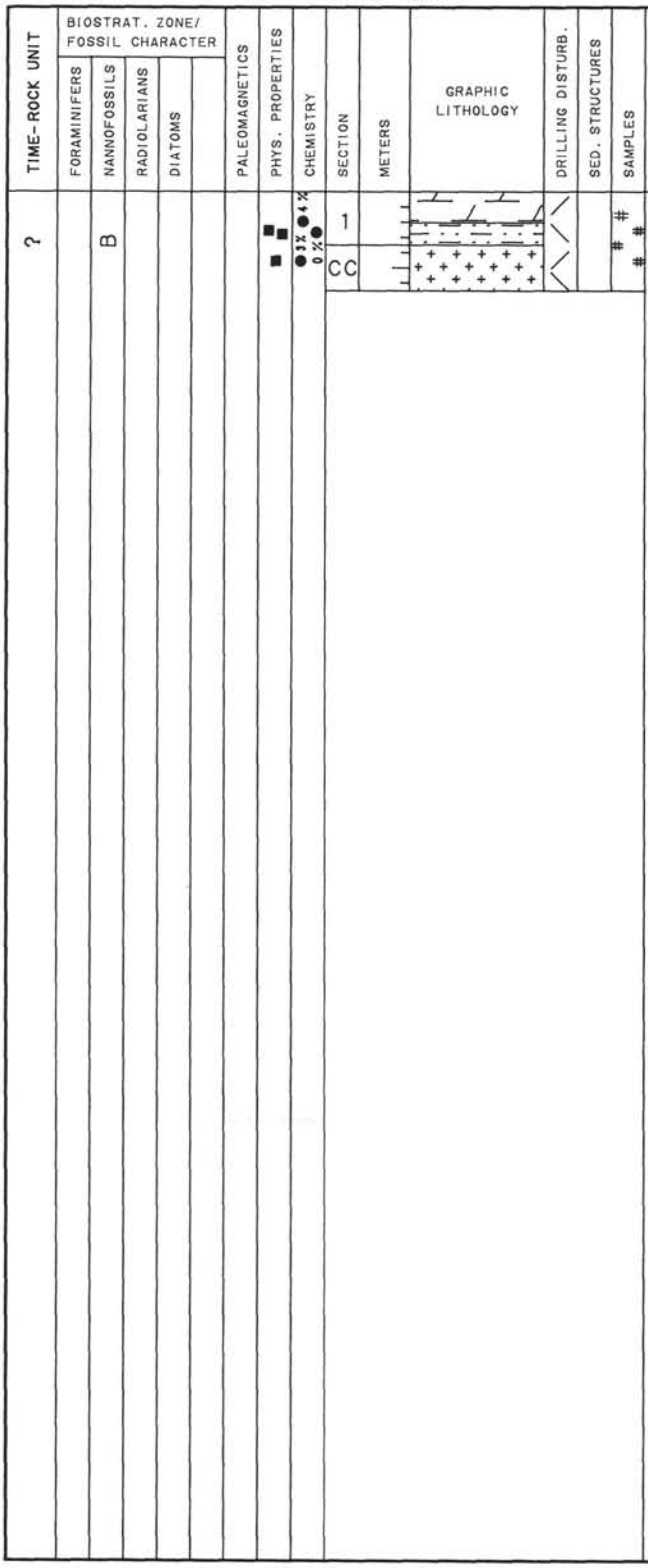

LITHOLOGIC DESCRIPTION

MIXED LITHOLOGIES

The core consists of disordered and unoriented, subrounded pieces, ranging in size from 1 to 5 cm. Lithologies present include:

(1) Light brown (10YR 5/3), brecciated dolomite with large veins filled by white dolomite (Section 1, 0-13 cm).

(2) Yellowish red (5YR 5/6) clay, containing cuttings of lithology 4 (Section 1, 13-17 cm).

(3) Dark yellowish brown (10YR 4/6) silicic breccia containing clasts of metamorphic quartzite, strained quartz clasts and rare feldspar (Section 1, 17-21 cm).

(4) Dark reddish brown (5YR 4/4) to dusky red (5YR 2.5/1), low-grade metamorphic claystone/siltstone with iron pisolites (as much as 2 mm in diameter). Major components are detrital quartz, micas (including chlorite, sericite and muscovite), Fe-Oxides (Section 1, 21-36 cm and CC, 54-61 cm).

(5) Light pinkish gray, altered volcanic rock of ?dacitic composition with fine-grained spherulitic texture and small feldspar phenocrysts (Section CC, 0-13 cm and 21-26 cm).

THIN SECTION SUMMARY (%):

	1,34- 36 D	7,20- 23 D	1,24- 25 D
TEXTURE:			
Sand	10	–	Tr
Silt	90	–	20
Clay	–	–	80
COMPOSITION:			
Quartz	75	56	10
Feldspar	Tr	2	1
Rock Fragments	–	40	–
Mica (Serricite, Chlorite)	3	1	69
Calcite Cement	20	1	–
Accessory Minerals:			
Fe Oxide	2	Tr	20
Tourmaline, Epidote	–	Tr	Tr

PHYSICAL PROPERTIES DATA:

	1,21	1,25	CC,3
V_p	4.24	3.65	1.94
ρ_b	2.78	2.84	2.80

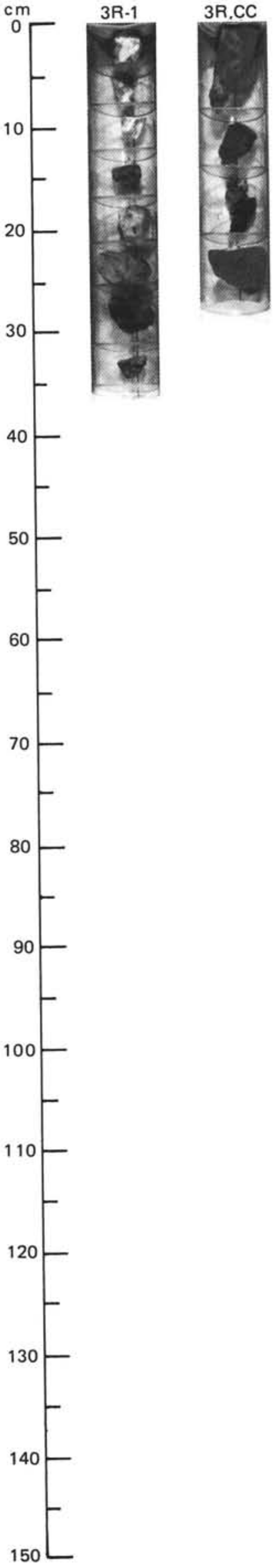
cm
0
10
20
30
40
50
60
70
80
90
100
110
120
130
140
150
3R-1
3R,CC

SITE 639 HOLE E CORE 4 R CORED INTERVAL 4987.7-4994.4 mbsl; 228.2-234.9 mbsf

TIME-ROCK UNIT	BIOSTRAT. ZONE/ FOSSIL CHARACTER					PALEOMAGNETICS	PHYS. PROPERTIES	CHEMISTRY	SECTION	METERS	GRAPHIC LITHOLOGY	DRILLING DISTURB.	SED. STRUCTURES	SAMPLES
	FORAMINIFERS	NANNOFOSSILS	RADIOLARIANS	DIATOMS										
							■	● % 0				/		#

LITHOLOGIC DESCRIPTION

METEMORPHOSED GRANULE CONGLOMERATE

The core consists of a single piece, 4 x 3 cm across, of metemorphosed polygenic granule conglomerate and very coarse-grained sandstone. Major components are quartz and rock fragments (siltstone, sandstones and metapelites). The matrix as well as the metapelitic rock fragments are recrystallized to chlorite, sericite, illite and biotite (low greenschist facies).

THIN SECTION SUMMARY (%):

	CC, 0-4 D
COMPOSITION:	
Quartz	10
Rock Fragments (Siltstone + Pelite)	70
Mica (Seric., Chlor., Biot., Ill.)	15
Accessory Minerals: Fe Oxide	5

PHYSICAL PROPERTIES DATA:

	CC,2
V_p	3.62
ρ_b	3.16

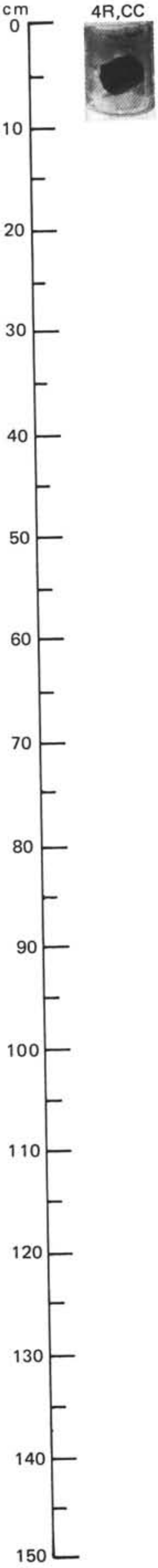
cm
4R,CC
0
10
20
30
40
50
60
70
80
90
100
110
120
130
140
150

SITE 639 HOLE F CORE 1 R CORED INTERVAL 4998.3-5007.8 mbsl; 237.8-247.3 mbsf

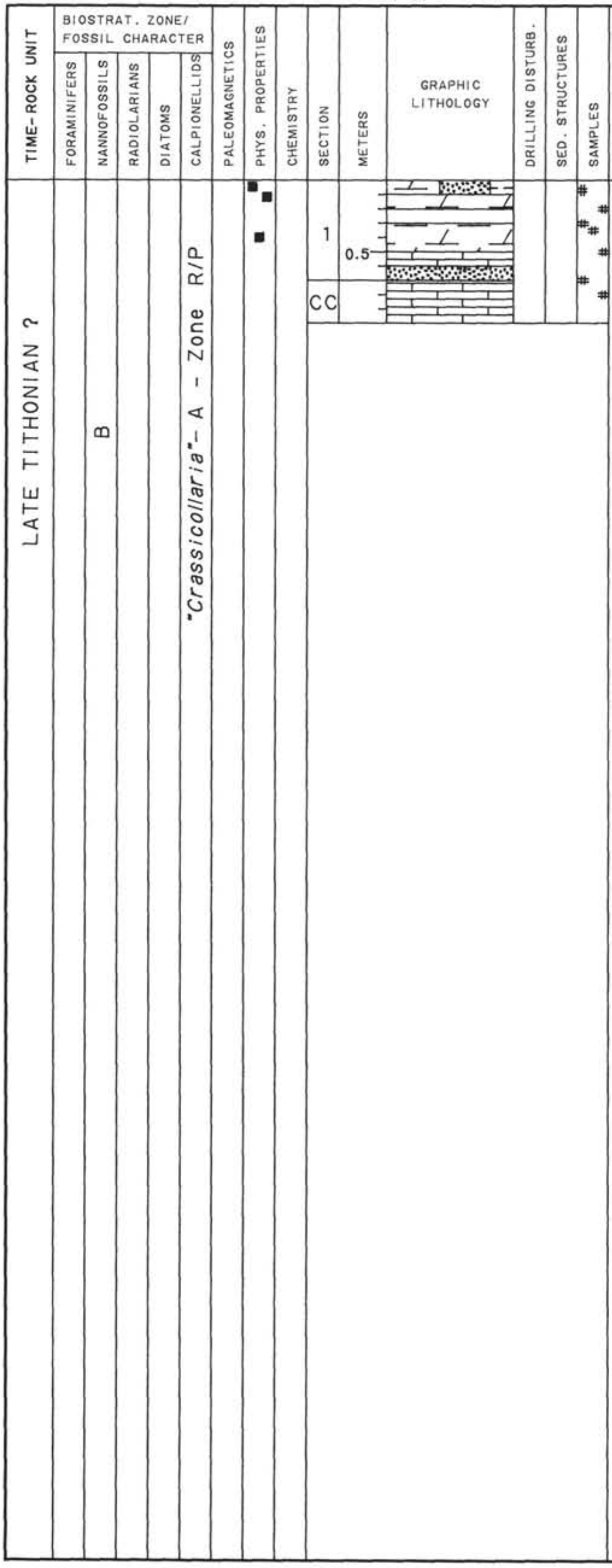

LITHOLOGIC DESCRIPTION

MIXED LITHOLOGIES

The core consists of disordered and unoriented pieces ranging in length from 1 to 12 cm. Lithologies include:

(1) Light brown (2.5Y 5/2) brecciated dolomite with yellow (2.5Y 7/8; 2.5Y 8/9) detrital dolomite matrix and large veins filled with white sparry dolomite (Section 1, 13-18 cm, 29-39 cm and 44-60 cm).

(2) Dark grayish brown (2.5Y 5/2) coarse-grained crystalline dolomite (Section 1, 39-44 cm and 64-67 cm).

(3) Dark yellowish brown (10YR 1/3) fine-grained quartzose sandstone (Section 1, 18-20 cm) and siltstone, with the matrix recrystallized to muscovite, sericite and chlorite.

(4) Reddish brown (2.5YR 4/2) to dark grayish brown (2.5Y 4/2) siltstone and very fine-grained sandstone with the matrix recrystallized to sericite and chlorite (Section 1, 9-13 cm). Some pieces are weakly foliated.

(5) Very pale brown (10YR 7/3) skeletal-fossiliferous lime mudstone to wackestone. Allochems include thin-shelled bivalves, gastropods, serpulid worm tubes and fine-grained mollusc debris (Section 1, 60-64 cm, 67-71 cm and CC, 0-26 cm).

THIN SECTION SUMMARY (%):

	1-1 0-8 D	1-1 0-8 D	1-1 0-8 D	1-1 8-12 D	1-1 18-24 D	1-1 35-39 D	1-1 44-57 D
TEXTURE:							
Sand	50	Tr	70	55	70	–	–
Silt	–	90	–	–	10	–	–
Clay	50	10	30	45	20	–	–
COMPOSITION:							
Quartz	50	70	70	50	65	–	–
Feldspar	5	Tr	Tr	2	–	–	–
Mica (Matrix; Sericite, Chlorite)	45	8	27	47	25	–	–
Clay	–	–	–	–	–	3	5
Dolomite	–	–	–	–	–	95	94
Cement (Quartz)	–	20	–	–	5	–	–
Accessory Minerals:							
Fe Oxide	Tr	2	3	1	5	2	1
Tourmaline	–	Tr	–	–	–	–	–

PHYSICAL PROPERTIES DATA:

	1,3	1,11	1,38
V_p	5.36	4.22	5.37

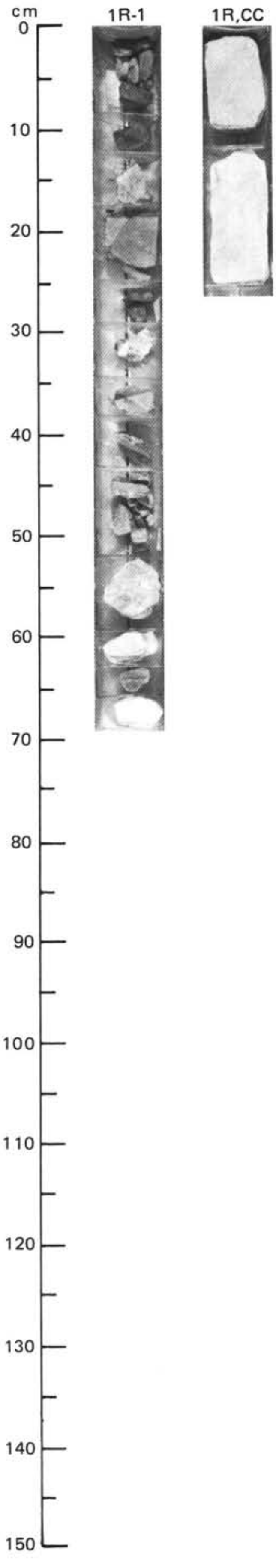
cm
0
10
20
30
40
50
60
70
80
90
100
110
120
130
140
150
1R-1
1R,CC

SITE 639 HOLE F CORE 2 R CORED INTERVAL 5007.8-5011.3 mbsl; 247.3-250.8 mbsf

TIME-ROCK UNIT	BIOSTRAT. ZONE/ FOSSIL CHARACTER				PALEOMAGNETICS	PHYS. PROPERTIES	CHEMISTRY	SECTION	METERS	GRAPHIC LITHOLOGY	DRILLING DISTURB.	SED. STRUCTURES	SAMPLES
	FORAMINIFERS	NANNOFOSSILS	RADIOLARIANS	DIATOMS									
						■■ ■		CC		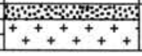			# # #

LITHOLOGIC DESCRIPTION

ALTERED SILICIC HYPABYSSAL ROCKS and QUARTZ SANDSTONE

The core consists of 4 pieces, 4-5 cm across, of:

1) Dark gray to black, brecciated medium-grained quartz sandstone (Sample CC, 0-7 cm).

2) Silicic, hypabyssal rock (?rhyolite-dacite) composed of feldspar, quartz, biotite and muscovite (Sample CC, 7-17 cm).

THIN SECTION SUMMARY (%):

	CC,1-4 D
TEXTURE:	
Sand	80
Clay	20
COMPOSITION:	
Quartz	75
Feldspar	3
Mica (matrix; sericite, chlorite)	20
Accessory Minerals: Fe Oxide Tourm.	2

PHYSICAL PROPERTIES DATA:

	CC,3	CC,10	CC,19
V_p	6.58	6.13	6.49
ρ_b	2.73	2.73	2.88

2R,CC